

**University of Alberta**

**Hydrolysis, Esterification and Glycerolysis of Lipids in  
Supercritical Carbon Dioxide Media**

by

**Paul Henri Luc Moquin**



**A thesis submitted to the Faculty of Graduate Studies and Research  
in partial fulfillment of the requirements for the degree of**

**Doctor of Philosophy**

in

**Bioresource and Food Engineering**

**Department of Agricultural, Food and Nutritional Science**

**Edmonton, Alberta**

**Spring 2008**



Library and  
Archives Canada

Bibliothèque et  
Archives Canada

Published Heritage  
Branch

Direction du  
Patrimoine de l'édition

395 Wellington Street  
Ottawa ON K1A 0N4  
Canada

395, rue Wellington  
Ottawa ON K1A 0N4  
Canada

*Your file    Votre référence*  
*ISBN: 978-0-494-45570-8*  
*Our file    Notre référence*  
*ISBN: 978-0-494-45570-8*

**NOTICE:**

The author has granted a non-exclusive license allowing Library and Archives Canada to reproduce, publish, archive, preserve, conserve, communicate to the public by telecommunication or on the Internet, loan, distribute and sell theses worldwide, for commercial or non-commercial purposes, in microform, paper, electronic and/or any other formats.

The author retains copyright ownership and moral rights in this thesis. Neither the thesis nor substantial extracts from it may be printed or otherwise reproduced without the author's permission.

**AVIS:**

L'auteur a accordé une licence non exclusive permettant à la Bibliothèque et Archives Canada de reproduire, publier, archiver, sauvegarder, conserver, transmettre au public par télécommunication ou par l'Internet, prêter, distribuer et vendre des thèses partout dans le monde, à des fins commerciales ou autres, sur support microforme, papier, électronique et/ou autres formats.

L'auteur conserve la propriété du droit d'auteur et des droits moraux qui protègent cette thèse. Ni la thèse ni des extraits substantiels de celle-ci ne doivent être imprimés ou autrement reproduits sans son autorisation.

---

In compliance with the Canadian Privacy Act some supporting forms may have been removed from this thesis.

Conformément à la loi canadienne sur la protection de la vie privée, quelques formulaires secondaires ont été enlevés de cette thèse.

While these forms may be included in the document page count, their removal does not represent any loss of content from the thesis.

Bien que ces formulaires aient inclus dans la pagination, il n'y aura aucun contenu manquant.

■+■  
**Canada**

## ABSTRACT

Hydrolysis, esterification and glycerolysis reactions were conducted in supercritical carbon dioxide (SC-CO<sub>2</sub>) media with the overall objective of enhancing fundamental knowledge about enzymatic and non-enzymatic lipid reactions conducted in SC-CO<sub>2</sub> media while providing key processing parameters and kinetic models for process design.

Reactions were conducted in a stirred batch reactor (for glycerolysis, esterification and hydrolysis) and in a continuous packed-bed enzymatic reactor (for hydrolysis). Samples were collected as a function of time and the concentrations of monoacylglycerol (MAG), diacylglycerol (DAG), free fatty acids (FFA) and triacylglycerol were determined using thin layer chromatography – flame ionization detector or supercritical fluid chromatography system. Tested processing parameters for batch reactions were: pressure (10-30 MPa), temperature (170-250 °C), supercritical media (CO<sub>2</sub> or N<sub>2</sub>) and initial reactant concentrations (glycerol/oil/water, glycerol/oleic acid, oil/water). For enzymatic reactions, SC-CO<sub>2</sub> flow rate, enzyme load and temperature were the investigated parameters.

Pressure had no impact on the maximum rate of MAG formation (MAG<sub>max</sub>) obtained during esterification but decreased MAG<sub>max</sub> during glycerolysis and delayed FFA production during non-enzymatic hydrolysis. High temperatures increased MAG<sub>max</sub> during esterification while supercritical media did not have any effect on MAG<sub>max</sub> during glycerolysis and esterification or on the maximum rate of

FFA formation ( $FFA_{max}$ ) during hydrolysis. An increase in initial water concentration increased  $MAG_{max}$  during glycerolysis and  $FFA_{max}$  during hydrolysis while an increase in initial glycerol content increased  $MAG_{max}$  during esterification.

For enzymatic hydrolysis, conversion rate was improved with enzyme load and SC-CO<sub>2</sub> flow rate but unaffected by temperature. More studies are therefore required to determine the true optimum for enzyme load and flow rate.

Extensive kinetic modeling taking into account all possible reaction steps for the batch reactions was performed and rate constants were established. Research findings lead to a better understanding of the complex mechanism involved in each reaction while providing the necessary data for optimal process design targeting the production of MAG, DAG or FFA. This research contributes to the development of novel environmentally friendly approaches to value-added processing of oilseeds such as canola, an important local agricultural commodity.



---

**DEDICATION**

To Gérard and Thérèse Moquin

## ACKNOWLEDGEMENTS

First and foremost I would like to express my deep and sincere gratitude to Professor Feral Temelli for being such an incredible mentor and for all the valuable contributions she made to this work. I am very grateful for her wide knowledge and her logical way of thinking as well as for her insistent and constant enthusiasm, patience, advice, support and generosity. Without her this thesis would not be for, although this work is authored by me, the ideas and views were jointly developed.

I wish to thank Dr. Helena Sovová, for inviting me to her laboratory in Prague where she provided me with great guidance, advice and training.

My sincere thanks are due to Dr. Levente Diosady, Dr. Selma Guigard, Dr. David Bressler and Dr. Jonathan Curtis for their detailed review, constructive criticism and excellent advice.

I warmly thank Dr. Peter Sporns, Dr. Monica Palcic, Professor Jerry King, Dr. Marleny Saldaña and Dr. Terry Gannon for their advice and guidance.

I am grateful to Dr. Kelvin Lien, Mei Sun and Doris Chan for their technical assistance as well as to Bernhard Seifried, Byron Yépez, Sandra Spence and Li Sun for their advice and many enlightening discussions.

Finally, my loving thanks to my parents, Gérard and Thérèse, and my wife Kamila for their understanding, endless patience and encouragement when it was most required. I am also grateful for the support of my family members and friends.

This work was funded by the Natural Sciences and Engineering Research Council of Canada. Such funding was greatly appreciated.



**Chapter 2. Kinetic modeling of the glycerolysis reaction for soybean oil in supercritical carbon dioxide media..... 65**

2.1. Introduction.....	65
2.2. Experimental procedures.....	67
2.2.1. Experimental parameters.....	67
2.2.2. Kinetic modeling.....	68
2.2.3. Determination of rate constants .....	71
2.3. Results and discussion .....	74
2.3.1. Chemistry of the glycerolysis of soybean oil.....	74
2.3.2. Kinetics –constraint and assumption .....	75
2.3.3. Trends in calculated rate constants .....	76
2.3.4. Effect of water.....	78
2.3.5. Effect of glycerol/oil ratio.....	80
2.3.6. Effect of pressure .....	80
2.4. Conclusion .....	81
2.5. References .....	82

**Chapter 3. Kinetic modeling of glycerolysis – hydrolysis of canola oil in supercritical carbon dioxide media using dynamic equilibrium data..... 84**

3.1. Introduction.....	84
3.2. Materials and methods .....	86
3.2.1. Materials.....	86
3.2.2. Experimental set up and reaction protocols .....	87
3.2.3. Lipid analysis .....	89
3.2.4. Statistical analysis .....	90
3.2.5. Kinetic modeling.....	91
3.2.6. Determination of rate constants .....	91
3.3. Results and discussion .....	94
3.3.1. Composition and reaction rates.....	94
3.3.2. SC-CO <sub>2</sub> effect.....	99
3.3.3. Effect of water.....	100
3.3.4. Effect of pressure .....	103
3.3.5. Mechanism of the reaction.....	105
3.4. Conclusion .....	108
3.5. References .....	109

**Chapter 4. Production of monoolein from oleic acid and glycerol in supercritical carbon dioxide media: a kinetic approach..... 112**

4.1. Introduction .....	112
4.2. Materials and methods .....	114
4.2.1. Materials.....	114
4.2.2. Reaction protocols.....	115
4.2.3. Lipid analysis .....	116
4.2.4. Experimental design and statistical analysis .....	116
4.2.5. Kinetic modeling.....	117
4.2.6. Determination of rate constants .....	120
4.3. Results and discussion .....	122
4.3.1. Composition and kinetic calculations .....	122
4.3.2. Temperature effect .....	125
4.3.3. Pressure effect .....	126
4.3.4. Effect of supercritical media .....	128
4.3.5. Effect of initial reagent concentration.....	130
4.3.6. Mechanism of the reaction .....	132
4.4. Conclusion .....	135
4.5. References .....	136

**Chapter 5. Kinetic modeling of hydrolysis of canola oil in supercritical media ..... 138**

5.1. Introduction .....	138
5.2. Materials and methods .....	141
5.2.1. Materials.....	141
5.2.2. Reaction protocols.....	142
5.2.3. Lipid analysis .....	143
5.2.4. Experimental design and statistical analysis .....	143
5.2.5. Kinetic modeling.....	145
5.2.6. Determination of rate constants .....	146
5.3. Results and discussion .....	149
5.3.1. Composition and kinetic calculations .....	149
5.3.2. Temperature effect .....	152
5.3.3. Pressure effect .....	153
5.3.4. Effect of supercritical media .....	155

5.3.5. Effect of initial reagent concentration.....	156
5.3.6. Mechanism of the reaction .....	162
5.4. Conclusion .....	164
5.5. References .....	165

**Chapter 6. Continuous enzymatic hydrolysis of canola oil in super-critical carbon dioxide media: effects of temperature, enzyme load and carbon dioxide flow rate ..... 167**

6.1. Introduction.....	167
6.2. Materials and methods .....	169
6.2.1. Materials.....	169
6.2.2. Experimental set-up and design .....	170
6.2.3. Reaction protocols.....	174
6.2.4. Compositional analysis .....	174
6.2.5. Experimental design and statistical analysis .....	178
6.3. Results and discussion .....	179
6.3.1. Establishment of experimental test parameters.....	179
6.3.2. Composition of the product mixture .....	181
6.3.3. Response surface model.....	183
6.3.4. Temperature effect .....	188
6.3.5. Effect of enzyme load .....	189
6.3.6. Effect of SC-CO <sub>2</sub> flow rate .....	190
6.4. Conclusion .....	192
6.5. References.....	193

**Chapter 7. Summary, conclusions and recommendations ..... 195**

7.1. Comparison of reactions and dynamic equilibrium product compositions obtained .....	195
7.2. Effect of supercritical carbon dioxide.....	199
7.3. Effect of pressure and temperature .....	201
7.4. Effect of reactant concentrations.....	203
7.5. References .....	206

**Appendix A. Detailed equipment description and operation..... 207**

A.1. Supercritical high temperature batch reactor ..... 207

    A.1.1. Detailed description of the supercritical high  
        temperature batch reactor ..... 207

    A.1.2. Detailed operating procedure ..... 210

    A.1.3. References ..... 214

A.2. Supercritical continuous enzymatic reactor ..... 215

    A.2.1. Description of the continuous enzymatic reactor ..... 215

    A.2.2. Detailed operating procedure ..... 215

## LIST OF TABLES

Table	Page
1.1. Physical properties of selected components important for the lipid reactions under study [57].....	13
1.2. Summary of glycerolysis reactions conducted by various investigators: reactants, catalyst, processings parameter and yields .....	35
2.1. Effect of glycerol/oil ratio and water content on rate constants.....	77
3.1. Effect of pressure, water and media on the rate constants .....	99
4.1. Effect of glycerol to oleic acid molar ratio (gly/oleic) and pressure on rate constants at 250 °C .....	128
5.1. Effect of the initial canola oil to water molar ratio (o/w), pressure and supercritical media (SC-CO <sub>2</sub> and SC-N <sub>2</sub> ) on rate constants at 250 °C .....	162
6.1. Box-Behnken experimental design with natural and coded variables .....	178
6.2. Composition* of samples obtained between 5 and 6 h of continuous enzymatic hydrolysis of canola oil in supercritical carbon dioxide at 45 °C as a function of enzyme load and flow rate .....	182
6.3. Box-Behnken experimental design with percentage conversion obtained experimentally and those predicted by the response surface model .....	183
6.4. Analysis of variance results for the complete response surface quadratic model.....	184
6.5. Analysis of variance results for the reduced response surface quadratic model.....	185
7.1. Range of FFA, MAG, DAG and TAG concentrations obtained while conducting glycerolysis, esterification and hydrolysis at various initial reactant concentrations and pressures in SC-CO <sub>2</sub> .....	196



## LIST OF FIGURES

Figures	Page
1.1. Schematic phase diagram for pure CO <sub>2</sub> . TP indicates the triple point and CP indicates the critical point [30, 31]. .....	6
1.2. Density of CO <sub>2</sub> as a function of pressure at different temperatures. CP indicates the critical point [30]. .....	8
1.3. Structures of glycerol, oleic acid, monoolein, diolein and triolein [57].....	15
1.4. List of reactions involving esters [61] where the <i>R</i> , <i>R'</i> , <i>R''</i> and <i>R'''</i> represent different fatty acid chains and where FFA stands for free fatty acid .....	17
1.5. Reactions describing the reversible step-wise hydrolysis of TAG [62] where <i>R'</i> , <i>R''</i> and <i>R'''</i> represent different side chains and where MAG, DAG, TAG and FFA stands for monoacylglycerol, diacylglycerol, triacylglycerol and free fatty acid, respectively.....	18
1.6. Reactions describing the reversible step-wise esterification of free fatty acids (FFA) into triacylglycerol (TAG) [127] where <i>R'</i> , <i>R''</i> and <i>R'''</i> represent different side chains and where MAG and DAG stands for monoacylglycerol, diacylglycerol, respectively. ....	29
1.7. Equation (1.12) describes the overall simplified glycerolysis reaction while Eqations (1.13) and (1.14) provide the reversible stepwise glycerolysis of triacylglycerol (TAG) into monoacylglycerol (MAG) [159, 160] where <i>R'</i> , <i>R''</i> and <i>R'''</i> represent different side chains and DAG stands for diacylglycerol and FFA for free fatty acids.....	34
2.1. Rate constants as a function of pressure where the initial water content was 6% (w/w) and the initial Glycerol/Oil ratio was 15.....	78
2.2. MAG formation as a function of time where the initial Glycerol/Oil ratio was 25, pressure was 20.7 MPa and different levels (3-8%, w/w) of initial water content were used. Symbols represent experimental data obtained by Temelli et al. [7] and lines are best fit curves obtained by modeling the data.....	79

3.1. Schematic of the experimental apparatus: (1) filter, (2) rupture disk, (3) compressor, (4) on-off valve, (5) pressure gauge, (6) vent, (7) thermocouple, (8) reactor, (9) temperature controller, (10) sampling tube, (11) electric heater, (12) magnetic stirrer. ....	87
3.2. Thin layer chromatography-flame ionization detection chromatogram as a function of time for a sample collected after 4 h in SC-CO <sub>2</sub> at 250 °C, 30 MPa and 8% (w/w) initial water.....	95
3.3. Experimental data and fitted curves of the composition of the oil phase as a function of time obtained at 250 °C, 10 MPa and 8% (w/w) initial water. ....	96
3.4. Rate of MAG formation as a function of time calculated from Eq. (2.8a) using k-values from Table 3.1 and the concentrations obtained from the fitted data: (1) 10 MPa, 4% (w/w) initial water; (2) 30 MPa, 8% (w/w) initial water; (3) 20 MPa, 8% (w/w) initial water; (4) 10 MPa, 8% (w/w) initial water. ....	97
3.5. Effect of SC-N <sub>2</sub> and SC-CO <sub>2</sub> on MAG and DAG production at 250 °C, 10 MPa and 8% (w/w) initial water as a function of time: (■) MAG in SC-CO <sub>2</sub> media, (▲) DAG in SC-CO <sub>2</sub> media, (×) MAG in SC-N <sub>2</sub> media, (○) DAG in SC-N <sub>2</sub> media. Data points and curves are based on the kinetic model. ....	100
3.6. Effect of initial water content on MAG production at 250 °C and 10 MPa as a function of time where (×), (■), (○) are 0, 4 and 8% (w/w) initial water, respectively. Data points and curves are based on the kinetic model. ....	101
3.7. Effect of pressure on MAG production at 250 °C and 8% (w/w) initial water as a function of time. Data points and curves are based on the kinetic model. ....	104
4.1. Experimental data and fitted curves of the composition of the oil phase as a function of time obtained at 250 °C, 10MPa and using a 1:0.1 initial glycerol to oleic acid ratio. ....	123
4.2. Effect of temperature on monoolein production at 10 MPa using 1:0.1 glycerol to oleic acid ratio as a function of time where (○), (×) and (□) represent 170, 200 and 250 °C, respectively. ....	125

4.3. Effect of pressure and supercritical media on concentration of reaction species at 250 °C and using a 1:0.1 initial glycerol to oleic acid ratio as a function of time where (----), (—) and (—) represent modeled data for 10 MPa in supercritical carbon dioxide (SC-CO <sub>2</sub> ), 30 MPa in SC-CO <sub>2</sub> and 10 MPa in supercritical nitrogen, respectively.....	127
4.4. Change in water concentration as a function of time for reactions conducted at 10 MPa and 250 °C where (----), (—) and (—) represent esterification reactions conducted using 1:0.1, 1:1 and 1:2 initial glycerol/oleic acid molar ratio, respectively. ....	130
4.5. Effect of initial glycerol to oleic acid ratio on product composition at 250 °C and 10 MPa as a function of time where (×), (■), (○) represent 1:2, 1:1 and 1:0.1 initial glycerol to oleic acid ratio, respectively. OA, MO, DO, TO correspond to the plot of the concentration of oleic acid, monoolein, diolein and triolein, respectively. Data points and curves are based on modeled data. ....	131
4.6. Change in glycerol and MO concentration as a function of time during esterification reactions conducted at 10 MPa and 250 °C where (----) represent MO and (—) represent glycerol concentrations and where (▲), (○) and (×) represent reactions conducted using 1:0.1, 1:1 and 1:2 initial glycerol/oleic acid molar ratio, respectively.....	133
5.1. Experimental hydrolysis data and fitted curves of the composition of the canola oil phase as a function of time obtained at 1:17 o/w, 250 °C and 10 MPa. All individual points are measured data except for those for glycerol which were calculated based on material balance. ....	150
5.2. Effect of pressure, temperature and media on FFA composition using a 1:17 o/w as a function of time where (●) represent reactions conducted in SC-CO <sub>2</sub> at 200 °C and 10 MPa, (○) represent runs conducted in SC-N <sub>2</sub> at 250 °C and 10 MPa and where (▲) and (×) represent runs both conducted in SC-CO <sub>2</sub> at 250 °C but at 30 MPa and 10 MPa, respectively. Data points and curved are modeled data. ....	153

5.3. Rate of FFA formation as a function of time calculated from the fitted data: (1) 10 MPa, 1:70 o/w, SC-CO <sub>2</sub> ; (2) 10 MPa, 1:17 o/w, SC-N <sub>2</sub> ; (3) 10 MPa, 1:17 o/w, SC-CO <sub>2</sub> ; (4) 30 MPa, 1:17 o/w, SC-CO <sub>2</sub> ; (5) 10 MPa, 1:3 o/w, SC-CO <sub>2</sub> .....	154
5.4. Production of FFA and TAG during hydrolysis of canola oil at 250 °C, 10 MPa where (Δ), (■) and (□) are 1:3, 1:17 and 1:70 o/w, respectively. Data points and curves are modeled data. ....	157
5.5. Production of DAG and MAG during hydrolysis of canola oil at 250 °C, 10 MPa where (Δ), (■) and (□) are 1:3, 1:17 and 1:70 o/w, respectively. Data points and curves are modeled data. ....	158
5.6. Change in water concentration as a function of time for esterification (Chapter 4) and hydrolysis reactions conducted at 10 MPa and 250 °C. (●) represent hydrolysis data conducted using 1:3 initial oil/water molar ratio; (----), (—) and (—) represent esterification reactions conducted using 1:0.1, 1:1 and 1:2 initial glycerol/oleic acid molar ratio, respectively.....	160
5.7. Change in water concentration as a function of time for hydrolysis and glycerolysis (Chapter 3) reactions conducted at 10 MPa and 250 °C. (▲) represent hydrolysis data conducted using 1:17 initial oil/water molar ratio and (O) and (×) represent glycerolysis data for reactions conducted using 4 and 8% (w/w of glycerol) initial water, respectively. ....	161
6.1. Schematic of the experimental system used to conduct continuous enzymatic reactions in supercritical carbon dioxide: (1) compressor, (2) on-off valve, (3) check valve, (4) back-pressure regulator, (5) rupture disk, (6) pressure gauge, (7) high-performance liquid chromatography pumps, (8) oven, (9) mixer, (10) enzymatic reactor, (11) micro-metering valve, (12) sample collection tube, (13) rotameter, (14) gas meter. ....	171
6.2. Typical supercritical fluid chromatogram of a sample collected from the enzymatic hydrolysis of canola oil in supercritical carbon dioxide (SC-CO <sub>2</sub> ) after 6 h of continuous reaction; (1,2) internal standard, (3,4) FFA, (5) MAG, (6-8) DAG, (9-11) TAG.....	182

6.3. Effect of temperature and supercritical carbon dioxide flow rate on conversion during the continuous enzymatic hydrolysis of canola oil using 1.5 g of enzyme.....	186
6.4. Effect of temperature and enzyme load on conversion during continuous enzymatic hydrolysis of canola oil using supercritical carbon dioxide flow rate of 1.5 L/min.....	187
6.5. Effect of enzyme load and supercritical carbon dioxide flow rate on conversion during continuous enzymatic hydrolysis of canola oil at 50 °C.....	188
7.1. Products formed as a function of time during hydrolysis, glycerolysis and esterification conducted at 10 MPa and 250°C: (▲) amount of FFA formed by hydrolysis using 1:17 initial oil/water molar ratio, (■) amount of MAG formed by glycerolysis using 8% (w/w of glycerol) initial water, and (○) and (----) amount of monoolein formed by esterification using 1:0.1 initial glycerol/oleic acid molar ratio when time zero is set at 0 and 2.5 h, respectively.....	197
A.1.1. Nova Swiss test autoclave with the given name of each part.....	208
A.1.2. Three dimensional scale drawing of some parts of the SC-HTBR system.....	209
A.1.3. Scale drawing of the temperature controller.....	210
A.1.4. Diagram of bolts and fittings position on the nut.....	212
A.1.5. Schematic of the front control panel of the Nova Swiss compressor.....	212
A.1.6. Knob positions on the magnetic stirrer.....	213
A.2.1. Schematic of the experimental system used to conduct continuous enzymatic reactions in supercritical carbon dioxide.....	216

## LIST OF SYMBOLS

$C_{exp}$	Experimental molar concentration obtained using mathematical expressions that best fitted the experimental data
$C_{exp t}$	Experimental molar concentration obtained using mathematical expressions that best fitted the experimental data at time $t$
$C_{pred}$	Predicted concentration obtained using the following expression: $C _t + r_{pred} \cdot \Delta t$
$C _t$	Previously obtained concentration at time $t$
$C _{t+\Delta t}$	Concentration at time $t + \Delta t$ which is equal to $C_{pred}$
$\% Conv$	Percentage enzymatic hydrolysis conversion defined as the percentage of the total fatty acid in free form or $[N_{FFA}/(N_{FFA}+N_{MAG}+2 \cdot N_{DAG}+3 \cdot N_{TAG})] \cdot 100$
$\% Conversion$	Conversion rate of non-enzymatic hydrolysis defined as $= \frac{[FFA]_t}{3 \times [TAG]_0} \times 100$
DAG	Diacylglycerol(s)
FFA	Free fatty acid(s)
$FFA_{max}$	The maximum rate of free fatty acids formation during non-enzymatic hydrolysis
$[FFA]_t$	Molar concentration of free fatty acids at time $t$
$\% H_2O_{added}$	Percentage of water (as wt % of glycerol) added to the reaction system used by Temelli et al. [7] and reported in Ch. 2
$\infty$	Dynamic equilibrium
$k_1$	Rate constant (g/h·mol) for the following reaction: $TAG + Gly \rightarrow MAG + DAG$
$k_2$	Rate constant (g/h·mol) for the following reaction: $MAG + DAG \rightarrow TAG + Gly$

$k_3$	Rate constant (g/h·mol) for the following reaction: DAG + Gly $\rightarrow$ 2 MAG
$k_4$	Rate constant (g/h·mol) for the following reaction: 2 MAG $\rightarrow$ DAG + Gly
$k_5$	Rate constant (g/h·mol) for the following reaction: TAG + MAG $\rightarrow$ 2 DAG
$k_6$	Rate constant (g/h·mol) for the following reaction: 2 DAG $\rightarrow$ TAG + MAG
$k_7$	Rate constant (g/h·mol) for the following reaction: TAG + H <sub>2</sub> O $\rightarrow$ DAG + FFA
$k_8$	Rate constant (g/h·mol) for the following reaction: DAG + FFA $\rightarrow$ TAG + H <sub>2</sub> O
$k_9$	Rate constant (g/h·mol) for the following reaction: DAG + H <sub>2</sub> O $\rightarrow$ MAG + FFA
$k_{10}$	Rate constant (g/h·mol) for the following reaction: MAG + FFA $\rightarrow$ DAG + H <sub>2</sub> O
$k_{11}$	Rate constant (g/h·mol) for the following reaction: MAG + H <sub>2</sub> O $\rightarrow$ Gly + FFA
$k_{12}$	Rate constant (g/h·mol) for the following reaction: Gly + FFA $\rightarrow$ MAG + H <sub>2</sub> O
MAG	Monoacylglycerol(s)
N	Average number of moles
n	Number of moles
$n^{\text{in}}$	Number of moles fed into the system
$n^{\text{out}}$	Number of moles produced by the system
$P_c$	Critical pressure

$r_{pred}$	Predicted rate of change
$r'_{pred}$	Estimated rate of change
$R^2$	Correlation coefficient
Rate-50%	Rate of monoolein formation during esterification at 50% equilibrium concentration
$t$	Value at a given time
TAG	Triacylglycerol(s)
$[TAG]_0$	Initial molar concentration of triacylglycerol
$t_{-50\%}$	Time it took a given reaction to reach half of its equilibrium concentration
$T_c$	Critical temperature
$W_{total}$	Total weight of the reactants
$x_1$	Coded variable for temperature in the Box-Behnken experimental design
$x_2$	Coded variable for enzyme load in the Box-Behnken experimental design
$x_3$	Coded variable for flow rate in the Box-Behnken experimental design
$X$	Mole fraction obtained during enzymatic hydrolysis for samples collected between 5 and 6 h
$Y_{exp}$	Experimental percentage enzymatic hydrolysis conversion defined as the percentage of the total fatty acid in free form
$Y_{pred}$	Predicted percentage enzymatic hydrolysis conversion defined as the percentage of the total fatty acid in free form
$\beta$	Coefficients determined using the Box-Behnken Design
$\Delta t$	The time interval between each calculated concentrations



## LIST OF EQUATIONS

Equation	Page
Eq. 2.1	$\text{TAG} + 2 \text{Gly} \rightleftharpoons 3 \text{MAG} \dots\dots\dots 68$
Eq. 2.2	$\text{TAG} + \text{Gly} \xrightleftharpoons[k_2]{k_1} \text{MAG} + \text{DAG} \dots\dots\dots 68$
Eq. 2.3	$\text{DAG} + \text{Gly} \xrightleftharpoons[k_4]{k_3} 2 \text{MAG} \dots\dots\dots 68$
Eq. 2.4	$\text{TAG} + \text{MAG} \xrightleftharpoons[k_6]{k_5} 2 \text{DAG} \dots\dots\dots 69$
Eq. 2.5	$\text{TAG} + \text{H}_2\text{O} \xrightleftharpoons[k_8]{k_7} \text{DAG} + \text{FFA} \dots\dots\dots 69$
Eq. 2.6	$\text{DAG} + \text{H}_2\text{O} \xrightleftharpoons[k_{10}]{k_9} \text{MAG} + \text{FFA} \dots\dots\dots 69$
Eq. 2.7	$\text{MAG} + \text{H}_2\text{O} \xrightleftharpoons[k_{12}]{k_{11}} \text{Gly} + \text{FFA} \dots\dots\dots 69$
Eq. 2.8a	$\begin{aligned} \frac{d[\text{MAG}]}{dt} = & k_1[\text{Gly}][\text{TAG}] - k_2[\text{DAG}][\text{MAG}] \\ & + 2k_3[\text{Gly}][\text{DAG}] - 2k_4[\text{MAG}]^2 - k_5[\text{TAG}][\text{MAG}] \\ & + k_6[\text{DAG}]^2 + k_9[\text{DAG}][\text{H}_2\text{O}] - k_{10}[\text{MAG}][\text{FFA}] \\ & - k_{11}[\text{H}_2\text{O}][\text{MAG}] + k_{12}[\text{Gly}][\text{FFA}] \dots\dots\dots 70 \end{aligned}$

$$\begin{aligned} \text{Eq. 2.8b} \quad \frac{d[\text{DAG}]}{dt} &= k_1[\text{Gly}][\text{TAG}] - k_2[\text{DAG}][\text{MAG}] \\ &- k_3[\text{Gly}][\text{DAG}] + k_4[\text{MAG}]^2 + 2k_5[\text{TAG}][\text{MAG}] \\ &- 2k_6[\text{DAG}]^2 + k_7[\text{TAG}][\text{H}_2\text{O}] - k_8[\text{DAG}][\text{FFA}] \\ &- k_9[\text{DAG}][\text{H}_2\text{O}] + k_{10}[\text{MAG}][\text{FFA}] \dots\dots\dots 70 \end{aligned}$$

$$\begin{aligned} \text{Eq. 2.8c} \quad \frac{d[\text{TAG}]}{dt} &= -k_1[\text{Gly}][\text{TAG}] + k_2[\text{DAG}][\text{MAG}] \\ &- k_5[\text{TAG}][\text{MAG}] + k_6[\text{DAG}]^2 - k_7[\text{TAG}][\text{H}_2\text{O}] \\ &+ k_8[\text{DAG}][\text{FFA}] \dots\dots\dots 70 \end{aligned}$$

$$\begin{aligned} \text{Eq. 2.8d} \quad \frac{d[\text{FFA}]}{dt} &= k_7[\text{TAG}][\text{H}_2\text{O}] - k_8[\text{DAG}][\text{FFA}] + k_9[\text{DAG}][\text{H}_2\text{O}] \\ &- k_{10}[\text{MAG}][\text{FFA}] + k_{11}[\text{H}_2\text{O}][\text{MAG}] - k_{12}[\text{Gly}][\text{FFA}] \dots\dots\dots 70 \end{aligned}$$

$$\begin{aligned} \text{Eq. 2.8e} \quad \frac{d[\text{H}_2\text{O}]}{dt} &= -k_7[\text{TAG}][\text{H}_2\text{O}] + k_8[\text{DAG}][\text{FFA}] - k_9[\text{DAG}][\text{H}_2\text{O}] \\ &+ k_{10}[\text{MAG}][\text{FFA}] - k_{11}[\text{H}_2\text{O}][\text{MAG}] + k_{12}[\text{Gly}][\text{FFA}] \dots\dots\dots 70 \end{aligned}$$

$$\begin{aligned} \text{Eq. 2.8f} \quad \frac{d[\text{Gly}]}{dt} &= -k_1[\text{Gly}][\text{TAG}] + k_2[\text{DAG}][\text{MAG}] - k_3[\text{Gly}][\text{DAG}] \\ &+ k_4[\text{MAG}]^2 + k_{11}[\text{MAG}][\text{H}_2\text{O}] - k_{12}[\text{Gly}][\text{FFA}] \dots\dots\dots 70 \end{aligned}$$

$$\text{Eq. 2.9} \quad \% \text{ Water (w/w)} = \frac{(\text{Gly/Oil})(n_{\text{TAG}0})(92.09 \text{ g/mol})(\% \text{H}_2\text{O Added} + 0.04)}{W_{t\text{total}}} \dots\dots 70$$

$$\text{Eq. 2.10} \quad C'_{\text{pred}} = C'_{|t+\Delta t} = C|_t + r'_{\text{pred}} \Delta t \dots\dots\dots 73$$

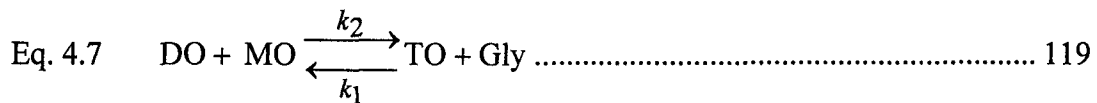
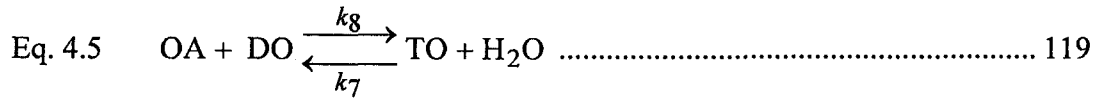
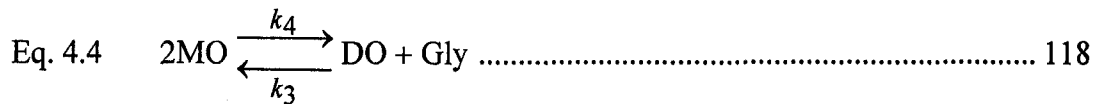
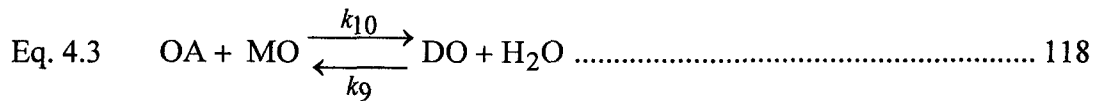
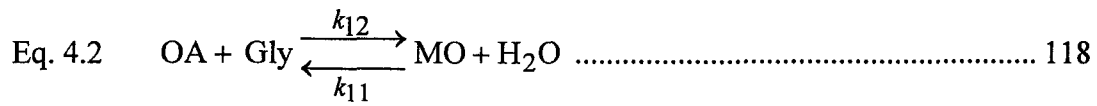
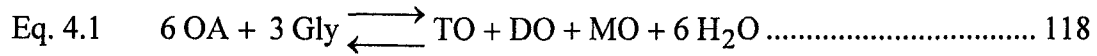
$$\text{Eq. 2.11} \quad C_{\text{pred}} = C|_{t+\Delta t} = C|_t + r_{\text{pred}} \Delta t \dots\dots\dots 73$$

$$\text{Eq. 3.1} \quad [\text{Gly}]_t = ([\text{Oil}]_0 + [\text{Gly}]_0) - ([\text{TAG}]_t + [\text{DAG}]_t + [\text{MAG}]_t) \dots\dots\dots 91$$

$$\text{Eq. 3.2} \quad C_{\text{pred}} = C|_{t+\Delta t} = C_{\text{exp}}|_t + r_{\text{pred}} \Delta t \dots\dots\dots 93$$

$$\text{Eq. 3.3} \quad k_9 = \frac{k_3([\text{Gly}]_\infty)([\text{DAG}]_\infty) + k_4([\text{MAG}]_\infty)^2 + k_{10}([\text{MAG}]_\infty)([\text{FFA}]_\infty)}{([\text{DAG}]_\infty)([\text{H}_2\text{O}]_\infty)} \dots\dots 93$$

$$\text{Eq. 3.4} \quad k_{12} = \frac{k_3([\text{Gly}]_\infty)([\text{DAG}]_\infty) + k_4([\text{MAG}]_\infty)^2 + k_{11}([\text{MAG}]_\infty)([\text{H}_2\text{O}]_\infty)}{([\text{Gly}]_\infty)([\text{FFA}]_\infty)} \dots\dots 93$$



$$\begin{aligned} \text{Eq. 4.8a} \quad \frac{d[\text{MO}]}{dt} &= k_1[\text{Gly}][\text{TO}] - k_2[\text{DO}][\text{MO}] + 2k_3[\text{Gly}][\text{DO}] \\ &- 2k_4[\text{MO}]^2 - k_5[\text{TO}][\text{MO}] + k_6[\text{DO}]^2 + k_9[\text{DO}][\text{H}_2\text{O}] \\ &- k_{10}[\text{MO}][\text{OA}] - k_{11}[\text{H}_2\text{O}][\text{MO}] + k_{12}[\text{Gly}][\text{OA}] \dots\dots\dots 119 \end{aligned}$$

$$\begin{aligned} \text{Eq. 4.8b} \quad \frac{d[\text{DO}]}{dt} &= k_1[\text{Gly}][\text{TO}] - k_2[\text{DO}][\text{MO}] - k_3[\text{Gly}][\text{DO}] + k_4[\text{MO}]^2 \\ &+ 2k_5[\text{TO}][\text{MO}] - 2k_6[\text{DO}]^2 + k_7[\text{TO}][\text{H}_2\text{O}] \\ &- k_8[\text{DO}][\text{OA}] - k_9[\text{DO}][\text{H}_2\text{O}] + k_{10}[\text{MO}][\text{OA}] \dots\dots\dots 119 \end{aligned}$$

$$\begin{aligned} \text{Eq. 4.8c} \quad \frac{d[\text{TO}]}{dt} &= -k_1[\text{Gly}][\text{TO}] + k_2[\text{DO}][\text{MO}] - k_5[\text{TO}][\text{MO}] \\ &+ k_6[\text{DO}]^2 - k_7[\text{TO}][\text{H}_2\text{O}] + k_8[\text{DO}][\text{OA}] \dots\dots\dots 119 \end{aligned}$$

$$\begin{aligned} \text{Eq. 4.8d} \quad \frac{d[\text{OA}]}{dt} &= k_7[\text{TO}][\text{H}_2\text{O}] - k_8[\text{DO}][\text{OA}] + k_9[\text{DO}][\text{H}_2\text{O}] \\ &- k_{10}[\text{MO}][\text{OA}] + k_{11}[\text{H}_2\text{O}][\text{MO}] - k_{12}[\text{Gly}][\text{OA}] \dots\dots\dots 119 \end{aligned}$$

$$\begin{aligned} \text{Eq. 4.8e} \quad \frac{d[\text{H}_2\text{O}]}{dt} &= -k_7[\text{TO}][\text{H}_2\text{O}] + k_8[\text{DO}][\text{OA}] - k_9[\text{DO}][\text{H}_2\text{O}] \\ &+ k_{10}[\text{MO}][\text{OA}] - k_{11}[\text{H}_2\text{O}][\text{MO}] + k_{12}[\text{Gly}][\text{OA}] \dots\dots\dots 120 \end{aligned}$$

$$\begin{aligned} \text{Eq. 4.8f} \quad \frac{d[\text{Gly}]}{dt} &= -k_1[\text{Gly}][\text{TO}] + k_2[\text{DO}][\text{MO}] - k_3[\text{Gly}][\text{DO}] \\ &+ k_4[\text{MO}]^2 + k_{11}[\text{MO}][\text{H}_2\text{O}] - k_{12}[\text{Gly}][\text{OA}] \dots\dots\dots 120 \end{aligned}$$

$$\text{Eq. 4.9} \quad [\text{Gly}]_t = [\text{Gly}]_0 - ([\text{TO}]_t + [\text{DO}]_t + [\text{MO}]_t) \dots\dots\dots 120$$

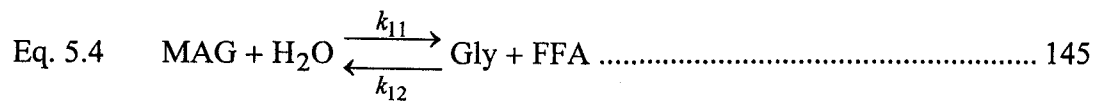
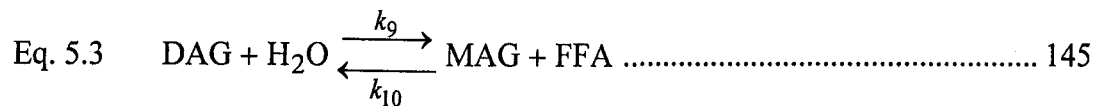
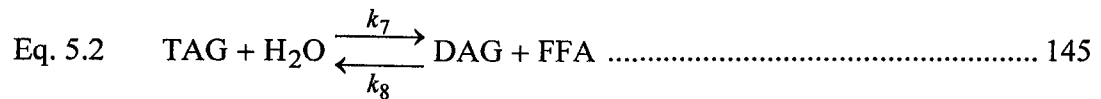
$$\text{Eq. 4.10} \quad C_{\text{pred}} = C|_{t+\Delta t} = C_{\text{exp}}|_t + r_{\text{pred}} \Delta t \dots\dots\dots 121$$

$$\begin{aligned} &-k_1([\text{Gly}]_\infty)([\text{TO}]_\infty) + k_2([\text{DO}]_\infty)([\text{MO}]_\infty) \\ &+ k_3([\text{Gly}]_\infty)([\text{DO}]_\infty) - k_4([\text{MO}]_\infty)^2 \\ &- 2k_5([\text{TO}]_\infty)([\text{MO}]_\infty) + 2k_6([\text{DO}]_\infty)^2 \\ &- k_7([\text{TO}]_\infty)([\text{H}_2\text{O}]_\infty) + k_8([\text{DO}]_\infty)([\text{OA}]_\infty) \\ &+ k_9([\text{DO}]_\infty)([\text{H}_2\text{O}]_\infty) \end{aligned}$$

$$\text{Eq. 4.11} \quad k_{10} = \frac{\dots\dots\dots}{([\text{MO}]_\infty)([\text{OA}]_\infty)} \dots\dots\dots 122$$

$$\text{Eq. 4.12} \quad k_{12} = \frac{-k_1([\text{Gly}]_\infty)([\text{TO}]_\infty) + k_2([\text{DO}]_\infty)([\text{MO}]_\infty) - k_3([\text{Gly}]_\infty)([\text{DO}]_\infty) + k_4([\text{MO}]_\infty)^2 + k_{11}([\text{MO}]_\infty)([\text{H}_2\text{O}]_\infty)}{([\text{Gly}]_\infty)([\text{OA}]_\infty)} \dots\dots\dots 122$$

$$\text{Eq. 5.1} \quad \% \text{ Conversion} = \frac{[\text{FFA}]_t}{3 \times [\text{TAG}]_0} \times 100 \dots\dots\dots 144$$



$$\text{Eq. 5.6a} \quad \frac{d[\text{MAG}]}{dt} = -k_5[\text{TAG}][\text{MAG}] + k_6[\text{DAG}]^2 + k_9[\text{DAG}][\text{H}_2\text{O}] - k_{10}[\text{MAG}][\text{FFA}] - k_{11}[\text{H}_2\text{O}][\text{MAG}] + k_{12}[\text{Gly}][\text{FFA}] \dots\dots\dots 146$$

$$\text{Eq. 5.6b} \quad \frac{d[\text{DAG}]}{dt} = 2k_5[\text{TAG}][\text{MAG}] - 2k_6[\text{DAG}]^2 + k_7[\text{TAG}][\text{H}_2\text{O}] - k_8[\text{DAG}][\text{FFA}] - k_9[\text{DAG}][\text{H}_2\text{O}] + k_{10}[\text{MAG}][\text{FFA}] \dots\dots\dots 146$$

$$\text{Eq. 5.6c} \quad \frac{d(\text{TAG})}{dt} = -k_5[\text{TAG}][\text{MAG}] + k_6[\text{DAG}]^2 - k_7[\text{TAG}][\text{H}_2\text{O}] + k_8[\text{DAG}][\text{FFA}] \dots\dots\dots 146$$

$$\text{Eq. 5.6d} \quad \frac{d[\text{FFA}]}{dt} = k_7[\text{TAG}][\text{H}_2\text{O}] - k_8[\text{DAG}][\text{FFA}] + k_9[\text{DAG}][\text{H}_2\text{O}] - k_{10}[\text{MAG}][\text{FFA}] + k_{11}[\text{H}_2\text{O}][\text{MAG}] - k_{12}[\text{Gly}][\text{FFA}] \dots\dots\dots 146$$

$$\text{Eq. 5.6e} \quad \frac{d[\text{H}_2\text{O}]}{dt} = -k_7[\text{TAG}][\text{H}_2\text{O}] + k_8[\text{DAG}][\text{FFA}] - k_9[\text{DAG}][\text{H}_2\text{O}] + k_{10}[\text{MAG}][\text{FFA}] - k_{11}[\text{H}_2\text{O}][\text{MAG}] + k_{12}[\text{Gly}][\text{FFA}] \dots\dots\dots 146$$

$$\text{Eq. 5.6f} \quad \frac{d[\text{Gly}]}{dt} = k_{11}[\text{MAG}][\text{H}_2\text{O}] - k_{12}[\text{Gly}][\text{FFA}] \dots\dots\dots 146$$

$$\text{Eq. 5.7} \quad C_{\text{pred}} = C|_{t+\Delta t} = C_{\text{exp}}|_t + r_{\text{pred}} \cdot \Delta t \dots\dots\dots 148$$

$$\text{Eq. 5.8} \quad k_{10} = \frac{-2k_5([\text{TAG}]_{\infty})([\text{MAG}]_{\infty}) + 2k_6([\text{DAG}]_{\infty})^2 - k_7([\text{TAG}]_{\infty})([\text{H}_2\text{O}]_{\infty}) + k_8([\text{DAG}]_{\infty})([\text{FFA}]_{\infty}) + k_9([\text{DAG}]_{\infty})([\text{H}_2\text{O}]_{\infty})}{([\text{MAG}]_{\infty})([\text{FFA}]_{\infty})} \dots\dots\dots 148$$

$$\text{Eq. 5.9} \quad k_{12} = \frac{k_{11}([\text{MAG}]_{\infty})([\text{H}_2\text{O}]_{\infty})}{([\text{Gly}]_{\infty})([\text{FFA}]_{\infty})} \dots\dots\dots 148$$

$$\text{Eq. 6.1} \quad \% \text{ Conv} = \frac{N_{\text{FFA}}}{N_{\text{FFA}} + N_{\text{MAG}} + 2 \cdot N_{\text{DAG}} + 3 \cdot N_{\text{TAG}}} \times 100 \dots\dots\dots 176$$

$$\begin{aligned} \text{Eq. 6.2} \quad X_{TAG} &= \frac{N_{TAG}}{N_{TAG} + N_{MAG} + N_{DAG} + N_{FFA}} \dots\dots\dots 176 \\ &= \frac{n_{TAG}^{out}}{n_{TAG}^{out} + n_{MAG}^{out} + n_{DAG}^{out} + n_{FFA}^{out}} \end{aligned}$$

$$\text{Eq. 6.3} \quad 0 = [n_{TAG}^{out} \cdot (X_{TAG} - 1)] + (n_{DAG}^{out} \cdot X_{TAG}) + (n_{MAG}^{out} \cdot X_{TAG}) + (n_{FFA}^{out} \cdot X_{TAG}) \dots\dots 177$$

$$\text{Eq. 6.4} \quad 0 = (n_{TAG}^{out} \cdot X_{DAG}) + [n_{DAG}^{out} \cdot (X_{DAG} - 1)] + (n_{MAG}^{out} \cdot X_{DAG}) + (n_{FFA}^{out} \cdot X_{DAG}) \dots\dots 177$$

$$\text{Eq. 6.5} \quad 0 = (n_{TAG}^{out} \cdot X_{FFA}) + (n_{DAG}^{out} \cdot X_{FFA}) + (n_{MAG}^{out} \cdot X_{FFA}) + [n_{FFA}^{out} \cdot (X_{FFA} - 1)] \dots\dots 177$$

$$\text{Eq. 6.6} \quad n_{TAG}^{in} = n_{TAG}^{out} + n_{DAG}^{out} + n_{MAG}^{out} + n_{Glycerol}^{out} \dots\dots\dots 177$$

$$\text{Eq. 6.7} \quad 0 = n_{DAG}^{out} + 2 \cdot n_{MAG}^{out} + 3 \cdot n_{Glycerol}^{out} - n_{FFA}^{out} \dots\dots\dots 177$$

$$\begin{aligned} \text{Eq. 6.8} \quad y &= \beta_0 + \beta_1 x_1 + \beta_2 x_2 + \beta_3 x_3 + \beta_{12}(x_1)(x_2) + \beta_{13}(x_1)(x_3) + \\ &\beta_{23}(x_2)(x_3) + \beta_{11}(x_1)^2 + \beta_{22}(x_2)^2 + \beta_{33}(x_3)^2 \dots\dots\dots 179 \end{aligned}$$

$$\begin{aligned} \text{Eq. 6.9} \quad y &= 32.393 + 0.837 x_1 + 4.030 x_2 + 4.060 x_3 + 2.934 x_2 x_3 \\ &- 2.753 (x_2)^2 + 1.687 (x_3)^2 \dots\dots\dots 185 \end{aligned}$$

# **1. Introduction and literature review**

## **1.1. Scope and thesis objectives**

Claims that Canada relies too heavily on its natural resources and does not process its agricultural raw materials locally [1] calls for an increase in local processing of home grown crops for value addition. One of Canada's major crops is canola and its oil has a triacylglycerol (TAG) content between 94.4 and 99.1% of total lipids [2] and a high oleic acid content that makes it a serious rival to soybean oil as a healthy unsaturated oil [3]. Nonetheless, transforming canola oil and the excess glycerol generated as a side product of the hydrolysis [4] and the biodiesel industry [5] into monoacylglycerol (MAG) and diacylglycerol (DAG) designer oil mixtures used in a number of food, pharmaceutical and industrial products [6-9] represents a tremendous opportunity for Canada. Furthermore, finding a novel way of producing MAG and DAG in an environmentally responsible manner would ensure a more sustainable development. Indeed, production of MAG and DAG using supercritical carbon dioxide (SC-CO<sub>2</sub>), which is carbon dioxide (CO<sub>2</sub>) above its critical temperature (31.03 °C) and pressure (7.38 MPa), would present a novel and more environmentally friendly processing approach. In fact, SC-CO<sub>2</sub> constitutes a beneficial reaction media for a number of non-enzymatic and enzymatic lipid reactions. Indeed, manipulating the temperature and pressure of reactions in SC-CO<sub>2</sub> media offers the opportunity to adjust the reaction environment by controlling the solvating power, diffusion effects, and the products formed. This



implies that the high diffusivity of these fluids allows faster penetration of the substrate and accelerates the reaction [10]. Some experimental data also suggest that supercritical technology can enhance the yield of one product with respect to another to a greater extent compared to what can be achieved in a conventional liquid medium [11]. Moreover, CO<sub>2</sub> is a solvent of choice for food applications because it has a low critical temperature, is inexpensive, abundant, safe to handle and easily removed upon depressurization.

An extensive number of studies have been conducted on extraction in SC-CO<sub>2</sub>, which have led this technology to its current use in a number of industrial applications, such as coffee decaffeination and production of oil, hops and spice extracts, as well as in various decontamination processes [12]. However, unlike SC-CO<sub>2</sub> extraction, reactions in SC-CO<sub>2</sub> have not yet been as widely studied and only a few reviews are available [10, 13-18]. Furthermore, only a limited number of investigators have focused on non-enzymatic lipid reactions even though further research in this field appears promising. Indeed, lighter coloured products have been obtained using SC-CO<sub>2</sub> and, given that the products can be quickly removed from SC-CO<sub>2</sub> media upon depressurization, reaction reversion is minimized [19].

Among the non-enzymatic reactions investigated, glycerolysis was successfully conducted using soybean oil at high temperature (250 °C) and high pressure (20 - 40 MPa) in SC-CO<sub>2</sub> media [20]. The main products were high quality light coloured MAG and DAG, which are important functional lipids used as ingredients in a variety of product applications. Given that MAG and DAG could

be obtained using canola oil as a feedstock, the establishment of optimal process conditions for glycerolysis of canola oil in SC-CO<sub>2</sub> would offer a way to add value to canola oil through novel process development. In contrast with non-enzymatic reactions in SC-CO<sub>2</sub>, more research has been conducted on enzymatic lipid reactions in SC-CO<sub>2</sub> and considerable fundamental knowledge has been accumulated. For instance, it was found that compared to organic solvent media, enzymatic reactions proceed at a much faster rate in SC-CO<sub>2</sub> media [21]. It has also been established that the mass transport from the bulk of the solution to the enzyme surface is faster in SC-CO<sub>2</sub> than that in hexane [22]. Furthermore, Hakoda et al. [23], who worked with immobilized lipase (Lipozyme IM, *Mucor miehei*), claimed that the solubility of water in SC-CO<sub>2</sub> was an important parameter because it affected the amount of water adsorbed on the support material used for enzyme immobilization. Rezaei and Temelli [24], who conducted continuous enzymatic hydrolysis in SC-CO<sub>2</sub> using the same lipase as Hakoda et al. [23], investigated two SC-CO<sub>2</sub> flow rate levels (1.0 and 3.7 L/min, measured at ambient conditions) and reported higher conversion at the lower flow rate studied thereby concluding that higher conversion could be achieved if lower flow rates were used. However, Sovova and Zarevucka [25] later conducted reactions at lower SC-CO<sub>2</sub> flow rates (<0.5 L/min) and reported lower conversions at lower flow rates but were not able to establish if the effect was significant or not. They also reported a trend indicating negligible temperature effect [25] while Rezaei and Temelli [24] reported an

increase in glycerol formation with temperature. Additional research is therefore required to clarify such results.

Few non-enzymatic studies involving reactions of vegetable oils and fatty esters have gone beyond basic experimental results with respect to consideration of reaction kinetics [26-29] and only Darnoko and Cheryan [26] noted the fact that ester hydrolysis reactions were taking place in parallel with transesterification. The literature lacks information on the kinetics of glycerolysis, esterification and hydrolysis reactions in SC-CO<sub>2</sub> media. Such information is essential for a better understanding of the reaction mechanism as well as for the design of reaction equipment and processes.

Therefore, the overall objectives for this thesis research were to:

- A. further the fundamental knowledge about enzymatic and non-enzymatic lipid reactions conducted in SC-CO<sub>2</sub> media and
- B. provide key processing parameters necessary to develop and enhance novel environmentally friendly processes, which will produce value added products using locally available feedstock.

The specific objectives were to:

- a) model the kinetics of glycerolysis of soybean oil in SC-CO<sub>2</sub> media using previously reported data (Chapter 2),
- b) conduct glycerolysis of canola oil in SC-CO<sub>2</sub> media, assess the effect of processing parameters, develop a kinetic model using equilibrium data and establish the mechanism of the reaction to

describe the glycerolysis-hydrolysis reaction in SC-CO<sub>2</sub> media (Chapter 3),

- c) conduct esterification of oleic acid with glycerol in SC-CO<sub>2</sub> to determine the effects of processing parameters, develop a kinetic model and establish the mechanism of the reaction (Chapter 4),
- d) conduct hydrolysis of canola oil in SC-CO<sub>2</sub> to determine the effects of processing parameters, develop a kinetic model and establish the mechanism of the reaction (Chapter 5), and
- e) conduct enzymatic hydrolysis of canola oil in SC-CO<sub>2</sub> media and investigate the effects of operating conditions to maximize production of free fatty acids (Chapter 6).

## **1.2. Literature review**

### *1.2.1. SC-CO<sub>2</sub> media*

#### *1.2.1.1. The supercritical state*

Pure CO<sub>2</sub> exists in nature under the solid (dry ice), liquid and vapour (gaseous) states, depending on its temperature and pressure. A phase diagram for pure CO<sub>2</sub> plotted as a function of temperature and pressure is presented in Figure 1.1. The point where all three phases of CO<sub>2</sub> occur, at -56.6 °C and 0.5 MPa, is commonly referred to as the triple point (TP) and can be identified on such a plot. It is also possible to identify a point where the phase boundary between a vapour and

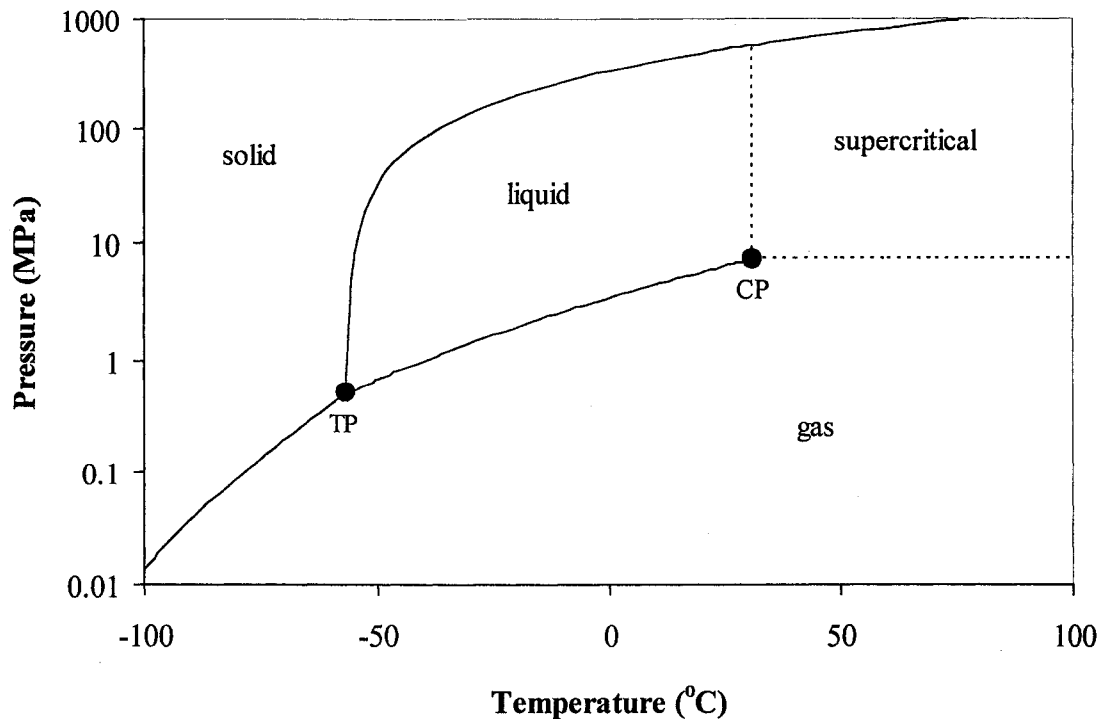


**Figure 1.1.** Schematic phase diagram for pure CO<sub>2</sub>. TP indicates the triple point and CP indicates the critical point [30, 31].

a liquid ends. This point is referred to as the critical point (CP) and marks the point where differences between vapour and liquid states disappear. When CO<sub>2</sub> is above this point, but below 570 MPa [31], which is the pressure required to condense it into a solid, it is SC-CO<sub>2</sub>. The critical pressure for CO<sub>2</sub> is 7.38 MPa and its critical temperature is 304.1 K or 31.03 °C [32]. When CO<sub>2</sub> is in the liquid phase at temperature below 31.03 °C, but not too far below, CO<sub>2</sub> is referred to as a “subcritical liquid”; similarly, when it is below but in the vicinity of 7.38 MPa, it is called a “subcritical gas”. SC-CO<sub>2</sub> and, to a certain extent, subcritical CO<sub>2</sub> has

inherent solvent-like properties for non-polar compounds and can also be used as a reaction medium.

### *1.2.1.2. Physical properties of SC-CO<sub>2</sub>*

#### *1.2.1.2.1. Density*

SC-CO<sub>2</sub> is a dense fluid, with a density of 466 kg/m<sup>3</sup> at the critical point [33]. The relatively high density of SC-CO<sub>2</sub> (Fig. 1.2) above the critical point leads to high solvating power. Also, as seen in Figure 1.2, variations in temperature and pressure cause changes in the density of SC-CO<sub>2</sub>, which provide some flexibility or tunability of the solvent power of SC-CO<sub>2</sub>. Interestingly, around the critical point density fluctuates greatly; therefore, when these fluctuations are of the same order of magnitude as the wavelength of visible light, light is scattered and the fluid becomes opaque – a phenomenon known as critical opalescence [33].

#### *1.2.1.2.2. Polarity*

When choosing a solvent or a media for a given reaction, it is important to consider the type of interaction forces that will take place between the solvent/media and the solute because solutes with similar polarity to that of the solvent/media will preferably be dissolved. For this reason, it is important to consider the dielectric constant and the polarity or polarizability of SC-CO<sub>2</sub>. The dielectric constant for SC-CO<sub>2</sub> at its critical point is about 1.3 and it only increases to approximately 1.6 at 100 °C and 79.8 MPa when SC-CO<sub>2</sub> density doubles to

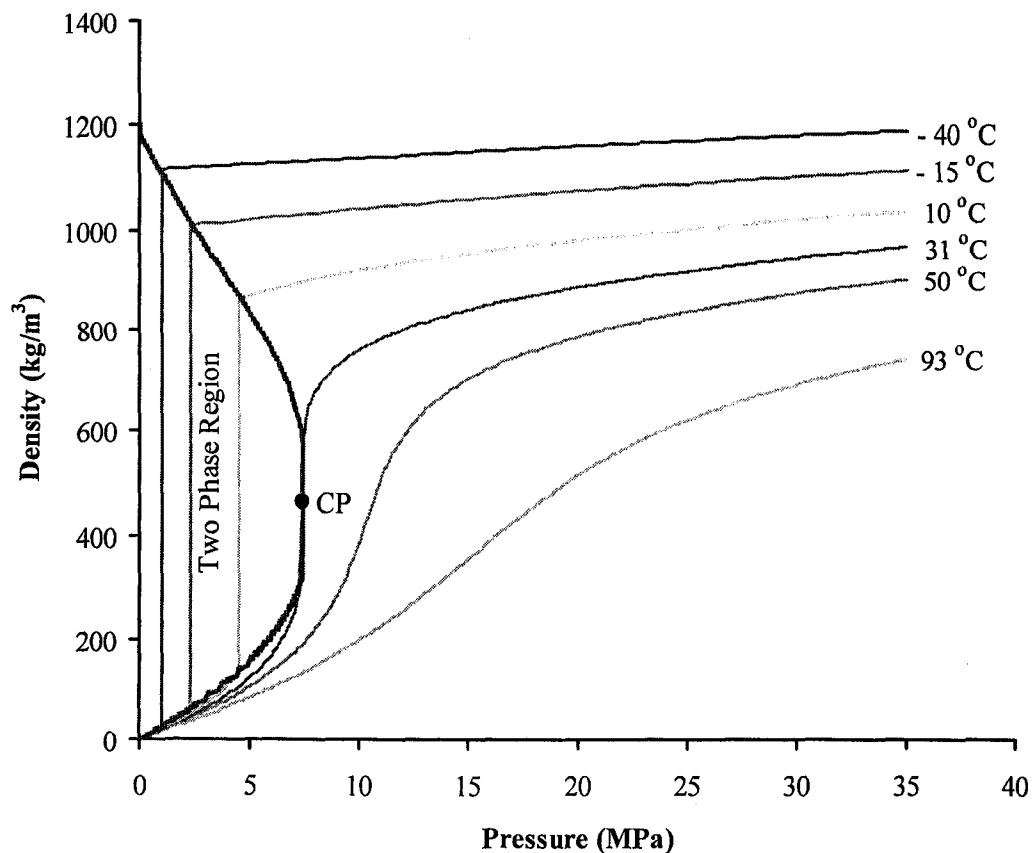


**Figure 1.2.** Density of CO<sub>2</sub> as a function of pressure at different temperatures. CP indicates the critical point [30].

932 kg/m<sup>3</sup> [33]. Such an increase appears negligible compared to that of supercritical water where the dielectric constant increases dramatically from approximately 5 at the critical point to approximately 14 when the critical density of water is doubled [33]. Apart from exhibiting a low dielectric constant, SC-CO<sub>2</sub> is also non-polar, which means that it has poor solvent power for polar solutes compared to other supercritical fluids, such as supercritical water [10], but it is excellent for use with non-polar solutes such as hydrocarbons. Polarity of SC-CO<sub>2</sub>

can also be enhanced with the addition of a co-solvent such as ethanol or water to increase SC-CO<sub>2</sub> solvent power towards slightly polar solutes.

#### *1.2.1.2.3. Properties impacting mass transfer*

SC-CO<sub>2</sub> offers improved mass transfer properties compared to liquid CO<sub>2</sub>. Indeed, SC-CO<sub>2</sub> has lower diffusion coefficient than liquid CO<sub>2</sub>. It also has a very low viscosity, which improves fluidity thereby improving mass transfer. Finally, SC-CO<sub>2</sub> decreases interfacial tension and this translates into the formation of smaller droplets thereby improving mass transfer.

#### *1.2.1.3. Brief history of SC-CO<sub>2</sub>*

The critical point of a substance was first reported by Cagniard de La Tour in 1822 [34] as he observed the disappearance of the gas-liquid meniscus of ether as it approached the critical pressure and temperature. He called this new state of matter “l'état particulier” (peculiar state of matter) and suggested that it be used as a reaction medium as he observed that near-critical water was capable of decomposing glass [34]; however, he did not study CO<sub>2</sub>. In 1869, Andrews [35] carefully studied the effect of pressure and temperature on CO<sub>2</sub> and coined the term “critical point” when referring to the point where CO<sub>2</sub> stands midway between the gas and liquid phases. Since then, van derWaals and Maxwell considerably enhanced our understanding of the behaviour of gases and their work is still at the core of our current understanding [33].



As the fundamental science improved, industrial applications soon followed. In 1931, Auerbach patented the use of subcritical liquid CO<sub>2</sub> for the extraction and fractionation of lipids [36]. Later, in 1940 Pilat and Godlewicz [37] patented a fractionation process using a mixture of propane or butane and CO<sub>2</sub>. This patent, which was assigned to Shell Development Company, claimed that it did not infringe on Auerbach's patent because no liquid CO<sub>2</sub> was used since at higher pressures the system was operated above the critical point of CO<sub>2</sub>. These initial patents were followed by a number of others, but it is the work of Zosel [38, 39] that attracted the industry's attention by showing that extraction with CO<sub>2</sub> offered benefits to the food industry. Indeed, this study led to industrial coffee decaffeination and hops extraction in Germany in the late 70s and early 80s.

One major breakthrough, which is often overlooked, is the development of the autoclave or high pressure "bomb" by Ipatieff [40] while doing his Doctorate in Chemistry on "catalytic reactions under high pressure and temperature" in the beginning of the 1900s. Throughout the years, a number of investigators studied reactions involving SC-CO<sub>2</sub> as a reactant. Briner [41, 42] explored the reactivity and decomposition of SC-CO<sub>2</sub>, Sargent [43] copolymerized supercritical C<sub>2</sub>H<sub>4</sub> and SC-CO<sub>2</sub> in the presence of benzoyl peroxide at 72-88 °C and 100 MPa, Buckley and Ray [44] formed polymeric ureas by treating carbamates with SC-CO<sub>2</sub> at 200 °C and 50 MPa and Stevens [45] formed polycarbonates by copolymerization of ethylene and SC-CO<sub>2</sub>. Aside from being used as a reactant, SC-CO<sub>2</sub> was also used as a reaction medium. For instance, Tacke et al. [46-48] conducted a high efficiency

and selective Pd catalyzed hydrogenation of edible oils and fatty acids in SC-CO<sub>2</sub> and reported higher catalyst productivity [49]. The use of SC-CO<sub>2</sub> media to conduct enzymatic reactions was initially reported in the mid-1980s by three different research groups [50-52]. Since then, much has been published on enzymatic reactions conducted in SC-CO<sub>2</sub> media. Indeed, within the last three years, these studies have been extensively reviewed [18, 53-56].

#### *1.2.1.4. Motivation for the use of SC-CO<sub>2</sub>*

The main motivation for using SC-CO<sub>2</sub> as a reaction medium is that it offers environmental, processing, chemical, health and safety benefits.

Numerous reports claim that SC-CO<sub>2</sub> is environmentally benign even though CO<sub>2</sub> is a known “green-house gas”. The fact is that CO<sub>2</sub> is abundant in nature and that using SC-CO<sub>2</sub> as reaction media would not increase CO<sub>2</sub> emissions but would rather offer a chance to use and recycle CO<sub>2</sub> recovered from, for instance, the ammonia production industry and or naturally occurring deposits [10]. In addition, the use of SC-CO<sub>2</sub> media would allow the replacement of some more hazardous organic solvents currently used. However, aside from these advantages, it is also important to consider the environmental impact, including energy consumption, of a process that would use SC-CO<sub>2</sub>. It is true that SC-CO<sub>2</sub> media as opposed to liquid organic solvents (such as hexane) is easily removed upon depressurization and does not require energy intensive operations such as evaporation and distillation. However, pressurization of CO<sub>2</sub> requires energy. For

this reason, combining unit operations requiring only one CO<sub>2</sub> compression stage, such as the use of continuous extraction, reaction and fractionation operations in SC-CO<sub>2</sub> media would be beneficial. Unfortunately, such systems are not yet in place due to limited fundamental research in this area.

The previously mentioned properties of SC-CO<sub>2</sub> media make it suitable for reactions conducted in continuous-flow processes capable of handling high throughput. The adjustable solvating power, low cost along with the absence of solvent residue in the final product also makes SC-CO<sub>2</sub> media attractive to the cosmetic, pharmaceutical, food and even the electronic manufacturing industries [10].

Some of the benefits offered by the use of SC-CO<sub>2</sub> in chemical reactions are higher diffusivity and greater miscibility with other gases thereby leading in some cases to higher reaction rates as well as better control over solvent power by varying the type and concentration of co-solvent [33].

Besides all these advantages, SC-CO<sub>2</sub> media offer health and safety benefits matched by only a few traditional liquid solvents. Indeed, this media is relatively inert, non-carcinogenic, non-mutagenic, non-flammable and thermodynamically stable.

#### *1.2.1.5. Application of SC-CO<sub>2</sub> media to lipid reactions*

In this thesis research, a number of reactions were conducted to transform canola oil, which is rich in oleic acid, into MAG or free fatty acids (FFA) in SC-

CO<sub>2</sub> media. For this reason, it seems fitting to review some of the physical properties of the compounds used. Table 1.1 provides an overview of some of the key properties and Figure 1.3 shows the chemical structures of the main compounds studied in this work.

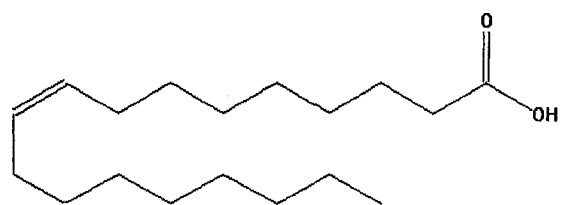
SC-CO<sub>2</sub> can be used as a solvent to either extract a valuable fraction or to remove undesirable fractions from a given material, as a reactant in a chemical reaction or as a reaction medium. Given that SC-CO<sub>2</sub> is a non-polar solvent, it is a well suited media for lipid reactions. However, when SC-CO<sub>2</sub> is added to a system,

**Table 1.1.** Physical properties of selected components important for the lipid reactions under study [57]

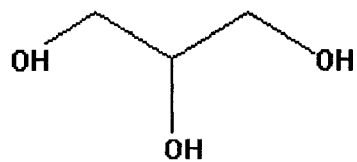
Solute	Properties					
	Formula	Molecular Weight (g/mol)	Melting point (°C)	Boiling point* (°C)	Density (g/cm <sup>3</sup> )	Solubility**
Oleic acid	C <sub>18</sub> H <sub>34</sub> O <sub>2</sub>	282.46	13.4	360 <sup>a</sup> , 286 <sup>b</sup>	0.8935 @ 20 °C	i H <sub>2</sub> O; msc. EtOH, eth, ace, bz, chl, etc.
Monoolein	C <sub>21</sub> H <sub>40</sub> O <sub>4</sub>	356.54	35	239 <sup>c</sup>	0.9420 @ 20 °C	i H <sub>2</sub> O; s EtOH, eth, chl
Diolein	C <sub>39</sub> H <sub>72</sub> O <sub>5</sub>	620.99	50.1	--	--	--
Triolein	C <sub>57</sub> H <sub>104</sub> O <sub>6</sub>	885.43	-4	237 <sup>d</sup>	0.915 @ 15 °C	i H <sub>2</sub> O; sl EtOH; vs eth; s chl, peth
Glycerol	C <sub>3</sub> H <sub>8</sub> O <sub>3</sub>	92.09	18.1	290 <sup>a</sup>	1.2613 @ 20 °C	Msc H <sub>2</sub> O, EtOH; sl eth; i bz, etc, chl
Water	H <sub>2</sub> O	18.015	0	99.974 <sup>a</sup>	0.9970 @ 25 °C	vs EtOH, MeOH, ace

\* Measured at the following pressures: 0.1<sup>a</sup>, 0.0133<sup>b</sup>, 0.0004<sup>c</sup>, and 0.002<sup>d</sup> MPa

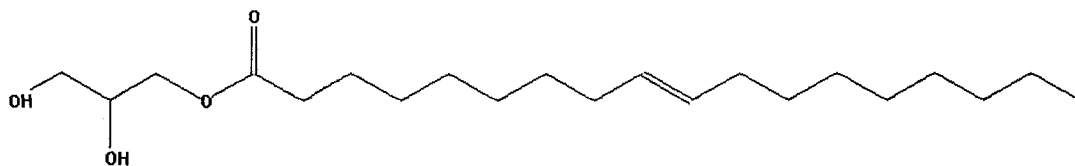
\*\* msc: miscible, sl: slightly soluble, s: soluble, vs: very soluble, i: insoluble, ace: acetone, bz: benzene, chl: chloroform, etc: carbon tetrachloride, EtOH: ethanol, eth: diethyl ether, peth: petroleum ether



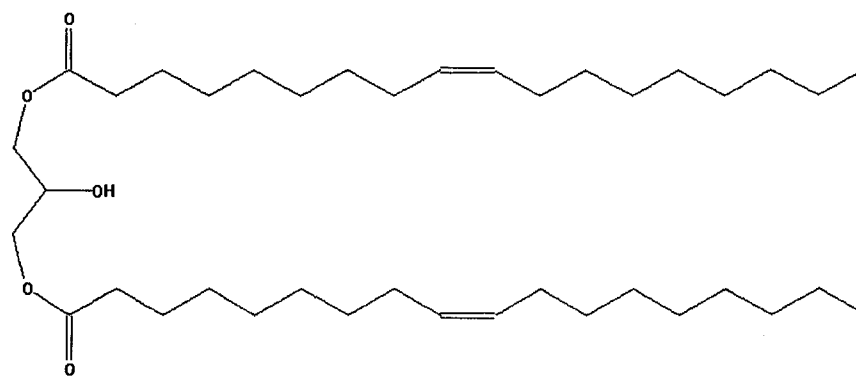
Oleic acid (*cis*-9-Octadecenoic acid)



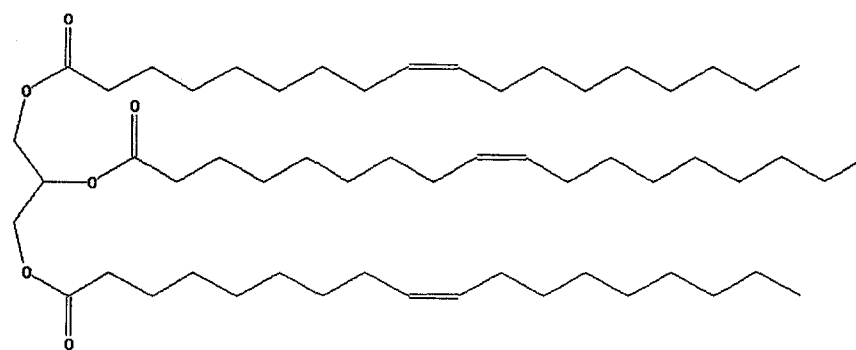
Glycerol (1,2,3-Propanetriol)



Monoolein (Glycerol 1-oleate)



Diolein (Glycerol 1,3-di-9-octadecenoate, *cis*, *cis*)



Triolein (Glycerol trioleate)

**Figure 1.3.** Structures of glycerol, oleic acid, monoolein, diolein and triolein [57].

the physical properties that were previously outlined for pure CO<sub>2</sub> are slightly affected. In addition, changes in phase behaviour should also be taken into account. Indeed, when SC-CO<sub>2</sub> and one or more components are mixed in a closed system at fixed temperature and pressure, two or more phases may coexist at equilibrium, especially if a reaction producing other chemical species occurs under the test conditions. A practical approach to identify the number of phases in such a mixture is to conduct the reaction in a phase equilibria cell equipped with a set of high pressure windows, sampling valves that allow the sampling of the different phases and an accurate piston-like system that allows to return the system to its original pressure after taking a sample without having to add more CO<sub>2</sub>. Unfortunately, such a system is often temperature and pressure limited. Another way to observe phase behaviour is to conduct the reaction in a beryllium cell, which is transparent to X-rays and use X-rays to observe the phase behaviour at high temperatures (up to 450 °C) and pressures up to 30 MPa [58]. Obviously, the more components involved in a given reaction, the more complex is the phase behaviour. Also, the addition of chemical species to a known system can greatly change the phase behaviour for the new system. For this reason, much research is needed in this field.

In addition to phase behaviour, another physical factor that must be taken into consideration when designing equipment and conducting reactions in SC-CO<sub>2</sub> is the fact that dry ice or solid CO<sub>2</sub> forms when liquid CO<sub>2</sub> or SC-CO<sub>2</sub> is quickly depressurized. This effect is known as the Joule-Thomson effect [59]. Due to this

effect, micro-metering needle valves or backpressure regulators used to control the SC-CO<sub>2</sub> flow rate in a typical supercritical system must be heated to prevent blockage caused by the accumulation of dry ice in the needle valve. In addition, SC-CO<sub>2</sub> equipment should be surrounded by polycarbonate shield to protect the operator from possible dry ice spray from a leaking connection.

### *1.2.2. Lipid reactions used to produce FFA*

#### *1.2.2.1. Interest in producing FFA*

FFA produced through fat hydrolysis are widely used as feed stock for other industrial processes. For instance, they are used to make soap, candles, emulsifiers, polymers, lubricants and when added to a nitrogen atom they find applications in even more different products such as food-packaging materials, water repellent textiles (Zelan or Velan type), mold-releasing agents, printing ink, and liquid detergents [60].

#### *1.2.2.2. Hydrolysis reaction*

Figure 1.4 shows some of the important lipid reactions and hydrolysis, Eq. (1.1), is one of them. The hydrolysis reaction accounts for the breakdown of TAG into FFA and glycerol in the presence of water. However, the stepwise nature of the hydrolysis reaction (Fig. 1.5) involves the production of MAG and DAG as intermediates and explains why they may still be present in the final product of partially hydrolyzed TAG. Hydrolysis is also referred to as “fat splitting” and it is

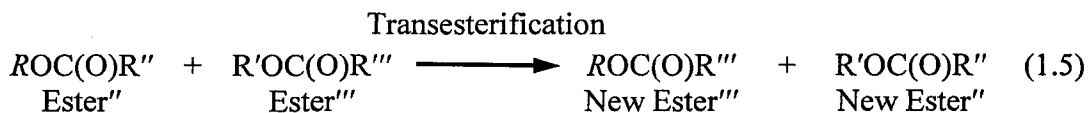
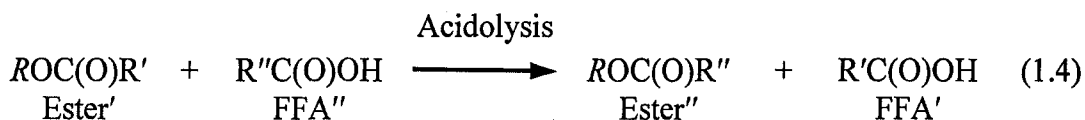
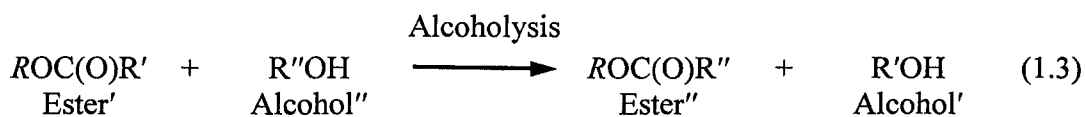
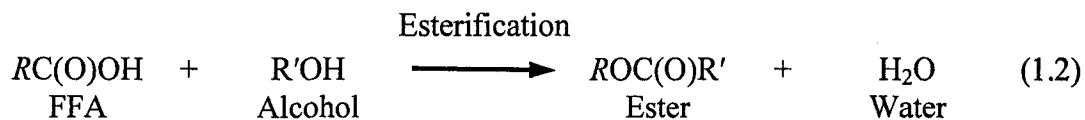
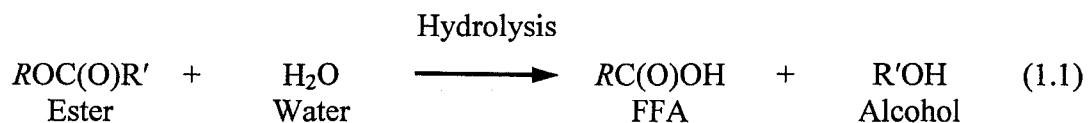


**Figure 1.4.** List of reactions involving esters [61] where the  $R$ ,  $R'$ ,  $R''$  and  $R'''$  represent different fatty acid chains and where FFA stands for free fatty acid.

conventionally conducted in three different ways: using pressurized steam, using lipase at ambient temperature and using an alkali [63]. The addition of alkali is generally referred to as saponification because it produces soaps that must be acidified to produce FFA. Such a saponification/acidification process is complicated by, among other things, the formation of a gel or an emulsion and the disposal of large quantities of salt water thereby making pressurized steam and lipase hydrolysis preferred approaches to saponification [64]. For this reason, this thesis will focus on pressurized steam and lipase hydrolysis.



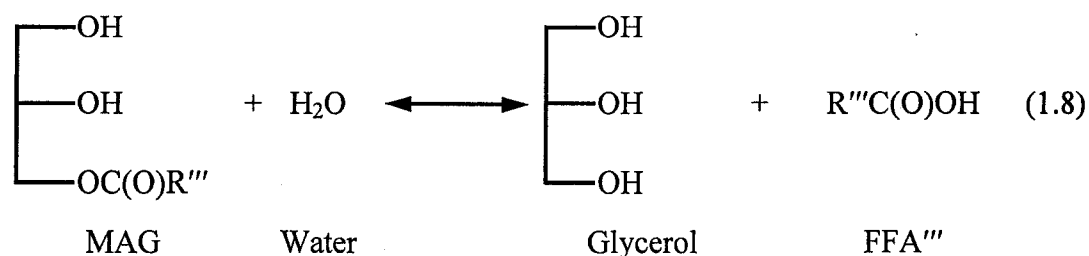
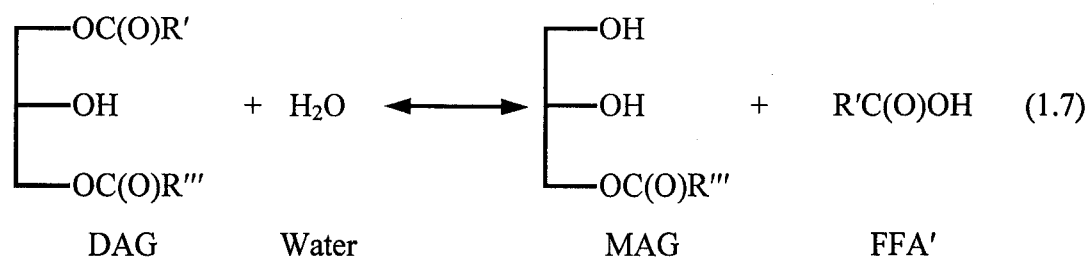
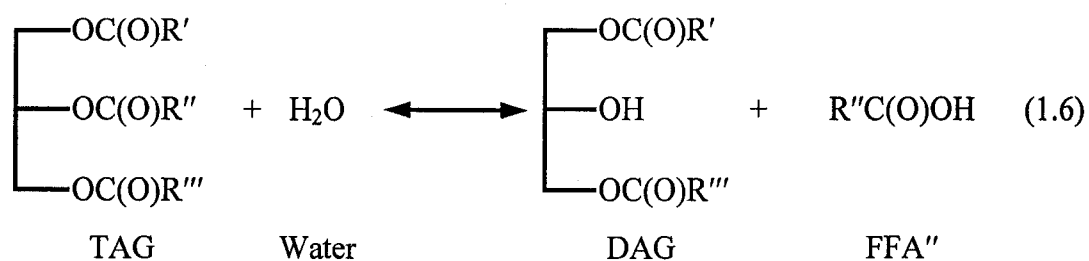


**Figure 1.5.** Reactions describing the reversible step-wise hydrolysis of TAG [62] where R', R'' and R''' represent different side chains and where MAG, DAG, TAG and FFA stands for monoacylglycerol, diacylglycerol, triacylglycerol and free fatty acid, respectively.

#### 1.2.2.2.1. Brief history of hydrolysis

Hydrolysis of oil was conducted as early as 1770 when Scheele produced glycerine by heating olive oil and litharge [4]. He later observed that glycerine could also be produced from other vegetable oils and animal fats thereby calling it

“the sweet principle of fats” because of the sweet taste of glycerine [65]. However, it was not until the beginning of the 1800s that Gay-Lussac and Chevreul first reported the hydrolysis (saponification) process [66]. Chevreul used hydrolysis to isolate many fatty acids. He was the first to isolate butyric acid and he patented a process to make cleaner and less smelly candles from stearic acid [66]. Later, in 1860, Tilghman [67] patented a hydrolysis process where countercurrent fat and water flow through an autoclave along with high pressure steam; however, the process received little attention. In 1902, Connstein et al. [68] first observed the hydrolysis of castor oil at room temperature using castor bean lipase and the process has been used commercially on a small scale ever since [69]. Twitchell patented in 1898 [70] the use of oleosulfonic acid (oleic acid + sulphuric acid) along with sulphuric acid to hydrolyze fat with steam at atmospheric pressure. In the 1930s, the Colgate-Emery continuous hydrolysis process operating at 260 °C and 4.8-5.2 MPa was patented [71, 72]. In 1939, Eisenlohr patented [73] a hydrolysis process that offered some advantages over the Colgate-Emery process using 260-320 °C and 24 MPa.

#### *1.2.2.2.2. Conventional hydrolysis*

From a chemical point of view the challenge in conducting hydrolysis is that the reactants are completely incompatible with each other. Indeed, on one side there is water, which is hydrophilic and on the other there is TAG, which is hydrophobic. Furthermore, solubility data for TAG in water and water in TAG at high

temperatures are not available partly because at higher temperatures hydrolysis of TAG occurs. For this reason, investigators focused on the solubility of fatty acids in water [74, 75] and water in fatty acids [76], which is similar but not identical to that of TAG in water and water in TAG [69]. It was found that the solubility of water in FFA is greater than the solubility of FFA in water [74-76]. Assuming that the same holds true for TAG and that reactants form two phases at operating conditions, then the reaction would take place in the oil phase for Lascaray [77] already confirmed that the hydrolysis reaction did not take place at the interface of TAG and water. Solubility of water in TAG might also be dependent on the fatty acid composition of TAG. In fact, it is known that the solubility of water in fatty acids increases when shorter fatty acids are used [76]. Other ways of increasing TAG and water solubility are to increase the reaction temperature or add an emulsifier. Another viable technique is to recycle a portion of the product back into the next batch because the products of hydrolysis, namely MAG, DAG and FFA, are more hydrophilic than TAG and could therefore decrease the initial induction period.

Increasing the solubility of the hydrolysis reactants is fundamental to increasing the rate of hydrolysis. Although it was originally thought that mineral acids, some bases and metal oxides could be used to catalyze the reaction, it is now suspected that these are only acting directly or indirectly to form emulsifiers, which improve the miscibility of water in TAG [69]. This would explain why such

“catalysts” are not required for the Colgate-Emery continuous hydrolysis process and Eisenlohr’s process since the conditions employed increase reactants solubility.

A number of kinetic studies were conducted on the hydrolysis reaction [62, 78-80]. Hartman [79] determined that the Twitchell process was of first order throughout and assumed that the reaction takes place in the oil phase; thereby supporting Lascaray’s view. Later, Patil et al. [62] developed a model for the thermal hydrolysis of oil at 180-280 °C. The model contained four equilibrium parameters and one rate parameter and assumed that hydrolysis occurs in the oil phase, that the first step (breakdown of TAG into DAG) was rate limiting and that the mass transfer of glycerol and water across the phases is faster than the reaction [62]. The model was said to give an excellent description of the current and previously published hydrolysis data [62]. More recently, Minami and Saka [80] suggested that hydrolysis is a second-order reaction and established a mechanism for the autocatalytic hydrolysis of oil. Although their approach provides a more detailed mechanistic approach than that of Patil et al. [62], it does stipulate that since fatty acids are acting as an acid catalyst, their concentration should be multiplied by all the terms in the differential rate equation for TAG, DAG and MAG to account for their autocatalytic mechanism. Minami and Saka [80] also assumed that the rate constant for TAG was equal to those of DAG and MAG without providing any reasoning for this approach apart from the fact that their study was focused on the effect of FFA on the autocatalytic reaction. Such an

approach seemed to adequately model FFA but no mention was made of its ability to model TAG, DAG, and MAG.

#### *1.2.2.2.3. Hydrolysis in supercritical and subcritical media*

Even though the popular Colgate-Emery continuous hydrolysis process is capable of achieving 97% conversion of TAG into FFA, when unsaturated oils are processed products are dark coloured and require distillation [63]. For this reason, some investigations have recently been aimed at conducting hydrolysis in either subcritical water or SC-CO<sub>2</sub>. For instance, King et al. [81] conducted hydrolysis reactions in subcritical water at 270-340 °C, 13 MPa and high water to oil ratios and reported improved conversion times and yields compared to those currently obtained in the fat splitting industry. However, at such high temperatures, FFA isomerization from *cis* to *trans* occurred [81, 82]. Pinto and Lanças [83] also investigated the effect of subcritical water by conducting 40 min hydrolysis reactions of corn oil using a molar ratio of 1:355 oil to water and reported, based on gas chromatography analysis, no conversion at 150 and 200 °C, but 80% conversion at 250 °C and 100% conversion at 280 °C.

Few studies are available on the non-enzymatic hydrolysis of oil in SC-CO<sub>2</sub> media. One of those rare studies is by Fujita and Himi [84] where hydrolysis of triolein was conducted in SC-CO<sub>2</sub> media. The investigators report that, based on a thin-layer chromatography analysis, the hydrolysis efficiency was almost 100% at 8 MPa and 250 °C, and less than half of that at 200 °C while no hydrolysis occurred

at 100 °C. One of the advantages of conducting hydrolysis in SC-CO<sub>2</sub> was that the hydrolysis vessel could also serve as an extraction vessel for FFA by simply decreasing the temperature from 250 °C to 80 °C and increasing the pressure from 8 MPa to 20 MPa [84]. In addition, no degradation of oleic acid could be detected using liquid chromatography [84].

Upon reviewing the available literature for kinetic studies on non-enzymatic hydrolysis of oil in SC-CO<sub>2</sub>, no studies were found.

#### *1.2.2.2.4. Enzymatic hydrolysis*

Lipase catalyzed hydrolysis is an alternative method to obtain FFA. It is especially useful when working with thermally and oxidatively unstable oils such as fish oils because it can be conducted at lower temperatures. Furthermore, the fact that lipases are more selective than inorganic catalysts results in fewer side reactions thereby delivering a cleaner product [85] while providing the opportunity to produce a wide variety of products with different composition and properties [63].

Due to the considerable amount of research activity in this field, lipase hydrolysis has become more cost effective. For instance, to decrease the amount of enzyme required for a given reaction, lipase has been immobilized on a support material, which not only simplifies enzyme separation from the product but also retains the amount of water necessary for the proper activation of the enzyme when it is placed in contact with fresh reactants [63, 86]. Unfortunately, not all support

materials are food grade, but a few are and more are expected to reach the market as the demand for them increases. In addition, it is believed that with the recent progress in genetic engineering and modern processing technologies more efficient and less costly biocatalysts will be available [87].

Lipases are biocatalysts taken from different organisms and therefore have inherent requirements. They generally operate best at body temperature and at atmospheric pressure, although some lipases isolated from organisms living at the bottom of the ocean function best at higher pressures. Besides having optimal temperature and pressure requirements, lipases operate best in certain reaction vessels and within given water content, agitation level and solvent media.

Enzymes are generally denatured at room temperature by copper, iron and nickel ions [88]. For this reason, enzymatic hydrolysis is generally conducted in stainless steel or glass-lined equipment.

The innate function of a lipase is to catalyze the hydrolysis of TAG. However, when a sufficient quantity of water is not present some lipases will catalyze the reverse reaction and start forming TAG from FFA [89]. For this reason, establishing optimal water content is an important consideration.

Another important factor is that lipases are activated by the oil-water interface, a characteristic that distinguishes them from esterases [90]. Hence, lipase hydrolysis of TAG must occur in a heterogeneous system. Therefore, higher reaction rates are achieved when the substrate is finely dispersed or adequately mixed in the aqueous phase.

For any enzyme to maintain its native state, it must be surrounded by a minimum of a single layer of water molecules [91]. Thus, enzymatic reactions must be conducted in a hydrophobic solvent because a hydrophilic solvent would strip the essential water layer around the enzyme thereby inactivating it. In addition, lipases are believed to be “trapped” in their active conformation when present in a hydrophobic solvent because not enough water is available to lubricate them and give them conformational flexibility [92].

#### *1.2.2.2.5. Enzymatic hydrolysis in SC-CO<sub>2</sub> media*

One possible hydrophobic solvent for enzymatic reactions is SC-CO<sub>2</sub>, which allows high mass transfer rate, control over the reaction conditions and easy separation of the reaction products. Initial rate of hydrolysis was reported to be greater in SC-CO<sub>2</sub> compared to that in hexane when the water content was increased [93]. However, the use of SC-CO<sub>2</sub> media may have some disadvantages. For instance, Hobbs and Thomas [18] recently reported that there was a lack of consistency in the literature regarding enzyme activity in SC-CO<sub>2</sub>, which complicated the optimization of such new biocatalytic systems. In addition, it was claimed that CO<sub>2</sub> reacts with lysine residues on the surface of the enzymes, but while some reports claim this to be an advantage [94-96], others claim that it causes enzyme inactivation [97-99]. Moreover, it is thought that CO<sub>2</sub> reacts with water to form carbonic acid, which decreases the pH level and may inhibit enzyme activity



depending on the conditions used [100, 101]. However, if this is the case, addition of a buffer, such as sodium bicarbonate, could alleviate this problem [102].

A number of lipase hydrolysis studies were conducted in SC-CO<sub>2</sub> [24, 25, 103-117] and most of the work focused on three enzymes: Lipozyme IM from *Mucor miehei* [24, 25, 103, 105, 108, 116], Novozyme 435 from *Candida antarctica* [103, 104, 107], and lipase from *Candida rugosa* [106, 107, 111, 115, 117]. These enzymes appeared to be quite active in SC-CO<sub>2</sub>. In fact, it was reported that the lipase from *Candida rugosa* previously treated with SC-CO<sub>2</sub> had 2.5 times more activity than an untreated lipase [106]. This gain in activity was attributed to a size reduction of particles and the purification of the enzyme that occurred during the SC-CO<sub>2</sub> treatment [106]. Although SC-CO<sub>2</sub> might initially boost the activity of an enzyme, a lipase has a lifespan and will eventually lose its catalytic effect. Rezaei and Temelli [24] who investigated hydrolysis of canola oil in SC-CO<sub>2</sub> at 38 MPa and 55 °C reported a drop in conversion rate over a 24 h period. This drop in lipase activity over time was also recently confirmed by Oliveira et al. [118].

Rezaei and Temelli [24] were among the first to report the continuous enzymatic hydrolysis of oil in SC-CO<sub>2</sub>. They found that by pumping oil and water through a packed bed of Lipozyme from *Mucor miehei*, a 63-67% TAG conversion could be achieved at 24-38 MPa, 35-55 °C and 3.7 L/min CO<sub>2</sub> flow rate after 4 h of reaction [24]. The investigators also predicted that complete hydrolysis of oil could be achieved using lower CO<sub>2</sub> flow rates, higher enzyme loads and/or a lower oil

flow rate [24]. Since then a few studies using lipases from *Aspergillus niger* [112] and *Candida rugosa* [115] have reported optimization of enzymatic hydrolysis in a batch reactor but to our knowledge none have attempted to optimize the continuous enzymatic hydrolysis of oil.

### *1.2.3. Lipid reactions used to produce MAG*

Figure 1.4 showed some of the common lipid reactions used to produce MAG. In this thesis research, the emphasis was mainly on alcoholysis and esterification using glycerol. When an alcoholysis reaction is conducted using glycerol, the reaction is commonly referred to as glycerolysis. In some cases, glycerolysis is used to refer to all ester-glycerol reactions; however, in this work it is used to describe the reaction of TAG or diacylglycerol (DAG) rich oil/fat with glycerol. For this reason, the reaction of methyl esters with glycerol is not considered and reactions between FFA and glycerol are referred to as esterification.

#### *1.2.3.1. Interest in producing MAG*

The demand for MAG is high; in the year 2000, it was estimated to be approximately 200,000 metric tons [119]. Such a high demand should not come as a surprise since 75% of the world production of food emulsifiers comes from MAG and their derivatives [120]. Indeed, MAG are used in many food applications. According to Birnbaum [121], MAG's first commercial application was in margarine and puff pastry shortening. Today, they are found in a wide variety of food products including, among many others, cakes, pastries, coffee whiteners, egg

substitutes, spreads, pudding, ice cream, peanut butter, whipping cream and even wiener wrap [121]. In food products, MAG does not only act as an emulsifier but can also enhance starch complexation, protein interaction, crystal modification, aeration and foam stabilisation [121]. The fact that they are non-ionic and quite robust in acidic and basic conditions also contributes to their popularity in the food industry [122]. MAG also has intriguing characteristics: they can form various self-assembly structures when hydrated to different extents. Such technology depends on a thorough understanding of their phase behaviour at different hydration levels but current research in this field has shown that MAG can be used as delivery vehicles to improve taste, aroma, health benefits and structure of food without necessarily adding new ingredients since, in most cases, MAG are already present [123]. Apart from their use in food products, MAG are also used as the starting material for alkyd resins [124-126], detergents, protective coating materials and many other industrially important compounds [64]. Their use has also been extended to the pharmaceutical industries where they are often used in beauty and health products.

#### *1.2.3.2. Esterification reaction*

Generally speaking, an esterification reaction occurs when a FFA is combined with glycerol or another alcohol to produce an ester and water. However, given the focus of this thesis, the reaction between free fatty acids and glycerol will

be referred to as esterification only. The complete steps for the esterification are given in Figure 1.6.

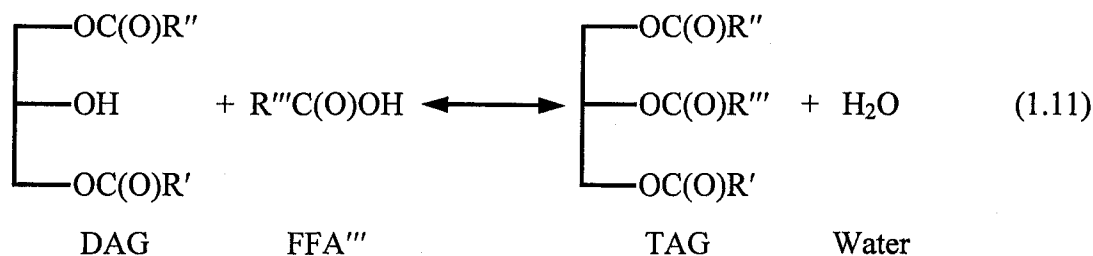
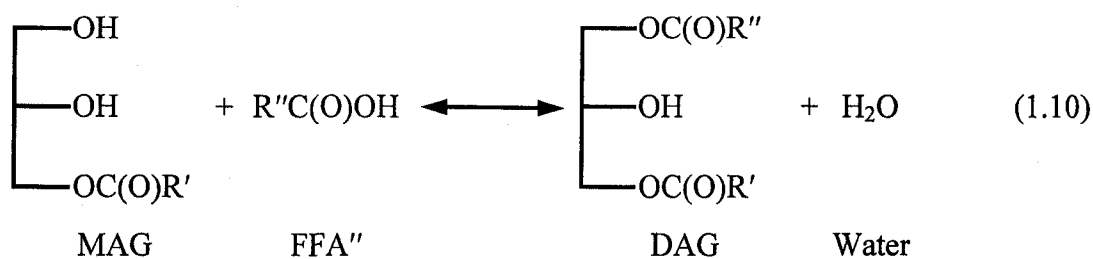
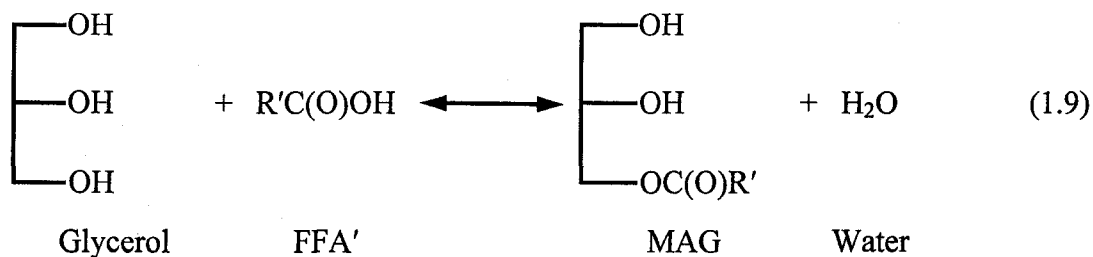


**Figure 1.6.** Reactions describing the reversible step-wise esterification of free fatty acids (FFA) into triacylglycerol (TAG) [127] where R', R'' and R''' represent different side chains and where MAG and DAG stand for monoacylglycerol and diacylglycerol, respectively.

#### *1.2.3.2.1. Brief history of esterification*

The first recorded use of the esterification reaction to produce a synthetic fat was by Pelouze and Gelis in 1844 [128] who, following the work initiated by Chevreul in 1814, reported the formation of a yellowish oil when a mixture of butyric acid, glycerol and sulphuric acid was slightly heated. This initial work was continued by Berthelot who reported in 1853 that 18 carbon fatty acids could also react with glycerol at higher temperatures [129]. Since then, considerable amount of work was performed on the esterification reaction. Older reviews [130, 131] provide an interesting perspective of the ideas and issues considered at that time but more recent reviews are also available [64, 132, 133]. Although these reports are quite elaborate, it appears fitting to illustrate how esterification is typically carried out.

#### *1.2.3.2.2. Conventional esterification*

When conducting esterification of long chain fatty acids and glycerol, temperatures between 175 and 250 °C are applied. Such temperatures provide the required high activation energy [134] while increasing the miscibility of glycerol in FFA, which is key for increasing MAG formation [134, 135] if esterification is not conducted in an organic solvent such as phenol [135] or pyridine [136] in which both glycerol and FFA are soluble. Apart from the reaction temperature, the rate of MAG formation depends on the proportion of the reactants and rate of mechanical mixing.

Given that esterification of glycerol is the reverse of fat hydrolysis, it has been postulated that, in order for the esterification reaction to proceed to completion, the water formed by the association of the hydroxyl group of the FFA and the hydrogen of the alcohol [137, 138] has to be removed either by flowing a stream of inert gas (such as nitrogen or CO<sub>2</sub>) or by maintaining a vacuum on the reactants [132, 139]. Interestingly, Garner [140] reported that better coloured products were achieved using a stream of CO<sub>2</sub> compared to those obtained using nitrogen or reduced pressure. Nevertheless, Hartman [141] obtained a conversion rate similar to that of Feuge et al. [139] while conducting the esterification reaction without the removal of the water formed during the reaction. Indeed, after having reacted equivalent proportions of mixed fatty acids and glycerol over 5 h at 180 °C, Hartman [141] reported 65.5 to 77.4% esterified fatty acids, which was very close to the 75.5% obtained by Feuge et al. [139] while reacting peanut oil fatty acids at 178 °C. This is an interesting observation that questions the need for water removal during the esterification reaction.

Another method used to increase the rate of MAG formation is to lower the activation energy using a catalyst. In the past, acid catalysts were used [131, 142]; however, more sophisticated catalysts such as hypophosphoric acid, dibutyl tin oxide, titanium dichloride diacetate, and zinc dust are now suggested [64]. Nevertheless, the use of a catalyst often complicates the process because in some cases they cause the formation of undesirable colours and products (such as acrolein [132]), which has to be removed by bleaching or refining [64]. Furthermore, some

catalysts are inactivated by high temperature or by impurities in reactants [132]. In addition, catalyst removal at the end of the reaction leads to yield loss [64]. For all of the above reasons, non-catalyzed esterification is often preferred [64].

A number of investigators studied the kinetics of the esterification of FFA with glycerol [127, 136, 139, 141, 143-147]. Hartman [141] studied the kinetics of the non-catalyzed esterification of various FFA with glycerol and found, as did Feuge et al. [139], that the reaction was of second order. Hartman [141] conducted the esterification reaction using eight different FFA with completely different miscibilities in glycerol and observed no differences in esterification rate. He explained this finding by the fact that the MAG formed during the reaction increased the solubility of glycerol and FFA. Since then, depending on the reaction parameters and the presence or absence of a catalyst, second or third order kinetic models have been proposed for this reaction [136, 139, 143-146]. However, recent studies using sodium, potassium and zinc carboxylates as a catalyst, reported that the reaction in question was a consecutive first order reaction in nitrogen where MAG was an intermediate product [127, 147].

#### *1.2.3.2.3. Esterification in SC-CO<sub>2</sub> media*

With the current advances in supercritical fluid technology, an alternative would be to conduct uncatalyzed, non-enzymatic esterification in SC-CO<sub>2</sub> media. SC-CO<sub>2</sub> is an excellent reaction medium mainly because, apart from offering tunable solvent properties, oxygen free atmosphere and no residual solvent in the

product, it simplifies FFA separation from the product mixture, which is a major challenge with conventional processing methods. However, the literature lacks studies on non-enzymatic esterification in SC-CO<sub>2</sub>.

#### *1.2.3.2.4. Enzymatic esterification in SC-CO<sub>2</sub>*

In the presence of low water, high FFA and high glycerol concentrations, most lipases will catalyze FFA esterification. This reaction has been studied in SC-CO<sub>2</sub> media to take advantage of all the previously mentioned positive attributes of this media. A number of investigators chose to limit their studies to the esterification of oleic acid with an alcohol in SC-CO<sub>2</sub> media and reported encouraging results [21, 100, 148-158]. Among these, Laudani et al.'s [157, 158] recent reports demonstrate the potential bright future of enzymatic esterification in SC-CO<sub>2</sub>.

#### *1.2.3.3. Glycerolysis reaction*

Production of MAG by glycerolysis, as seen in Figure 1.7, requires TAG rich oil or fat and glycerol. As seen in Table 1.2, TAG reactants are not in short supply since a wide variety of vegetable/fish oil or animal fats can be used to produce MAG. As previously mentioned, glycerol is the by-product of the hydrolysis and biodiesel industries. Considering the current popularity of biodiesel, it is safe to assume that there will be no shortage of glycerol either. In fact, in an



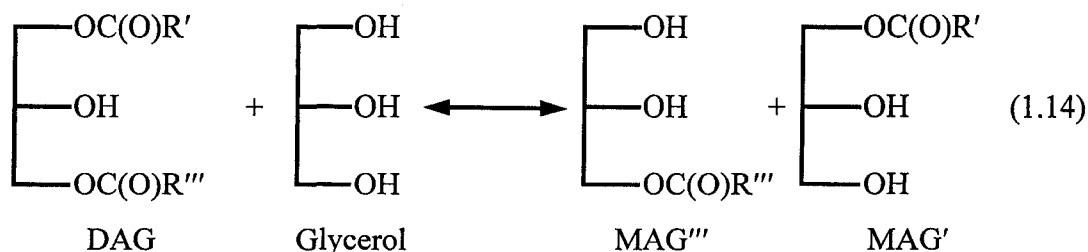
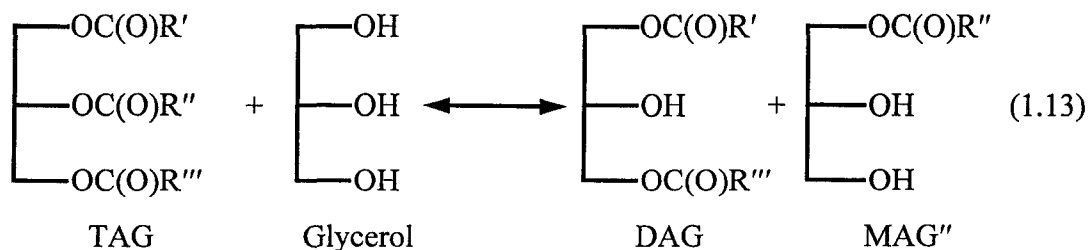
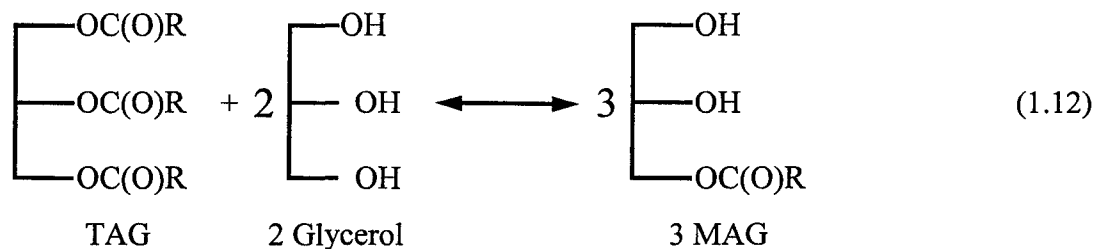


**Figure 1.7.** Equation (1.12) describes the overall simplified glycerolysis reaction while Equations (1.13) and (1.14) provide the reversible stepwise glycerolysis of triacylglycerol (TAG) into monoacylglycerol (MAG) [159, 160] where R', R'' and R''' represent different side chains and where DAG stands for diacylglycerol and FFA for free fatty acids.

attempt to offset the cost of biodiesel, some investigators such as Muniyappa et al. [161] have been considering glycerolysis as a means to convert glycerol to higher value products such as MAG.

**Table 1.2.** Summary of glycerolysis reactions conducted by various investigators: reactants, catalyst, processing parameters and yields.

Reactants		Catalyst		Processing Conditions					Yield*		Ref.
TAG source	Oil to Glycerol molar ratio	Compound	Amount (wt%)	T (°C)	P (kPa)	Time (h)	Solvent Media / Gas used	Mixing Rate	MAG Yield (%)	Detection Method <sup>s</sup>	
Butterfat	1:1.5	NaOH	0.1	200	NS	2	N <sub>2</sub>	NS	51	TLC-GC	[162]
Butteroil	1:4.6	NaOH	0.1	200	NS	2	N <sub>2</sub>	NS	55	SEC-GC	[163]
Castor oil	1:8	None	n/a	240-249	4826-5171	2	SC-CO <sub>2</sub>	NS	91	NS	[19]
Castor oil	1:8	None	n/a	240-250	700-1034	2	SC-CO <sub>2</sub>	NS	83	NS	[19]
Castor oil	1:8	None	n/a	240-250	700-1034	2	N <sub>2</sub>	NS	73	NS	[19]
Castor oil	1:3	LiOH	0.04	240	~101	1.5	N <sub>2</sub>	Moderate	46*	NS	[125]
Castor oil	1:3	LiOH	0.1	240-280	~101	0.5	N <sub>2</sub>	Moderate	48*	NS	[125]
Castor oil	1:3	KOH	0.1	240	~101	0.5	N <sub>2</sub>	Moderate	46*	NS	[125]
Coconut oil	1:2	NaOH	0.08	180	Suction	6	N <sub>2</sub>	High speed	44-45*	[164]	[165]
Coconut oil	1:17	None	n/a	240-250	700-1034	2	SC-CO <sub>2</sub>	NS	75	NS	[19]
Coconut oil	1:17	None	n/a	240-250	700-1034	2	N <sub>2</sub>	NS	65	NS	[19]
Cottonseed oil	1:14	NaOH	~0.4	250	NS	NS	NS	Continuous counter-current column	70	NS	[166]

Table 1.2. (continued)

Reactants		Catalyst		Processing Conditions					Yield*		Ref.
TAG source	Oil to Glycerol molar ratio	Compound	Amount (wt%)	T (°C)	P (kPa)	Time (h)	Solvent Media / Gas used	Mixing Rate	MAG Yield (%)	Detection Method <sup>s</sup>	
Cottonseed oil	1:1.1	Na <sub>2</sub> CO <sub>3</sub>	0.1	190	NS	1	NS	NS	7*	[167]	[168]
Fish oil (Herring, Menhaden, Salmon, Sardine, Tuna oil)	1:4	KOH	0.1	220	NS	0.75 - 1	N <sub>2</sub>	Vigorous stirring	54-58*	[169]	[170]
Fish oil (Sardine oil)	1:2	NaOH	0.08	180	Suction	6	N <sub>2</sub>	High speed	44-45*	[164]	[165]
Groundnut oil	1:1.1	Na <sub>2</sub> CO <sub>4</sub>	0.1	190	NS	1	NS	NS	25*	[167]	[168]
Lard	1:1.5	CH <sub>3</sub> ONa	1	70	NS	16	Pyridine	NS	77*	[169]	[171]
Lard	1:5	NaOH + Previous batch <sup>50%MAG</sup>	0.3 <sup>NaOH</sup> 10 <sup>50%MAG</sup>	264	NS	0.5	NS	NS	50*	NS	[172]
Linseed oil	1:2	NaOH	0.08	180	Suction	6	N <sub>2</sub>	High speed	44-45*	[164]	[165]
Linseed oil	1:2.5	CaO	0.02	220-250	NS	NS	NS	NS	39-53	NS	[124]
Linseed oil	1:2.4	NaOH	0.18	225	NS	>1.3	N <sub>2</sub>	NS	35	NS	[173]
Linseed oil	1:2.4	NaOC <sub>3</sub> H <sub>5</sub> (OH) <sub>2</sub>	0.11	200	NS	>1.3	N <sub>2</sub>	NS	25	NS	[173]
Oleo oil	1:7	CH <sub>3</sub> ONa	0.6	100	NS	4	Pyridine	NS	76*	[169]	[171]

Table 1.2. (continued)

Reactants		Catalyst		Processing Conditions					Yield*		Ref.
TAG source	Oil to Glycerol molar ratio	Compound	Amount (wt%)	T (°C)	P (kPa)	Time (h)	Solvent Media / Gas used	Mixing Rate	MAG Yield (%)	Detection Method <sup>§</sup>	
Peanut, Sesame oil	1:2	NaOH	0.08	180	Suction	6	N <sub>2</sub>	High speed	44-45*	[164]	[165]
Soybean (hard fat)	1:5 - 1:39	CH <sub>3</sub> ONa	0.3 - 2	30 - 130	NS	0.08 - 96	Pyridine	NS	33 - 78*	[169]	[171]
Soybean oil	1:25	none	n/a	250	20700	4	SC-CO <sub>2</sub>	1040 rpm	49	SFC	[20]
Soybean oil	1:2.5	NaOH	0.18	245	Vacuum, 80	0.7	N <sub>2</sub>	800 rpm	54	HPLC	[160]
Soybean oil	1:2.5	NaOH	0.18	230	NS	0.4	None	3600 rpm	56	HPLC	[29]
Tallow	1:3200	NaOH	0.0001	280	NS	0.17	N <sub>2</sub>	NS	90% after distillation	NS	[174]
Triolein	1:12	Sepiolite-Cs	4	240	NS	5	N <sub>2</sub>	400 rpm	34	GC	[175]
Triolein	1:12	Hydrotalcite	4	240	NS	5	N <sub>2</sub>	400 rpm	72	GC	[175]
Triolein	1:12	MgO	4	240	NS	5	N <sub>2</sub>	400 rpm	73	GC	[175]
Tristearin	2.5:1	Alkyl-guanidines	10 mol%	110	1.6	8	None	Vigorous stirring	40	TLC-NMR	[176]

\* MAG: monoacylglycerol; when an asterix appears after a yield, it means that only alpha monoacylglycerol was considered.

§ SFC: supercritical fluid chromatography, SEC: size exclusion chromatography, HPLC: high performance chromatography, TLC: thin layer chromatography, GC: gas chromatography, NMR: <sup>1</sup>H nuclear magnetic resonance, NS: not-specified

It is not uncommon to find, still today, the glycerolysis reaction defined using Eq. (1.12) in Figure 1.7. Unfortunately, this equation over simplifies this complex and difficult to manage reaction that is glycerolysis and provides a mere overview of the overall reaction. Indeed, this model does not account for the formation of 2-monoglycerides (previously referred to as beta-monoglycerides) along with the 1-monoglycerides and it does not consider the production of DAG, which is always present as an intermediate product [159]. For this reason, glycerolysis should be described by the stepwise reversible reactions defined by Eqs. (1.13) and (1.14) in Figure 1.7. The last step of this series of equations includes the transesterification of TAG with MAG to form DAG, which occurs in parallel with the other glycerolysis reactions.

#### *1.2.3.3.1. Brief history of glycerolysis*

Glycerolysis was developed more recently than either hydrolysis or esterification. One early mention of glycerolysis was in Grun's 1924 American patent where, in the initial step of production of a synthetic butter, he described what is now known as catalyzed glycerolysis [177]. This initial patent was followed by the famous 1940 Procter and Gamble Co. [178, 179] and 1945 Colgate-Palmolive-Peet Co. [180] patents. Following these initial patents, a considerable number of articles appeared in the scientific literature and Sonntag [159] thoroughly reviewed them while clarifying some half-truths. For instance, it was initially believed that FA from TAG were randomly distributed among the available

hydroxyl groups [139, 165]; however, although this is a good approximation, it is now known to be false due to the differences in relative chemical reactivity of glycerol's first and second hydroxyl groups [159]. It was also initially reported that the composition of the end product depended on the amount of glycerol, which was miscible in the oil phase [165], but such an assumption did not take into account the increase in glycerol-oil miscibility due to the accumulation of MAG and DAG throughout the reaction [132]. Besides, when glycerolysis is conducted for an extensive period of time, equilibrium between DAG, MAG, TAG and glycerol is eventually reached. The product of glycerolysis therefore consists of a mixture from which MAG must be extracted. Generally, such separation is achieved by decanting or centrifuging glycerol out of the oil and then recovering MAG either by washing with an aqueous solution or inorganic salts (5% sodium sulphate), using vacuum distillation or vacuum-steam distillation [174].

#### *1.2.3.3.2. Conventional glycerolysis*

Over the years, a number of studies (Table 1.2) have been aimed at understanding the effects of TAG/glycerol initial ratio, temperature, mixing rate, chemical catalyst, solvent, enzymatic catalyst and addition of emulsifiers on the level of MAG production and such studies have considerably enhanced our understanding of glycerolysis. The following is an attempt at summarizing some of these findings.

The use of excess glycerol over the 2 moles stoichiometric requirement is a well accepted method of increasing the yield of MAG by displacing the equilibrium of all the reactions described in Figure 1.7 towards the formation of MAG [29, 132]. This fact has been known since 1945 when it was initially reported that satisfactory results can be obtained using 3 to 10 times the stoichiometric amount of MAG required but that 10 moles of glycerol to one of TAG gives the highest MAG yield [180]. One drawback, as pointed out by Birnbaum [172], is that the use of a high ratio of glycerol to fat is costly to separate from the final product. However, judging from his patent, the only solution found by Birnbaum was to reduce the initial molar concentration of glycerol from 10 to 5 moles of glycerol for one mole of TAG and add 10 wt% of the previously obtained batch containing 50% MAG [172].

Temperature was identified as a major parameter early on. Indeed, Edeler and Richardson [178] reported in the 1930s that glycerol did react with fats at temperatures  $>200$  °C to form DAG and probably some MAG. However, it was later concluded that the solubility of oil in glycerol was temperature dependent [165, 181]. Indeed, it is now known that the solubility of glycerol in TAG is less than 5 wt% at room temperature but that it increases to approximately 45-55 wt% at 250 °C [29]. For this reason, temperatures of 175-250 °C are required to aid in the mass transfer of TAG to the glycerol phase as well as to increase the mutual solubility of TAG and glycerol phases [161]. Higher temperatures were also

considered but due to the decomposition of some fatty acids, especially those with double bonds, temperatures  $>250\text{ }^{\circ}\text{C}$  are not recommended [161].

Due to the limited miscibility between glycerol and TAG at the MAG formation temperatures, mixing is usually required to increase the interfacial area and the mass transfer between the phases [29], especially at the initial stages of the reaction where an increase in mixing intensity is reported to decrease the initial lag time [28]. Nevertheless, the use of a higher mixing rate, 3600 vs 360 rpm, which was recently investigated in a continuous glycerolysis process [29], revealed only a small increase in MAG production as MAG approached equilibrium. However, results obtained at lower mixing levels showed the diffusion limitations, which affects the interfacial transport between the glycerol and oil phases [29], thereby indicating that the reaction rate is mass transfer limited [182]. Negi et al. [182], who studied the reaction of fatty acid methyl esters with glycerol, hypothesized that when a high mixing rate is applied glycerol forms finely dispersed droplets in the oil phase and, since the total film volume around these droplets is higher than the volume of the continuous phase, the reaction occurs at the interface of these thin films. Such hypothesis, although plausible, remains to be proven and only reinforces the fact that knowledge of mass transfer in these complex reaction systems is still far from complete.

In an attempt to maximize MAG yields, a number of investigators conducted glycerolysis using chemical catalysts. The first to apparently patent such a process was Grun in 1924 [177]. According to his patent, tin metal was used to



catalyze oil and fat glycerolysis to yield the required level of MAG needed for the production of a synthetic butter [177]. In 1940, Proctor and Gamble Co. patented the use of commercial sodium soap or alcoholates such as  $\text{NaOC}_2\text{H}_5$  or  $\text{KOC}_2\text{H}_5$  as catalysts for the production of MAG [178, 179]. Five years later, a patent assigned to Colgate-Palmolive-Peet Co., showing a more thorough understanding of glycerolysis, claimed that the following catalysts were suitable to catalyze the glycerolysis reaction: sodium hydroxide, sodium methylate, sodium carbonate and other alkali metal salts, barium oxide, lime, tetramethyl ammonium hydroxide, hydrochloric acid, trichloroacetic acid, phosphoric acid, sulfuric acid, aluminum chloride, boron fluoride, and glycerine sulphonic acids [180]. Since then, many base and acid catalysts have been used to conduct glycerolysis. Generally, base catalysts were favoured industrially because they are less corrosive than acidic compounds [183]. Finding the optimal concentration of a catalyst required still remains an open question. It is true that, although high amounts of catalyst considerably increase MAG yields, the use of small amounts of catalysts (0.03-0.10 mol per equivalent TAG) is preferred in order to reduce the amount of soap formed [180].

Over the years, a number of studies have been conducted using different fats and oils, catalysts, and processing conditions (Table 1.2). It is important to keep in mind that MAG yields vary from one study to the next not only due to processing conditions but because of differences in analytical methods and basis of comparison used. For instance, in some studies the percentage of theoretical MAG yield is reported while in others only the weight percent of MAG is provided; often times,

little information is given to explain MAG yield calculations. Among all these studies, the work of Rheineck et al. [173] is worth highlighting for they hypothesized that the real catalyst was not NaOH but rather sodium glyceroxide ( $\text{NaOC}_3\text{H}_5(\text{OH})_2$ ), which is produced when glycerol and NaOH are together under glycerolysis conditions. To prove their point, they patiently prepared sodium glyceroxide (which is a very tedious procedure) and conducted glycerolysis using 0.11% of it at 200 °C. The results proved them right for they reached equilibrium approximately 40 min earlier using sodium glyceroxide than when conducting glycerolysis at the same temperature using 0.18% NaOH catalyst [173]. Other investigators have also tried to explain the role of catalysts on the glycerolysis reaction. Some have suggested that TAG might react with the catalyst to form soaps which was, at least in part, acting as an emulsifier to enhance the miscibility between the alcohol and fat/oil phase [161].

Regardless of their exact mechanism of action, the use of catalysts in glycerolysis oftentimes requires special considerations. For instance, some catalysts can cause undesirable colour in the final product whereas others, such as hydrated lime,  $\text{Ca}(\text{OH})_2$ , causes a low colour development and is therefore preferred for the manufacture of MAG in the food industry [175]. Furthermore, the addition of a catalyst also implies extra processing steps to neutralize it and then to remove the neutralization product formed (salt or other component) from the MAG rich oil. The catalyst should always be inactivated prior to cooling otherwise the reaction will quickly reverse itself, due to the low miscibility of glycerol and oil at lower

temperatures, thereby causing approximately 30% decrease in MAG yield [159]. Neutralization of the catalyst also avoids soapy taste, unstable colour and foaming [175]. If a base catalyst is used, neutralization is generally achieved by adding phosphoric acid [159]. The salt formed by neutralization is later removed by filtration using clays: a process which requires a large amount of solvent and causes considerable yield loss due to MAG adsorption on the clay [175]. When hydrated lime is neutralized with phosphoric acid, calcium hydrogen phosphate is formed and, due to the high temperature, it is converted to polymeric metaphosphate, which makes filtration problematic [159]. As previously mentioned, the use of hydrated lime is preferred by the food industry but it requires a quick cool-down thereby increasing processing costs.

One way to conduct glycerolysis at milder temperatures and obtain >75% MAG is to conduct catalyzed glycerolysis in pyridine [171, 184]. The reason for this is that glycerol and oil/fat are both miscible in hot pyridine, avoiding mass transfer limitations between different phases. Other solvents, such as tetrahydrofuran (THF) have also been used to increase the rate of catalyzed alcoholysis by solubilizing oil and methanol [185]. However, a clear drawback of these methods is that pyridine and THF are not food grade and that an extra solvent removal step is required. In the case of pyridine, this extra step is achieved by washing the product with hot salted water, following catalyst neutralization by dilute hydrochloric acid, and then deodorizing at 200 °C and 0.133 kPa for 15 min [171].

Glycerolysis has also been catalyzed using enzymes. Work in this area was initiated by Yamane et al. [186] who initially obtained 20.4% MAG using *Pseudomonas fluorescens* lipase and later demonstrated that by conducting glycerolysis at 42 °C for 8-16 h and then at 5 °C for up to 4 days, a yield of approximately 90 wt% MAG could be obtained and that the reaction could be further optimized by carefully monitoring the level of water, TAG to glycerol ratio and amount of lipase [187]. Since these initial studies, and since Bornscheuer's review [188] on lipase-catalyzed synthesis of MAG, a considerable amount of work has been conducted [189-210]. These studies clearly demonstrated that the use of lipase to catalyze the glycerolysis reaction is advantageous and offers perhaps the greatest potential for future MAG production. Unfortunately, they still require long processing times.

Few non-enzymatic studies involving reactions of vegetable oils and fatty acid esters have gone beyond basic experimental results with respect to consideration of reaction kinetics [26, 27, 29, 160, 211] and only one of these studies [26] noted the fact that ester hydrolysis reactions were taking place in parallel with transesterification. In addition, as pointed out by Zhou et al. [185], some of these studies have used catalysts such as sodium or potassium hydroxide, which dissolves in the alcohol phase, and have failed to recognize that their reaction was initially mass-transfer controlled. Indeed, Zhou et al. [185] claimed that if the catalyst was found in the alcohol phase, TAG had to be first transferred into that phase in order for the reaction to occur and consequently, accurate rate constants

could only be achieved if such catalyzed reactions would be conducted in a solvent, such as THF, which would solubilize the reactants and catalyst.

#### *1.2.3.3.3. Glycerolysis in SC-CO<sub>2</sub>*

To avoid product oxidation during glycerolysis the reaction is usually either conducted under reduced pressure, to remove the air, or reactants are blanketed with an inert gas [161]. As shown in Table 1.2, nitrogen is usually used. However, Arrowsmith's patent [180] included the use of CO<sub>2</sub> and a 1962 Indian patent by Kochhar and Bhatnagar [19] even claimed that a pressurized aqueous solution of CO<sub>2</sub> catalyzed the glycerolysis reaction and produced a MAG yield of 85-91% without the use of molecular distillation. As pointed out by Sonntag [159], this process has not been widely known and appreciated for it suggests two things, firstly that SC-CO<sub>2</sub> could play a part in the reaction and secondly that the reaction did not have to be kept anhydrous, as it had previously been thought, but that the presence of water was actually beneficial. Furthermore, such a process did not require the addition of an objectionable catalyst, could use commercial glycerol with 2-5% water, produced a lighter coloured product without undesirable odours, and did not undergo reversion of MAG because the "catalyst" was removed upon depressurization [19]. To test the validity of this process, Temelli et al. [20] conducted glycerolysis of soybean oil using glycerol with 0-8% water in SC-CO<sub>2</sub> at various pressures (20.7-62.1 MPa) and obtained 49.2% MAG without the use of a metal catalyst. Although the high yields previously reported were not obtained,

MAG yields did increase with water concentration and upon pressurizing CO<sub>2</sub> above its critical pressure [20] and the glyceride products were much lighter in colour compared to those synthesized using metal catalysts [212]. Nevertheless, no kinetic study was found on the glycerolysis of oil in SC-CO<sub>2</sub> media.

### **1.3. Concluding remarks and perspective for further research**

Considering the current state of knowledge summarized above for the reactions of fats and oils, it appears advantageous to conduct non-catalyzed non-enzymatic hydrolysis, esterification and glycerolysis in SC-CO<sub>2</sub>. Given that little kinetic information is available to explain when and how much MAG, DAG, TAG and FFA are present as a function of time for such reactions, it is very compelling to conduct detailed kinetic studies for hydrolysis, esterification and glycerolysis. Such studies would obviously assist in understanding the effect of each processing parameter in order to optimize the process but it would also permit us to model each reaction. It also appears practical to initiate our kinetic study with the glycerolysis reaction because data previously obtained by Temelli et al. [20] are readily available.

It appears equally enticing to continue the work initiated by Sovova and Zarevucka [25] and Rezaei and Temelli [24] by using a continuous enzymatic hydrolysis system to better understand the impact of processing parameters on the lipase catalyzed hydrolysis of vegetable oil with the ultimate goal of optimization and design of such a system for potential scale up.

#### 1.4. References

- [1] O.P. Dwivedi, P. Kyba, P.J. Stoett, R. Tiessen, Sustainable Development and Canada: National & International Perspectives, Broadview Press, Peterborough, ON, 2001.
- [2] T. Mag, Canola and Rapeseed. Production, Chemistry, Nutrition and Processing Technology, Avi Book, Van Nostrand Reinhold, New York, NY, 1990.
- [3] G.H. Johnson, D.R. Keast, P.M. Kris-Etherton, Dietary modeling shows that the substitution of canola oil for fats commonly used in the united states would increase compliance with dietary recommendations for fatty acids. *J. Am. Diet. Assoc.* 107 (2007) 1726-1734.
- [4] K. Schroeder, Glycerine, in: F. Shahidi (Eds.), Industrial and Nonedible Products from Oils and Fats, John Wiley & Sons, Hoboken, NJ, 2005,
- [5] J.C. Thompson, B.B. He, Characterization of crude glycerol from biodiesel production from multiple feedstocks. *Appl. Eng. Agric.* 22 (2006) 261-265.
- [6] Anonymous, Lubricant compositions. *Res. Discl.* (2006) 690.
- [7] A.M. Fernandez, U. Held, A. Willing, W.H. Breuer, New green surfactants for emulsion polymerization. *Prog. Org. Coatings* 53 (2005) 246-255.
- [8] G.M. Eccleston, Functions of mixed emulsifiers and emulsifying waxes in dermatological lotions and creams. *Colloids Surf. A Physicochem. Eng. Asp.* 123-124 (1997) 169-182.
- [9] N. Garti, What can nature offer from an emulsifier point of view: Trends and progress? *Colloids Surf. A Physicochem. Eng. Asp.* 152 (1999) 125-146.
- [10] E.J. Beckman, Supercritical and near-critical CO<sub>2</sub> in green chemical synthesis and processing. *J. Supercrit. Fluids* 28 (2004) 121-191.
- [11] J.W. King, Advances in critical fluid technology for food processing. *Food Sci. Technol. Today* 14 (2000) 186.
- [12] G. Brunner, Supercritical fluids: Technology and application to food processing. *J. Food Eng.* 67 (2005) 21-33.

- [13] A.A. Clifford, E. Kiran, J.M.H. Levelt Senger, Reactions in supercritical fluids, in: *Supercritical Fluids Fundamentals for Application*, Kluwer Academic Publishers, Dordrecht, 1994, p. 449.
- [14] T. Clifford, K. Bartle, Chemical reactions in supercritical fluids. *Chem. Ind.* 17 (1996) 449.
- [15] M.A. McHugh, V.J. Krukonis, *Supercritical Fluid Extraction: Principles and Practice*, Butterworth-Heinemann, Toronto, ON, 1994, p.502.
- [16] P.E. Savage, S. Gopalan, T.I. Mirzan, C.J. Martino, E.E. Brock, Reactions at supercritical conditions: applications and fundamentals. *AIChE J.* 41 (1995) 1723.
- [17] T. Matsuda, T. Harada, K. Nakamura, Biocatalysis in supercritical CO<sub>2</sub>. *Curr. Org. Chem.* 9 (2005) 299-315.
- [18] H.R. Hobbs, N.R. Thomas, Biocatalysis in supercritical fluids, in fluorosolvents, and under solvent-free conditions. *Chem. Rev.* 107 (2007) 2786-2820.
- [19] R.K. Kochhar, R.K. Bhatnagar, An improved process for the manufacture of monoacylglycerols, Indian Patent 1962.
- [20] F. Temelli, J.W. King, G.R. List, Conversion of oils to monoglycerides by glycerolysis in supercritical carbon dioxide media. *J. Am. Oil Chem. Soc.* 73 (1996) 699.
- [21] Z.R. Yu, S.S.H. Rizvi, J.A. Zollweg, Enzymatic esterification of fatty acid mixtures from milk fat and anhydrous milk fat with canola oil in supercritical carbon dioxide. *Biotechnol. Prog.* 8 (1992) 508-513.
- [22] N.N. Gandhi, N.S. Patil, S.B. Sawant, J.B. Joshi, P.P. Wangikar, D. Mukesh, Lipase-catalyzed esterification. *Catal. Rev. Sci. Eng.* 42 (2000) 439-480.
- [23] M. Hakoda, N. Shiragami, A. Enomoto, K. Nakamura, Effect of moisture on enzymatic reaction in supercritical carbon dioxide. *Bioproc. Biosyst. Eng.* 24 (2002) 355-361.
- [24] K. Rezaei, F. Temelli, Lipase-catalyzed hydrolysis of canola oil in supercritical carbon dioxide. *J. Am. Oil Chem. Soc.* 77 (2000) 903.
- [25] H. Sovova, M. Zarevucka, Lipase-catalysed hydrolysis of blackcurrant oil in supercritical carbon dioxide. *Chem. Eng. Sci.* 58 (2003) 2339-2350.



- [26] D. Darnoko, M. Cheryan, Kinetics of palm oil transesterification in a batch reactor. *J. Am. Oil Chem. Soc.* 77 (2000) 1263-1267.
- [27] B. Freedman, R.O. Butterfield, E.H. Pryde, Transesterification kinetics of soybean oil. *J. Am. Oil Chem. Soc.* 63 (1986) 1375-1380.
- [28] H. Nouredini, D. Zhu, Kinetics of transesterification of soybean oil. *J. Am. Oil Chem. Soc.* 74 (1997) 1457-1463.
- [29] H. Nouredini, D.W. Harkey, M.R. Gutsman, A continuous process for the glycerolysis of soybean oil. *J. Am. Oil Chem. Soc.* 81 (2004) 203-207.
- [30] S. Angus, B. Armstrong, K.M. Reuck, International Thermodynamic Tables of the Fluid State. Carbon Dioxide, Pergamon Press, Oxford, 1976.
- [31] P.W. Bridgman, Change of Phase under Pressure. I. The phase diagram of eleven substances with especial reference to the melting curve. *Phys. Rev.* 3 (1914) 126-141, 153-203.
- [32] Y. Suehiro, M. Nakajima, K. Yamada, M. Uematsu, Critical parameters of  $\{x\text{CO}_2 + (1 - x)\text{CHF}_3\}$  for  $x = (1.0000, 0.7496, 0.5013, \text{ and } 0.2522)$ . *J. Chem. Thermodyn.* 28 (1996) 1153-1164.
- [33] P.G. Jessop, W. Leitner, Supercritical fluids as media for chemical reactions, in: *Chemical Synthesis Using Supercritical Fluids*, Wiley-VCH, Weinheim, Germany, 1999, p. 1-36.
- [34] Cagniard de La Tour, C., Exposé de quelques résultats obtenus par l'action combinée de la chaleur et de la compression sur certains liquides, tels que l'eau, l'alcool, l'éther sulfurique et l'essence de pétrole rectifiée. *Ann. Chim. Phys.* 21 (1822) 127-132,-178-182.
- [35] T. Andrews, The bakerian lecture: On the continuity of the gaseous and liquid states of matter. *Phil. Trans. Roy. Soc.* 159 (1869) 575-590.
- [36] E.B. Auerbach, Process for treating, separating and purifying oils, United States Patent 1,805,751, 1931.
- [37] S. Pilat, M. Godlewicz, Method of separating high molecular mixtures, United States Patent 2,188,013, 1940.
- [38] K. Zosel, Separation with supercritical gases: practical applications. *Angew. Chem. Int. Ed. Engl.* 17 (1978) 702-709.

- [39] K. Zosel, Selective separation in supercritical gas phase, in: K.D. Timmerhaus, M.S. Bauber. (Eds.), High Pressure Science and Technology, vol. 1, 1977, p.561.
- [40] V.N. Ipatieff, The Life of a Chemist, Stanford University Press, Stanford, 1946.
- [41] E. Briner, A. Wroczynski, Action chimique des pressions élevées; compression du protoxyde d'azote et d'un mélange d'azote et d'hydrogène; décomposition de l'oxyde de carbone par la pression. Compt. rend. 150 (1910) 1324-1327.
- [42] E. Briner, A. Wroczynski, Réactions chimiques dans les mélanges gazeux soumis aux pressions très élevées. Compt. Rend. 148 (1909) 1518-1519.
- [43] D.E. Sargent, Polymers from ethylene and carbon dioxide, United States Patent 2,462,680, 1949.
- [44] G.D. Buckley, N.H. Ray, Manufacture of polymeric ureas, United States Patent 2,550,767, 1951.
- [45] H.C. Stevens, Method of preparing high molecular weight polycarbonates, United States Patent 3,248,415, 1966.
- [46] T. Tacke, S. Wieland P. Panster, Hardening of fats and oils in supercritical CO<sub>2</sub>, in: High Pressure Chemical Engineering, Elsevier, Amsterdam, 1996, p. 17-21.
- [47] T. Tacke, S. Wieland P. Panster, Selective and complete hardening of edible oils and free fatty acids in supercritical fluids, 4th International Symposium on Supercritical Fluids, 1997, p.511.
- [48] T. Tacke, S. Wieland, P. Panster, M. Bankmann, R. Brand, H. Magerlein, Hardening of unsaturated fats, fatty acids or fatty acid esters, United States Patent 5,734,070, 1998.
- [49] M. Poliakoff, T.M. Swan, T. Tacke, M.G. Hitzler, S.K. Ross, S. Wieland, Supercritical hydrogenation, WO 97/38955, 1997.
- [50] T.W. Randolph, H.W. Blanch, J.M. Prausnitz, G. Wilke, Enzymatic catalysis in a supercritical fluid. Biotechnol. Lett. 7 (1985) 325.
- [51] D.A. Hammond, M. Karel, A.M. Klibanov, V.J. Krukonis, Enzymatic reactions in supercritical gases. Appl. Biochem. Biotech. 11 (1985) 393.

- [52] K. Nakamura, Y.M. Chi, Y. Yamada, T. Yano, Lipase activity and stability in supercritical carbon dioxide. *Chem. Eng. Commun.* 45 (1986) 207-212.
- [53] T. Matsuda, K. Watanabe, T. Harada, K. Nakamura, Enzymatic reactions in supercritical CO<sub>2</sub>: Carboxylation, asymmetric reduction and esterification. *Catal. Today* 96 (2004) 103-111.
- [54] T. Matsuda, T. Harada, K. Nakamura, Organic synthesis using enzymes in supercritical carbon dioxide. *Green Chem.* 6 (2004) 440-444.
- [55] K. Rezaei, F. Temelli, E. Jenab, Effects of pressure and temperature on enzymatic reactions in supercritical fluids. *Biotechnol. Adv.* 25 (2007) 272-280.
- [56] Z. Knez, M. Habulin, M. Primožič, Enzymatic reactions in dense gases. *Biochem. Eng. J.* 27 (2005) 120-126.
- [57] D.R. Lide, G. Baysinger, L.I. Berger, R.N. Goldberg, H.V. Kehiaian, K. Kuchitsu, G. Rosenblatt, D.L. Roth, D. Zwillinger, *CRC Handbook of Chemistry and Physics*, 87th Edition, Taylor and Francis, Boca Raton, FL, 2007.
- [58] H. Cai, J.M. Shaw, K.H. Chung, Hydrogen solubility measurements in heavy oil and bitumen cuts. *Fuel* 80 (2001) 1055-1063.
- [59] J.R. Roebuck, The Joule-thomson effect in carbon dioxide. *J. Am. Chem. Soc.* 64 (1942) 400-411.
- [60] R.W. Johnson, E. Fritz, N.O.V. Sonntag, D.T.A. Huibers, G. Buehler, W.C. Eisenhard, R.A. Reck, D.V. Kinsman, R.T. McIntyre, H.F. Reid, B.A.M. Oude Alink, P. Rakoff, J. Nidock, F.F. Aplan, K.S. Ennor M.L., Schlossman, *Fatty acids in Industry: Process, Properties, Derivatives, Applications*, Marcel Dekker, Inc., New York, NY, 1989, p. 667.
- [61] D.G. Hayes, Enzyme-catalyzed modification of oilseed materials to produce eco-friendly products. *J. Am. Oil Chem. Soc.* 81 (2004) 1077-1103.
- [62] T.A. Patil, D.N. Butala, T.S. Raghunathan, H.S. Shankar, Thermal hydrolysis of vegetable oils and fats. 1. Reaction kinetics. *Ind. Eng. Chem. Res.* 27 (1988) 727-735.
- [63] N. Senanayake, F. Shahidi, Modification of fats and oils via chemical and enzymatic methods, in: F. Shahidi (Eds.), *Edible oil and fat products: specialty oils and oil products*, John Wiley & Sons, Hoboken, NJ, 2005, p. 555-584.

- [64] N.O.V. Sonntag, Fat splitting, esterification and interesterification, in: D. Swern (Eds.), *Bailey's Industrial Oil and Fat Products*, John Wiley & Sons, New York, NY, 1979, p. 97-173.
- [65] L.L. Lamborn, *Modern Soaps, Candles, and Glycerin*, Van Nostrand Co., New York, NY, 1906, p. 542.
- [66] F. Aftalion, *A History of the International Chemical Industry*, University of Pennsylvania Press, Pennsylvania, PA, 1991, p. 410.
- [67] R.A. Tilghman, Improvement in method of decomposing fats into fatty acids and glycerine, United States Patent 28,315, 1860.
- [68] W. Connstein, E. Hoyer, H. Wartenberg, Enzymatic adipolysis. *Ber. Chem. Ges.* 35 (1902) 3988.
- [69] N.O.V. Sonntag, Fat splitting and glycerol recovery, in: *Fatty Acids in Industry: Processes, Properties, Derivatives, Applications*, Marcel Dekker, New York, NY, 1989, p. 23-72.
- [70] E. Twitchell, Process of decomposing fats or oils into fatty acids and glycerin, United States Patent 601,603, 1898.
- [71] M.H. Ittner, Hydrolysis of fats and oils, United States Patent 2,139,589, 1938.
- [72] V. Mills, Continuous countercurrent hydrolysis of fat, United States Patent 2,156,863, 1939.
- [73] G.W. Eisenlohr, Process of hydrolyzing oils and fats, United States Patent 2,154,835, 1939.
- [74] D.N. Eggenberger, F.K. Broome, A.W. Ralston, H.J. Harwood, The solubilities of the normal saturated fatty acids in water. *J. Org. Chem.* 14 (1949) 1108-1110.
- [75] L.M. John, J.W. McBain, The hydrolysis of soap solutions. II. The solubilities of higher fatty acids. *J. Am. Oil Chem. Soc.* 25 (1948) 40-41.
- [76] C.W. Hoerr, W.O. Pool, A.W. Ralston, The effect of water on the solidification points of fatty acids. *Solubility of water in fatty acids. Oil Soap* 19 (1942) 126-128.
- [77] L. Lascaray, Mechanism of fat splitting. *Ind. Eng. Chem.* 41 (1949) 786-790.

- [78] A. Sturzenegger, H. Sturm, Hydrolysis of fats at high temperatures. *Ind. Eng. Chem.* 43 (1951) 510-515.
- [79] L. Hartman, Kinetics of the Twitchell hydrolysis. *Nature* 167 (1951) 199-199.
- [80] E. Minami, S. Saka, Kinetics of hydrolysis and methyl esterification for biodiesel production in two-step supercritical methanol process. *Fuel* 85 (2006) 2479-2483.
- [81] J.W. King, R.L. Holliday, G.R. List, Hydrolysis of soybean oil in a subcritical water flow reactor. *Green Chem.* 1 (1999) 261-264.
- [82] R.L. Holliday, J.W. King, G.R. List, Hydrolysis of vegetable oils in sub- and supercritical water. *Ind. Eng. Chem. Res.* 36 (1997) 932-935.
- [83] J.S.S. Pinto, F.M. Lanças, Hydrolysis of corn oil using subcritical water. *J. Braz. Chem. Soc.* 17 (2006) 85-89.
- [84] K. Fujita, M. Himi, Hydrolysis of glycerol trioleate and extraction of its fatty acid under CO<sub>2</sub> supercritical conditions. *Nippon Kagaku Kaishi* 1 (1995) 79-82.
- [85] C. Scrimgeour, Chemistry of Fatty Acids, in: F. Shahidi (Eds.), *Edible Oil and Fat Products: Chemistry, Properties, and Health Effects*, John Wiley & Sons, Hoboken, NJ, 2005, p. 1-43.
- [86] F.X. Malcata, H. Reyes, H. Garcia, C. Hill, C. Amundson, Immobilized lipase reactors for modification of fats and oils. A review. *J. Am. Oil Chem. Soc.* 67 (1990) 890-910.
- [87] E. Vulfson, Enzymatic synthesis of food ingredients in low-water media. *Trends Food Sci. Technol.* 4 (1993) 209-215.
- [88] W.M. Linfield, Enzymatic fat splitting, *Proceedings of the World Conference on Biotechnology for the Fats and Oils Industry*, 1988, p.131.
- [89] M.T. Patel, R. Nagarajan, A. Kilara, Lipase-catalyzed biochemical reactions in novel media: A review. *Chem. Eng. Commun.* 152-53 (1996) 365-404.
- [90] H.L. Brockmann, *Lipases*, Elsevier, New York, NY, 1984, p. 4.
- [91] A. Zaks, A.M. Klibanov, Enzymatic catalysis in nonaqueous solvents. *J. Biol. Chem.* 263 (1988) 3194-3201.

- [92] K. Griebenow, A.M. Klibanov, On protein denaturation in aqueous-organic mixtures but not in pure organic solvents. *J. Am. Oil Chem. Soc.* 118 (1996) 11695-11700.
- [93] Y.M. Chi, K. Nakamura, T. Yano, Enzymatic interesterification in supercritical carbon dioxide. *Agric. Biol. Chem.* 52 (1988) 1541.
- [94] Y. Ikushima, N. Saito, M. Arai, H.W. Blanch, Activation of a lipase triggered by interactions with supercritical carbon dioxide in the near-critical region. *J. Phys. Chem.* 99 (1995) 8941.
- [95] Y. Ikushima, Supercritical fluids: An interesting medium for chemical and biochemical processes. *Adv. Colloid Interface Sci.* 71-72 (1997) 259-280.
- [96] N. Mase, T. Sako, Y. Horikawa, K. Takabe, Novel strategic lipase-catalyzed asymmetrization of 1,3-propanediacetate in supercritical carbon dioxide. *Tetrahedron Lett.* 44 (2003) 5175-5178.
- [97] S. Kamat, G. Critchley, E.J. Beckman, A.J. Russell, Biocatalytic synthesis of acrylates in organic solvents and supercritical fluids: 3. Does carbon dioxide covalently modify enzymes? *Biotechnol. Bioeng.* 46 (1995) 610.
- [98] M. Habulin, Z. Knez, Activity and stability of lipases from different sources in supercritical carbon dioxide and near-critical propane. *J. Chem. Technol. Biot.* 76 (2001) 1260-1266.
- [99] K.L. Toews, R.M. Shroll, C.M. Wai, N.G. Smart, pH-Defining equilibrium between water and supercritical CO<sub>2</sub>. Influence on SFE of organics and metal chelates. *Anal. Chem.* 67 (1995) 4040-4043.
- [100] A. Marty, W. Chulalaksananukul, R.M. Willemot, J.S. Condoret, Kinetics of lipase-catalyzed esterification in supercritical CO<sub>2</sub>. *Biotechnol. Bioeng.* 39 (1992) 273-280.
- [101] N. Fontes, M.C. Almeida, S. Garcia, C. Peres, J. Partridge, P.J. Halling, S. Barreiros, Supercritical fluids are superior media for catalysis by cross-linked enzyme microcrystals of subtilisin Carlsberg. *Biotechnol. Prog.* 17 (2001) 355-358.
- [102] J.D. Holmes, D.C. Steytler, G.D. Rees, B.H. Robinson, Bioconversions in a water-in-CO<sub>2</sub> microemulsion. *Langmuir* 14 (1998) 6371-6376.
- [103] H. Frykman, J.M. Snyder, J.W. King, Screening catalytic lipase activities with an analytical supercritical fluid extractor. *J. Am. Oil Chem. Soc.* 75 (1998) 517.

- [104] J.W. Hampson, T.A. Foglia, Effect of moisture content on immobilized lipase-catalyzed triacylglycerol hydrolysis under supercritical carbon dioxide flow in a tubular fixed-bed reactor. *J. Am. Oil Chem. Soc.* 76 (1999) 777.
- [105] K. Rezaei, F. Temelli, On-line extraction-reaction of canola oil using immobilized lipase in supercritical CO<sub>2</sub>. *J. Supercrit. Fluids* 19 (2001) 263.
- [106] H. Yan, H. Noritomi, K. Nagahama, A rise in the hydrolysis activity of *Candida rugosa* lipase caused by pressurized treatment with supercritical carbon dioxide. *Kobunshi Ronbunshu* 58 (2001) 674-678.
- [107] M. Habulin, Z. Knez, High-pressure enzyme hydrolysis of oil. *Eur. J. Lipid Sci. Technol.* 104 (2002) 381-386.
- [108] J.L. Martinez, K. Rezaei, F. Temelli, Effect of water on canola oil hydrolysis in an online extraction-reaction system using supercritical CO<sub>2</sub>. *Ind. Eng. Chem. Res.* 41 (2002) 6475-6481.
- [109] Z. Knez, M. Habulin, M. Primožic, Hydrolases in supercritical CO<sub>2</sub> and their use in a high-pressure membrane reactor. *Bioproc. Biosyst. Eng.* 25 (2003) 279-284.
- [110] M. Primožič, M. Habulin, Z. Knez, Thermodynamic properties of the enzymatic hydrolysis of sunflower oil in high-pressure reactors. *J. Am. Oil Chem. Soc.* 80 (2003) 785-788.
- [111] H. Yan, K. Nagahama, Activity of free *candida rugosa* lipase in hydrolysis reaction of tuna oil under high pressure carbon dioxide. *J. Chem. Eng. Jpn.* 36 (2003) 557.
- [112] M. Primožič, M. Habulin, Z. Knez, Parameter optimization for the enzymatic hydrolysis of sunflower oil in high-pressure reactors. *J. Am. Oil Chem. Soc.* 80 (2003) 643-646.
- [113] M. Primožič, M. Habulin, Z. Knez, Modeling of kinetics for the enzymatic hydrolysis of sunflower oil in a high-pressure reactor. *J. Am. Oil Chem. Soc.* 82 (2005) 543-547.
- [114] M. Habulin, M. Primožič, Z. Knez, Enzymatic reactions in high-pressure membrane reactors. *Ind. Eng. Chem. Res.* 44 (2005) 9619-9625.
- [115] N.K. Guthalugu, M. Balaraman, U.S. Kadimi, Optimization of enzymatic hydrolysis of triglycerides in soy deodorized distillate with supercritical carbon dioxide. *Biochem. Eng. J.* 29 (2006) 220-226.

- [116] M. Bártlová, P. Bernášek, J. Sýkora, H. Sovová, HPLC in reversed phase mode: Tool for investigation of kinetics of blackcurrant seed oil lipolysis in supercritical carbon dioxide. *J. Chromatogr. B Anal. Technol. Biomed. Life Sci.* 839 (2006) 80-84.
- [117] W.J. Ting, K.Y. Tung, R. Giridhar, W.T. Wu, Application of binary immobilized *Candida rugosa* lipase for hydrolysis of soybean oil. *J. Mol. Catal. B Enzym.* 42 (2006) 32-38.
- [118] D. Oliveira, A.C. Feihmann, A.F. Rubira, M.H. Kunita, C. Dariva, J.V. Oliveira, Assessment of two immobilized lipases activity treated in compressed fluids. *J. Supercrit. Fluids* 38 (2006) 373-382.
- [119] R. Janis, J. Krejci, A. Klasek, Preparation of 1-monoacylglycerols from glycidol and fatty acids catalyzed by the chromium(III)-fatty acid system. *Eur. J. Lipid Sci. Technol.* 102 (2000) 351-354.
- [120] N.J. Krog, Food emulsifiers and their chemical and physical properties, in: S.E. Friberg and K. Larson, (Eds.), *Food Emulsions*, Marcel Dekker, New York, NY, 1997, p. 141-188.
- [121] H. Birnbaum, The monoglycerides: manufacture, concentration, derivatives and applications. *Bakers Digest* 55 (1981) 6-18.
- [122] E. Boyle, Monoglycerides in food systems: Current and future uses. *Food Technol.* 51 (1997) 52-59.
- [123] L. Sagalowicz, M.E. Leser, H.J. Watzke, M. Michel, Monoglyceride self-assembly structures as delivery vehicles. *Trends Food Sci. Technol.* 17 (2006) 204-214.
- [124] N.A. Ghanem, F.F. Abd El-Mohsen, The glycerolysis step in the production of oil-modified alkyd resins - the effects of the acid and iodine values of mixed triglycerides. *J. Oil Col. Chem. Assoc.* 49 (1966) 490-499.
- [125] N.A. Ghanem, Z.H.A. El-Latif, M.A. El-Azmirl, The glycerolysis step in production of oil-modified alkyd resins: Part V - glycerolysis of castor-oil and dehydrated castor-oil. *J. Oil Col. Chem. Assoc.* 55 (1972) 114-127.
- [126] N.A. Ghanem, F.F. Abd El-Mohsen, The glycerolysis step in production of oil modified alkyd resins: Part IV - some new aspects. *J. Oil Col. Chem. Assoc.* 50 (1967) 441-450.



- [127] H. Szelag, W. Zwierzykowski, Esterification kinetics of glycerol with fatty acids in the presence of sodium and potassium soaps. *Fett-Lipid* 100 (1998) 302-307.
- [128] J. Pelouze, A. Gelis, Mémoire sur l'acide butyrique. *Ann. Chim. Phys.* 10 (1844) 434-456.
- [129] M. Berthelot, Sur les combinaisons de la glycérine avec les acides. *Compt. rend.* 37 (1853) 398-405.
- [130] H.A. Goldsmith, Polyhydric alcohol esters of fatty acids: Their preparation, properties, and uses. *Chem. Rev.* 33 (1943) 257-349.
- [131] L. Hartman, Advances in the synthesis of glycerides of fatty acids. *Chem. Rev.* 58 (1958) 845-867.
- [132] N.O.V. Sonntag, Esterification and interesterification. *J. Am. Oil Chem. Soc.* 56 (1979) 751A-754A.
- [133] W.C. Eisenhard, Esterification, in: R.W. Johnson and E. Fritz, (Eds.), *Fatty acids in industry: processes, properties, derivatives, application*, Marcel Dekker, New York, NY, 1989, p. 139-152.
- [134] R.B.R. Choudhury, The preparation and purification of monoglycerides. II Direct esterification of fatty acids with glycerol. *J. Am. Oil Chem. Soc.* 39 (1962) 345-347.
- [135] T.P. Hilditch, J.G. Rigg, Experiments on the direct esterification of higher fatty acids with glycerol and with ethylene glycol. *J. Chem. Soc.* (1935) 1774-1778.
- [136] M.M. Emtir, F.S. Guner, O.S. Kabasakal, A.T. Erciyes, E. Ekinci, Kinetics of esterification reaction between glycerol and oleic acid in the presence of pyridine. *Fett Wiss. Technol.* 97 (1995) 347-351.
- [137] I. Roberts, H.C. Urey, A study of the esterification of benzoic acid with methyl alcohol using isotopic oxygen. *J. Am. Chem. Soc.* 60 (1938) 2391-2393.
- [138] I. Roberts, H.C. Urey, The mechanisms of acid catalyzed ester hydrolysis, esterification and oxygen exchange of carboxylic acids. *J. Am. Chem. Soc.* 61 (1939) 2584-2587.
- [139] R.O. Feuge, E.A. Kraemer, A.E. Bailey, Modification of vegetable oils - reesterification of fatty acids with glycerol. *Oil Soap* 22 (1945) 202-207.

- [140] T.L. Garner, The formation of glycerides and their isomers. -Part I. J. Soc. Chem. Ind. 47 (1928) 278T-280T.
- [141] L. Hartman, Esterification rates of some saturated and unsaturated fatty acids with glycerol. J. Am. Oil Chem. Soc. 43 (1966) 536-538.
- [142] R.O. Feuge, Derivatives of fats for use as foods. J. Am. Oil Chem. Soc. 39 (1962) 521-527.
- [143] L.H. Dunlap, J.S. Heckles, Catalyzed esterification of oleic acid. J. Am. Oil Chem. Soc. 37 (1960) 281-285.
- [144] F.S. Guner, A. Sirkecioglu, S. Yilmaz, A.T. Erciyas, A. Erdem-Senatalar, Esterification of oleic acid with glycerol in the presence of sulfated iron oxide catalyst. J. Am. Oil Chem. Soc. 73 (1996) 347-351.
- [145] P.J. Flory, Kinetics of condensation polymerization; the reaction of ethylene glycol with succinic acid. J. Am. Chem. Soc. 59 (1937) 466-470.
- [146] N. Sanchez, M. Martinez, J. Aracil, Selective esterification of glycerine to 1-glycerol monooleate. 1. Kinetic modeling. Ind. Eng. Chem. Res. 36 (1997) 1524-1528.
- [147] A. Macierzanka, H. Szelag, Esterification kinetics of glycerol with fatty acids in the presence of zinc carboxylates: preparation of modified acylglycerol emulsifiers. Ind. Eng. Chem. Res. 43 (2004) 7744-7753.
- [148] A. Shishikura, K. Fujimoto, T. Suzuki, K. Arai, Improved lipase-catalyzed incorporation of long-chain fatty-acids into medium-chain triglycerides assisted by supercritical carbon-dioxide extraction. J. Am. Oil Chem. Soc. 71 (1994) 961-967.
- [149] Z. Knez, V. Rizner, M. Habulin, D. Bauman, Enzymatic-synthesis of oleyl oleate in dense fluids. J. Am. Oil Chem. Soc. 72 (1995) 1345-1349.
- [150] S. Colombie, R.J. Tweddell, J.S. Condoret, A. Marty, Water activity control: A way to improve the efficiency of continuous lipase esterification. Biotechnol. Bioeng. 60 (1998) 362-368.
- [151] I. Krmelj, M. Habulin, Z. Knez, D. Bauman, Lipase-catalyzed synthesis of oleyl oleate in pressurized and supercritical solvents. Fett-Lipid 101 (1999) 34-38.
- [152] R. Goddard, J. Bosley, B. Al-Duri, Lipase-catalysed esterification of oleic acid and ethanol in a continuous packed bed reactor, using supercritical CO<sub>2</sub>

- as solvent: approximation of system kinetics. *J. Chem. Technol. Biot.* 75 (2000) 715.
- [153] R. Goddard, J. Bosley, B. Al-Duri, Esterification of oleic acid and ethanol in plug flow (packed bed) reactor under supercritical conditions investigation of kinetics. *J. Supercrit. Fluids* 18 (2000) 121-130.
- [154] S. Hazarika, P. Goswami, N.N. Dutta, A.K. Hazarika, Ethyl oleate synthesis by Porcine pancreatic lipase in organic solvents. *Chem. Eng. J.* 85 (2002) 61-68.
- [155] C.G. Laudani, M. Habulin, M. Primožič, Z. Knez, G. DellaPorta, E. Reverchon, Optimisation of n-octyl oleate enzymatic synthesis over *Rhizomucor miehei* lipase. *Bioprocess Biosyst. Eng.* 29 (2006) 119-127.
- [156] M.A. Jackson, I.K. Mbaraka, B.H. Shanks, Esterification of oleic acid in supercritical carbon dioxide catalyzed by functionalized mesoporous silica and an immobilized lipase. *Appl. Catal. A Gen.* 310 (2006) 48-53.
- [157] C.G. Laudani, M. Habulin, Z. Knez, G.D. Porta, E. Reverchon, Immobilized lipase-mediated long-chain fatty acid esterification in dense carbon dioxide: Bench-scale packed-bed reactor study. *J. Supercrit. Fluids* 41 (2007) 74-81.
- [158] C.G. Laudani, M. Habulin, Z. Knez, G.D. Porta, E. Reverchon, Lipase-catalyzed long chain fatty ester synthesis in dense carbon dioxide: Kinetics and thermodynamics. *J. Supercrit. Fluids* 41 (2007) 92-101.
- [159] N.O.V. Sonntag, Glycerolysis of fats and methyl-esters - status, review and critique. *J. Am. Oil Chem. Soc.* 59 (1982) A795-A802.
- [160] H. Nouredini, V. Medikonduru, Glycerolysis of fats and methyl esters. *J. Am. Oil Chem. Soc.* 74 (1997) 419-425.
- [161] P.R. Muniyappa, S.C. Brammer, H. Nouredini, Improved conversion of plant oils and animal fats into biodiesel and co-product. *Bioresource Technol.* 56 (1996) 19-24.
- [162] T. Yang, H. Zhang, H.L. Mu, A.J. Sinclair, X.B. Xu, Diacylglycerols from butterfat: Production by glycerolysis and short-path distillation and analysis of physical properties. *J. Am. Oil Chem. Soc.* 81 (2004) 979-987.
- [163] K. Campbell-Timperman, J.H. Choi, R. Jimenez-Flores, Mono- and diglycerides prepared by chemical glycerolysis from a butterfat fraction. *J. Food Sci.* 61 (1996) 44-53.

- [164] American Oil Chemists' Society, Official and Tentative Methods, Chicago, 1958, p. 11-57.
- [165] R.B.R. Choudhury, The preparation and purification of monoglycerides.1. Glycerolysis of oils. J. Am. Oil Chem. Soc. 37 (1960) 483-486.
- [166] S.S. Chang, L.H. Wiedermann, Continuous manufacture of monoglycerides, United States Patent 3,079,412, 1963.
- [167] American Oil Chemists' Society, Official and Tentative Methods, Champaign, IL, 1977,
- [168] U. Bajwa, G.S. Bains, Studies on the glycerolysis of groundnut oil and cottonseed oil. J. Food Sci. Tech. Mys. 24 (1987) 81-83.
- [169] W.D. Pohle, V.C. Mehlenbacher, A modification of the periodic acid method for the determination of monoglycerides and free glycerol in fats and oils. J. Am. Oil Chem. Soc. 28 (1950) 54-56.
- [170] E.H. Gruger, D.C. Malins, E.J. Gauglitz, Glycerolysis of marine oils and the preparation of acetylated monoglycerides. J. Am. Oil Chem. Soc. 37 (1960) 214-217.
- [171] K.F. Mattil, R.J. Sims, The glycerolysis of fat in tertiary aromatic nitrogenous bases to increase monoglyceride yield. J. Am. Oil Chem. Soc. 29 (1952) 59-61.
- [172] H. Birnbaum, Process for preparing monoglycerides of fatty acids, United States Patent 2,875,221, 1959.
- [173] A.E. Rheineck, R. Bergseth, B. Sreeniva, Glycerolysis of linseed oil - a compositional study. J. Am. Oil Chem. Soc. 46 (1969) 447-451.
- [174] W.G. Alsop, I.J. Krems, Process for the preparation of higher fatty acid monoglycerides, United States Patent 3,083,216, 1963.
- [175] A. Corma, S. Iborra, S. Miquel, J. Primo, Catalysts for the production of fine chemicals - production of food emulsifiers, monoglycerides, by glycerolysis of fats with solid base catalysts. J. Catal. 173 (1998) 315-321.
- [176] L.M.G. Aguiar, R.M. Vargas, Preparation of monoglycerides by guanidine-catalyzed processes. J. Am. Oil Chem. Soc. 75 (1998) 755-756.
- [177] A. Grun, Method of manufacturing nutritious fats, United States 1505560, 1924.

- [178] A. Edeler, A.S. Richardson, Process for manufacturing fatty esters, United States Patent 2,206,168, 1940.
- [179] A. Edeler, A.S. Richardson, Process for manufacturing fatty esters, United States Patent 2,206,167, 1940.
- [180] C.J. Arrowsmith, J. Ross, Process for preparing fatty materials, United States Patent 1945.
- [181] R.O. Feuge, A.E. Bailey, Modification of vegetable oil - the practical preparation of mono- and diglycerides. *Oil Soap* 23 (1946) 259-264.
- [182] D.S. Negi, F. Sobotka, T. Kimmel, G. Wozny, R. Schomacker, Glycerolysis of fatty acid methyl esters: 1. Investigations in a batch reactor. *J. Am. Oil Chem. Soc.* 84 (2007) 83-90.
- [183] U. Schuchardt, R. Sercheli, R.M. Vargas, Transesterification of vegetable oils: A review. *J. Brazilian Chem. Soc.* 9 (1998) 199-210.
- [184] C. Franzke, F. Kretzschmann, D. Kubel, L. Zahn, E. Hollstein, Studies on the yields of monoglycerides obtained by catalytic glycerolysis of triglycerides. *Nahrung* 11 (1967) 639-643.
- [185] W. Zhou, S.K. Konar, D.G.B. Boocock, Ethyl esters from the single-phase base-catalyzed ethanolysis of vegetable oils. *J. Am. Oil Chem. Soc.* 80 (2003) 367-371
- [186] T. Yamane, M.M. Hoq, S. Itoh, S. Shimizu, Glycerolysis of fat by lipase. *J. Jpn. Oil Chem. Soc.* 35 (1986) 625-631.
- [187] G.P. McNeill, T. Yamane, Further improvements in the yield of monoglycerides during enzymatic glycerolysis of fats and oils. *J. Am. Oil Chem. Soc.* 68 (1991) 6-10.
- [188] U.T. Bornscheuer, Lipase-catalyzed syntheses of monoacylglycerols. *Enzyme Microb. Technol.* 17 (1995) 578-586.
- [189] M.A. Jackson, J.W. King, Lipase-catalyzed glycerolysis of soybean oil in supercritical carbon dioxide. *J. Am. Oil Chem. Soc.* 74 (1997) 103-106.
- [190] M.A. Jackson, J.W. King, G.R. List, W.E. Neff, Lipase-catalyzed randomization of fats and oils in flowing supercritical carbon dioxide. *J. Am. Oil Chem. Soc.* 74 (1997) 635-639.

- [191] B. Cheirsilp, W. Kaewthong, A. H-Kittikun, Kinetic study of glycerolysis of palm olein for monoacylglycerol production by immobilized lipase. *Biochem. Eng. J.* 35 (2007) 71-80.
- [192] R. Pawongrat, X. Xu, A. H-Kittikun, Synthesis of monoacylglycerol rich in polyunsaturated fatty acids from tuna oil with immobilized lipase AK. *Food Chem.* 104 (2007) 251-258.
- [193] J.H. Lee, F. Yu, P.L. Vu, M.S. Choi, C.C. Akoh, K.T. Lee, Compositional study on rice bran oil after lipase-catalyzed glycerolysis and solvent fractionations. *J. Food. Sci.* 72 (2007) C163-C167.
- [194] M.L. Damstrup, J. Abildskov, S. Kiil, A.D. Jensen, F.V. Sparsø, X. Xu, Evaluation of binary solvent mixtures for efficient monoacylglycerol production by continuous enzymatic glycerolysis. *J. Agric. Food Chem.* 54 (2006) 7113-7119.
- [195] J.A. Laszlo, D.L. Compton, Enzymatic glycerolysis and transesterification of vegetable oil for enhanced production of feruloylated glycerols. *J. Am. Oil Chem. Soc.* 83 (2006) 765-770.
- [196] Z. Guo, B. Chen, R.L. Murillo, T. Tan, X. Xu, Functional dependency of structures of ionic liquids: Do substituents govern the selectivity of enzymatic glycerolysis. *Org. Biomol. Chem.* 4 (2006) 2772-2776.
- [197] Z. Guo, X. Xu, Lipase-catalyzed glycerolysis of fats and oils in ionic liquids: A further study on the reaction system. *Green Chem.* 8 (2006) 54-62.
- [198] M.L. Damstrup, T. Jensen, F.V. Sparsø, S.Z. Kiil, A.D. Jensen, X. Xu, Production of heat-sensitive monoacylglycerols by enzymatic glycerolysis in tert-pentanol: Process optimization by response surface methodology. *J. Am. Oil Chem. Soc.* 83 (2006) 27-33.
- [199] T. Yang, M. Rebsdorf, U. Engelrud, X. Xu, Monoacylglycerol synthesis via enzymatic glycerolysis using a simple and efficient reaction system. *J. Food Lipids* 12 (2005) 299-312.
- [200] M.L. Damstrup, T. Jensen, F.V. Sparsø, S.Z. Kiil, A.D. Jensen, X. Xu, Solvent optimization for efficient enzymatic monoacylglycerol production based on a glycerolysis reaction. *J. Am. Oil Chem. Soc.* 82 (2005) 559-564.
- [201] C. Yin, T. Liu, T. Tan, Enzymatic glycerolysis of Chinese vegetable tallow fraction by lipase and study of the mechanism. *Chinese J. Chem. Eng.* 13 (2005) 656-662.

- [202] T. Tan, C. Yin, The mechanism and kinetic model for glycerolysis by 1,3 position specific lipase from *Rhizopus arrhizus*. *Biochem. Eng. J.* 25 (2005) 39-45.
- [203] Z. Guo, X. Xu, New opportunity for enzymatic modification of fats and oils with industrial potentials. *Org. Biomol. Chem.* 3 (2005) 2615-2619.
- [204] W. Kaewthong, S. Sirisansaneeyakul, P. Prasertsan, A. H-Kittikun, Continuous production of monoacylglycerols by glycerolysis of palm olein with immobilized lipase. *Process Biochem.* 40 (2005) 1525-1530.
- [205] T. Yang, M. Rebsdorf, U. Engelrud, X. Xu, Enzymatic production of monoacylglycerols containing polyunsaturated fatty acids through an efficient glycerolysis system. *J. Agric. Food Chem.* 53 (2005) 1475-1481.
- [206] M. Tüter, H.A. Aksoy, Enzymatic glycerolysis of palm and palm kernel oils. *Chem. Eng. Commun.* 192 (2005) 14-17.
- [207] W. Kaewthong, A. H-Kittikun, Glycerolysis of palm olein by immobilized lipase PS in organic solvents. *Enzyme Microb. Technol.* 35 (2004) 218-222.
- [208] Y. Watanabe, Y. Shimada, Y. Yamauchi-Sato, M. Kasai, T. Yamamoto, K. Tsutsumi, Y. Tominaga, A. Sugihara, Synthesis of MAG of CLA with *penicillium camembertii* lipase. *J. Am. Oil Chem. Soc.* 79 (2002) 891-896.
- [209] Y.M. Xia, K.C. Zhang, G.Y. Shi, X.H. Li, Y. Fang, Enzymatic synthesis of monoglycerides in microaqueous media by using lipase from *Pseudomonas fluorescens*. *Sheng Wu Gong Cheng Xue Bao* 18 (2002) 84-88.
- [210] C. Torres, B. Lin, C.G. Hill, Lipase-catalyzed glycerolysis of an oil rich in eicosapentaenoic acid residues. *Biotechnol. Lett.* 24 (2002) 667-673.
- [211] R.O. Butterfield, Kinetic rate constants determined by a digital computer. *J. Am. Oil Chem. Soc.* 46 (1969) 429-431.
- [212] J.W. King, Critical fluid technology for the processing of lipid-related natural products. *C. R. Chim.* 7 (2004) 647-659.

## **2. Kinetic modeling of the glycerolysis reaction for soybean oil in supercritical carbon dioxide media<sup>1</sup>**

### **2.1. Introduction**

Monoacylglycerols (MAG) have many applications as ingredients. Indeed, MAG are used as emulsifiers, encapsulators [1], moisture barriers [2], lubricant [3] and anti-staling agents [1] and are found in foods, nutraceuticals [4], control release medicinal tablets [5], anti-inflammation dental pastes, as well as in hair and skin products [1].

The conventional manufacture of MAG (as reviewed in Section 1.2.3.3.2) is energy-intensive, requires the addition and removal of catalysts such as NaOH, KOH, Ca(OH)<sub>2</sub>, CaO, SrO [6] and can lead to dark colours and burnt flavours in the final product [1, 5]. As an alternative to the conventional method of producing MAG, glycerolysis can be conducted in the presence of a supercritical fluid, which has been demonstrated to accrue positive benefits [5, 7].

Kochhar and Bhatnagar [8] initially reported that a heated aqueous solution of carbon dioxide (CO<sub>2</sub>) enhanced the rate of MAG production during glycerolysis but CO<sub>2</sub> is not used as an adjunct in conventional glycerolysis because it reacts with

---

<sup>1</sup> A version of this chapter was published in the Journal of American Oil Chemists' Society (82: 613-717, 2005).



the alkali catalyst. However, supercritical carbon dioxide (SC-CO<sub>2</sub>) offers many advantages (Sections 1.2.1.4. and 1.2.3.3.3).

In 1996, Temelli et al. [7] demonstrated that glycerolysis of soybean oil could be accomplished in the presence of SC-CO<sub>2</sub> and water. They found that the optimum reaction temperature was 250 °C and reported a significant ( $p < 0.05$ ) decrease in MAG formation with pressure above 20 MPa. As expected, they found that reversal of glycerolysis was negligible and, in some cases, MAG concentration even increased towards the end of the reaction period studied. Similarly, Jackson and King [5] used an immobilized lipase in the presence of flowing SC-CO<sub>2</sub> to facilitate glycerolysis, and reported that the reaction was dependent on the water content of the reagents. They found that when the water level was increased from 0.7% to 4.2%, MAG production decreased from 84% to 67% [5]. Such a trend facilitates control over the composition of the final product. Jackson and King [5] also suggested that the reaction took place in a heterogeneous multiphase mixture.

As discussed in Chapter 1 (Section 1.2.3.3.2), few studies have considered reaction kinetics of non-enzymatic lipid reactions [3, 9-12]. Among these studies, Darnoko and Cheryan [11] were the only ones to report that ester hydrolysis reactions were taking place in parallel with transesterification.

The literature lacks information on the kinetics of glycerolysis reactions in the presence of SC-CO<sub>2</sub> media. Such information is essential to better understand the reaction mechanism as well as to design reaction equipment and processes. Therefore, the objective of this study was to model the kinetics of glycerolysis of

soybean oil in SC-CO<sub>2</sub> media, taking into account that hydrolysis reactions can also occur in parallel with glycerolysis, using previously reported data [7].

## **2.2. Experimental procedures**

### *2.2.1. Experimental parameters*

The materials and experimental protocols used to study glycerolysis of soybean oil and other vegetable oils with glycerol in the presence of SC-CO<sub>2</sub> were described by Temelli et al. [7]. Reactions were conducted by Temelli et al. [7] at 250 °C and pressures of 20.7, 41.4, 62.1 MPa, glycerol-oil molar ratios of 15, 20, 25, and water concentration varying from 3 to 8% (w/w) using a stirred batch reactor. Samples were collected every 0.5 h for 4 h and the composition of the lipid phase (MAG, diacylglycerol (DAG), triacylglycerol (TAG) and free fatty acids (FFA), in moles per 100 g of sample) was determined. The change in the glycerol content over time was not taken into account by Temelli et al. [7] but was calculated in this study based on the initial glycerol/oil ratio and the amount of products formed. To account for the moisture in the glycerol reagent used, the actual water concentration was calculated by adding the average amount of water in glycerol, which corresponded to 4 g of water per 100 g of glycerol, to the concentrations reported by Temelli et al. [7].

### 2.2.2. Kinetic modeling

Modeling was carried out to estimate rate constants for all possible reactions. This approach requires a thorough understanding of the sequential reaction steps taking place. The overall glycerolysis reaction is given by Eq. (2.1).



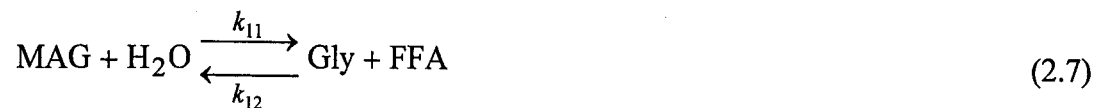
The overall reaction occurs in two consecutive steps [3, 6]. In the first step (Eq. (2.2)), the transfer of a fatty acid from TAG to glycerol (Gly) gives MAG and DAG. In the second step (Eq. (2.3)), MAG is formed by the transfer of a fatty acid from DAG to glycerol.



Assuming that Eqs. (2.2) and (2.3) are reversible,  $k_{1-4}$  represent the rate constants for each step. In Eqs. (2.2) and (2.3), it is assumed that the available acyl groups are randomly distributed among the TAG, DAG and MAG moieties and that water is not participating in these reactions [3]. Thus, by using excess glycerol, a higher yield of total MAG can be obtained [6]. Higher conversions can also be achieved by continuously removing MAG from the product mixture as they are being formed, thereby preventing the breakdown of MAG due to Eq. (2.4).



The above glycerolysis scheme does not account for the presence of FFA in the product mixture. Since water is present in the reaction system [7], ester hydrolysis must be taken into account as a competitive reaction. Hydrolysis can also occur in a stepwise manner. In the first step, a TAG becomes DAG by releasing a FFA after ester hydrolysis (Eq. (2.5)). In the second step, DAG is hydrolyzed giving MAG and a FFA (Eq. (2.6)). MAG can then be further hydrolyzed into glycerol and FFA or, if glycerol is in excess, glycerol can react with FFA to produce even more MAG (Eq. (2.7)).



As in glycerolysis, each step of Eqs. (2.5)-(2.7) is reversible and their respective rate constants are  $k_{7-12}$ . By taking into account all of the reaction steps described in Eqs. (2.2)-(2.7), the rate of change in concentration for each of the reaction components can then be described by the following differential rate equations (Eqs. (2.8a)-(2.8f)), where Gly is glycerol:

$$\begin{aligned} \frac{d[\text{MAG}]}{dt} = & k_1[\text{Gly}][\text{TAG}] - k_2[\text{DAG}][\text{MAG}] + 2k_3[\text{Gly}][\text{DAG}] \\ & - 2k_4[\text{MAG}]^2 - k_5[\text{TAG}][\text{MAG}] + k_6[\text{DAG}]^2 \\ & + k_9[\text{DAG}][\text{H}_2\text{O}] - k_{10}[\text{MAG}][\text{FFA}] - k_{11}[\text{H}_2\text{O}][\text{MAG}] \\ & + k_{12}[\text{Gly}][\text{FFA}] \end{aligned} \quad (2.8a)$$

$$\begin{aligned} \frac{d[\text{DAG}]}{dt} = & k_1[\text{Gly}][\text{TAG}] - k_2[\text{DAG}][\text{MAG}] - k_3[\text{Gly}][\text{DAG}] \\ & + k_4[\text{MAG}]^2 + 2k_5[\text{TAG}][\text{MAG}] - 2k_6[\text{DAG}]^2 \\ & + k_7[\text{TAG}][\text{H}_2\text{O}] - k_8[\text{DAG}][\text{FFA}] - k_9[\text{DAG}][\text{H}_2\text{O}] \\ & + k_{10}[\text{MAG}][\text{FFA}] \end{aligned} \quad (2.8b)$$

$$\begin{aligned} \frac{d[\text{TAG}]}{dt} = & -k_1[\text{Gly}][\text{TAG}] + k_2[\text{DAG}][\text{MAG}] - k_5[\text{TAG}][\text{MAG}] \\ & + k_6[\text{DAG}]^2 - k_7[\text{TAG}][\text{H}_2\text{O}] + k_8[\text{DAG}][\text{FFA}] \end{aligned} \quad (2.8c)$$

$$\begin{aligned} \frac{d[\text{FFA}]}{dt} = & k_7[\text{TAG}][\text{H}_2\text{O}] - k_8[\text{DAG}][\text{FFA}] + k_9[\text{DAG}][\text{H}_2\text{O}] \\ & - k_{10}[\text{MAG}][\text{FFA}] + k_{11}[\text{H}_2\text{O}][\text{MAG}] - k_{12}[\text{Gly}][\text{FFA}] \end{aligned} \quad (2.8d)$$

$$\begin{aligned} \frac{d[\text{H}_2\text{O}]}{dt} = & -k_7[\text{TAG}][\text{H}_2\text{O}] + k_8[\text{DAG}][\text{FFA}] - k_9[\text{DAG}][\text{H}_2\text{O}] \\ & + k_{10}[\text{MAG}][\text{FFA}] - k_{11}[\text{H}_2\text{O}][\text{MAG}] + k_{12}[\text{Gly}][\text{FFA}] \end{aligned} \quad (2.8e)$$

$$\begin{aligned} \frac{d[\text{Gly}]}{dt} = & -k_1[\text{Gly}][\text{TAG}] + k_2[\text{DAG}][\text{MAG}] - k_3[\text{Gly}][\text{DAG}] \\ & + k_4[\text{MAG}]^2 + k_{11}[\text{MAG}][\text{H}_2\text{O}] - k_{12}[\text{Gly}][\text{FFA}] \end{aligned} \quad (2.8f)$$

The initial water concentration was calculated using Equation (2.9),

$$\% \text{ Water (w/w)} = \frac{(\text{Gly/Oil})(n_{\text{TAG}_0})(92.09 \text{ g/mol})(\% \text{H}_2\text{O}_{\text{Added}} + 0.04)}{Wt_{\text{total}}} \quad (2.9)$$

where % water (w/w) is the initial amount of water as a percentage of the total weight of the reactants (oil, glycerol and water) added to the system, Gly/Oil is the glycerol-oil molar ratio,  $n_{TAG_0}$  is the initial number of moles of TAG, 92.09 g/mol is the molecular weight of glycerol, % H<sub>2</sub>O<sub>Added</sub> is the percentage of water (as wt % of glycerol) added to the reaction system as reported by Temelli et al. [7], 0.04 is the percentage of water (w/w) in the glycerol reagent used by Temelli et al. [7] and  $Wt_{total}$  is the total weight of the reactants. Since the actual concentration of water was known at time zero, it was also possible to estimate the change in water concentration over time. This was achieved by subtracting the experimental FFA concentration from the calculated water concentration obtained in Eq. (2.9), since formation of every mole of FFA requires the utilization of one mole of water (Eqs. (2.5)-(2.7)).

### 2.2.3. Determination of rate constants

To calculate  $k_{1-12}$  in Eqs. (2.8a)-(2.8f), the change of concentrations over time for each chemical species (TAG, DAG, MAG, FFA, water and glycerol) had to be known. Unfortunately, no experimental data or direct algebraic equations were available to establish the change of concentration over time for glycerol. Therefore, in the first set of calculations, glycerol was assumed to be in excess and the rate of change in glycerol concentration was omitted to determine a set of  $k$ -values, called  $k'_{1-12}$ . Then, in the second set of calculations, Equation (2.8f) and  $k'_{1-12}$  were used

to determine the rate of change in glycerol concentration, which was then used to determine  $k_{1-12}$ .

To facilitate calculations, the experimentally determined [7] change of concentrations over time for TAG, DAG, MAG, and FFA as well as the calculated change of concentration over time for water were converted into mathematical expressions. This was achieved using a curve fitting computer program [13], which had a built-in “curve finder” capable of fitting >35 regression models as well as custom models and then ranking the fits from best to worst. Using this program, TAG data were best described by a Harris Model [ $y = 1/(a+b \cdot t^c)$ ] ( $R^2$  range 0.94 - 0.99), DAG by a Logistic Model [ $y=a/(1+b \cdot e^{-c \cdot t})$ ] ( $R^2$  range 0.89 - 0.99), FFA by a MMF Model [ $y=(a \cdot b+c \cdot t^d)/(b+t^d)$ ] ( $R^2$  range 0.90-0.99), MAG by two segments of linear fit [ $y=a+b \cdot t$ ] ( $R^2$  range 0.93-0.99) and H<sub>2</sub>O by linear fit ( $R^2$  range 0.69 - 0.93) where  $a, b, c, d$  were fixed constants determined by the program and  $t$  was the time. Using these mathematical expressions, molar concentration ( $C_{\text{exp}}$ ) for each component (TAG, DAG, MAG, FFA and H<sub>2</sub>O) was obtained for every 12 min time interval over the 4 h reaction period.

To calculate  $k'_{1-12}$ , the  $C_{\text{exp}}$  values were introduced into Eqs. (2.8a)-(2.8e) along with variable  $k'_{1-12}$  values and the estimated rate of change ( $r'_{\text{pred}}$ ) in the concentration of TAG, DAG, MAG, FFA and H<sub>2</sub>O was obtained. The following expression was then used to obtain the predicted concentration ( $C'_{\text{pred}}$ ) for each component:

$$C'_{\text{pred}} = C'_{|t+\Delta t} = C|_t + r'_{\text{pred}} \cdot \Delta t \quad (2.10)$$

where  $C|_{t+\Delta t}$  is the concentration at time  $t + \Delta t$ ,  $C|_t$  is the previously obtained concentration at time  $t$  and  $\Delta t$  is the time interval. The summed squared error (SSE) between  $C_{\text{exp}}$  and  $C'_{\text{pred}}$  was then obtained using the expression  $\Sigma(C_{\text{exp}} - C'_{\text{pred}})^2$ . Using the Generalized Reduced Gradient (GRG2) nonlinear optimization code [14] and the constraint that  $k'$  had to be positive and less than or equal to 1, the sum of SSE for all components between 0-4 h was minimized to obtain  $k'_{1-12}$ .

The rate of change for glycerol was then estimated by introducing the newly calculated  $k'_{1-12}$  and the original experimentally determined molar concentrations into Eq. (2.8f). The molar concentration for glycerol was then obtained using Eq. (2.10) and described by a linear fit equation. From this linear fit,  $C_{\text{exp}}$  for glycerol was obtained ( $R^2 > 0.80$ ) for every 12 min time interval over the 4 h reaction period.

To calculate  $k_{1-12}$ , the  $C_{\text{exp}}$  for TAG, DAG, MAG, FFA, and glycerol were introduced into Eqs. (2.8a)-(2.8f) along with variable  $k_{1-12}$  and the rate of change,  $r_{\text{pred}}$ , of each component was obtained. The following expression was then used to obtain the predicted concentration ( $C_{\text{pred}}$ ) for each component:

$$C_{\text{pred}} = C|_{t+\Delta t} = C|_t + r_{\text{pred}} \Delta t \quad (2.11)$$

Using the GRG2 program [14] and the constraints described above, the SSE between  $C_{\text{exp}}$  and  $C_{\text{pred}}$  for all components over the 4 h period was minimized to obtain the actual  $k_{1-12}$ . In all cases, 98% of the variation in  $C_{\text{pred}}$  was accounted for in the model.



The rate constants,  $k'_{1-12}$  and  $k_{1-12}$ , were calculated for three sets of experimental parameters [7]: water concentrations of 3-8% w/w (at 20.7 MPa, and Gly/Oil ratio of 25), glycerol/oil ratio of 15, 20, 25 (at 41.4 MPa, and 4% water) and pressures of 20.7, 41.1, 62.1 MPa (at Gly/Oil ratio of 15, and 6% water).

### **2.3. Results and discussion**

#### *2.3.1. Chemistry of the glycerolysis of soybean oil*

The mechanism proposed for the glycerolysis reaction in the presence of SC-CO<sub>2</sub> media is described in Eqs. (2.2)-(2.4). This mechanism is based on the chemical equation for glycerolysis of oils as given by Sonntag [6]. While this mechanism accounts for the production of MAG and DAG, it does not explain the formation of FFA observed by Temelli et al. [7]. Therefore, both the hydrolysis and the glycerolysis reactions were considered. The hydrolysis reactions are described in Eqs. (2.5)-(2.7). This additional parallel process might be further complicated by the different phases potentially present inside the reactor, namely the lipid phase, aqueous phase (glycerol and water) and critical phase. Unfortunately, when conducting this study it was not known if the reactions described in the preceding equations were taking place in one or more phases, thus the system was assumed to be homogeneous under the tested conditions for the purpose of kinetic modeling carried out in this study. This assumption greatly simplified calculations for if the

system had been considered non-homogeneous potential mass transfer controlled steps would have complicated the kinetic study.

Eqs. (2.2)-(2.7) are reversible reactions, which are controlled by concentration effects and reaction equilibrium. These equations are also consecutive reactions where the product of one is the substrate for the subsequent step. For instance, Eq. (2.1) consists of two steps: first TAG reacts with Gly to form MAG plus DAG, then this newly formed DAG reacts with a second Gly molecule to form more MAG. If the rate constant of the first step of the reaction is larger than that of the second step, then the second step of the reaction controls the net rate at which MAG is produced. Eqs. (2.2)-(2.7) are further complicated by the fact that glycerolysis and hydrolysis occur simultaneously. This means that both reactions occur in parallel and that the DAG formed in Eq. (2.2) can be used up in Eqs. (2.3)-(2.6). Such parallel reactions add another level of complexity to the system, which has not been reported previously. The challenge is then to obtain the kinetic parameters to describe the relationships between the different reaction steps.

### 2.3.2. Kinetics – constraint and assumptions

The aim of kinetic modeling is to find a reaction mechanism that is consistent with the experimental kinetic data. To achieve this, it was necessary to set the following constraint:  $k_{1-12}$  should have positive values between zero and one. Such an upper limit had to be set for the  $k$ -values in the absence of equilibrium concentrations for the different species. Assumptions were made to obtain the

change in glycerol concentration as a function of time. Because excess glycerol was used, where the initial concentration of glycerol was at least 15 times that of TAG [7], it was assumed that the molar concentration of glycerol did not change appreciably throughout the 4 h reaction. Consequently, the reactions involving glycerol were assumed to follow pseudo first order kinetics. This meant that the glycerol concentration was not required to calculate the  $k'$ -values because the effect of glycerol was embedded into them. It was then assumed that these  $k'$ -values could be used to obtain the change in glycerol concentration as a function of time. This approach allowed the determination of actual  $k_{1-12}$  values in the second step. Later, determination of the glycerol content as a function of time through material balance and reaction stoichiometry confirmed these results.

### 2.3.3. Trends in calculated rate constants

The values for  $k_{1-12}$  are presented in Table 2.1 for different levels of water content and glycerol/oil ratio and in Figure 2.1 for different levels of pressure. Based on these results, one could assume that reactions described by Eqs. (2.2)-(2.6) were not reversible. In addition, only the reverse reaction of Eq. (2.7) occurred. This was particularly evident when glycerol was considered to be in excess. Indeed, in some cases the  $k_{12}$  obtained by assuming excess glycerol were double those obtained using the estimate for glycerol concentration. This clearly demonstrates the importance of the excess glycerol on the reaction rate. Aside from

**Table 2.1.** Effect of glycerol/oil ratio and water content on rate constants

Rate constant (g/h mol)	<i>k</i> -values <sup>a</sup>			<i>k</i> -values <sup>b</sup>				
	Initial Glycerol/Oil ratio			Initial water concentration (% w/w)				
	15	20	25	3	4	6	7	8
<i>k</i> <sub>1</sub>	0.04	0.03	0.02	0.04	0.04	0.04	0.04	0.05
<i>k</i> <sub>2</sub>	0	0	0	0	0	0	0	0
<i>k</i> <sub>3</sub>	0	0	0	0.06	0.02	0.03	0	0
<i>k</i> <sub>4</sub>	0	0	0	0	0	0	0	0
<i>k</i> <sub>5</sub>	1.00	1.00	1.00	1.00	1.00	1.00	1.00	1.00
<i>k</i> <sub>6</sub>	0	0	0	0	0	0	0	0
<i>k</i> <sub>7</sub>	0.07	0.06	0.04	0.06	0.07	0.07	0.07	0.07
<i>k</i> <sub>8</sub>	0	0	0	0	0	0	0	0
<i>k</i> <sub>9</sub>	0.09	0.02	0.07	0	0.41	0.28	0.36	0.39
<i>k</i> <sub>10</sub>	0	0	0	0	0	0	0	0
<i>k</i> <sub>11</sub>	0	0	0	0	0	0	0	0
<i>k</i> <sub>12</sub>	0.09	0.07	0.08	0.09	0.30	0.13	0.13	0.13

<sup>a</sup>Initial water content = 4% (w/w), Pressure = 41.4 MPa.

<sup>b</sup>Initial Glycerol/oil ratio = 25, Pressure = 20.7 MPa.

*k*<sub>12</sub> values, *k*<sub>1</sub> values demonstrated a similar trend, making it evident that only reaction steps involving glycerol were affected by the pseudo first order kinetics assumption. Apart from this, *k*<sub>5</sub>-values equal to the upper limit assumed for this study were consistently obtained under all tested conditions. This is probably due to the large excess of TAG in the reactants and to the accumulation of MAG with time, which dramatically switches the equilibrium of the reaction towards the production of DAG.

### 2.3.4. Effect of water

During the initial stages of this study, in an effort to simplify the reaction kinetics, water was assumed to be in excess. However, this assumption did not hold and was eliminated from further consideration; especially at the lower water concentration where  $k_4$  values were found to be larger than  $k_3$ , a situation that might not be chemically feasible considering the high initial glycerol concentration. Indeed, a reaction that would produce glycerol would act against a large concentration gradient, unless low amount of glycerol is present in the oil phase.

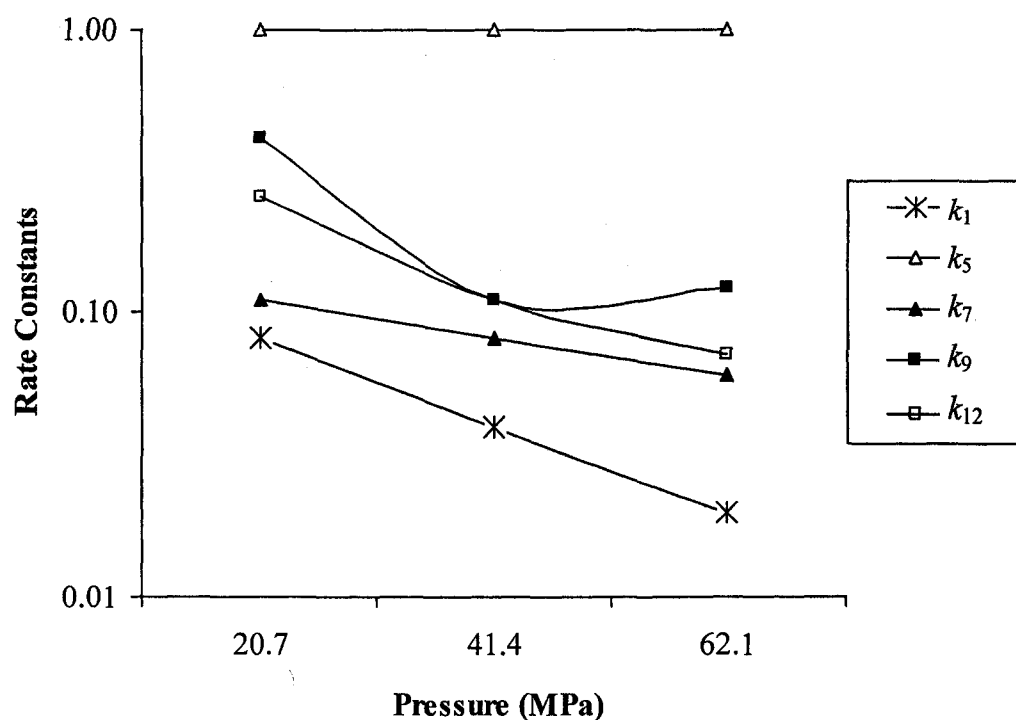


**Figure 2.1.** Rate constants as a function of pressure where the initial water content was 6% (w/w) and the initial Glycerol/Oil ratio was 15.

Figure 2.2 shows that, up to 3.5 h, more MAG was produced with an initial water content of 8% (w/w) compared to that at lower water levels. With the exception of the initial water concentration of 3% (w/w), comparable amounts of MAG were produced at all water levels at the end of the 4 h reaction period. These results therefore demonstrate the positive influence of water on MAG production.

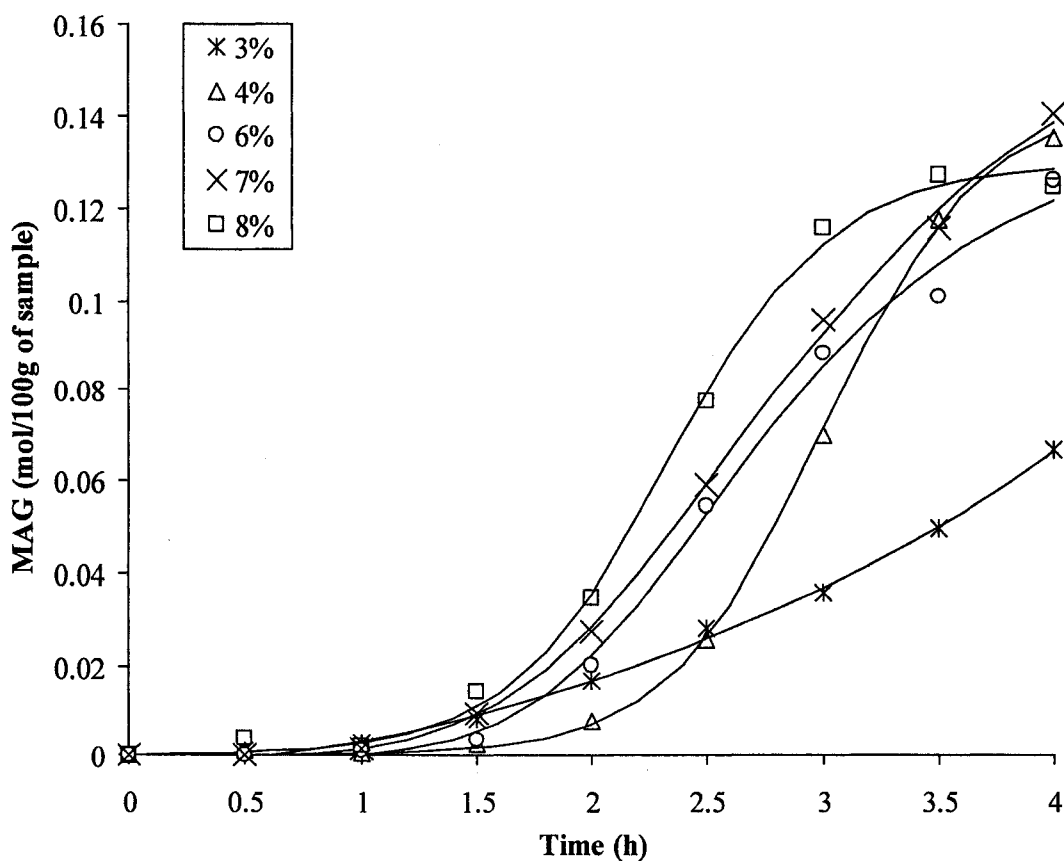


**Figure 2.2.** MAG formation as a function of time where the initial Glycerol/Oil ratio was 25, pressure was 20.7 MPa and different levels (3-8%, w/w) of initial water content were used. Symbols represent experimental data obtained by Temelli et al. [7] and lines are best fit curves obtained by modeling the data.

The rate constants reported in Table 2.1 were expected to have similar values at different water levels because they were conducted at the same pressure (20.7 MPa), temperature (250 °C) and glycerol/oil ratio of 25. However, this does not seem to be the case when lower water concentrations are used. In fact, at 3% (w/w) water the forward reaction of Eq. (2.3) occurred while that of Eq. (2.6) did not thereby indicating a tendency towards glycerolysis at lower water concentrations. On the other hand, the opposite was true at higher water concentrations tested, where hydrolysis was more predominant. Although such differences might be a reflection of changes in phase behaviour, it certainly calls for further investigation. Another important observation is the difference in  $k_{12}$ -value (Table 2.1) obtained for reaction at 4% initial water concentration compared to those at other water levels thereby suggesting that these conditions favour esterification.

#### 2.3.5. *Effect of glycerol/oil ratio*

As expected, only minor differences were seen between rate constants obtained at 15, 20 and 25 glycerol/oil ratio as presented in Table 2.1. Such differences are within experimental error.

#### 2.3.6. *Effect of pressure*

Figure 2.1 provides rate constants obtained at three tested pressures and suggest a marked pressure effect. It appears that a pressure of 20.7 MPa favours the TAG breakdown because  $k_1$  and  $k_7$  are higher than those obtained at 41.4 and 62.1

MPa. A pressure of 20.7 MPa also increases the reverse reaction of Eq. (2.7). Such results suggest that an increase in pressure, which causes dilution of reactants because higher amounts of SC-CO<sub>2</sub> are solubilized in the oil phase, decreases the rate of glycerolysis. Changes in pressure might also affect the phase behaviour. In addition, it is also possible that the phase behaviour might be changing over time as reaction progresses and emulsifiers such as MAG and DAG are formed.

Results in Figure 2.1 also provide a simple mechanistic description of the overall reaction and permits the identification of the rate limiting step. First TAG are broken down by three reactions (forward reactions of Eqs. (2.2), (2.4), (2.5)) to form MAG, FFA and DAG. DAG are then hydrolyzed by the forward reaction of Eq. (2.6) to form MAG and FFA. Finally, the FFA are used in the reverse reaction of Eq. (2.7) to form more MAG. Out of all these reactions, the ones responsible for the initial breakdown of TAG are the slowest and therefore rate limiting. Consequently, parameters affecting the rate of those reactions must be optimized in order to enhance the efficiency of this process further.

#### **2.4. Conclusions**

In this study, rate constants for the parallel glycerolysis and hydrolysis reactions were estimated for different levels of glycerol/oil ratio, water content and pressure using previously published data [7]. Rate constants were obtained by minimizing the summed squared error between the values calculated from the experimental data and those obtained from the kinetic model. The results suggested



that, at the levels tested, water content and pressure had an effect on rate constants but glycerol/oil ratio did not. Within the assumptions and the limitations of the model, modeling the reaction also demonstrated that glycerol and water concentrations had to be considered in the determination of rate constants, that all reactions considered were non-reversible, the reaction between TAG and MAG to form DAG seemed to be predominant, the esterification reaction seemed to be favoured at 4% water level and that the reactions initially responsible for the breakdown of TAG were slowest and therefore rate limiting. Findings provide rate constant estimates necessary for the optimization of supercritical processes involving glycerolysis reactions for the production of MAG from vegetable oils.

## 2.5. References

- [1] E. Boyle, Monoglycerides in food systems: Current and future uses, *Food Technol.* 51 (1997) 52-59.
- [2] E.A. Flack, N. Krog, The functions and applications of some emulsifying agents commonly used in Europe, *Food Trade Rev.* 40 (1970) 27-33.
- [3] H. Nouredini, D.W. Harkey, M.R. Gutsman, A continuous process for the glycerolysis of soybean oil, *J. Am. Oil Chem. Soc.* 81 (2004) 203-207.
- [4] Z.Y. Li, O.P. Ward, Lipase-catalyzed esterification of glycerol and n-3 polyunsaturated fatty acid concentrate in organic solvent, *J. Am. Oil Chem. Soc.* 70 (1993) 745-748.
- [5] M.A. Jackson, J.W. King, Lipase-catalyzed glycerolysis of soybean oil in supercritical carbon dioxide, *J. Am. Oil Chem. Soc.* 74 (1997) 103-106.
- [6] N.O.V. Sonntag, Glycerolysis of fats and methyl esters – status, review and critique, *J. Am. Oil Chem. Soc.* 59 (1982) 795A-802A.

- [7] F. Temelli, J.W. King, G.R. List, Conversion of oils to monoglycerides by glycerolysis in supercritical carbon dioxide media, *J. Am. Oil Chem. Soc.* 73 (1996) 699-706
- [8] R.K. Kochar, R.K. Bhatnagar, An improved process for the manufacture of monoacylglycerols, *Indian Patent.* 71 (1962) 979
- [9] H. Nouredini, D. Zhu, Kinetics of transesterification of soybean oil, *J. Am. Oil Chem. Soc.* 74 (1997) 1457-1463.
- [10] B. Freedman, R.O. Butterfield, E.H. Pryde, Transesterification kinetics of soybean oil, *J. Am. Oil Chem. Soc.* 63 (1986) 1375-1380.
- [11] D. Darnoko, M. Cheryan, Kinetics of palm oil transesterification in a batch reactor, *J. Am. Oil Chem. Soc.* 77 (2000) 1263-1267
- [12] R.O. Butterfield, Kinetic rate constants determined by a digital computer, *J. Am. Oil Chem. Soc.* 46 (1969) 429-431.
- [13] D.G. Hyams, CurveExpert Version 1.37, Chadwick Court, Hixson, TN, 2001.
- [14] L. Lasdon, W. Allan, Microsoft Excel Solver (GRG2), Frontline Systems, Inc. Incline Village, NV, 2002.

### **3. Kinetic modeling of glycerolysis – hydrolysis of canola oil in supercritical carbon dioxide media using dynamic equilibrium data<sup>1</sup>**

#### **3.1. Introduction**

Recent developments in supercritical fluid technology have shown that these fluids have a promising future in green chemistry. In fact, in addition to being exceptional extraction solvents, supercritical fluids have also been shown to be useful as reaction media. As discussed in Chapters 1 and 2, one important industrial reaction that appears to be well suited for supercritical fluids is the glycerolysis reaction [1] since conventional glycerolysis requires strict and energy-intensive operating conditions. Conducting glycerolysis in supercritical carbon dioxide (SC-CO<sub>2</sub>) simplifies the conventional process because it does not require the addition and removal of any catalyst [1, 2]. Furthermore, due to the high temperature required, it is possible to reach the desirable working pressure with minimal pressurization.

Monoacylglycerol (MAG) and diacylglycerol (DAG) are the most valuable products of glycerolysis. MAG's emulsifying properties have long been exploited by food, pharmaceutical and lubricant manufacturers (Section 1.2.3.1). DAG, on the

---

<sup>1</sup> A version of this chapter was published in the Journal of Supercritical Fluids (37:417-424, 2006).

other hand, has recently attracted attention as a fat that could prevent obesity [3] and atherosclerosis [4], while being beneficial to diabetics [5]

Even though MAG is the most abundant product of the glycerolysis reaction, as shown in Table 1.2, MAG yield varies widely depending on initial reactant concentration and processing conditions. Therefore, to ensure consistently high MAG yields, a more thorough understanding of the reaction kinetics is required. However, the literature lacks the required kinetic studies for the conventional process and the study reported in Chapter 2 is the only known attempt at understanding the kinetics of glycerolysis in SC-CO<sub>2</sub> media. However, in the absence of dynamic equilibrium data, it was only possible to obtain approximate rate constants. Nonetheless, the study reported in Chapter 2 clearly demonstrated that glycerolysis reactions alone might not account for the production of MAG and DAG. Indeed, water is often inadvertently added to the reactants due to the hydrophilic properties of glycerol. When this occurs, hydrolysis takes place in parallel to glycerolysis, resulting in the formation of free fatty acids (FFA). The previously reported study (Chapter 2) also showed that, to understand and optimize such a complex system, the rate constants of six reversible independent reactions had to be determined. Based on these findings, it was hypothesized that some catalytic effect is occurring under the investigated conditions of 250 °C as glycerolysis could only occur at a reasonable rate if the reactants were heated to 287 °C [6]. However, the nature of any potential catalysis occurring in SC-CO<sub>2</sub> media is

not known. The objectives of this study were therefore to obtain reliable rate constants by using the concentrations of species at dynamic equilibrium, gain a better understanding of the catalytic agent that might be involved in the glycerolysis-hydrolysis reaction in supercritical media and assess the effect of SC-CO<sub>2</sub> under different conditions on the reaction rates.

### **3.2. Materials and methods**

#### *3.2.1. Materials*

The reactants were commercially refined, bleached and deodorized canola oil graciously donated by Canbra Foods Ltd. (Lethbridge, AB), anhydrous glycerol (Gly) from J.T. Baker (Phillipsburg, NJ, USA), deionized distilled water (DDW), and 99.8% bone dry (water level < 3 ppm) CO<sub>2</sub> and 99.95% compressed nitrogen (N<sub>2</sub>) from Praxair Canada Inc. (Mississauga, ON). Thin layer chromatography-flame ionization detection (TLC-FID) system determinations were performed using analytical grade glacial acetic acid from BDH Inc. (Toronto, ON), and laboratory grade ethyl ether and HPLC grade hexane from Fisher Scientific (Fairlawn, NJ, USA). The TLC reference standard containing 25% (w/w) of each of oleic acid, monoolein, diolein and triolein was obtained from Nu-Chek Prep Inc. (Elysian, MN, USA).

### 3.2.2. Experimental set up and reaction protocols

The reaction was conducted in batch mode in a Nova Swiss (Nova-Werke AG, Effretikon, Switzerland) high pressure, electrically heated, magnetically stirred 200 mL autoclave setup as shown in Figure 3.1. A total volume of 75 mL of reactants, consisting of canola oil, glycerol and DDW were added to the autoclave: the glycerol/oil molar ratio was 34:1 and DDW was 0, 4 or 8% (w/w of glycerol). When mixing reactants for the anhydrous reactions (0% water), the autoclave was flushed with a flow of dry nitrogen to prevent the accumulation of moisture from

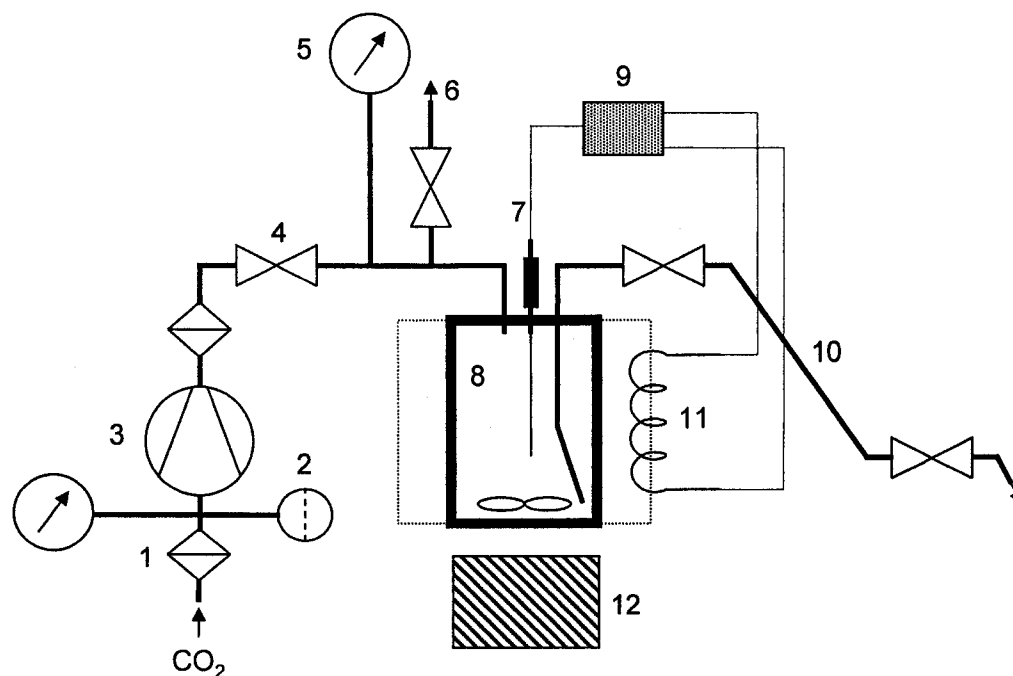


**Figure 3.1.** Schematic of the experimental apparatus: (1) filter, (2) rupture disk, (3) compressor, (4) on-off valve, (5) pressure gauge, (6) vent, (7) thermocouple, (8) reactor, (9) temperature controller, (10) sampling tube, (11) electric heater, (12) magnetic stirrer.

the air. Once the autoclave was sealed, the reaction mixture was purged with CO<sub>2</sub> or N<sub>2</sub> and constantly stirred (~100 rpm). Tank pressure CO<sub>2</sub> or N<sub>2</sub> (~6 MPa) was then added to the autoclave before increasing the temperature to 250 °C. Once the desired temperature was established, the autoclave was pressurized to 10, 20 or 30 MPa and the mixing rate was increased to 250 ± 30 rpm. Samples (1 mL) were collected by building vacuum in the sampling tube and then filling the sampling tube with reaction mixture taken 2 mm from the bottom of the autoclave. The sampling port on the system made sample collection during the reaction possible without significantly affecting the pressure inside the autoclave. The length of the sampling tube between the two on-off valves was designed to be slightly longer than the total length of tubing extending from the bottom of the autoclave to the first on-off valve. During sample collection, the first sample, which comprised of the stagnant material left in the tube since the last sampling, was discarded, the content of the sampling tube was sucked dry by vacuum and then a second sample was taken. Samples were collected every 30 min for 4 h reactions and every hour for 10 h reactions. For 14 h reactions, samples were collected every two hours but after 10 h a sample was collected every hour. These different sampling protocols were implemented in order to maximize kinetic data while minimizing the disturbance of the equilibrium of the reactions.

### 3.2.3. Lipid analysis

The samples, collected as a function of time throughout the reactions conducted at different conditions, separated into two phases upon standing at ambient conditions. In this study, only the composition of the oil layer was analyzed using TLC-FID. The oil was separated into triacylglycerol (TAG), DAG, MAG and FFA on Chromarods-SIII (silica gel type) and quantified using an Iatroscan TH-10 (IATRON-Laboratories Inc., Tokyo, Japan). The analysis was performed by plotting 0.6  $\mu\text{L}$  of a solution containing 0.03 g oil and 5 mL hexane on previously scanned and dried (120 °C for 20 min) chromarods, developing the rods in a solution of hexane/diethyl ether/acetic acid (80:20:1) for 20 min, evaporating the solvent at 120 °C for 10 min and scanning at hydrogen pressure of 113 kPa, air flow rate of 2 L/min, and a scan speed of 30 s/rod in the Iatroscan. For each duplicated analysis, samples were randomly plotted on nine of the ten rods and the TLC external standard was plotted on the remaining rod. Chromatograms were recorded and integrated by Shimadzu CLASS-VP<sup>TM</sup> version 4.2 (Columbia, MD, USA) software. Extensive calibration runs demonstrated that the area percent was  $25 \pm 2\%$  for each of the components of the external standard, which contained 25% (w/w) of each of oleic acid, monoolein, diolein and triolein. The area percentage was therefore used to obtain the weight percentage with a response factor of one within  $< 10\%$  variation. This approach is consistent with Indrasena et al. [7] who reported that the main neutral lipid classes can be monitored closely with the TLC-FID



method using area percentages. It is also in agreement with data obtained by Stephens et al. [8] showing that the FID detector yields response factors that are consistently at or close to one. Molar concentrations were calculated by dividing the '% Area' by an average weight. For DAG, MAG and FFA, the molecular weights used were 621.0, 356.6 and 282.5 a.m.u, respectively, which represent diolein, monoolein and oleic acid, since oleic acid is the most abundant fatty acid in canola oil [9]. For TAG, the average molecular weight of canola oil, 879 a.m.u, was used [10]. All concentrations are reported as mol per 100 g of oil.

#### 3.2.4. *Statistical analysis*

The experimental design was a  $3 \times 3$  split plot with each block consisting of a replicate. A complete set of replicated 4 h runs were conducted in SC-CO<sub>2</sub> at 10, 20 and 30 MPa and 0, 4 and 8% (w/w) water. Later, replicated 14 h runs were conducted in SC-CO<sub>2</sub> at 10 MPa and 4 and 8% (w/w) water. Replicated 10 h reactions were also conducted in SC-CO<sub>2</sub> at 20 and 30 MPa and 8% (w/w) water. Two replicated runs were done in SC-N<sub>2</sub> at 10 MPa and 8% (w/w) water. The composition of the samples obtained for each of the above runs was analyzed in duplicate by TLC-FID analyses and the variance, as obtained by analyzing all the TLC reference standard chromatograms, was less than 10%. Analysis of variance of the maximum rate of MAG formation was performed using the Mixed Model procedure of SAS Statistical Software version 9.1 and means for different treatments were compared using Student's t-test [11]. Results were reported as

statistically significant when the p-value was smaller than or equal to 0.05 ( $p \leq 0.05$ ); however, where applicable, the exact p-value obtained by the above software was reported.

### 3.2.5. *Kinetic modeling*

As previously reported in Section 2.2.2, glycerolysis (Eqs. (2.2)-(2.4)) and hydrolysis (Eqs. (2.5)-(2.7)) reactions could potentially occur simultaneously. By amalgamating the reaction steps described in Eqs. (2.2)-(2.7), the rate of change in concentration for each of the reaction components was described by the differential rate equations presented previously, Eqs. (2.8a)-(2.8f).

### 3.2.6. *Determination of rate constants*

The change in water concentration as a function of time was not determined experimentally but rather calculated as a function of time based on reaction stoichiometry using the initial amount of water and the FFA content. Indeed, Eqs. (2.5)-(2.7) illustrate that the production of one mol of FFA requires one mol of water and therefore the change in water concentration can be obtained by subtracting the molar content of FFA per 100 g of oil from that of water. The change in glycerol was also not determined experimentally and had to be calculated from the following material balance equation:

$$[\text{Gly}]_t = ([\text{Oil}]_0 + [\text{Gly}]_0) - ([\text{TAG}]_t + [\text{DAG}]_t + [\text{MAG}]_t) \quad (3.1)$$

where  $[\text{Oil}]_0$  and  $[\text{Gly}]_0$  are the initial molar concentrations of oil and glycerol, respectively, and  $[\text{Gly}]_t$ ,  $[\text{TAG}]_t$ ,  $[\text{DAG}]_t$  and  $[\text{MAG}]_t$  are the molar concentrations of the respective components at time  $t$ .

For modeling purposes, all the individual TLC-FID analyses for duplicated runs were combined and the change in concentration over time for each component was expressed using a mathematical expression. The equation of best fit was obtained using a curve fitting computer program [12]. Using this program, TAG data were described by a Harris Model  $[y = 1/a + b \cdot x^c]$  ( $R^2$  range 0.98 - 0.99), and FFA, MAG and water by a Logistic Model  $[y = a/(1 + b \cdot e^{-c \cdot t})]$  where the  $R^2$  range for each component was 0.74 - 0.87, 0.96 - 0.98, 0.73 - 0.78, respectively. The changes in concentration of glycerol and DAG were slightly different after 4 h and therefore two distinct models had to be used to fit the data. Glycerol data were described by a Harris model up to 4 h and then by a MMF Model  $[y = (a \cdot b + c \cdot t^d)/(b + t^d)]$  ( $R^2$  range 0.94 - 0.98), and DAG by a Rational Function  $[y = (a + bx)/(1 + cx + dx^2)]$  and Weibull Model  $[y = a - b \cdot \exp(-c \cdot x^d)]$  ( $R^2$  range 0.72 - 0.90). In each model,  $a$ ,  $b$ ,  $c$  and  $d$  were fixed constants determined by the program and  $t$  was the time. Using these mathematical expressions, experimental molar concentration ( $C_{\text{exp}}$ ) for each component (TAG, DAG, MAG, FFA and  $\text{H}_2\text{O}$ ) was obtained every 12 min over a 4 h period. These  $C_{\text{exp}}$  were then introduced into Eqs. (2.8a)-(2.8f) along with variable  $k$ -values ( $k_{1-12}$ ) and the rate of change ( $r_{\text{pred}}$ ) of each

component was obtained over the same period as for  $C_{\text{exp}}$ . The following expression was then used to obtain the predicted concentration ( $C_{\text{pred}}$ ) for each component:

$$C_{\text{pred}} = C|_{t+\Delta t} = C_{\text{exp}}|_t + r_{\text{pred}} \Delta t \quad (3.2)$$

where  $C_{\text{exp}}|_t$  is the concentration at time  $t$ ,  $\Delta t$  is the time interval (12 min) and  $C|_{t+\Delta t}$  is the concentration at  $t + \Delta t$ . The summed squared error (SSE) between  $C_{\text{exp}}$  and  $C_{\text{pred}}$  was then obtained for each component using the expression  $\Sigma(C_{\text{exp}} - C_{\text{pred}})^2$ .

Two  $k$ -values,  $k_9$  and  $k_{12}$ , were calculated by introducing dynamic equilibrium data obtained after 10 h in the following equilibrium equations:

$$k_9 = \frac{k_3([\text{Gly}]_\infty)([\text{DAG}]_\infty) + k_4([\text{MAG}]_\infty)^2 + k_{10}([\text{MAG}]_\infty)([\text{FFA}]_\infty)}{([\text{DAG}]_\infty)([\text{H}_2\text{O}]_\infty)} \quad (3.3)$$

$$k_{12} = \frac{k_3([\text{Gly}]_\infty)([\text{DAG}]_\infty) + k_4([\text{MAG}]_\infty)^2 + k_{11}([\text{MAG}]_\infty)([\text{H}_2\text{O}]_\infty)}{([\text{Gly}]_\infty)([\text{FFA}]_\infty)} \quad (3.4)$$

where  $[\text{Gly}]_\infty$ ,  $[\text{DAG}]_\infty$ ,  $[\text{MAG}]_\infty$ ,  $[\text{FFA}]_\infty$  and  $[\text{H}_2\text{O}]_\infty$  are mol/100 g oil at 10 h. Eqs. (3.3) and (3.4) were derived from Eqs. (2.8a)-(2.8f) where the rate of change is zero at equilibrium.  $[\text{TAG}]$  was equal to zero at equilibrium, which meant that any reaction producing TAG did not occur. Hence,  $k_2$ ,  $k_6$  and  $k_8$  were equal to zero.

Using the Generalized Reduced Gradient (GRG2) nonlinear optimization code [13], the above  $k$ -values and the constraint that  $k$  had to be positive, the SSE for all components was minimized while changing  $k_1$ ,  $k_3$ ,  $k_4$ ,  $k_5$ ,  $k_7$ ,  $k_{10}$  and  $k_{11}$  to determine these rate constants.

### 3.3. Results and discussion

#### 3.3.1. *Composition and reaction rates*

The compositional analysis of the oil by TLC-FID offered a relatively fast separation of the complex reaction mixture into TAG, DAG, MAG and FFA by TLC followed by quantification by FID. As reported by Fraser et al. [14], as long as an adequate standard mixture is used, fast and accurate analysis can be conducted using TLC-FID. Even though it would be desirable to analyze the total mixture including water and glycerol components, there is no rapid method to analyze them simultaneously with the lipid components. In addition, it is the oil layer that is the desirable product industrially, which separates from glycerol upon cooling of the reaction mixture at the end of the reaction time.

A TLC-FID chromatogram of the oil mixture collected at 4 h of reaction in SC-CO<sub>2</sub> at 250 °C, 30 MPa and 8% (w/w) initial water is shown in Figure 3.2. This is a typical TLC-FID chromatogram obtained by scanning the rod from top to bottom. Two distinctive overlapping peaks were obtained for the different DAG isomers, as well as a clearly defined peak for MAG and a slight overlap between the baseline of TAG and FFA. In the chromatogram of oil mixtures collected after 10 h, an extra peak corresponding to glycerol appeared at the origin (0.48 min) indicating that glycerol did not elute with the solvent system used. The only explanation for

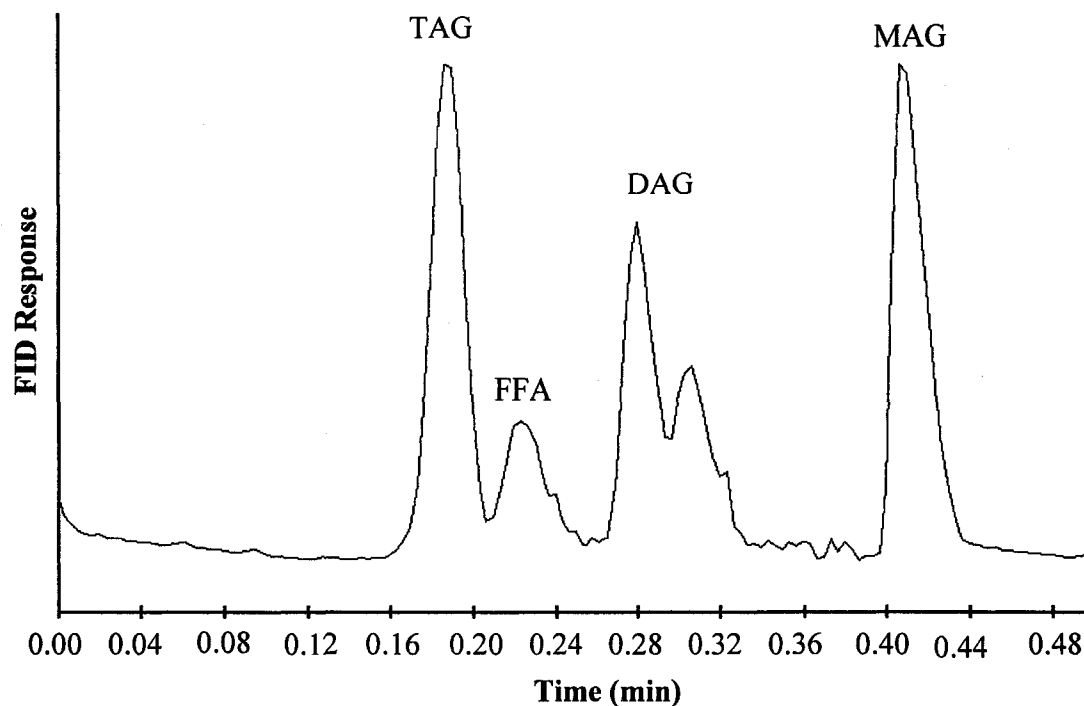


**Figure 3.2.** Thin layer chromatography-flame ionization detection chromatogram as a function of time for a sample collected after 4 h in SC-CO<sub>2</sub> at 250 °C, 30 MPa and 8% (w/w) initial water.

the presence of glycerol in the oil layer was that glycerol was emulsified by the large amount of MAG and DAG present in the samples collected at 10 h.

Figure 3.3 shows the composition data and the fitted curves of the oil phase obtained as a function of time. The rapid increase in MAG after 2 h and the exponential decrease in TAG are apparent. Furthermore, TAG concentration becomes negligible as the system reaches dynamic equilibrium at 9 h.

Upon conducting a material balance, it became apparent that the total amount of fatty acids decreased over time. Indeed, there was approximately 11%

difference between the total number of moles of fatty acids between 0 and 10 h samples. Although most of this difference was probably due to the multiple samples removed over 10 h, it is also possible that the sampling and analysis protocol may have contributed to this difference because as the reaction progressed and more emulsifiers were formed, the boundary between oil and glycerol layers was less obvious thereby complicating representative sampling of the oil layer for analysis. Nevertheless, under the circumstances, such a difference most probably had a

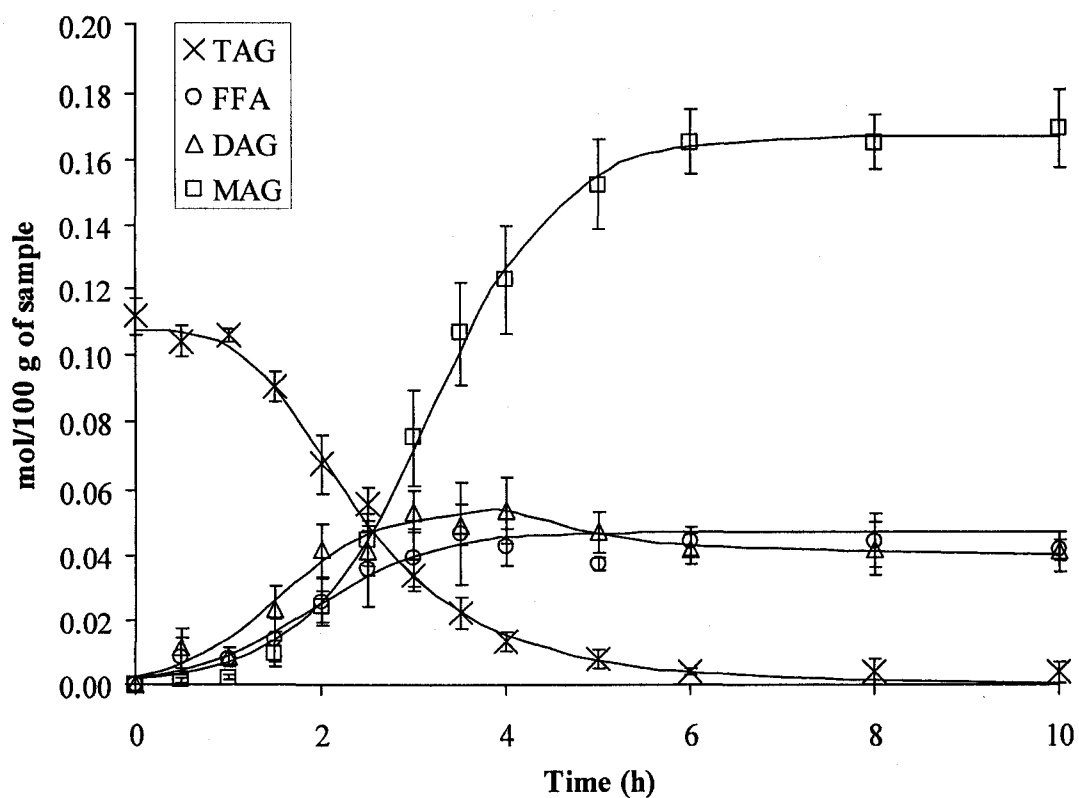


**Figure 3.3.** Experimental data and fitted curves of the composition of the oil phase as a function of time obtained at 250 °C, 10 MPa and 8% (w/w) initial water.

negligible effect on the calculated rate constants.

To ensure that true dynamic equilibrium was reached, the reaction was conducted for up to 14 h but there was no change in concentrations after 10 h.

Figure 3.4 shows the rate of MAG formation as a function of time for reactions ran

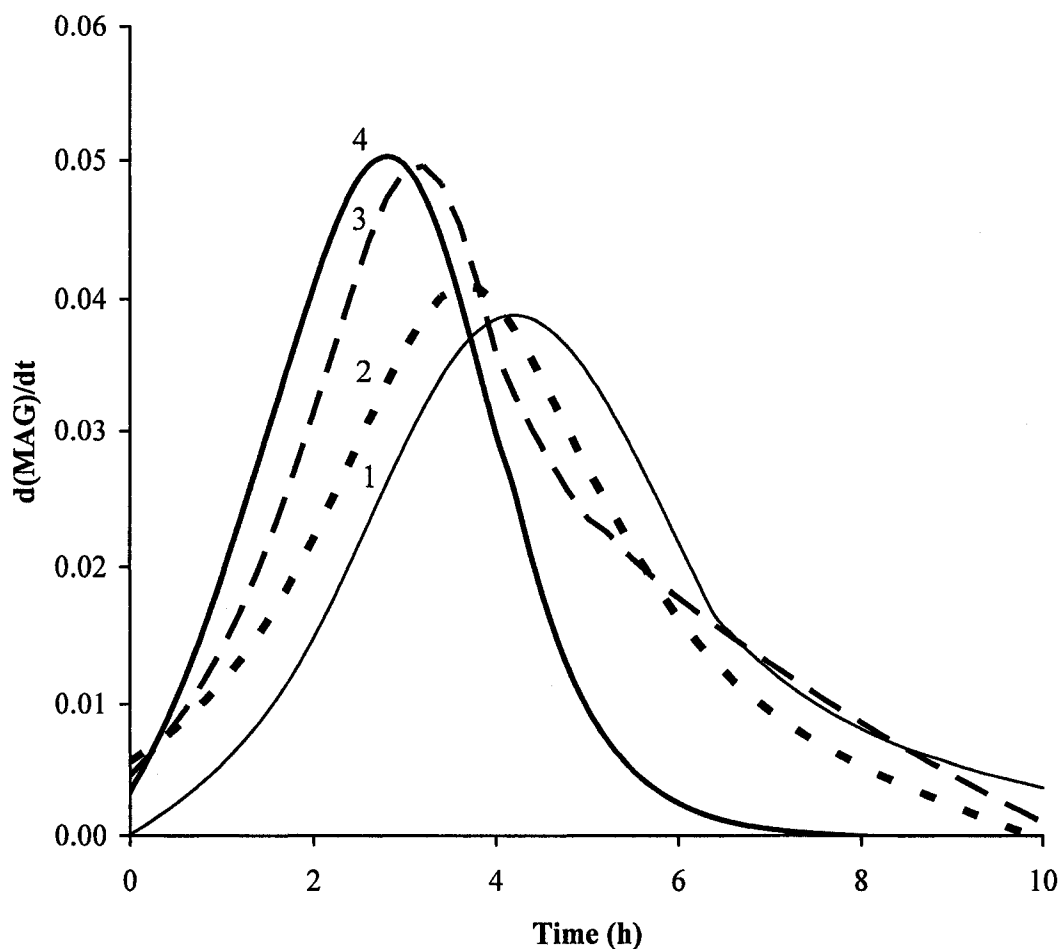


**Figure 3.4.** Rate of MAG formation as a function of time calculated from Eq. (2.8a) using  $k$ -values from Table 3.1 and the concentrations obtained from the fitted data: (1) 10 MPa, 4% (w/w) initial water; (2) 30 MPa, 8% (w/w) initial water; (3) 20 MPa, 8% (w/w) initial water; (4) 10 MPa, 8% (w/w) initial water.



under different pressures and initial water contents. The maximum rate of MAG formation, which is found at the inflection point, was used to compare the different tested conditions. The spread in the bell shape curves in Figure 3.4 as well as the time at which maximum rate of MAG formation is reached, also illustrates the differences in efficiency between the various conditions. For instance, reactions with 8% (w/w) initial water content conducted at 10 MPa peaked at 2.8 h while those conducted at 30 MPa peaked at 3.6 h. To establish kinetic data, it was important to understand the reactions taking place. As previously noted in Chapter 2, the reversible, consecutive glycerolysis (Eqs. (2.2)-(2.4)) and hydrolysis (Eqs. (2.5)-(2.7)) reactions are occurring in parallel to each other. The approach taken to establish the  $k$ -values for these equations and to understand the effect of water and SC-CO<sub>2</sub> on the glycerolysis-hydrolysis reactions required the establishment of a mechanism that was consistent with the experimental data. In order to do this, some assumptions were established. The first assumption was that  $k_{1-12}$  have positive values. The second assumption was that, due to the negligible amount of TAG at equilibrium, all reactions producing TAG should be assigned a rate constant of zero because they most probably did not occur and hence,  $k_2$ ,  $k_6$  and  $k_8$  should be zero. The final assumption was that, two independent equilibrium equations (Eqs. (3.3)-(3.4)) derived by evaluating the differential rate equations (Eqs. (2.8a)-(2.8f)) for dynamic equilibrium conditions, could be used to calculate the rate constants presented in Table 3.1.

### 3.3.2. SC-CO<sub>2</sub> effect

The initial hypothesis for this study was that the formation of MAG was catalyzed by the possible presence of carbonic acid, which usually occurs when water and CO<sub>2</sub> are mixed. However, results plotted in Figure 3.5 refuted this initial hypothesis. Indeed, the maximum rate of MAG formation in SC-CO<sub>2</sub> was similar ( $p > 0.05$ ) to that in SC-N<sub>2</sub>, thereby demonstrating that SC-CO<sub>2</sub> does not contribute to catalysis. The question then remained, is the system catalyzed and if so by what.

**Table 3.1.** Effect of pressure, water and media on the rate constants

Rate Constants (g/h·mol)	SC-CO <sub>2</sub>					SC-N <sub>2</sub>
	10 MPa 0% H <sub>2</sub> O	10 MPa 4% H <sub>2</sub> O	10 MPa 8% H <sub>2</sub> O	20 MPa 8% H <sub>2</sub> O	30 MPa 8% H <sub>2</sub> O	10 MPa 8% H <sub>2</sub> O
$k_1$	0.01	0	0	0	0	0
$k_2$	0	0	0	0	0	0
$k_3$	0.04	0.11	0.17	0.15	0.12	0.13
$k_4$	0	0.54	1.05	0.90	0.54	1.02
$k_5$	2.28	6.58	6.52	9.09	4.75	11.62
$k_6$	0	0	0	0	0	0
$k_7$	0	0.07	0.08	0.05	0.06	0.03
$k_8$	0	0	0	0	0	0
$k_9$	0	0.09	0.06	0.15	0.04	0.19
$k_{10}$	0	0	0	0	0	0
$k_{11}$	0	0	0	0	0	0
$k_{12}$	0	0.02	0.02	0.05	0.01	0.07

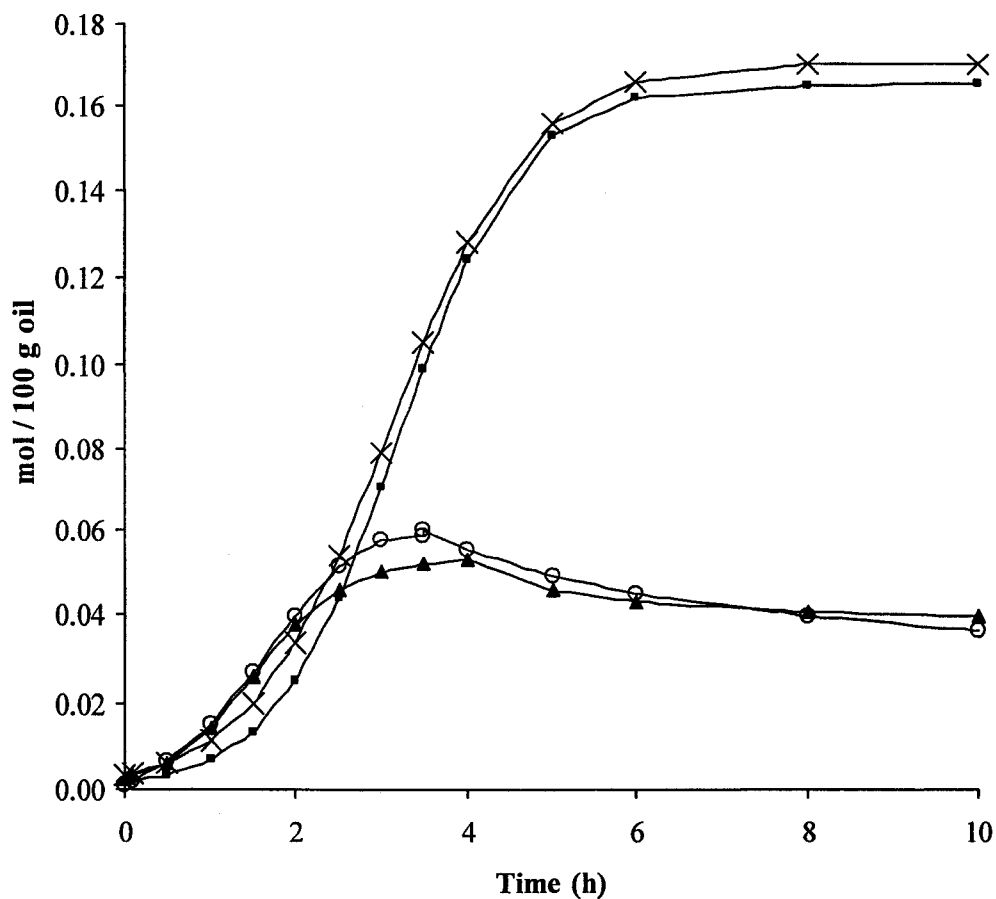


**Figure 3.5.** Effect of SC-N<sub>2</sub> and SC-CO<sub>2</sub> on MAG and DAG production at 250 °C, 10 MPa and 8% (w/w) initial water as a function of time: (■) MAG in SC-CO<sub>2</sub> media, (▲) DAG in SC-CO<sub>2</sub> media, (×) MAG in SC-N<sub>2</sub> media, (○) DAG in SC-N<sub>2</sub> media. Data points and curves are based on the kinetic model.

### 3.3.3. Effect of water

Figure 3.6 shows the amount of MAG produced in reactions containing different initial water contents. Using the maximum rate of MAG formation from Figure 3.4, it was possible to conclude that the rate of MAG formation for reactions

conducted using 4% (w/w) initial water at 10 MPa was significantly higher ( $p = 0.0002$ ) than that of anhydrous reactions and that it was significantly lower ( $p = 0.0052$ ) than that of reactions conducted using 8% (w/w) initial water. From these results, one could wonder if MAG formation was only due to hydrolysis. However, if this was the case, the molar concentration of MAG could not be greater

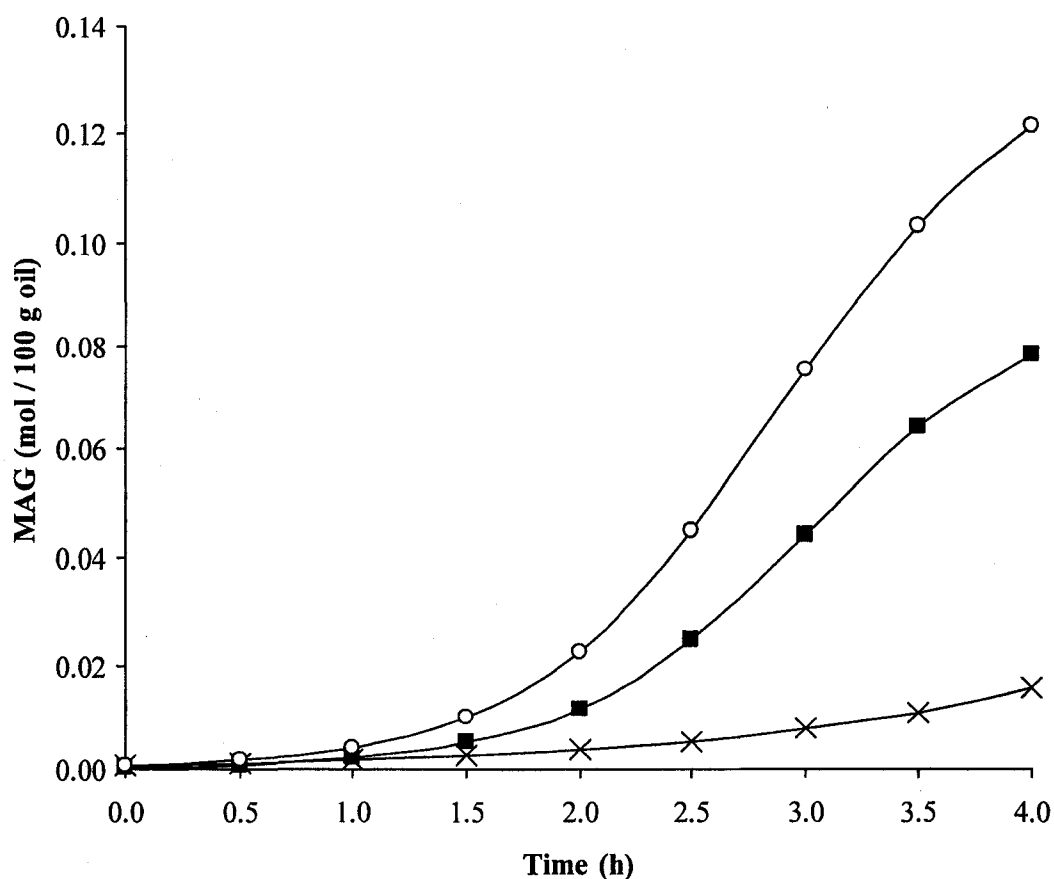


**Figure 3.6.** Effect of initial water content on MAG production at 250°C and 10 MPa as a function of time where (×), (■), (○) are 0, 4 and 8% (w/w) initial water, respectively. Data points and curves are based on the kinetic model.

than that of TAG at  $t = 0$ . Yet, as shown in Figure 3.3, the molar concentration of MAG after 5 h was above that of initial TAG. This means that some glycerol accepted FFA and/or some glycerolysis reaction occurred. Results shown in Table 3.1 for reactions conducted in the presence of water demonstrated that glycerol did accept FFA and DAG also reacted with glycerol to form MAG. Indeed, the rate constants (Table 3.1) for reactions with 4 and 8% initial water had some values above zero for  $k_3$  and  $k_{12}$ . Table 3.1 also shows that reactions conducted with different initial water contents have differences in rate constants. It is important to note that under anhydrous conditions only the forward reactions of Eqs. (2.2)-(2.4) occur. This means that TAG is broken down by Eqs. (2.2) and (2.4) and the DAG formed by both of these reactions are further broken down by Eq. (2.3). In the presence of water, the rate of Eq. (2.4) increases and the hydrolysis of TAG (Eq. (2.5)) take over Eq. (2.2) and quickly hydrolyse TAG into DAG and FFA. The reverse of Eq. (2.3) also contributed to the increase in DAG concentration thereby explaining the rapid rise in DAG as observed in Figure 3.3. The production of MAG is less rapid than that of DAG because the reactions producing MAG have lower rate constants. Indeed, out of the forward reaction of Eq. (2.3) and the reverse reaction of Eq. (2.7), only Eq. (2.3) (controlled by  $k_3$ ) seems to increase with increased initial water content thereby indicating that it has a role to play in the increased production of MAG at the initial water level of 8% (w/w).

Besides affecting the rate constants, water could also help catalyze the reaction. In fact, at the reaction temperature studied (250°C), the self-dissociation constant for water is three times that of water under ambient conditions thereby increasing the number of hydronium and hydroxide ions present and promoting acid/base catalyzed reactions [15]. Furthermore, hydrolysis of TAG forms FFA, which could also be catalyzing the reaction. This potential catalytic effect of water would also partly account for the substantially lower MAG production under anhydrous conditions.

#### 3.3.4. *Effect of pressure*

Based on the results presented in Figure 3.7 and on the maximum rate of MAG production in Figure 3.4, it was possible to conclude that while keeping the level of initial water at 8% (w/w), the rate of MAG formation for reactions conducted at 20 MPa was significantly higher ( $p = 0.0119$ ) than that at 30 MPa whereas the rates obtained at 10 and 20 MPa were similar ( $p > 0.05$ ). In fact, the rate of MAG formation was favoured at 10 and 20 MPa compared to that at 30 MPa (Fig. 3.7). However, Figure 3.4 makes it quite evident that the rates of MAG formation at 10 MPa and 4% (w/w) initial water and 30 MPa and 8% (w/w) initial water were similar. This observation could be due to a decrease in water-oil interaction as the pressure of the system is increased from 10 to 30 MPa. Indeed, Takenouchi and Kennedy [16] who examined the phase equilibria of water-CO<sub>2</sub>

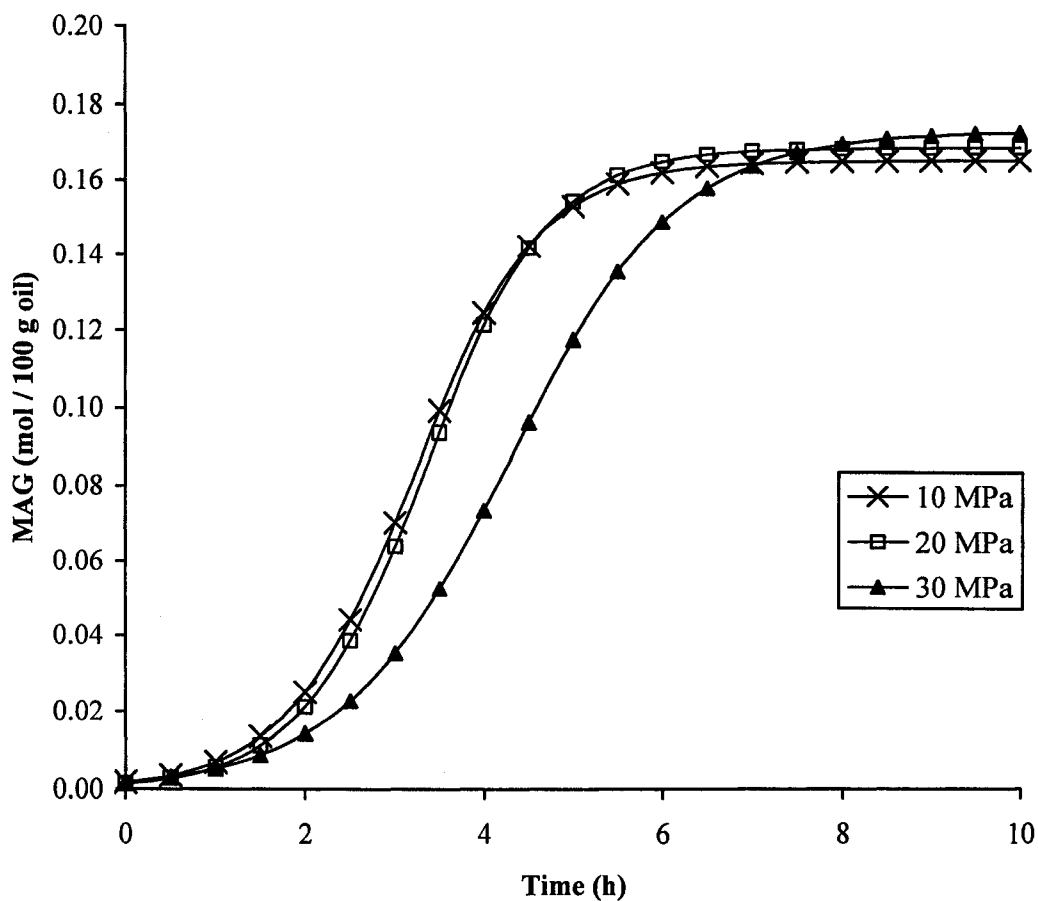


**Figure 3.7.** Effect of pressure on MAG production at 250 °C and 8% (w/w) initial water as a function of time. Data points and curves are based on the kinetic model.

reported that at temperatures below 265 °C, water and CO<sub>2</sub> are not completely miscible and that 2.8% and 5.8% of CO<sub>2</sub> was present in the liquid phase at 10 and 30 MPa, respectively. Assuming these findings [16] apply to the more complex reaction system under investigation in this study, while considering the fact that upon a pressure increase from 10 to 30 MPa more CO<sub>2</sub> was introduced into the

system, then it is possible that less water was present in a liquid phase, which was presumably rich in oil. This means less water was available to react with the oil or similar water levels compared to reactions conducted at 4% water and 10 MPa, thereby explaining why similar rate constants were achieved.

The fact that glycerolysis-hydrolysis reaction rates are similar at 10 and 20 MPa has economical significance because it means that a low pressure is sufficient to achieve the same amount of MAG. Furthermore, it appears that reactions conducted at 10 MPa would not even require the use of a compressor or high pressure pump. Indeed, it was found that when the initial pressure inside the sealed autoclave was 5.5-6 MPa (equivalent to the pressure of the gas cylinder), the pressure increased to 10 MPa upon heating the system to 250°C. It is believed that this finding will greatly reduce the capital and operating cost of glycerolysis-hydrolysis reaction conducted under SC-CO<sub>2</sub> or SC-N<sub>2</sub> media.

### 3.3.5. *Mechanism of the reaction*

It is important to have a good understanding of the phase behaviour of the complex system under investigation and how it influences the reaction. From the above discussion, it is quite evident that water level and pressure did influence the reaction rate of the system and that the progressive formation of MAG and DAG, which are powerful emulsifiers, changed the phase behaviour over the course of the reaction. It is thus possible to suppose that the phase behaviour of the system and



therefore the mass transfer considerations are changing as the reaction progresses. Although the initial phase behaviour or how it evolved over time is not known at this point, it is possible to consider the different mechanisms that may be involved in the glycerolysis-hydrolysis reactions.

Under ambient conditions, oil and glycerol are immiscible and the main reason for conducting glycerolysis reactions at 250 °C is to increase the solubility of glycerol in oil. With the addition of SC-CO<sub>2</sub>, it is possible that there may be three phases (liquid – liquid – vapor) inside the reactor. It is thought that reactions described by Eqs. (2.2), (2.3), (2.5-2.7) are heterogeneous reactions occurring at the interface between the different phases. The rate of these reactions was therefore dependent on mixing rate and the viscosity of the system. The rate of the homogenous reaction, Eq. (2.4) was not affected by phase interactions and this might partially explain the high  $k_5$  values.

As seen in Figure 3.3, DAG production reaches a plateau much sooner than MAG and MAG final concentration is much higher than that of DAG. To understand these results, one can consider what may be taking place in the reactor during the glycerolysis-hydrolysis reactions using reactions conducted at 10 MPa and 8% initial water as an example. At the beginning of the reaction, since neither DAG nor MAG was present in the mixture, only the reaction described by Eq. (2.5) was taking place. As a result, the production of DAG was slightly higher than that of MAG. Later, as the concentration of MAG, DAG and FFA increased but were

still smaller than that of TAG, formation of DAG by reactions described by Eqs. (2.4) and (2.5) and consumption of MAG (Eq. (2.4)) were faster than the formation of MAG by Eqs. (2.3) and (2.7). However, when the amount of TAG became lower, reactions described by Eqs. (2.4) and (2.5) became slower. The reactions given by Eqs. (2.3) and (2.7) then became dominant and, due to the relatively large concentration of glycerol and water, the forward reaction for Eq. (2.3) and the reverse for Eq. (2.7) prevailed. Thus, the amount of MAG increased and the amount of DAG decreased. Finally, when the concentration of TAG became negligible, reactions given by Eqs. (2.3) and (2.6) solely took place and dynamic equilibrium was established.

To explain the fact that there is a significant difference between 20 and 30 MPa but not between 10 and 20 MPa, one could consider the potential dilution and/or differential viscosity effect that could only be experienced above 20 MPa. With an increase in pressure, the amount of CO<sub>2</sub> in a liquid phase would increase [16]. Considering the non-polar nature of CO<sub>2</sub>, it is expected that more CO<sub>2</sub> would be present in the oil layer as opposed to the glycerol layer, thereby reducing the viscosity of the oil layer to a greater extent than that of the glycerol layer [17]. This leads to an increase in interfacial tension between the oil and glycerol phases. Such conditions would not be beneficial to MAG formation at the interface.

One might also wonder why the rate constant  $k_4$  was higher than  $k_3$  considering the large excess of glycerol. The answer may again lie in the phase

behaviour of the system. As the reaction progressed, more MAG and/or DAG were present to effectively emulsify the glycerol inside the oil layer. Another interesting observation that might be related to this emulsification phenomenon and which is quite apparent in Figure 3.3 is the slow breakdown of DAG between 4 and 5 h. Considering all the reactions in Eqs. (2.2)-(2.7), only the forward reaction of Eq. (2.3) ( $k_3$ ) could explain the breakdown of DAG at these conditions. It is therefore apparent that towards the end of the reaction, enough DAG and glycerol were present to drastically shift the dynamic equilibrium toward the production of MAG. However, this shift would not be possible if the large excess of MAG reported in Figure 3.3 was present in the oil layer. This evidence therefore supports our previous supposition that, under the studied conditions, MAG was not found in the oil layer but rather at the interface. Needless to say, further work is needed using autoclaves with windows and phase equilibria units to visually confirm the changes in phase behaviour of this complex system.

### **3.4. Conclusions**

Glycerolysis-hydrolysis reactions were conducted at 250°C, 10-30 MPa, using anhydrous glycerol-to-canola oil molar ratio of 34:1 and initial water content of 0 to 8% (w/w). Reactions were also conducted in supercritical nitrogen at 250°C, 10 MPa, and 8% (w/w) initial water. The maximum rate of MAG formation at 20 MPa was significantly higher ( $p \leq 0.05$ ) than that at 30 MPa, but similar ( $p > 0.05$ )

to that at 10 MPa; a finding that has economical impact because a pressure of 10 MPa can be reached without the use of a high pressure pump. Rates of MAG formation in SC-CO<sub>2</sub> and SC-N<sub>2</sub> media were similar ( $p > 0.05$ ) thereby demonstrating that SC-CO<sub>2</sub> does not contribute to catalysis. The maximum rate of MAG production at 10 MPa was significantly higher ( $p \leq 0.001$ ) for reaction with 4% (w/w) initial water compared with anhydrous reactions and was significantly lower ( $p \leq 0.05$ ) compared to that of reaction with 8% (w/w) initial water. Although this study was unable to identify the catalytic reagent, it did show that water played a more important role than what was previously thought. Reactions were carried out up to 14 h and dynamic equilibrium was reached at 9 h. The average dynamic equilibrium composition (mol %) obtained at 9-10 h for the reactions conducted at 10-30 MPa with 4-8% (w/w) water was 66-71% MAG, 13-15% DAG, 13-17% FFA and 0-1% TAG. Such findings lead to a better understanding of the complex mechanisms of simultaneous glycerolysis – hydrolysis reactions and are critical for optimal process design targeting the MAG and DAG products.

### 3.5. References

- [1] F. Temelli, J.W. King, G.R. List, Conversion of oils to monoglycerides by glycerolysis in supercritical carbon dioxide media. *J. Am. Oil Chem. Soc.* 73 (1996) 699-706.
- [2] M.A. Jackson, J.W. King, Lipase-catalyzed glycerolysis of soybean oil in supercritical carbon dioxide. *J. Am. Oil Chem. Soc.* 74 (1997) 103.

- [3] B.D. Flickinger, N. Matsuo, Nutritional characteristics of DAG oil. *Lipids* 38 (2003) 129-132.
- [4] H. Takase, K. Shoji, T. Hase, I. Tokimitsu, Effect of diacylglycerol on post-prandial lipid metabolism in non-diabetic subjects with and without insulin resistance. *Atherosclerosis* 180 (2005) 197-204.
- [5] N. Tada, K. Shoji, M. Takeshita, H. Watanabe, H. Yoshida, T. Hase, N. Matsuo, I. Tokimitsu, Effects of diacylglycerol ingestion on postprandial hyperlipidemia in diabetes. *Clin. Chim. Acta* 353 (2005) 87-94.
- [6] N.O.V. Sonntag, Glycerolysis of fats and methyl-esters - status, review and critique. *J. Am. Oil Chem. Soc.* 59 (1982) A795-A802.
- [7] W.M. Indrasena, K. Henneberry, C.J. Barrow, J.A. Kralovec, Qualitative and quantitative analysis of lipid classes in fish oils by thin-layer chromatography with an Iatroscan flame ionization detector (TLC-FID) and liquid chromatography with an evaporative light scattering detector (LC-ELSD). *J. Liq. Chromatogr. Relat. Technol.* 28 (2005) 2581-2595.
- [8] R.D. Stephens, P.A. Mulawa, M.T. Giles, K.G. Kennedy, P.J. Groblicki, S.H. Cadle, K.T. Knapp, An experimental evaluation of remote sensing-based hydrocarbon measurements: A comparison to FID measurements. *J. Air Waste Manage. Assoc.* 46 (1996) 148-158.
- [9] B.J. Siemens, J.K. Daun, Determination of the fatty acid composition of canola, flax, and solin by near-infrared spectroscopy. *J. Am. Oil Chem. Soc.* 82 (2005) 153-157.
- [10] A.J. Wright, S.E. McGauley, S.S. Narine, W.M. Willis, R.W. Lencki, A.G. Marangoni, Solvent effects on the crystallization behavior of milk fat fractions. *J. Agric. Food Chem.* 48 (2000) 1033-1040.
- [11] SAS Institute Inc., Version 9.1, Cary, NC, 2003.
- [12] D.G. Hyams, CurveExpert Version 1.37, Chadwick Court, Hixson, TN, 2001.
- [13] L. Lasdon, W. Allan, Microsoft Excel Solver (GRG2), Frontline Systems, Inc., Incline Village, NV, 2002.
- [14] A.J. Fraser, D.R. Tocher, J.R. Sargent, Thin-layer chromatography - flame ionization detection and the quantitation of marine neutral lipids and phospholipids, *J. Exp. Mar. Biol. Ecol.* 88 (1985) 91-99.

- [15] J.R. Vick Roy, A.O. Converse, Biomass hydrolysis with sulfur dioxide and water in the region of the critical point, in: J.M.L. Penninger, M. Radosz, M.A. McHugh and V.J. Krukoni (Eds.), *Supercritical Fluid Technology*, Elsevier Science Publishers B.V., Amsterdam, Netherlands, 1985, p. 397-414.
- [16] S. Takenouchi, G.C. Kennedy, The binary system H<sub>2</sub>O-CO<sub>2</sub> at high temperature and pressures. *Am. J. Sci.* 262 (1964) 1055-1074.
- [17] P. Kashulines, S.S.H. Rizvi, P. Harriott, J.A. Zollweg, Viscosities of fatty acids and methylated fatty acids saturated with supercritical carbon dioxide. *J. Am. Oil Chem. Soc.* 68 (1991) 912-921.

## **4. Production of monoolein from oleic acid and glycerol in supercritical carbon dioxide media: a kinetic approach<sup>1</sup>**

### **4.1. Introduction**

As consumers become more aware and concerned about the impact of the food they eat and the substances they commonly use on their health and general well-being, there is a growing interest in designer lipids. Among the lipid classes, surfactants, such as monoacylglycerols (MAG), are desired by the food, cosmetic, pharmaceutical and chemical industries [1-4]. Production of tailor-made designer MAG with targeted fatty acids therefore offers promising industrial opportunities.

As previously discussed in Section 1.2.3, a fat mixture high in MAG can be produced through glycerolysis of glycerol and oil and through esterification of free fatty acids (FFA) with glycerol. However, out of these two methods, the esterification method is best suited for the production of designer MAG because, unlike in glycerolysis, the desired FFA can easily be selected prior to MAG formation [5]. Although it has been known since the mid-1800s that glycerides could be formed by heating free fatty acids and glycerol [6], it still is not fully understood [7]. One of the issues is that although esterification of FFA with glycerol could theoretically form MAG on its own, it is usually accompanied by

---

<sup>1</sup> A version of this chapter was published in the *Journal of Supercritical Fluids* (44:40-47, 2008).

interesterification [8] and, depending on the success of the dehydration mechanism, hydrolysis.

Conventional production of MAG by esterification commonly involves the use of catalysts, which lower the activation energy of reaction. However, the use of a catalyst often complicates the process and leads to coloured products and yield loss [9]. Consequently, non-catalyzed esterification is often preferred [9].

There are a number of advantages in conducting esterification in SC-CO<sub>2</sub> (Section 1.2.3.2.3). A major advantage is that a SC-CO<sub>2</sub> esterification unit can follow an on-line extraction unit recovering FFA from a bulk source and channelling it through the reactor using SC-CO<sub>2</sub>.

Although most of the research on esterification is quite old (Section 1.2.3.2), with the advent of designer lipids there is now a renewed interest in this area. Furthermore, the esterification reaction is so central to lipid chemistry that its understanding is important for the improvement of other more complex systems. For instance, in the glycerolysis-hydrolysis studies reported in Chapters 2 and 3, formation of high levels of MAG partly depended on the esterification of FFA with glycerol. However, no detailed compositional data are available on the esterification of FFA with glycerol in SC-CO<sub>2</sub> at 250 °C. Preliminary runs showed promising results in terms of the production of MAG-rich oil. However, additional information about the optimum processing parameters and kinetics of the reaction is needed for process development targeting high-value lipid products. The objectives of this study were therefore to generate such information by studying the non-



catalyzed esterification of oleic acid (OA) with glycerol in SC-CO<sub>2</sub>, to determine the effects of temperature (170-250 °C), pressure (10-30 MPa) and initial molar ratio of the reactants on the conversion rate to establish the mechanism of the reaction and to develop a kinetic model to predict the extent of the reaction at any time under particular conditions.

## **4.2. Materials and methods**

### *4.2.1. Materials*

The materials used for reactions were free fatty acids (> 70% oleic acid) from Fisher Scientific (Fair Lawn, NJ, USA), anhydrous glycerol (gly) from J.T. Baker (Phillipsburg, NJ, USA), deionized distilled water (DDW), and 99.8% bone dry (water level < 3 ppm) CO<sub>2</sub> and 99.95% compressed nitrogen from Praxair Canada Inc. (Mississauga, ON). Thin Layer Chromatography-Flame Ionization Detector System (TLC-FID) determinations were performed using HPLC grade hexane and laboratory grade ethyl ether from Fisher Scientific (Fairlawn, NJ, USA) and analytical grade glacial acetic acid from BDH Inc. (Toronto, ON). TLC reference standard (>99%) containing 25% (w/w) of each of oleic acid, monoolein, diolein and triolein was obtained from Nu-Chek Prep Inc. (Elysian, MN, USA).

#### 4.2.2. Reaction protocols

Reactions were conducted in the batch system described previously in Section 3.2.2. A total volume of 61 mL of reactants, consisting of oleic acid and glycerol were added to the 200 mL autoclave: the glycerol to oleic acid molar ratio (gly/oleic) was 1:0.1, 1:1 and 1:2. When mixing reactants, the autoclave was flushed with a gentle flow of dry nitrogen to avoid any residual oxygen and moisture from the air. Once the autoclave was sealed, the reaction mixture was purged with CO<sub>2</sub> and constantly stirred (~100 rpm). CO<sub>2</sub> at tank pressure (~6 MPa) was then added to the autoclave before increasing the temperature to 170, 200 or 250 °C. Once the desired temperature was established, the autoclave was pressurized to 10 or 30 MPa and the mixing rate was increased to 250 ± 30 rpm. For reactions conducted in supercritical nitrogen (SC-N<sub>2</sub>) media (T<sub>c</sub> = -146.96 °C, P<sub>c</sub> = 3.40 MPa [10]), nitrogen was used to purge the reaction mixture and to fill the autoclave prior to increasing the temperature to 250 °C and the pressure to 10 MPa.

Samples (1 mL) were collected using the previously described protocol in Section 3.2.2 so as to ensure that a representative sample of the reaction mixture was collected. Samples were collected every 30 min but after 3 h a sample was collected every hour for a total of up to 6.5 h. This sampling protocol was implemented in order to maximize kinetic data while minimizing the disturbance of the equilibrium of the reaction mixture.

#### 4.2.3. *Lipid analysis*

The samples collected as a function of time throughout the reactions conducted at different conditions separated into two phases upon standing at ambient conditions. Only the composition of the oil layer was analyzed using TLC-FID. The oil was separated into triolein (TO), diolein (DO), monoolein (MO) and oleic acid (OA) on Chromarods-SIII (silica gel type) and quantified using an Iatroscan TH-10 (IATRON-Laboratories Inc., Tokyo, Japan). The analysis was done and the area percentages for each component were calculated as previously described in Section 3.2.3 while using molecular weights of 885.45, 620.99, 356.54 and 282.45 a.m.u. for TO, DO, MO, and OA, respectively. All concentrations were reported as mol per 100 g of oil.

#### 4.2.4. *Experimental design and statistical analysis*

Four sets of reactions were performed in two replicates at different levels of temperature, pressure, gly/oleic ratio and supercritical media. Temperature levels of 170, 200 and 250 °C were tested at 10 MPa using a 1:0.1 gly/oleic ratio in SC-CO<sub>2</sub> over 4.2 h and 6.5 h reactions. Pressure levels of 10 and 30 MPa were tested at 250 °C, using a 1:0.1 gly/oleic acid ratio in SC-CO<sub>2</sub> over 6.5 h reactions. Gly/oleic ratio of 1:0.1, 1:1 and 1:2 were tested at 250 °C and 10 MPa in SC-CO<sub>2</sub> over 6.5 h. The effect of SC-N<sub>2</sub> and SC-CO<sub>2</sub> were tested at 250 °C, 10 MPa and using a gly/oleic ratio of 1:0.1 over 6.5 h reactions. The order in which all of the above reactions were carried out was randomized and the composition of the samples

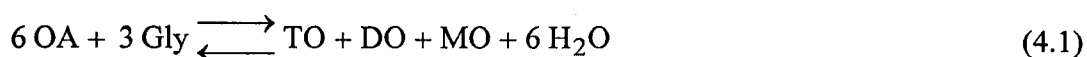
obtained was randomly analyzed in duplicate for each sample by TLC-FID analyses. The variance between TLC-FID analyses, as obtained by analyzing all the TLC reference standard chromatograms, was less than 4%.

The rate of MO formation at 50% of the dynamic equilibrium concentration (Rate-50%) was arbitrarily chosen as an unbiased mean to compare the various treatments. For this purpose, the MO experimental data for each replicate were modeled individually using an Exponential Association model. The time it took for each individual reaction to reach half of the 6 h MO dynamic equilibrium concentration ( $t$ -50%) was calculated from this model and Rate-50% was calculated by taking the instantaneous slope at  $t$ -50%. The analysis of variance of Rate-50% obtained for each replicated run of each treatment was performed using the Mixed Model procedure of SAS Statistical Software version 9.1 and means for different treatments were compared using Student's  $t$ -test [11]. Results were reported as statistically significant when the  $p$ -value was less than or equal to 0.05 ( $p \leq 0.05$ ); however, where applicable, the exact  $p$ -value obtained by SAS was reported.

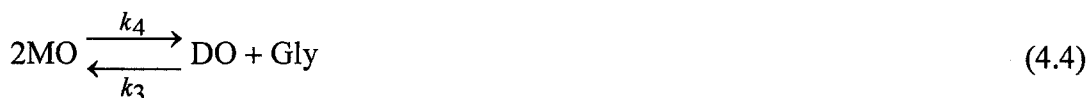
#### 4.2.5. *Kinetic modeling*

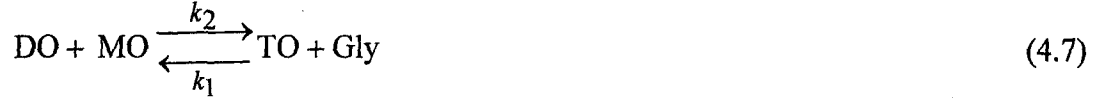
It is important to adequately describe all the possible reactions that are taking place in SC-CO<sub>2</sub> medium during the esterification of oleic acid with glycerol so as to accurately calculate rate constants and predict the mechanism of the reaction. The overall reversible reaction is described by Eq. (4.1) to show all possible species. However, to calculate the rate constants, the overall reaction

described by Eq. (4.1) must be broken down into a number of steps. Initially, only glycerol and OA are present; therefore, the forward reaction of Eq. (4.2) must first occur. Assuming that Eq. (4.2) is reversible,  $k_{12}$  and  $k_{11}$  represent the rate constants for each step. The numbers used to differentiate the  $k$ -values are the same as the ones that were arbitrarily given in Section 2.2.2 for the glycerolysis-hydrolysis reactions and were chosen to simplify the comparison between the two studies.



MO, initially formed by Eq. (4.2), is then available to form DO through the forward reactions of Eqs. (4.3) and (4.4). This DO is then directly responsible for the formation of TO through the possible forward reactions of Eqs. (4.5)-(4.7). Thus, DO may be involved in all of Eqs. (4.3)-(4.7) while, water, which is initially formed by the forward reaction of Eq. (4.2), could also be involved in the reverse reactions of Eqs. (4.2), (4.3) and (4.5).





From Eqs. (4.2)–(4.7), the rate of change in concentration for each reaction component can be described by the following differential rate equations, Eqs. (4.8a)–(4.8f):

$$\begin{aligned} \frac{d[\text{MO}]}{dt} = & k_1[\text{Gly}][\text{TO}] - k_2[\text{DO}][\text{MO}] + 2k_3[\text{Gly}][\text{DO}] - 2k_4[\text{MO}]^2 \\ & - k_5[\text{TO}][\text{MO}] + k_6[\text{DO}]^2 + k_9[\text{DO}][\text{H}_2\text{O}] - k_{10}[\text{MO}][\text{OA}] \\ & - k_{11}[\text{H}_2\text{O}][\text{MO}] + k_{12}[\text{Gly}][\text{OA}] \end{aligned} \quad (4.8a)$$

$$\begin{aligned} \frac{d[\text{DO}]}{dt} = & k_1[\text{Gly}][\text{TO}] - k_2[\text{DO}][\text{MO}] - k_3[\text{Gly}][\text{DO}] + k_4[\text{MO}]^2 \\ & + 2k_5[\text{TO}][\text{MO}] - 2k_6[\text{DO}]^2 + k_7[\text{TO}][\text{H}_2\text{O}] \\ & - k_8[\text{DO}][\text{OA}] - k_9[\text{DO}][\text{H}_2\text{O}] + k_{10}[\text{MO}][\text{OA}] \end{aligned} \quad (4.8b)$$

$$\begin{aligned} \frac{d[\text{TO}]}{dt} = & -k_1[\text{Gly}][\text{TO}] + k_2[\text{DO}][\text{MO}] - k_5[\text{TO}][\text{MO}] + k_6[\text{DO}]^2 \\ & - k_7[\text{TO}][\text{H}_2\text{O}] + k_8[\text{DO}][\text{OA}] \end{aligned} \quad (4.8c)$$

$$\begin{aligned} \frac{d[\text{OA}]}{dt} = & k_7[\text{TO}][\text{H}_2\text{O}] - k_8[\text{DO}][\text{OA}] + k_9[\text{DO}][\text{H}_2\text{O}] \\ & - k_{10}[\text{MO}][\text{OA}] + k_{11}[\text{H}_2\text{O}][\text{MO}] - k_{12}[\text{Gly}][\text{OA}] \end{aligned} \quad (4.8d)$$

$$\frac{d[\text{H}_2\text{O}]}{dt} = -k_7[\text{TO}][\text{H}_2\text{O}] + k_8[\text{DO}][\text{OA}] - k_9[\text{DO}][\text{H}_2\text{O}] + k_{10}[\text{MO}][\text{OA}] - k_{11}[\text{H}_2\text{O}][\text{MO}] + k_{12}[\text{Gly}][\text{OA}] \quad (4.8e)$$

$$\frac{d[\text{Gly}]}{dt} = -k_1[\text{Gly}][\text{TO}] + k_2[\text{DO}][\text{MO}] - k_3[\text{Gly}][\text{DO}] + k_4[\text{MO}]^2 + k_{11}[\text{MO}][\text{H}_2\text{O}] - k_{12}[\text{Gly}][\text{OA}] \quad (4.8f)$$

#### 4.2.6. Determination of rate constants

Water and glycerol concentrations as a function of time were not measured experimentally but calculated based on reaction stoichiometry. Given that, according to Eqs. (4.2), (4.3) and (4.5), one mole of water is produced for every mole of OA used and that the initial concentration of water was zero, any decrease in moles of OA must be equal to an increase in moles of water. The concentration of water at any given time was therefore obtained by subtracting the molar concentration of OA per 100 g of oil at that time from the initial molar concentration of OA. In contrast, the concentration of glycerol at a given time was calculated according to Eq. (4.9)

$$[\text{Gly}]_t = [\text{Gly}]_0 - ([\text{TO}]_t + [\text{DO}]_t + [\text{MO}]_t) \quad (4.9)$$

where  $[\text{Gly}]_0$  is the initial molar concentration of glycerol and  $[\text{Gly}]_t$ ,  $[\text{TO}]_t$ ,  $[\text{DO}]_t$ , and  $[\text{MO}]_t$  are the molar concentrations of the respective components at time  $t$ .

To establish the most reliable model possible, all the TLC-FID data generated in the 6.5 h replicated runs were combined and the change in concentration over time for each component was expressed using a mathematical

equation. The equation of best fit was obtained using a curve fitting computer program [12]. Using this program, OA, MO, TO, water and Gly were described by an Exponential Association Model  $[y=a(b-e^{-ct})]$  where the range of correlation coefficient ( $R^2$ ) for each component was 0.96-0.99, 0.86-96, 0.5-0.82, 0.95-0.99 and 0.92-0.99, respectively. The change in concentration of DO was slightly different after 2 h and therefore two distinct models had to be used to fit the data. A Rational Function  $[y=(a+bt)/(1+ct+dt^2)]$  ( $R^2$  range 0.88-0.93) was used to model the first 2 h and then a Polynomial Fit  $[y=a+bt+ct^2+dt^3+ht^4]$  ( $R^2$  range 0.81-0.82) was used. In each model,  $a$ ,  $b$ ,  $c$ ,  $d$  and  $h$  were fixed constants determined by the program and  $t$  was the time. Using these mathematical expressions, experimental molar concentration ( $C_{\text{exp}}$ ) for each component (OA, MO, DO, TO, water and glycerol) was obtained every 6 min over a 6 h period. These  $C_{\text{exp}}$  and variable  $k$ -values ( $k_{1-12}$ ) were introduced into Eqs. (4.8a)-(4.8f) and the predicted rate of change ( $r_{\text{pred}}$ ) of each component was obtained over the same time period as the  $C_{\text{exp}}$ . The predicted concentration ( $C_{\text{pred}}$ ) for each component was then calculated using the following expression:

$$C_{\text{pred}} = C|_{t+\Delta t} = C_{\text{exp}}|_t + r_{\text{pred}} \Delta t \quad (4.10)$$

where  $C_{\text{exp}}|_t$  is the concentration at time  $t$ ,  $\Delta t$  is the time interval (6 min) and  $C|_{t+\Delta t}$  is the predicted concentration at  $t+\Delta t$ . The summed squared error (SSE) between  $C_{\text{exp}}$  and  $C_{\text{pred}}$  was then calculated.

Two  $k$ -values,  $k_{10}$  and  $k_{12}$ , were calculated by introducing dynamic equilibrium data obtained after 6.5 h into Eqs. (4.11) and (4.12):



$$k_{10} = \frac{-k_1([\text{Gly}]_\infty)([\text{TO}]_\infty) + k_2([\text{DO}]_\infty)([\text{MO}]_\infty) + k_3([\text{Gly}]_\infty)([\text{DO}]_\infty) - k_4([\text{MO}]_\infty)^2 - 2k_5([\text{TO}]_\infty)([\text{MO}]_\infty) + 2k_6([\text{DO}]_\infty)^2 - k_7([\text{TO}]_\infty)([\text{H}_2\text{O}]_\infty) + k_8([\text{DO}]_\infty)([\text{OA}]_\infty) + k_9([\text{DO}]_\infty)([\text{H}_2\text{O}]_\infty)}{([\text{MO}]_\infty)([\text{OA}]_\infty)} \quad (4.11)$$

$$k_{12} = \frac{-k_1([\text{Gly}]_\infty)([\text{TO}]_\infty) + k_2([\text{DO}]_\infty)([\text{MO}]_\infty) - k_3([\text{Gly}]_\infty)([\text{DO}]_\infty) + k_4([\text{MO}]_\infty)^2 + k_{11}([\text{MO}]_\infty)([\text{H}_2\text{O}]_\infty)}{([\text{Gly}]_\infty)([\text{OA}]_\infty)} \quad (4.12)$$

where  $[\text{TO}]_\infty$ ,  $[\text{DO}]_\infty$ ,  $[\text{MO}]_\infty$ ,  $[\text{OA}]_\infty$ ,  $[\text{Gly}]_\infty$ , and  $[\text{H}_2\text{O}]_\infty$  are mol/100 g at dynamic equilibrium. Eqs. (4.11) and (4.12) were derived from Eqs. (4.8b) and (4.8f) where the rate of change for both DO and Gly at dynamic equilibrium is zero.

The Generalized Reduced Gradient (GRG2) nonlinear optimization code [13] was used to calculate the  $k$ -values. To simplify the calculation two constraints were included:  $k$  had to be positive and the rate of change for Eqs. (4.8a)-(4.8f) at dynamic equilibrium (6 h) had to be zero. Along with these constraints, Eqs. (4.11)-(4.12) were included in the system of equations and the program minimized the SSE for all components while changing  $k_{1-9}$  and  $k_{11}$ , thereby determining rate constants.

### 4.3. Results and discussion

#### 4.3.1. Composition and kinetic calculations

The compositional analysis was performed using TLC-FID because this method offers a relatively fast separation of the reaction mixture into OA, MO, DO,

TO by thin layer chromatography (TLC) followed by quantification by flame ionization detector (FID).

Figure 4.1 shows the change in composition of the oil phase and the fitted curves as a function of time. It is apparent that, under these conditions, the oleic acid quickly reacts with glycerol to form mainly MO but also DO. Traces of TO

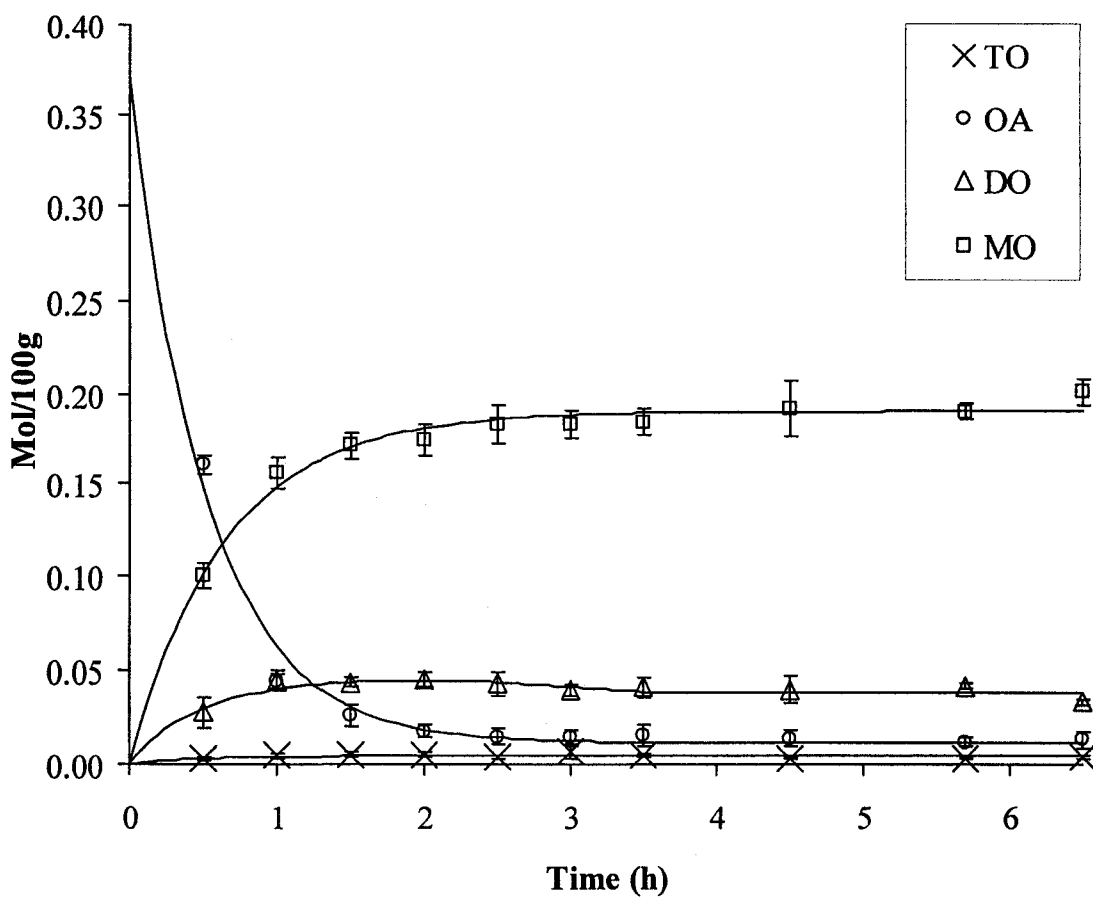


**Figure 4.1.** Experimental data and fitted curves of the composition of the oil phase as a function of time obtained at 250 °C, 10MPa and using a 1:0.1 initial glycerol to oleic acid ratio.

were also detected but the variation in the TO data made it difficult to find a reliable best-fit model, resulting in lower  $R^2$  values (0.5-0.82). On the other hand, the Exponential Association model chosen to describe the data for the other species, with the exception of DO, gave  $R^2$  values of 0.86-0.99 while models used to describe DO had  $R^2$  values of 0.81-0.93.

To obtain reliable kinetic data it is important to provide a model that appropriately describes the reaction. For this reason, in Figure 4.1 the first sample that was taken when the autoclave initially reached 250 °C was plotted at 0.5 h to account for the heat-up time from 100 to 250 °C. For reactions conducted at 170 and 200 °C the heat-up time was obviously shorter, as is quite apparent in Figure 4.2. In all cases, time zero was set to be the time corresponding to 100 °C during heating because, based on preliminary runs, the esterification of glycerol in SC-CO<sub>2</sub> only occurs at temperatures above 100 °C. Hence, in all calculations and figures, data points at time zero are describing the initial reactant concentrations at 100 °C.

Kinetic data were calculated using the reversible Eqs. (4.2)-(4.7). All  $k$ -values were calculated based on the two previously mentioned constraints. Simply stated, these constraints imply that  $k$ -values must be positive and that at dynamic equilibrium the rate of change in concentration for each chemical species is zero.

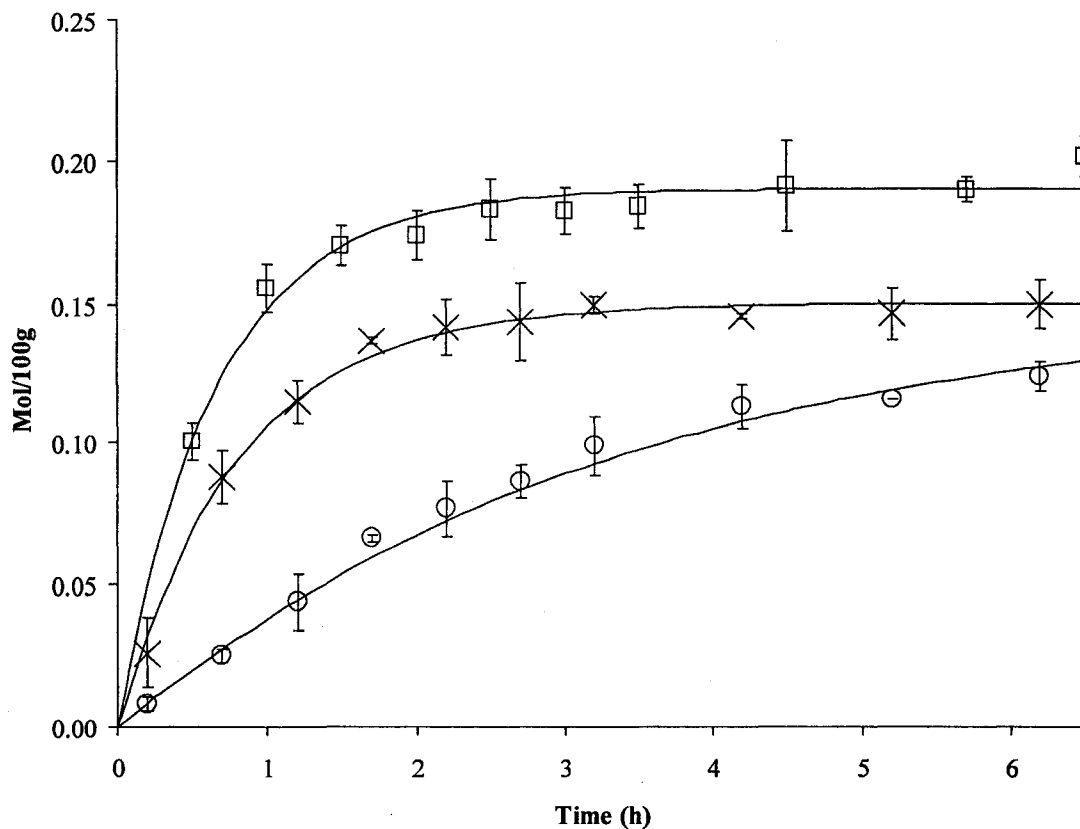


**Figure 4.2.** Effect of temperature on monoolein production at 10 MPa using 1:0.1 glycerol to oleic acid ratio as a function of time where (○), (×) and (□) represent 170, 200 and 250 °C, respectively.

#### 4.3.2. Temperature effect

Figure 4.2 shows the change in MO concentration over time at the three temperature levels studied. It is apparent that decreasing the temperature of the reaction from 250 to 200 and 170 °C drastically reduced the final MO concentration as well as the rate of MO production. To determine if this temperature effect was significant, the rate of change in MO concentration had to be compared based on a common time independent parameter. The common parameter chosen to compare

rates of MO production was concentration and, to remove all possible bias, half of the dynamic equilibrium concentration was selected as the exact point of comparison. Hence, as previously mentioned Rate-50% values were calculated for each individual run at each temperature and compared using statistical analysis. The results showed that, indeed, an increase in temperature significantly ( $p \leq 0.02$ ) increased the rate of MO production.

As mentioned above, a reaction conducted at 100 °C, 10 MPa and 1:0.1 gly/oleic during preliminary runs did not lead to any conversion as no MO, DO or TO was detected. Another run at 170 °C demonstrated that 6.5 h was not sufficient time to achieve dynamic equilibrium concentration and that much longer reaction time is needed in order to generate kinetic data. On the other hand, 2 h is sufficient to reach dynamic equilibrium at 250 °C. These results clearly demonstrate the need for heat for esterification of glycerol with oleic acid to take place without the addition of a catalyst. The reason for this is that increased temperature reduces the surface tension, increases the solubility of glycerol in fat [14] and provides the required activation energy for the esterification to take place [15].

#### *4.3.3. Pressure effect*

While keeping the temperature constant at 250 °C, the gly/oleic at 1:0.1 and varying the pressure between 10 and 30 MPa, it was possible to see that the Rate-50% was not affected by pressure ( $p = 0.75$ ). Indeed, as depicted in Figure 4.3 the

modeled curves obtained for runs conducted at 10 and 30 MPa overlap each other.

The rate constants presented in Table 4.1 for 10 and 30 MPa are also similar.

This absence of pressure effect was not expected since, as reported in Chapter 3, the rate of MAG formation during glycerolysis was significantly ( $p \leq 0.05$ ) higher at 10 MPa than that at 30 MPa. However, the lack of pressure effect for

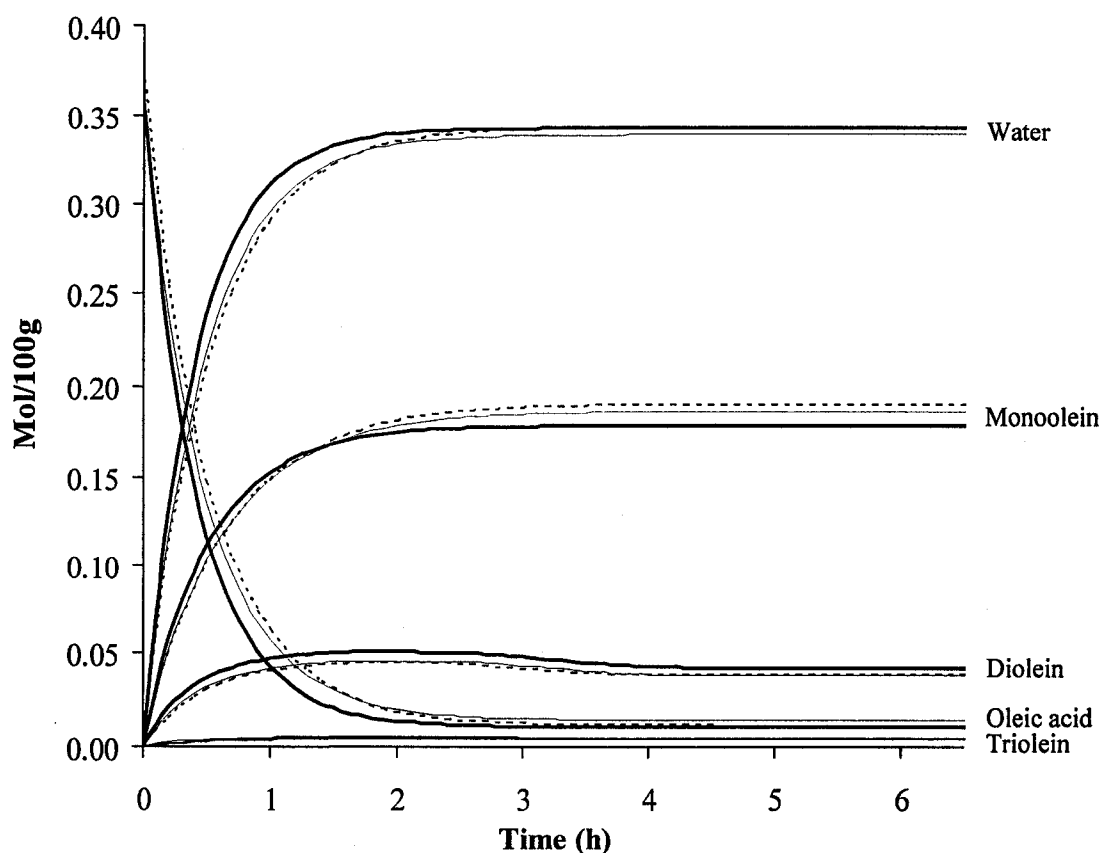


**Figure 4.3.** Effect of pressure and supercritical media on concentration of reaction species at 250 °C and using a 1:0.1 initial glycerol to oleic acid ratio as a function of time where (----), (—) and (—) represent modeled data for 10 MPa in supercritical carbon dioxide (SC-CO<sub>2</sub>), 30 MPa in SC-CO<sub>2</sub> and 10 MPa in supercritical nitrogen, respectively.

**Table 4.1.** Effect of glycerol to oleic acid molar ratio (gly/oleic) and pressure on rate constants at 250 °C

Rate constants (g/h mol)	SC-CO <sub>2</sub>				SC-N <sub>2</sub>
	10 MPa 1:2 gly/oleic	10 MPa 1:1 gly/oleic	10 MPa 1:0.1gly/oleic	30 MPa 1:0.1gly/oleic	10 MPa 1:0.1 gly/oleic
k <sub>1</sub>	0	0	0	0	0
k <sub>2</sub>	0	0	0	0	0
k <sub>3</sub>	18.80	10.81	0.14	0.06	0.08
k <sub>4</sub>	0	0.29	0.90	0.82	0.89
k <sub>5</sub>	15.55	12.88	2.15	3.18	3.79
k <sub>6</sub>	0	0	0	0	0
k <sub>7</sub>	0	0	0	0	0
k <sub>8</sub>	2.36	4.69	4.24	4.85	6.1
k <sub>9</sub>	4.35	0	2.35	3.35	2.56
k <sub>10</sub>	10.75	6.50	6.39	7.04	8.32
k <sub>11</sub>	3.03	1.63	0	0	0
k <sub>12</sub>	4.80	3.18	0.42	0.46	0.53

esterification could be explained by its relatively faster rate of MAG formation compared to that for the glycerolysis reaction and consequently MAG, which has excellent emulsifying properties decreasing the surface tension between oil and glycerol, being produced much sooner.

#### 4.3.4. *Effect of supercritical media*

It is well known that esterification reactions are acid catalyzed [16]. Even though initially the reaction mixture was anhydrous, water is formed throughout the

reaction and can lead to the formation of carbonic acid in the presence of CO<sub>2</sub>. Thus, it was originally hypothesized that carbonic acid, along with oleic acid, would contribute to catalyzing the reaction. Although the pH of a CO<sub>2</sub> and water mixture at high temperature (250 °C) can be estimated at subcritical conditions using equations reported by Hunter and Savage [17], there is not sufficient data to apply these equations for this complex reaction mixture under supercritical conditions. Furthermore, the availability of free water for carbonic acid formation is not known since the amount of water formed during the esterification step (Fig. 4.4) could also be bound to glycerol or used up in the hydrolysis reaction. As previously mentioned in Section 3.3.4, in a binary system of water-CO<sub>2</sub> [18], water and CO<sub>2</sub> were shown not to be completely miscible and only a small percentage of SC-CO<sub>2</sub> was present in the liquid phase at 250°C and 10 MPa. Even though properties of water and CO<sub>2</sub> might be similar in the more complicated system considered in this study, no data were available to confirm this. Therefore, to test the extent of carbonic acid's contribution to reaction catalysis, duplicated reactions were conducted in SC-N<sub>2</sub> at 250 °C, 10 MPa and using 1:0.1 gly/oleic. The results, presented in Figure 4.3, clearly demonstrate that there is no difference between SC-N<sub>2</sub> and SC-CO<sub>2</sub> media. As well, the rate constants are similar (Table 4.1). Thus, it appears that carbonic acid is not contributing as a catalyst, possibly due to insufficient amount of free water required to form carbonic acid. Also, since any carbonic acid formation would occur after the initial induction period, it is probably appearing too late for it



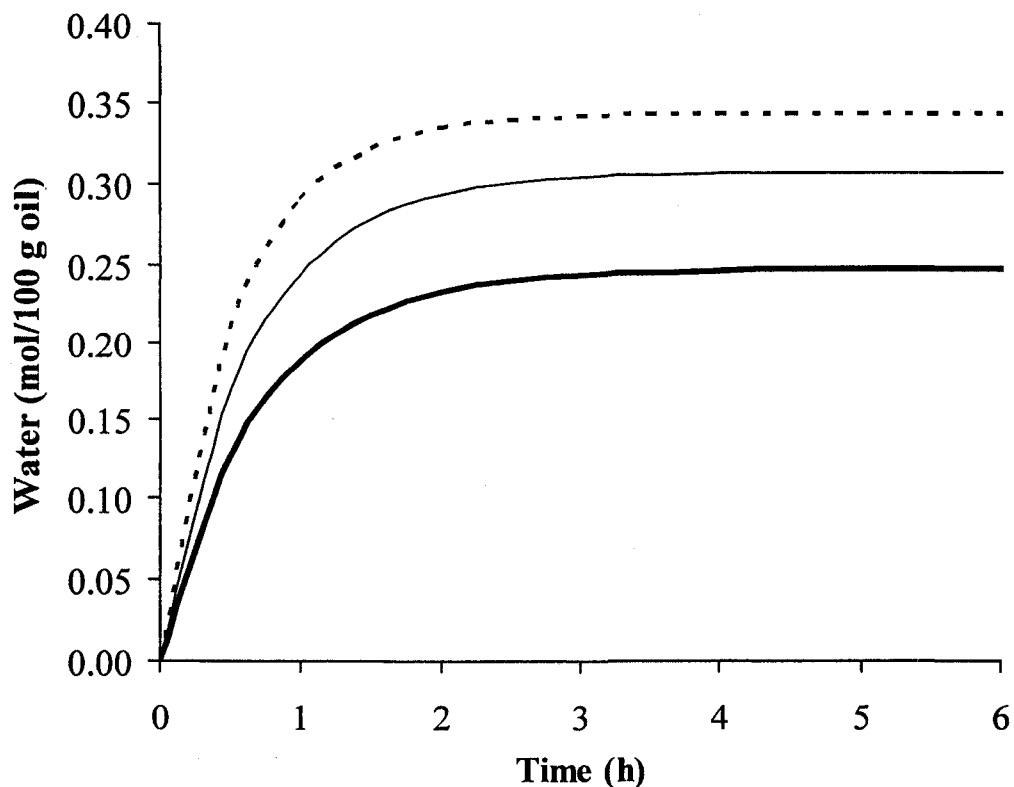


**Figure 4.4** Change in water concentration as a function of time for reactions conducted at 10 MPa and 250 °C where (----), (—) and (—) represent esterification reactions conducted using 1:0.1, 1:1 and 1:2 initial glycerol/oleic acid molar ratio, respectively.

to have an impact on reaction rate. Therefore, oleic acid seems to be the main catalytic agent and its effect is similar regardless of SC-CO<sub>2</sub> or SC-N<sub>2</sub> media.

#### 4.3.5. *Effect of initial reagent concentration*

It was originally thought that a decrease in glycerol and a corresponding increase in OA would promote the formation of DO and TO due to the lack of available glycerol backbone and the presence of excess OA. As demonstrated in

Figure 4.5, it is true that TO was increased substantially in the 1:2 gly/oleic reactions but its dynamic equilibrium concentration remained quite modest as a larger amount of OA remained unreacted compared to the other treatments. DO, on the other hand, was quite similar for 1:0.1, 1:1 and 1:2 gly/oleic while MO

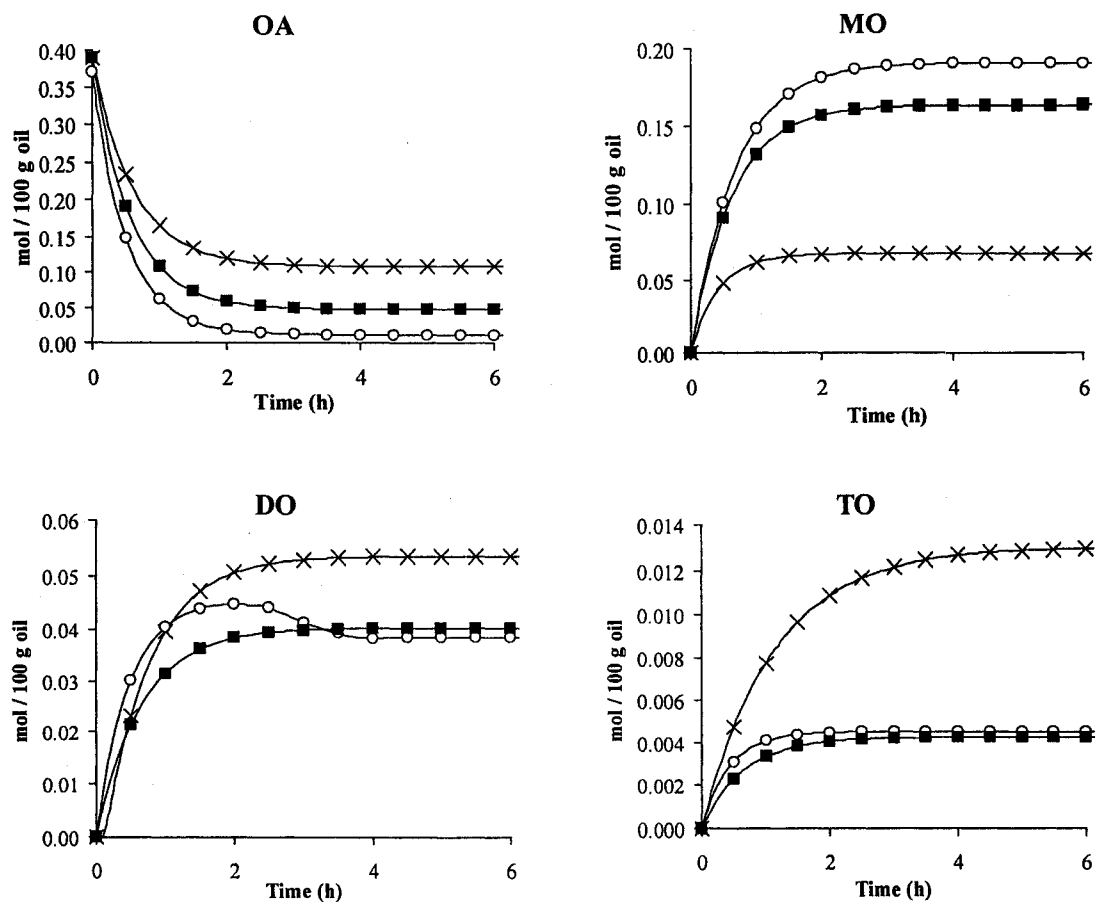


**Figure 4.5.** Effect of initial glycerol to oleic acid ratio on product composition at 250 °C and 10 MPa as a function of time where (×), (■), (○) represent 1:2, 1:1 and 1:0.1 initial glycerol to oleic acid ratio, respectively. OA, MO, DO, TO correspond to the plot of the concentration of oleic acid, monoolein, diolein and triolein, respectively. Data points and curves are based on modeled data.

decreased with a decrease in glycerol. Indeed, when Rate-50% for MO were compared, reactions conducted using 1:2 gly/oleic had a significantly ( $p \leq 0.001$ ) lower Rate-50% than those for both 1:1 and 1:0.1, which were similar ( $p = 0.90$ ). Such a difference in Rate-50% for reactions conducted at 1:1 and 1:2 gly/oleic suggest a marked difference in the mechanism of the reaction. Indeed, larger  $k_9$  and  $k_{11}$  in Table 4.1 suggest that reactions conducted at 1:2 gly/oleic are more influenced by hydrolysis than those conducted at 1:1 and 1:0.1 gly/oleic. When considering the influence of glycerol content on MAG production (Fig. 4.6), it is apparent that the level of glycerol for reactions conducted at 1:2 gly/oleic was very low and it is possible that this had an influence on the reaction. It is true that glycerol is a well known humectant due to its high water binding capacity. It is therefore possible that when an excess amount of glycerol was present during the esterification reaction, as was the case for reactions conducted at 1:0.1 gly/oleic, the water formed by the esterification reaction was quickly bound by glycerol and was therefore not available for hydrolysis. However, when lower amounts of glycerol were used, as was the case for reactions conducted at 1:2 gly/oleic, more free water was probably available and therefore hydrolysis was more predominant.

#### 4.3.6. *Mechanism of the reaction*

In light of the information presented in Table 4.1 and of the reactions previously referred to, it is possible to establish the mechanism of the esterification

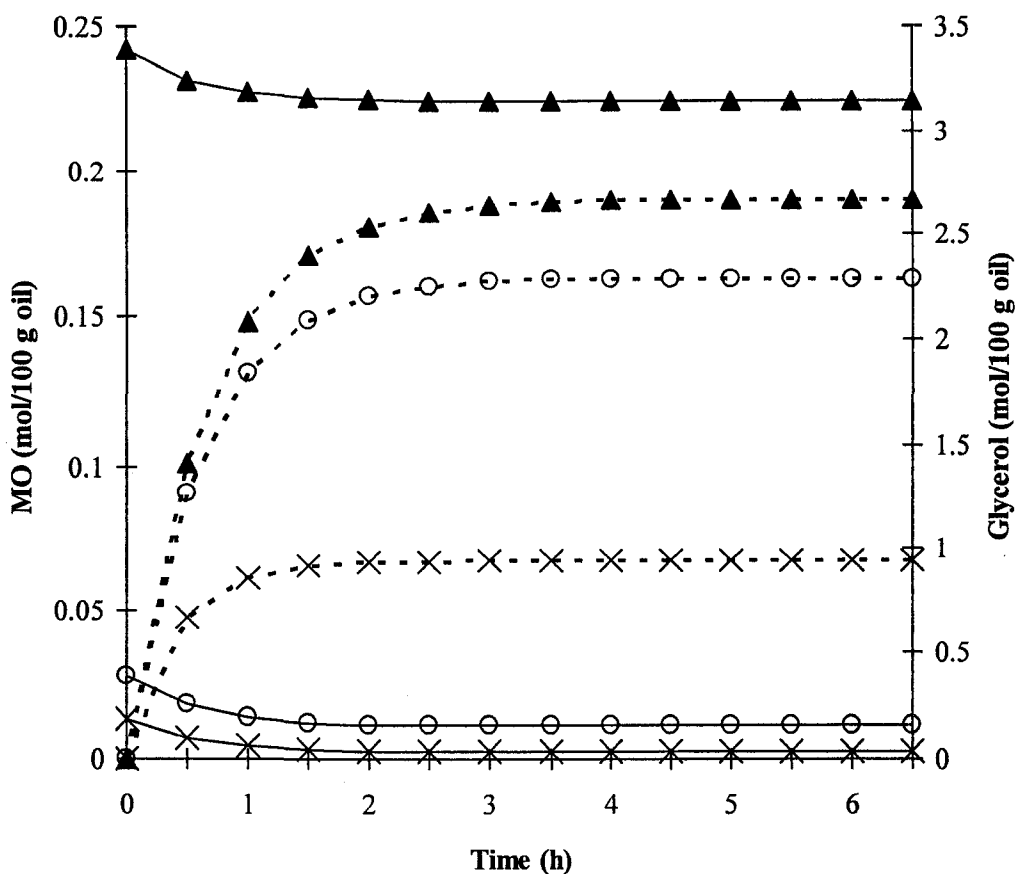


**Figure 4.6.** Change in glycerol and MO concentrations as a function of time during esterification reactions conducted at 10 MPa and 250 °C where (----) represent MO and (—) represent glycerol concentrations and where (▲), (○) and (×) represent reactions conducted using 1:0.1, 1:1 and 1:2 initial glycerol/oleic acid molar ratio, respectively.

of glycerol with OA within the limitations and assumptions of the kinetic model applied. To facilitate this discussion, one can consider the reactions conducted at 10 MPa, 250 °C and 1:0.1 gly/oleic. Initially, MO and water are formed via Eq. (4.2). Oddly enough, the rate constant for this reaction under these conditions is relatively small and could possibly be rate limiting. Once MO and water are present, the

forward reaction of Eq. (4.3) and, to a lesser extent, the forward reaction of Eq. (4.4) occurs and forms DO. DO can then react with water according to the reverse of Eq. (4.3), with glycerol according to the reverse of Eq. (4.4) and with OA according to Eq. (4.5). The latter is responsible for the formation of TO. Some of the TO formed can then quickly react with MO and form two moles of DO according to the reverse of Eq. (4.6). Under these conditions, Eq. (4.7), the forward reaction for Eq. (4.6), and the reverse reactions for Eqs. (4.2) and (4.5) do not occur. For all tested conditions, Eq. (4.7), reverse reaction of Eq. (4.5) and forward reaction of Eq. (4.6) did not occur.

As previously mentioned, no striking differences in k-values can be found between reactions conducted in different supercritical media and pressure (Table 4.1). Indeed, results are within experimental error and thereby suggest that the reaction is not affected by a change in media or pressure between 10 and 30 MPa.

According to the rate law, k-values should be independent of the concentrations of the species involved in the reaction [19]. However, different k-values were obtained for reactions conducted using different initial glycerol to oleic acid molar ratios. For instance, reactions conducted using 1:1 and 1:2 gly/oleic have larger  $k_3$ ,  $k_5$ ,  $k_{11}$  and  $k_{12}$  values than those at 1:0.1. The fact that different k-values are obtained when initial reactant concentrations are changed suggest that there are other physical interactions occurring, which were not examined in this study. The impacts of these other parameters are imbedded in the k-values shown in Table 4.1 but should be evaluated separately in future research. Of all the physical

interactions occurring, probably the most important one is the phase behaviour and the fact that phase behaviour and other physical properties might also be changing as reaction proceeds due to the formation of surfactants like MO. Following the changes in phase behaviour visually is a challenge since the reaction temperature (250 °C) is beyond the limits of typical commercially available phase equilibria monitoring units.

#### **4.4. Conclusions**

Esterification of FFA with glycerol in SC-CO<sub>2</sub> media was conducted to elucidate the reaction kinetics and provide the reaction mechanism. Reactions were conducted in SC-CO<sub>2</sub> at 10-30 MPa, 170-250 °C in a batch stirred reactor using an anhydrous glycerol to oleic acid initial molar ratio (gly/oleic) of 1:0.1, 1:1 and 1:2 and in supercritical nitrogen at 10 MPa and 250°C using 1:0.1 gly/oleic. The rate of MO formation at 50% of the dynamic equilibrium concentrations (Rate-50%) increased significantly ( $p \leq 0.05$ ) with temperature but was not affected by pressure or supercritical media ( $p > 0.05$ ). Rate-50% values for 1:0.1 and 1:1 gly/oleic were similar ( $p > 0.05$ ) but higher ( $p \leq 0.05$ ) than that for 1:2 gly/oleic. Dynamic equilibrium concentration of MO significantly ( $p \leq 0.05$ ) increased with increased initial glycerol concentration. The findings of this study provide some insight into this complex system and demonstrate that the esterification reaction can be carried

out successfully in SC-CO<sub>2</sub> media, but more research is required to enhance our fundamental understanding.

#### 4.5. References

- [1] Anonymous, Lubricant compositions. Res. Discl. (2006) 690.
- [2] A.M. Fernandez, U. Held, A. Willing, W.H. Breuer, New green surfactants for emulsion polymerization. Prog. Org. Coatings 53 (2005) 246-255.
- [3] G.M. Eccleston, Functions of mixed emulsifiers and emulsifying waxes in dermatological lotions and creams. Colloids Surf. A Physicochem. Eng. Asp. 123-124 (1997) 169-182.
- [4] N. Garti, What can nature offer from an emulsifier point of view: Trends and progress? Colloids Surf. A Physicochem. Eng. Asp. 152 (1999) 125-146.
- [5] F.S. Guner, A. Sirkecioglu, S. Yilmaz, A.T. Erciyas, A. Erdem-Senatalar, Esterification of oleic acid with glycerol in the presence of sulfated iron oxide catalyst. J. Am. Oil Chem. Soc. 73 (1996) 347-351.
- [6] T.P. Hilditch, J.G. Rigg, Experiments on the direct esterification of higher fatty acids with glycerol and with ethylene glycol. J. Chem. Soc. (1935) 1774-1778.
- [7] W.M. Willis, R.W. Lencki, A.G. Marangoni, Lipid modification strategies in the production of nutritionally functional fats and oils. Crit. Rev. Food Sci. 38 (1998) 639-674.
- [8] A.T. Gros, R.O. Feuge, Preparation of partial glycerides by direct esterification. J. Am. Oil Chem. Soc. 41 (1964) 727-731.
- [9] N.O.V. Sonntag, Fat splitting, esterification and interesterification, in: D. Swern (Eds.), Bailey's Industrial Oil and Fat Products, John Wiley & Sons, New York, NY, 1979, p. 97-173.

- [10] R.T. Jacobsen, R.B. Stewart, M. Jahangiri, Thermodynamic properties of nitrogen from the freezing line to 2000 K at pressures to 1000 MPa. *J. Phys. Chem. Ref. Data* 15 (1986) 735-909.
- [11] SAS Institute Inc., Version 9.1, Cary, NC, 2003.
- [12] D.G. Hyams, CurveExpert Version 1.37, Chadwick Court, Hixson, TN, 2001.
- [13] L. Lasdon, W. Allan, Microsoft Excel Solver (GRG2), Frontline Systems, Inc., Incline Village, NV, 2002.
- [14] N.O.V. Sonntag, Glycerolysis of fats and methyl-esters - Status, review and critique. *J. Am. Oil Chem. Soc.* 59 (1982) A795-A802.
- [15] R.B.R. Choudhury, The preparation and purification of monoglycerides. II Direct esterification of fatty acids with glycerol. *J. Am. Oil Chem. Soc.* 39 (1962) 345-347.
- [16] R.O. Feuge, Derivatives of fats for use as foods. *J. Am. Oil Chem. Soc.* 39 (1962) 521-527.
- [17] S.E. Hunter, P.E. Savage, Acid-catalyzed reactions in carbon dioxide-enriched high-temperature liquid water. *Ind. Eng. Chem. Res.* 42 (2003) 290-294.
- [18] S. Takenouchi, G.C. Kennedy, The binary system H<sub>2</sub>O-CO<sub>2</sub> at high temperature and pressures. *Am. J. Sci.* 262 (1964) 1055-1074.
- [19] S.H. Fogler, *Elements of Chemical Reaction Engineering*, Prentice Hall, Upper Saddle River, N J, 1999, p.69.



## **5. Kinetic modeling of hydrolysis of canola oil in supercritical media<sup>1</sup>**

### **5.1. Introduction**

Hydrolysis of triacylglycerol (TAG) from fats and oils to glycerol and free fatty acids (FFA) is an important reaction for the oleochemical industry. Typically, hydrolysis is carried out at 100-260 °C and 100-7000 kPa using 0.4-1.5 w/w initial water to oil ratio with or without catalysts [1].

According to a number of investigators [1, 2-4], hydrolysis occurs in a stepwise manner where TAG is initially hydrolyzed to diacylglycerol (DAG) then to monoacylglycerol (MAG) and finally to glycerol. Each of these steps is reversible [1, 3]; therefore, at dynamic equilibrium some DAG and MAG are present in the FFA product. The hydrolysis reaction of oil is further complicated by the occurrence of an induction period where reaction rate is initially low and then gradually increases up to its normal level. As previously pointed out by Hartman [5], such induction period does “obscure” the kinetics of the hydrolysis of oil. The induction period is due to the low solubility of water in TAG as opposed to its higher solubility in FFA [6]. At 250 °C, there is approximately 20% water in the lipid phase [2]. Thus, the induction period ends as soon as there is 10-20% FFA in the mixture and it can be shortened by adding FFA to the reactants [6, 7]. This

---

<sup>1</sup> A version of this chapter was accepted for publication in the Journal of Supercritical Fluids (in press).

approach led to the idea that FFA has an important role as an acid catalyst, which would autocatalyze the reaction [7]. The induction period is also affected by temperature and becomes quite short at 260 to 280 °C due to the increased solubility of water in oil with temperature [2, 4]. Actually, King et al. [8] did report that at 339 °C soybean oil is completely miscible with water and that at such a high temperature the hydrolysis of the oil was completed in a very short time. Hence, temperature not only affects the induction period but also the reaction rate. Lascaray [6] established that a 10 °C increase in temperature could increase the reaction rate by a factor of 1.2 to 1.5, which was later confirmed by Sturzenegger and Sturm [3]. Ackelberg [9] reported that the limit of 1.2 to 1.5 was due to the much slower process of diffusion. It is true that the rate of diffusion of water and glycerol into and out of the fat phase, which is also affected by temperature, does affect the hydrolysis reaction [4]. Conversely, one factor that is clearly not affected by temperature is the degree of hydrolysis because equal dynamic equilibrium endpoints are obtained at different temperatures [3, 7]. According to the law of mass action, the degree of hydrolysis of fats varies with the concentrations of water and glycerol and the degree of hydrolysis increased with an increase in the initial amount of water. For instance, during hydrolysis of beef tallow at 260°C, the degree of hydrolysis at 1:3 and 1:60 oil to water molar ratio was 52% and 93.9%, respectively [3].

According to Lascaray [6, 10], hydrolysis is mainly a homogeneous reaction occurring in the oil phase and only a minor portion of the reaction takes place at the

oil and water interface during the induction period. This explanation appeared to be well accepted at the time. More recently, King et al. [8] conducted continuous hydrolysis reaction at 300 °C in a view cell and reported that the oil moved slowly up the window as a sphere in which “a white solid” was initially formed and then the solid slowly dissolved as it traveled on through the cell. Such observation might confirm Ackelsberg’s [9] description that an emulsion is formed in the early stages but disappears as FFA is formed in the oil phase. Although these reports are clearly non-conclusive, they do suggest that hydrolysis occurs in a dynamic system where the physical properties are constantly changing.

Kinetic studies conducted on the hydrolysis reaction were reviewed in Chapter 1 (Section 1.2.2.2.2) which revealed, among other things, that the first step (breakdown of TAG into DAG) was rate limiting and that the mass transfer of glycerol and water across the phases is faster than the reaction [1]. A recent study [7] also suggested that hydrolysis was autocatalyzed by FFA and proposed a mechanism, which seemed to adequately model FFA but did not mention its ability to model TAG, DAG, and MAG.

Hydrolysis of fats and oils in subcritical water and supercritical CO<sub>2</sub> (SC-CO<sub>2</sub>) media has also been studied (Sections 1.2.2.2.2 and 1.2.2.2.3). For example, Fujita and Himi [11] conducted hydrolysis of triolein in SC-CO<sub>2</sub> media while developing a novel way of recovering FFA from algae. They concluded that complete hydrolysis could be successfully conducted without causing any

degradation of oleic acid and that the hydrolysis vessel could also serve as an extraction vessel for FFA [11].

The initial incentive to conduct this study was to investigate the hydrolysis reaction in SC-CO<sub>2</sub> media in order to improve our understanding of the previously studied (Chapter 3) glycerolysis-hydrolysis reaction. However, based on the literature review summarized above it is apparent that a better understanding of the hydrolysis reaction in SC-CO<sub>2</sub> is needed for potential industrial applications. Consequently, the objective of this study was to generate a comprehensive kinetic study of canola oil hydrolysis in SC-CO<sub>2</sub> in order to predict the extent of the reaction at any time under particular conditions, establish the mechanism of the reaction, and determine the effect of temperature (200-250 °C), pressure (10-30 MPa), supercritical media and initial molar ratios of the reactants on the product composition.

## **5.2. Materials and Methods**

### *5.2.1. Materials*

The materials used were commercially refined, bleached and deodorized canola oil graciously donated by Canbra Foods Ltd. (Lethbridge, AB), deionized distilled water (DDW), 99.8% bone dry (water level < 3 ppm) carbon dioxide (CO<sub>2</sub>) and 99.95% compressed nitrogen (N<sub>2</sub>) from Praxair Canada Inc. (Mississauga, ON). Thin Layer Chromatography-Flame Ionization Detector System (TLC-FID)

determinations were performed using HPLC grade hexane from Fisher Scientific (Fairlawn, NJ, USA), laboratory grade ethyl ether and analytical grade glacial acetic acid from BDH Inc. (Toronto, ON). TLC reference standard (>99%) containing 25% (w/w) of each of oleic acid, monoolein, diolein and triolein was obtained from Nu-Chek Prep Inc. (Elysian, MN, USA).

### 5.2.2. *Reaction protocols*

Hydrolysis reactions were conducted in the same batch-operated system described previously in Section 3.2.2, which consisted of a magnetically stirred autoclave with three ports used to introduce carbon dioxide on the top of the cell, collect a sample from the bottom and monitor the temperature of the reaction mixture. A total volume of 76 mL of reactants, consisting of canola oil and DDW were added to the autoclave: the initial oil to water molar ratio (o/w) was 1:3, 1:17 and 1:70. Once the autoclave was sealed, the reaction mixture was purged with either CO<sub>2</sub> or N<sub>2</sub> and constantly stirred (~100 rpm). Tank pressure CO<sub>2</sub> or N<sub>2</sub> (~6 MPa) was then added to the autoclave before increasing the temperature to 200 or 250 °C. Once the desired temperature was established, the autoclave was pressurized to 10 or 30 MPa and the mixing rate was increased to 250 ± 30 rpm.

Samples (1 mL) were collected using the previously described protocol (Section 3.2.2) to ensure that the samples taken as a function of time were representative of the reaction mixture at that time. Samples were collected every 30 min but after 3 h a sample was collected every hour up to 6 h. This sampling

protocol was implemented in order to maximize kinetic data without disturbing the equilibrium of the reaction mixture.

### 5.2.3. *Lipid analysis*

The samples collected as a function of time throughout the reactions conducted at different conditions separated into two phases upon standing at ambient conditions. Only the composition of the oil layer was analyzed using TLC-FID. The oil was separated into TAG, DAG, MAG and FFA on Chromarods-SIII (silica gel type) and quantified using an Iatroscan TH-10 (IATRON-Laboratories Inc., Tokyo, Japan). The analysis was done and the area percentages were calculated as previously described in Section 3.2.3. All concentrations were reported as mol per 100 g of oil using molar weights of 620.99, 356.54 and 282.45 a.m.u. for DAG, MAG and FFA, respectively. These molar weights represent those of diolein, monoolein and oleic acid, respectively, since oleic acid is the most abundant fatty acid in canola oil [12]. For TAG, the average molecular weight of canola oil, 879 a.m.u [13], was used to calculate the results obtained from hydrolysis.

### 5.2.4. *Experimental design and statistical analysis*

To test the effect of supercritical media, replicated 6 h reactions (250 °C, 10 MPa, 1:17 o/w) were conducted in both supercritical nitrogen (SC-N<sub>2</sub>) and in SC-CO<sub>2</sub>. To test the effect of pressure additional 6 h replicated runs (250 °C, 1:17 o/w,

SC-CO<sub>2</sub>) were also conducted at 30 MPa. The initial concentration effect was tested by conducting a set of replicated 6 h reactions (250 °C, 10 MPa, SC-CO<sub>2</sub>) using 1:3, 1:17 and 1:70 o/w. Finally, the temperature effect was observed in replicated 6 h reactions (10 MPa, 1:17 o/w, SC-CO<sub>2</sub>) conducted at 200 and 250 °C. The order in which all of the above reactions were carried out was randomized and the composition of the samples obtained was randomly analyzed in duplicate by TLC-FID analyses. The variance between TLC-FID analyses, as obtained by analyzing all the TLC reference standard chromatograms, was less than 6%.

The maximum rate of FFA formation (FFA<sub>max</sub>) was calculated by introducing the raw data along with the calculated *k*-values obtained from the kinetic model (described in Sections 5.2.5 and 5.2.6) into the differential rate equation for FFA. FFA<sub>max</sub> obtained for reactions conducted at different pressures, in different supercritical media and initial oil to water ratios were compared by conducting an analysis of variance using the mixed model procedure of SAS Statistical Software version 9.1 and means for different treatments were compared using Student's t-test [14]. Results were reported as statistically significant when the p-value was smaller than or equal to 0.05 ( $p \leq 0.05$ ) and in the discussion the exact p-values obtained by SAS were reported.

The conversion rate was defined and calculated as follows:

$$\% \text{ Conversion} = \frac{[\text{FFA}]_t}{3 \times [\text{TAG}]_0} \times 100 \quad (5.1)$$

where  $[FFA]_t$  was the molar concentration of FFA predicted by the model at time  $t$  and  $[TAG]_0$  was the initial molar concentration of TAG.

### 5.2.5. Kinetic modeling

Some investigators [1, 15] reported that hydrolysis occurs according to the reversible reactions described by Eqs. (5.2)-(5.4), where Gly and  $H_2O$  represent glycerol and water, respectively, and  $k_{7-12}$  represent the rate constants for each step. The numbers used to differentiate the  $k$ -values are the same as the ones that were arbitrarily given in Section 2.2.2 and were chosen to simplify the comparison between the two studies.



At first glance, Eqs. (5.2)-(5.4) alone might be able to explain the hydrolysis reaction; however, at the high temperature range studied, the reaction described by Eq. (5.5) can also occur within the oil mixture [16].





By considering the reaction steps described in Eqs. (5.2)-(5.5), the rate of change in concentration for each of the reaction components can then be described by the following differential rate equations, Eqs. (5.6a)-(5.6f).

$$\frac{d[\text{MAG}]}{dt} = -k_5[\text{TAG}][\text{MAG}] + k_6[\text{DAG}]^2 + k_9[\text{DAG}][\text{H}_2\text{O}] - k_{10}[\text{MAG}][\text{FFA}] - k_{11}[\text{H}_2\text{O}][\text{MAG}] + k_{12}[\text{Gly}][\text{FFA}] \quad (5.6a)$$

$$\frac{d[\text{DAG}]}{dt} = 2k_5[\text{TAG}][\text{MAG}] - 2k_6[\text{DAG}]^2 + k_7[\text{TAG}][\text{H}_2\text{O}] - k_8[\text{DAG}][\text{FFA}] - k_9[\text{DAG}][\text{H}_2\text{O}] + k_{10}[\text{MAG}][\text{FFA}] \quad (5.6b)$$

$$\frac{d[\text{TAG}]}{dt} = -k_5[\text{TAG}][\text{MAG}] + k_6[\text{DAG}]^2 - k_7[\text{TAG}][\text{H}_2\text{O}] + k_8[\text{DAG}][\text{FFA}] \quad (5.6c)$$

$$\frac{d[\text{FFA}]}{dt} = k_7[\text{TAG}][\text{H}_2\text{O}] - k_8[\text{DAG}][\text{FFA}] + k_9[\text{DAG}][\text{H}_2\text{O}] - k_{10}[\text{MAG}][\text{FFA}] + k_{11}[\text{H}_2\text{O}][\text{MAG}] - k_{12}[\text{Gly}][\text{FFA}] \quad (5.6d)$$

$$\frac{d[\text{H}_2\text{O}]}{dt} = -k_7[\text{TAG}][\text{H}_2\text{O}] + k_8[\text{DAG}][\text{FFA}] - k_9[\text{DAG}][\text{H}_2\text{O}] + k_{10}[\text{MAG}][\text{FFA}] - k_{11}[\text{H}_2\text{O}][\text{MAG}] + k_{12}[\text{Gly}][\text{FFA}] \quad (5.6e)$$

$$\frac{d[\text{Gly}]}{dt} = k_{11}[\text{MAG}][\text{H}_2\text{O}] - k_{12}[\text{Gly}][\text{FFA}] \quad (5.6f)$$

### 5.2.6. Determination of rate constants

The concentrations of glycerol and water as a function of time were not determined analytically but were calculated. The change in water concentration as a function of time was calculated based on stoichiometry by subtracting the production of FFA over time from the initial molar concentration of water because the use of one mole of water corresponds to the production of one mole of FFA

(Eqs. (5.2)-(5.4)). The molar concentration of glycerol as a function of time was calculated based on material balance where the glycerol at a given time was obtained by subtracting the sum of the molar concentrations of TAG, DAG and MAG at that given time from the initial amount of TAG.

To model the reaction, the composition data collected as a function of time and analyzed in duplicate by TLC-FID were converted into a mathematical expression using a curve fitting program [17]. Using this program, FFA and glycerol were modeled using a Logistic Model  $[y=a/(1+be^{-ct})]$  where the correlation coefficient ( $R^2$ ) range for each component was 0.98-0.994 and 0.88-0.98, respectively. TAG data were described by a Harris Model  $[y = 1/(a+bt^c)]$  ( $R^2 = 0.99$ ) for all conditions except for reactions conducted using 1:3 o/w; for those reactions a Harris Model ( $R^2 = 0.94$ ) and a Logistic Model ( $R^2 = 0.94$ ) were used. DAG and MAG, which were difficult to model due to the bell shape appearance encountered in reactions conducted using 1:17 and 1:70 o/w, were both modeled using a combination of a Rational Model  $[y=(a+bt)/(1+ct+dt^2)]$  ( $R^2$  range 0.71-0.92 and 0.53-0.96, respectively) and a Logistic Model ( $R^2$  range 0.53-0.96 and 0.61-0.94, respectively) for all conditions except for reactions using 1:3 o/w where DAG was modeled using a Logistic Model ( $R^2 = 0.94$ ) and an Exponential Association Model  $[y=a(1-e^{-bt})]$  ( $R^2 = 0.88$ ). Finally, for water a combination of Harris ( $R^2$  range 0.92-0.98) and Logistic ( $R^2$  range 0.69-0.98) Models was used. In each model,  $a$ ,  $b$ ,  $c$  and  $d$  were fixed constants determined by the program and  $t$  was the time. Using these mathematical expressions, experimental molar concentration

( $C_{\text{exp}}$ ) for each component (TAG, DAG, MAG, FFA, Gly and  $\text{H}_2\text{O}$ ) was obtained every 6 min over a 6 h period. These  $C_{\text{exp}}$  were then introduced into Eqs. (5.6a)-(5.6e) along with variable  $k$ -values ( $k_{5-12}$ ) and the rate of change ( $r_{\text{pred}}$ ) for each component was obtained over the same period as for  $C_{\text{exp}}$ . The following expression was then used to obtain the predicted concentration ( $C_{\text{pred}}$ ) for each component:

$$C_{\text{pred}} = C|_{t+\Delta t} = C_{\text{exp}}|_t + r_{\text{pred}} \cdot \Delta t \quad (5.7)$$

where  $C_{\text{exp}}|_t$  is the concentration at time  $t$ ,  $\Delta t$  is the time interval (6 min) and  $C|_{t+\Delta t}$  is the predicted concentration at  $t + \Delta t$ . The summed squared error (SSE) between  $C_{\text{exp}}$  and  $C_{\text{pred}}$  was then obtained for each component using the expression  $\Sigma(C_{\text{exp}} - C_{\text{pred}})^2$ .

Two  $k$ -values,  $k_{10}$  and  $k_{12}$ , were calculated by introducing dynamic equilibrium data obtained after 6 h in the following equilibrium equations:

$$k_{10} = \frac{-2k_5([\text{TAG}]_{\infty})([\text{MAG}]_{\infty}) + 2k_6([\text{DAG}]_{\infty})^2 - k_7([\text{TAG}]_{\infty})([\text{H}_2\text{O}]_{\infty}) + k_8([\text{DAG}]_{\infty})([\text{FFA}]_{\infty}) + k_9([\text{DAG}]_{\infty})([\text{H}_2\text{O}]_{\infty})}{([\text{MAG}]_{\infty})([\text{FFA}]_{\infty})} \quad (5.8)$$

$$k_{12} = \frac{k_{11}([\text{MAG}]_{\infty})([\text{H}_2\text{O}]_{\infty})}{([\text{Gly}]_{\infty})([\text{FFA}]_{\infty})} \quad (5.9)$$

where  $[\text{TAG}]_{\infty}$ ,  $[\text{DAG}]_{\infty}$ ,  $[\text{MAG}]_{\infty}$ ,  $[\text{FFA}]_{\infty}$ ,  $[\text{Gly}]_{\infty}$ , and  $[\text{H}_2\text{O}]_{\infty}$  are mol/100 g oil at dynamic equilibrium. Eqs. (5.8) and (5.9) were obtained by setting the rate of change of DAG and Gly to zero in Eqs. (5.6b) and (5.6f), respectively.

The Generalized Reduced Gradient (GRG2) nonlinear optimization code [18] was used to calculate the  $k$ -values. To simplify the calculation two constraints were included:  $k$  had to be positive and the rate of change for Eqs. (5.6a)-(5.6f) at 6 h had to be zero. Along with these constraints, Eqs. (5.8) and (5.9) were included in the system of equations and the program was asked to minimize the SSE for all components while changing  $k_{5,9}$  and  $k_{11}$  to determine the reaction rate constants.

### **5.3. Results and discussion**

#### *5.3.1. Composition and kinetic calculations*

In this study, as in the previous studies present in Chapter 3 and 4, the composition data were obtained using the relatively fast TLC separation and quantification using the reliable FID detector commonly used in gas chromatography. The use of such an analytical method was well suited for this study because it simplified the compositional analysis of hydrolyzed canola oil while providing enough detail to calculate the rate of the reaction.

Figure 5.1 presents the experimental data along with their fitted curves for the samples obtained in SC-CO<sub>2</sub> using 1:17 o/w, 250 °C and 10 MPa. It is apparent

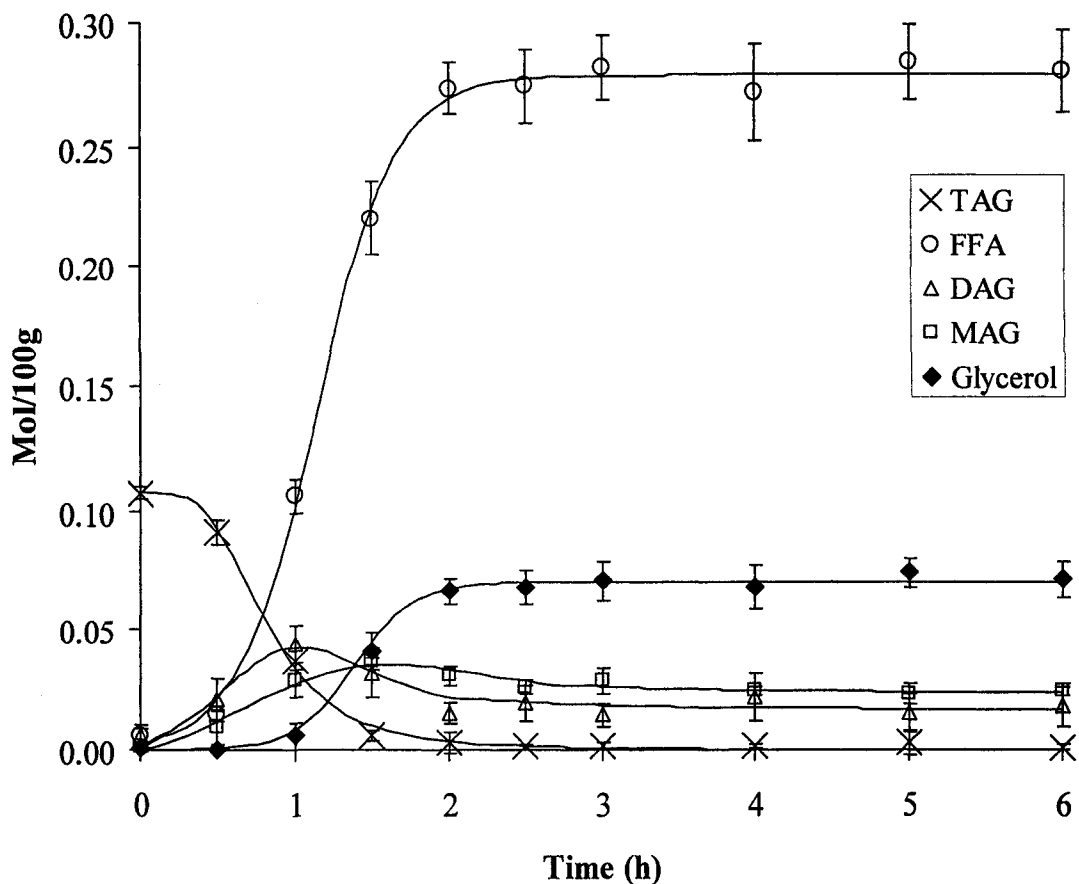


**Figure 5.1.** Experimental hydrolysis data and fitted curves of the composition of the oil phase as a function of time obtained at 1:17 o/w, 250 °C and 10 MPa. All individual points are measured data except for those for glycerol which were calculated based on material balance.

that dynamic equilibrium is achieved after 3 h and that the product consisted mainly of FFA with very small amounts of DAG and MAG and only traces of TAG. The induction period was less than 30 min given that time zero was defined as the time when the reactants in the autoclave reached 250 °C and 10 MPa. However, some reactions could have occurred during the last portion of the 30 min heat-up time and

would have been responsible for the minor amounts of DAG, MAG and FFA detected at time zero since none of them were initially present in the original canola oil used. The rate of hydrolysis at 100 °C was reported to be very low [6, 11]. Therefore, it is reasonable to assume that reactions only occurred during the last 10-15 min of the heating process when the temperature was increased from 100 to 250 °C. Thus, the induction period for the reaction conducted under these conditions is approximately 40 to 45 min. As previously mentioned, the induction period could be reduced by adding FFA to the reactants in order to enhance water and TAG solubility thereby autocatalyzing the reaction [7].

The induction period was followed by a dramatic decrease in TAG concentration after 0.5 h (Fig. 5.1). The FFA concentration, on the other hand, initially appeared to be sluggish but quickly ramped up to reach the fastest rate of FFA formation at 1 h. At 1 h, the concentration of DAG reached a maximum and then slowly decreased thereby resulting in a bell-shaped curve (Fig. 5.1). MAG concentration also formed a broad bell-shaped curve but its maximum was delayed and only appeared at 1.5 h. The tail of the bell-shaped curves for both MAG and DAG ended up at 2.5 to 3 h when the FFA concentration reached dynamic equilibrium and TAG concentration became negligible. Such observations are in agreement with the idea that hydrolysis occurs in a stepwise manner where TAG is initially hydrolyzed to DAG then to MAG and finally to glycerol and that the kinetic model should reflect this. Figure 5.1 also shows that the calculated glycerol formation slowly but consistently increased after 45 min and such behaviour

suggests that it did not participate in the reactions. Hence, glycerolysis reactions were not considered in the kinetic model.

### 5.3.2. *Temperature effect*

Lowering the temperature from 250 to 200 °C while keeping the other parameters constant (SC-CO<sub>2</sub>, 10 MPa, 1:17 o/w) showed a dramatic decrease in conversion rates. Indeed, the plot of FFA obtained under these conditions, as presented in Figure 5.2, clearly shows how little FFA was produced at 200 °C over time. This was expected since Fujita and Himi [11] had previously shown that a decrease in temperature from 250 to 200 °C was associated with >50% loss in TAG hydrolysis efficiency after 3 h of reaction. They also showed negligible TAG hydrolysis at 150 °C [11]. These results confirm that temperature has a considerable influence on the reaction rate of non-catalyzed hydrolysis. As previously mentioned, this effect is probably mainly due to the increase in solubility of water in oil with temperature [2, 4] but it is also possible that the change in SC-CO<sub>2</sub> density has a contribution although such effect could not be determined based on the current data.

Data collected at 200°C were not used to determine the reaction rate constants because dynamic equilibrium data were not generated. Higher reaction temperatures were not tested, even though increasing temperature would have probably increased the reaction rate further, because FFA isomerization occurs at

higher temperatures thereby forming *trans* FFA [2, 19], which may not be desirable depending on final product applications of FFA.

### 5.3.3. Pressure effect

In order to determine the effect of pressure, reactions were conducted in SC-CO<sub>2</sub> at 10 and 30 MPa while keeping the temperature constant at 250 °C and the initial reactant ratio at 1:17 o/w. Reactions conducted at 30 MPa took more time to

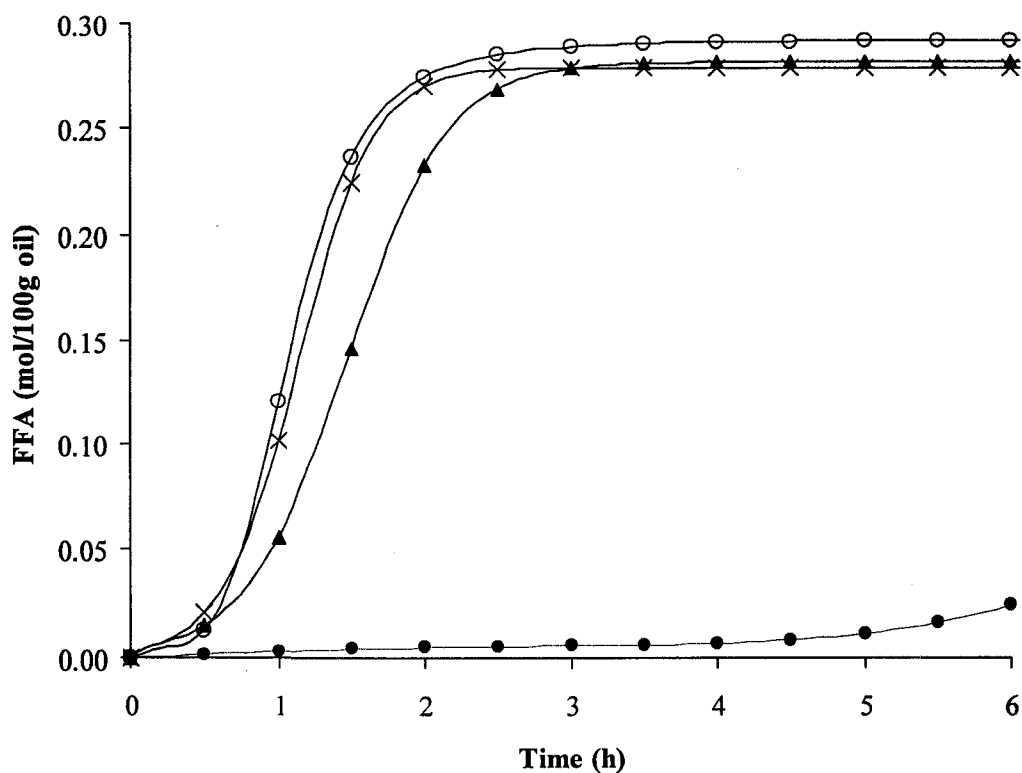


**Figure 5.2.** Effect of pressure, temperature and media on FFA composition using a 1:17 o/w as a function of time where (●) represent reactions conducted in SC-CO<sub>2</sub> at 200 °C and 10 MPa, (○) represent runs conducted in SC-N<sub>2</sub> at 250 °C and 10 MPa and where (▲) and (×) represent runs both conducted in SC-CO<sub>2</sub> at 250 °C but at 30 MPa and 10 MPa, respectively. Data points and curves are modeled data.



reach the FFA dynamic equilibrium concentration of 0.28 mol/100g oil or approximately 82% conversion compared to those conducted at 10 MPa (Fig. 5.2). However, statistical analysis showed that  $FFA_{max}$  obtained for reactions conducted at 10 and 30 MPa were not significantly different ( $p = 0.42$ ). As depicted in Figure 5.3, the curves for the rate of FFA formation as a function of time for reactions

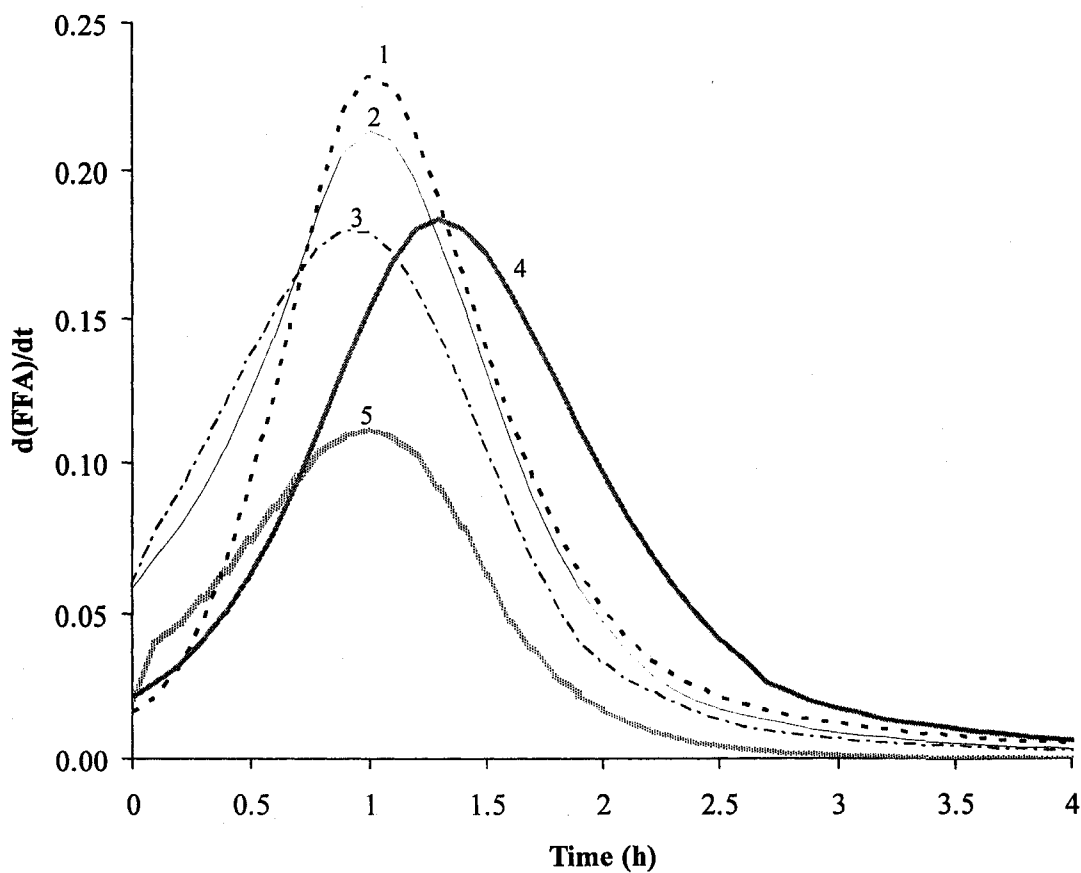


**Figure 5.3.** Rate of FFA formation as a function of time calculated from the fitted data: (1) 10 MPa, 1:70 o/w, SC-CO<sub>2</sub>; (2) 10 MPa, 1:17 o/w, SC-N<sub>2</sub>; (3) 10 MPa, 1:17 o/w, SC-CO<sub>2</sub>; (4) 30 MPa, 1:17 o/w, SC-CO<sub>2</sub>; (5) 10 MPa, 1:3 o/w, SC-CO<sub>2</sub>.

conducted at 10 and 30 MPa both peaked at the same rate. Nevertheless, Figure 5.3 also shows that the initial rates of FFA formation for reactions conducted at 10 MPa were higher than for those conducted at 30 MPa. In addition,  $FFA_{max}$  for reactions conducted at 10 MPa was reached at 0.9 h (54 min) whereas for those conducted at 30 MPa 1.3 h (78 min) was required; a 24 min difference which also corresponds to the extra time required for the reaction conducted at 30 MPa to reach FFA dynamic equilibrium concentration.

The longer time required at 30 MPa to reach FFA dynamic equilibrium could explain the pressure effect previously reported (Section 3.3.4) for the production of MAG during glycerolysis. Indeed, during glycerolysis, the rate of MAG formation was also favoured at 10 MPa compared to 30 MPa. However, in the esterification study (Section 4.3.3) pressure did not influence esterification. Therefore, one can conclude that pressure has a direct influence on the interaction between oil and water. As suggested earlier (Section 3.3.4), the nature of this effect could be due to a decrease in water-oil interaction as the pressure of the system is increased from 10 to 30 MPa as a result of increased level of  $CO_2$  in the system and dilution of oil phase. The system might also be mass transfer controlled; however, mass transfer aspects were not investigated in this study

#### *5.3.4. Effect of supercritical media*

Fujita and Himi [11] used SC- $CO_2$  both as a reaction medium and a separation solvent. However, it is not clear whether SC- $CO_2$  provides further

reaction benefits, possibly due to formation of carbonic acid, apart from its help in extracting FFA from the hydrolysis end products. To verify this, hydrolysis reactions were conducted at 250 °C, 10 MPa and using 1:17 o/w in SC-CO<sub>2</sub> and in SC-N<sub>2</sub>. As shown in Figure 5.2, formation of FFA was similar for reactions conducted in SC-CO<sub>2</sub> and SC-N<sub>2</sub>. In fact, although Figure 5.3 shows a slightly higher FFA<sub>max</sub> for reactions conducted in SC-N<sub>2</sub>, it was not significantly different ( $p = 0.12$ ) from that obtained in SC-CO<sub>2</sub> media. Even the initial rates of FFA formation were similar in both media (Fig. 5.3).

#### 5.3.5. *Effect of initial reagent concentrations*

Changes in product concentrations for reactions conducted using 1:3, 1:17 and 1:70 o/w while keeping the other parameters constant (SC-CO<sub>2</sub>, 10 MPa, 250 °C) are presented in Figure 5.4 for FFA and TAG and Figure 5.5 for MAG and DAG. TAG concentration became negligible at 4 h for reactions conducted at 1:17 and 1:70. This is in agreement with Fujita and Himi [11] who showed that hydrolysis efficiencies for a reaction conducted in SC-CO<sub>2</sub> at 250 °C and 8 MPa using 1:70 o/w are close to 100% after 4 h. However, Figures 5.4 and 5.5 also show a reality that was not reported previously, that is even if the hydrolysis efficiency is close to 100% in terms of TAG, DAG and MAG are still present along with FFA at 4 h. It is interesting to note that DAG and MAG both form bell-shaped curves for reactions conducted at 1:17 and 1:70 o/w with maximum reached at 1 and 1.5 h,

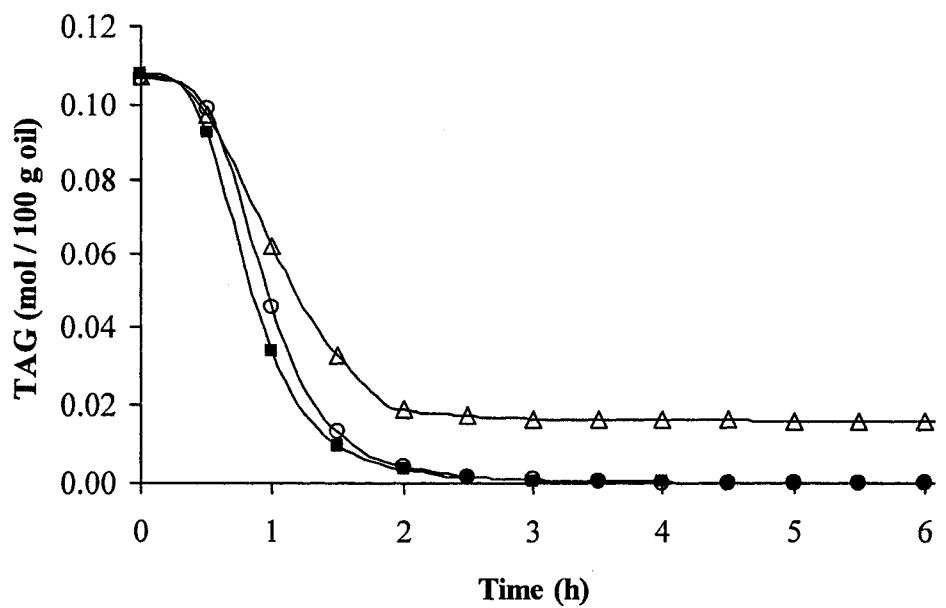
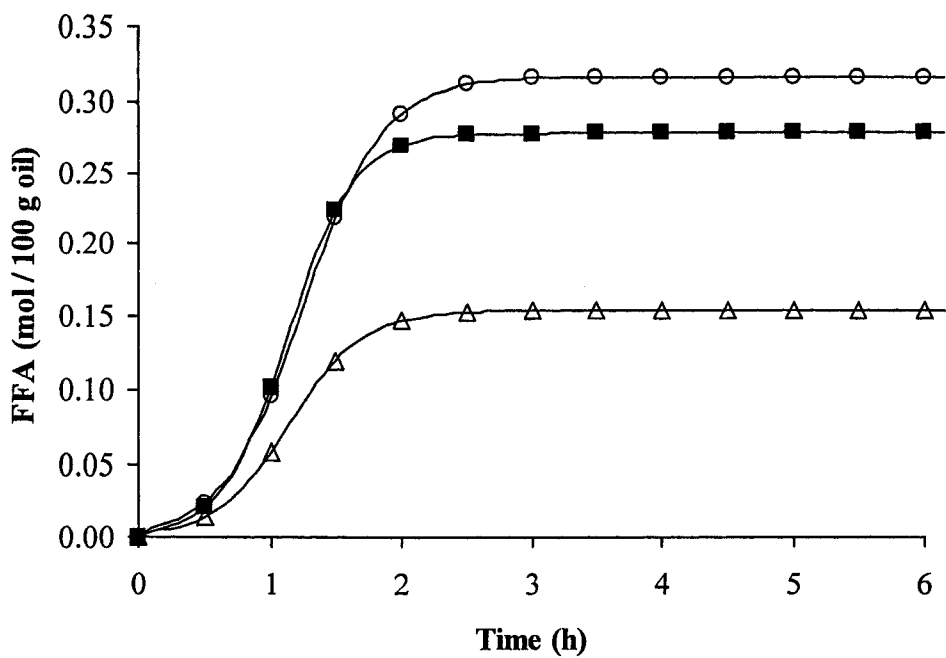


**Figure 5.4.** Production of FFA and TAG during hydrolysis of canola oil at 250 °C, 10 MPa where (Δ), (■) and (○) are 1:3, 1:17 and 1:70 o/w, respectively. Data points and curves are modeled data.

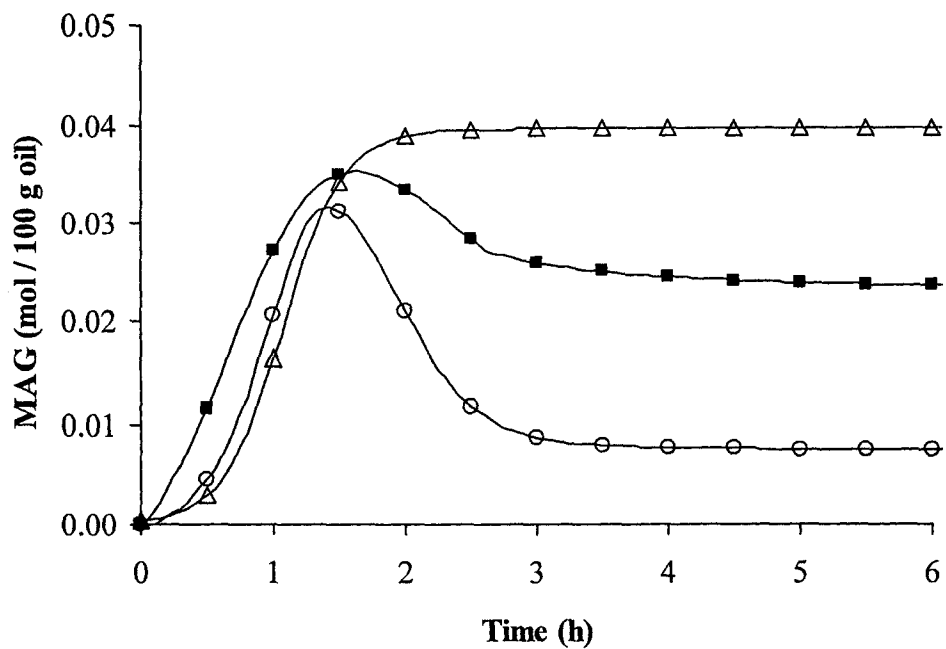
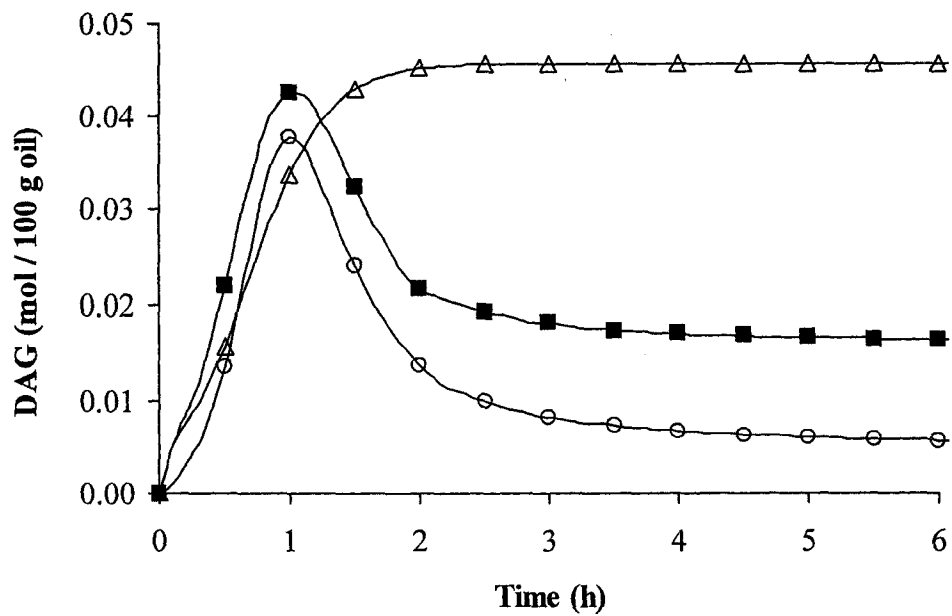


**Figure 5.5.** Production of DAG and MAG during hydrolysis of canola oil at 250 °C, 10 MPa where (Δ), (■) and (○) are 1:3, 1:17 and 1:70 o/w, respectively. Data points and curves are modeled data.

respectively. This indicates that the majority of TAG is transformed into DAG between 0.5 and 1 h and then DAG is progressively transformed into MAG between 1 and 1.5 h before finally becoming glycerol. As mentioned earlier, such a result is in agreement with Eqs. (5.2)-(5.4). The bell-shaped curve for MAG and DAG does not occur for reactions conducted at 1:3 o/w probably because there is not enough water available to further break them down and so DAG and MAG reach a plateau after 1 and 1.5 h, respectively. This was not expected since the 1:3 o/w ratio should have satisfied the stoichiometric requirements. However, as shown in Figure 5.6, the stoichiometric level of water corresponded closely with the amounts present when esterification reactions reached dynamic equilibrium. It is therefore possible that, as in the esterification reaction (Section 4.3.5), the glycerol produced during hydrolysis (Figure 5.1) bound the water thereby making it unavailable.

Figure 5.7 also shows that the initial water used for reaction conducted at 1:17 o/w level was close to the water initially present for the glycerolysis-hydrolysis reactions (Chapter 3) conducted using 8% w/w initial water in glycerol. However, unlike the hydrolysis reaction investigated in this study, the level of water did not decrease appreciably during glycerolysis-hydrolysis reactions (Chapter 3). A probable explanation for such a result might be that glycerolysis was occurring simultaneously with hydrolysis.

It is also apparent from Figure 5.4 that, even if an increase in initial water concentration from 1:17 to 1:70 does not seem to affect TAG breakdown, it does

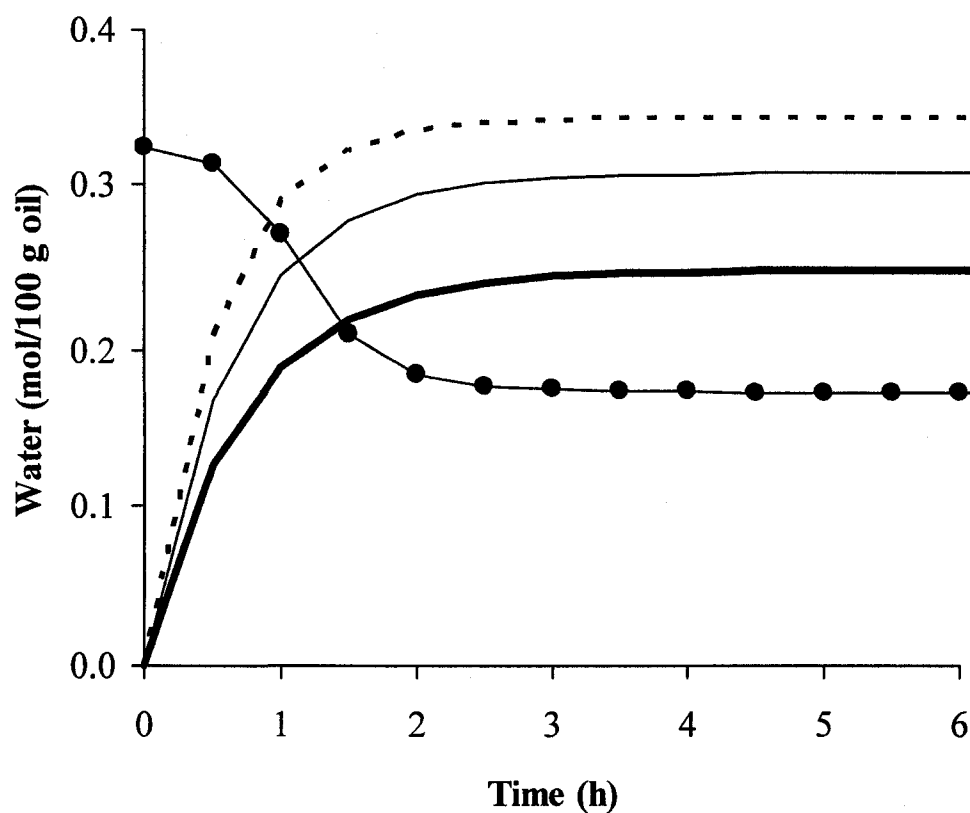


**Figure 5.6** Change in water concentration as a function of time for esterification (Chapter 4) and hydrolysis reactions conducted at 10 MPa and 250 °C. (●) represent hydrolysis data conducted using 1:3 initial oil/water molar ratio; (----), (—) and (—) represent esterification reactions conducted using 1:0.1, 1:1 and 1:2 initial glycerol/oleic acid molar ratio, respectively.

increase the amount of FFA formed. For instance, the conversion at 3 h was 45, 82 and 93% for 1:3, 1:17 and 1:70 o/w, respectively. From Figure 5.4, the rate for FFA formation between 1:17 and 1:70 appears to be somewhat similar; however, when the rate of change in FFA concentration is plotted as a function of time (Fig. 5.3), sharp differences become evident.  $FFA_{max}$  for reactions conducted using 1:17 o/w

was significantly different from those obtained for reactions conducted using 1:3 o/w ( $p \leq 0.0001$ ) and from those obtained using 1:70 initial o/w ( $p = 0.0003$ ).  $FFA_{\max}$  was also significantly different ( $p \leq 0.0001$ ) between reactions conducted using 1:3 and 1:70 o/w.

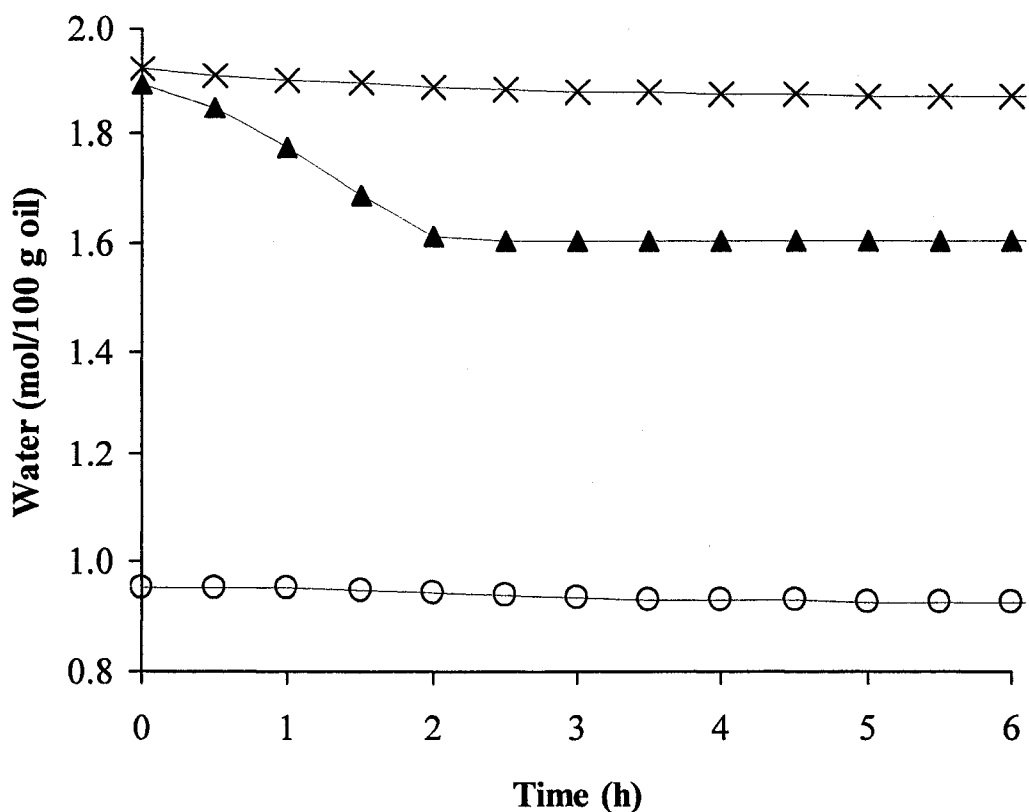


**Figure 5.7** Change in water concentration as a function of time for hydrolysis and glycerolysis (Chapter 3) reactions conducted at 10 MPa and 250 °C. (▲) represent hydrolysis data conducted using 1:17 initial oil/water molar ratio and (○) and (×) represent glycerolysis data for reactions conducted using 4 and 8% (w/w of glycerol) initial water, respectively.



### 5.3.6. Mechanism of the reaction

Based on Eqs. (5.2)-(5.5) and on the rate constants reported in Table 5.1, it is possible to establish how hydrolysis of TAG occurred for a reaction conducted in SC-CO<sub>2</sub> at 250 °C, 10 MPa using 1:17 o/w within the limitations and assumptions of the kinetic model used. At the beginning of the reaction, given that there were no FFA, DAG or MAG in the reactants, TAG and water reacted according to the forward reaction of Eq. (5.2). This initial step has the lowest *k*-value and was therefore the slowest or rate limiting step. The slow rate of this initial step also explains the induction period mentioned earlier. Although the forward reaction

**Table 5.1.** Effect of the initial canola oil to water molar ratio (o/w), pressure and supercritical media (SC-CO<sub>2</sub> and SC-N<sub>2</sub>) on rate constants at 250 °C

Rate constants (g/h mol)	SC-CO <sub>2</sub>				SC-N <sub>2</sub>
	10 MPa 1:3 o/w	10 MPa 1:17 o/w	10 MPa 1:70 o/w	30 MPa 1:17 o/w	10 MPa 1:17 o/w
<i>k</i> <sub>5</sub>	64.97	72.52	71.22	67.89	87.01
<i>k</i> <sub>6</sub>	20.52	0	0	0	0
<i>k</i> <sub>7</sub>	0.59	0.05	0.02	0.04	0.03
<i>k</i> <sub>8</sub>	0	0	0	0	0
<i>k</i> <sub>9</sub>	10.51	2.07	0.60	1.96	3.01
<i>k</i> <sub>10</sub>	13.98	3.82	10.31	2.48	5.78
<i>k</i> <sub>11</sub>	4.89	1.36	0.46	1.06	1.75
<i>k</i> <sub>12</sub>	15.58	3.08	0.86	3.33	3.36

of Eq. (5.2) is a limiting step, it is a decisive one because for all tested conditions  $k_8$  is zero meaning that the reverse reaction of Eq. (5.2) did not occur. Once DAG and FFA are formed by Eq. (5.2), DAG must react with water according to the forward reaction of Eq. (5.3) and form MAG and FFA. However, this forward step has a lower  $k$ -value than the reverse reaction, which means that the FFA formed in Eq (5.2) can react with newly formed MAG. Alternatively, MAG can also react with the initially high concentration of TAG according to the forward and non-reversible reaction of Eq. 5.5 and form two DAG. Given that the  $k$ -value ( $k_5$ ) for this reaction (Eq 5.5) is the highest rate constant, the concentration of DAG, as seen in Figure 5.5, reaches a maximum at 1 h and then decreases steadily as the concentration of TAG becomes depleted. MAG can also react with water according to the forward reaction of Eq. (5.4) to form glycerol and FFA. However, Eq. (5.4) is also reversible and this reverse reaction has a larger  $k$ -value. In addition, at the beginning of the reaction, there was arguably more FFA available than there was MAG and, according to Figure 5.1, glycerol did not accumulate until 45 min. Consequently, FFA and the glycerol recently formed most probably reacted to produce more MAG. This leads to the question of how FFA and glycerol accumulated eventually. The answer might be in potential changes in phase behaviour caused by the initial accumulation of DAG and then MAG. Indeed, without these intermediates (DAG and MAG), not enough water would have been emulsified into the oil mixture to push reactions of Eqs. (5.3) and (5.4) forward.

Looking at the reaction under this new light gives reason to Lascaray [6] who was claiming that hydrolysis was governed principally by physical phenomena.

The rate constants obtained when conducting reactions in SC-N<sub>2</sub> were similar to those obtained while conducting reactions under the same operating conditions in SC-CO<sub>2</sub> (Table 5.1). Such result thereby indicates that at tested conditions the mechanism of the reaction is not appreciably affected by the reaction media.

The rate constant of the limiting step,  $k_7$ , is small for reactions conducted using 1:17 o/w and 1:70 o/w (0.02-0.05). The  $k_7$  determined for SC-N<sub>2</sub> was 0.03, which is in agreement with the value of 0.0270, reported by Sturzenegger and Sturm [3] for peanut oil hydrolysis in nitrogen at 240 °C and ~7 MPa using ~1:23 o/w. Substantial change in higher rate constants ( $k_6, k_7, k_{9-12}$ ) obtained using lower initial molar concentration of water (1:3 o/w) are probably due to the complex phase behaviour and physical properties and, since these were not considered in this work, they should be studied further.

#### 5.4. Conclusions

Hydrolysis reactions of canola oil in SC-CO<sub>2</sub> were conducted at 250°C, 10-30 MPa, and using 1:3, 1:17 and 1:70 o/w. Reactions were also conducted in supercritical nitrogen at 10 MPa, 250°C and 1:17 o/w. Rate constants were obtained by kinetic modeling of the data. The maximum rate of FFA (FFA<sub>max</sub>) production was not affected ( $p > 0.05$ ) by supercritical media or pressure but it was delayed at

30 MPa.  $FFA_{max}$  increased significantly ( $p < 0.05$ ) as the amount of water was increased from 1:3 to 1:17 and 1:70 (o/w). Results suggested that more than stoichiometric amount of water should be initially added to the oil to ensure complete hydrolysis of TAG because a portion of the water is most probably bound by the glycerol produced in the reaction. Using the calculated rate constants, the mechanism of the hydrolysis of canola oil was determined. Results provide valuable information for optimization of industrial hydrolysis in SC-CO<sub>2</sub> media.

## 5.5. References

- [1] T.A. Patil, D.N. Butala, T.S. Raghunathan, H.S. Shankar, Thermal hydrolysis of vegetable oils and fats. 1. Reaction kinetics. *Ind. Eng. Chem. Res.* 27 (1988) 727-735.
- [2] V. Mills, H.K. McClain, Fat hydrolysis. *Ind. Eng. Chem.* 41 (1949) 1982-1985.
- [3] A. Sturzenegger, H. Sturm, Hydrolysis of fats at high temperatures. *Ind. Eng. Chem.* 43 (1951) 510-515.
- [4] E.A. Lawrence, Hydrolysis methods. *J. Am. Oil Chem. Soc.* 31 (1954) 542-544.
- [5] L. Hartman, Kinetics of the Twitchell hydrolysis. *Nature* 167 (1951) 199-199.
- [6] L. Lascaray, Industrial fat splitting. *J. Am. Oil Chem. Soc.* 29 (1952) 362-366.
- [7] E. Minami, S. Saka, Kinetics of hydrolysis and methyl esterification for biodiesel production in two-step supercritical methanol process. *Fuel* 85 (2006) 2479-2483.
- [8] J.W. King, R.L. Holliday, G.R. List, Hydrolysis of soybean oil in a subcritical water flow reactor. *Green Chem.* 1 (1999) 261-264.
- [9] O.J. Ackelsberg, Fat splitting. *J. Am. Oil Chem. Soc.* 35 (1958) 635-640.

- [10] L. Lascaray, Mechanism of fat splitting. *Ind. Eng. Chem.* 41 (1949) 786-790.
- [11] K. Fujita, M. Himi, Hydrolysis of glycerol trioleate and extraction of its fatty acid under CO<sub>2</sub> supercritical conditions. *Nippon Kagaku Kaishi* 1 (1995) 79-82.
- [12] B.J. Siemens, J.K. Daun, Determination of the fatty acid composition of canola, flax, and solin by near-infrared spectroscopy. *J. Am. Oil Chem. Soc.* 82 (2005) 153-157.
- [13] A.J. Wright, S.E. McGauley, S.S. Narine, W.M. Willis, R.W. Lencki, A.G. Marangoni, Solvent effects on the crystallization behavior of milk fat fractions. *J. Agric. Food Chem.* 48 (2000) 1033-1040.
- [14] SAS Institute Inc., Version 9.1, Cary, NC, 2003.
- [15] J.S.S. Pinto, F.M. Lanças, Hydrolysis of corn oil using subcritical water. *J. Braz. Chem. Soc.* 17 (2006) 85-89.
- [16] H. Nouredini, D.W. Harkey, M.R.A. Gutsman, Continuous process for the glycerolysis of soybean oil. *J. Am. Oil Chem. Soc.* 81 (2004) 203-207.
- [17] D.G. Hyams, CurveExpert Version 1.37, Chadwick Court, Hixson, TN, 2001.
- [18] L. Lasdon, W. Allan, Microsoft Excel Solver (GRG2), Frontline Systems, Inc., Incline Village, NV, 2002.
- [19] R.L. Holliday, J.W. King, G.R. List, Hydrolysis of vegetable oils in sub- and supercritical water. *Ind. Eng. Chem. Res.* 36 (1997) 932-935.

## **6. Continuous enzymatic hydrolysis of canola oil in supercritical carbon dioxide media: effects of temperature, enzyme load and carbon dioxide flow rate<sup>1</sup>**

### **6.1. Introduction**

Enzyme reactions in SC-CO<sub>2</sub> offer the advantages of mild reaction conditions, high mass transfer rate and control over reaction conditions while facilitating solvent-product separation. It is also a promising field of study since a continuous enzymatic reaction in SC-CO<sub>2</sub> could be incorporated as a unit operation into a continuous supercritical processing system. Indeed, by conducting continuous on-line extraction-hydrolysis-fractionation, canola oil in the seeds could be transformed into a number of higher value fractions with the same SC-CO<sub>2</sub> load thereby reducing the energy expenditure associated with pressurizing CO<sub>2</sub>. Although such a system would provide a number of other advantages, much fundamental work still needs to be conducted on continuous lipase hydrolysis in SC-CO<sub>2</sub> to see it to fruition.

As previously reviewed in Chapter 1, a number of enzymatic hydrolysis studies in SC-CO<sub>2</sub> have been conducted but few have focused on continuous lipase hydrolysis of oil in SC-CO<sub>2</sub> using Lipozyme IM from the fungi *Mucor miehei* and

---

<sup>1</sup> A version of this chapter is in preparation to be submitted to the Biochemical Engineering Journal for consideration for publication.

evaluated the effects of pressure, temperature, SC-CO<sub>2</sub> flow rate and enzyme load. For instance, Rezaei and Temelli [1] reported higher glycerol production at 10 MPa than at 24 or 38 MPa and attributed this result on the poor solubility of monoacylglycerol (MAG) and diacylglycerol (DAG) in SC-CO<sub>2</sub> at 10 MPa, which ensured a more complete hydrolysis of oil into glycerol and free fatty acids (FFA). Indeed, although more triacylglycerol (TAG) were hydrolyzed at 24 MPa compared to that at 10 MPa, the amount of MAG and DAG was almost equivalent to that of FFA. Such results indicate that operating at 10 MPa might ensure a more thorough hydrolysis than when higher pressures are used. On the other hand, these investigators also reported an increase in glycerol with temperature from 35 to 55 °C [1] while Sovova and Zarevúcka [2] reported that the effect of temperature in the range of 30 to 40 °C was negligible.

The effect of flow rate on hydrolysis conversion was also investigated by Rezaei and Temelli [1]. They reported higher glycerol content and lower MAG and DAG contents when a SC-CO<sub>2</sub> flow rate of 1.0 L/min was used rather than 3.7 L/min and concluded that lower flow rate increased conversion [1]. However, Sovova and Zarevúcka [2] reported lower conversions when conducting reactions at lower (< 0.5 L/min) flow rates.

The effect of enzyme load was examined by Sovova and Zarevúcka [2]; however, their experimental design did not allow them to directly observe the effect of enzyme load on conversion. In a separate study, which examined the possibility

of conducting on-line extraction-reaction of canola oil in SC-CO<sub>2</sub>, Rezaei and Temelli [3] considered the effect of enzyme load and reported that, although higher level of FFA production was anticipated when a higher level of enzyme load was used, less FFA had been obtained with an enzyme load of 2 and 5 g compared to that obtained with 1 g of enzyme. The authors [3] attributed this effect to the nature of the packed bed of enzyme and glass beads, which offered more resistance to oil-laden SC-CO<sub>2</sub> flow. Although this appears to be a satisfactory explanation, the effect of enzyme load should be re-examined to confirm such a finding. In addition, it appears fitting to also examine the effect of SC-CO<sub>2</sub> flow rate and temperature to shed more light on the previously mentioned conflicting results. Therefore, the objective of this study was to further investigate the effects of temperature, enzyme load and CO<sub>2</sub> flow rate on the overall conversion of canola oil into FFA by lipase-catalyzed hydrolysis using Lipozyme IM in a continuous flow supercritical reactor.

## **6.2. Materials and methods**

### *6.2.1. Materials*

The materials used were commercially refined, bleached and deodorized canola oil graciously donated by Canbra Foods Ltd. (Lethbridge, AB), deionized distilled water (DDW), 99.8% bone dry (water level < 3 ppm) carbon dioxide (CO<sub>2</sub>) from Praxair Canada Inc. (Mississauga, ON). The catalyst used was Lipozyme IM >100 U/g, a lipase from *Mucor miehei* immobilized on a macroporous ion-exchange



resin produced by Novozymes *BioChemika*, which was purchased from Sigma-Aldrich (St. Louis, MO, USA). Laboratory grade ethyl ether and Certified ACS grade petroleum ether were obtained from Fisher Scientific Ltd. (Nepean, ON). Ultra high purity grade (99.999%) hydrogen, extra dry nitrogen, prepurified helium, extra dry air and supercritical fluid chromatography grade (>99.998%) carbon dioxide were obtained from Praxair Products Inc. (Mississauga, ON). n-Docosane (99%) was obtained from Acros Organics (Fair Lawn, NJ, USA) while oleic acid (OA), monoolein (MO), diolein (DO) and triolein (TO) reference standards (>99%) were obtained from Nu-Chek Prep Inc. (Elysian, MN, USA).

#### 6.2.2. *Experimental set-up and design*

Continuous enzymatic reactions were conducted in a custom-made laboratory scale system (Fig. 6.1 and Appendix A.2) where carbon dioxide (CO<sub>2</sub>) was delivered at constant pressure using a compressor (Newport Scientific, Jessup, MD) equipped with a back-pressure regulator (Tescom 26-1721, Elk River, MN, USA) and canola oil and water were introduced at a constant flow rate using two HPLC pumps (Gilson 305 with manometric module 805, Middleton, WI, USA and Varian HP-0166, Walnut Creek, CA, USA, respectively). High pressure components of the system, which were in contact with the reactants and products, were 316 stainless steel pressure tested components such as check valves, on-off

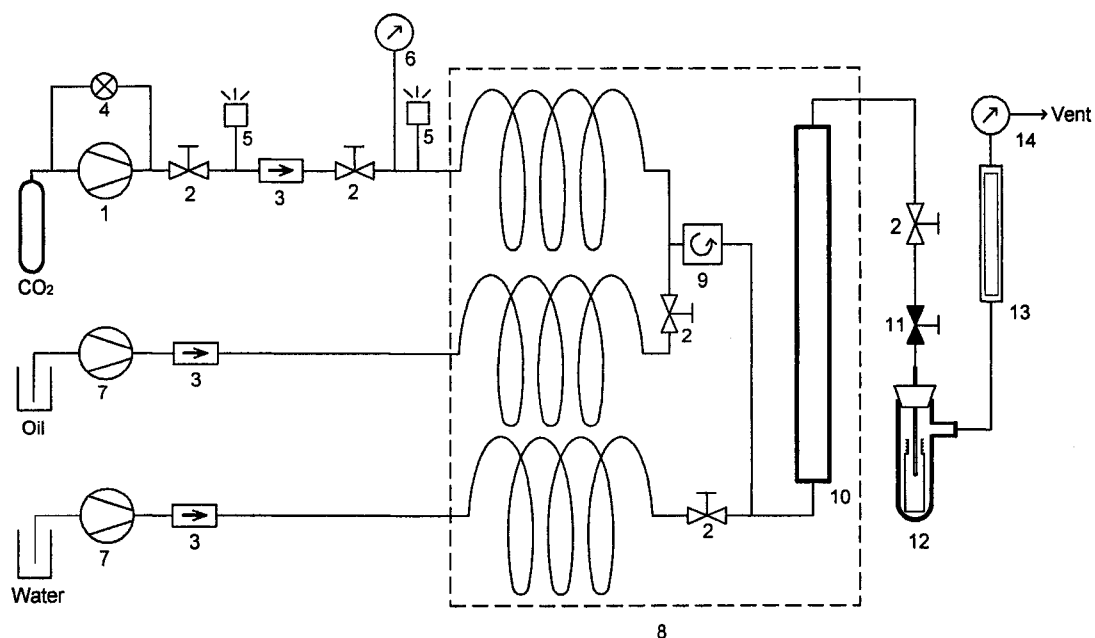


**Figure 6.1.** Schematic of the experimental system used to conduct continuous enzymatic reactions in supercritical carbon dioxide: (1) compressor, (2) on-off valve, (3) check valve, (4) back-pressure regulator, (5) rupture disk, (6) pressure gauge, (7) high-performance liquid chromatography pumps, (8) oven, (9) mixer, (10) enzymatic reactor, (11) micro-metering valve, (12) sample collection tube, (13) rotameter, (14) gas meter.

valves, tubing (Swagelok, Solon, OH, USA) and pressure gauge. All connecting lines were made using tubing with an outside diameter (O.D.) of 1.59 mm ( $1/16$  in) and an internal diameter (I.D.) of 0.51 mm (0.02 in) with the exception of the CO<sub>2</sub> feed line, which was made using 3.18 mm ( $1/8$  in) O.D. and 0.71 mm (0.028 in) I.D. tubing. Prior to mixing, reagents were pre-heated in the oven by passing them through coiled tubing that had the arbitrarily determined length of 2.3, 4.3 and 5.8 m for supercritical carbon dioxide (SC-CO<sub>2</sub>), water and oil, respectively. On the

oil and water lines the coiled tubing was followed by on-off valves that could be operated from outside the oven. This set-up permitted the heat-up of the reagents prior to their initial injection into the reactor. A cup-shaped sintered metal filter in a stainless steel fitting was used as a mixer to ensure that canola oil was well dispersed in SC-CO<sub>2</sub> prior to the addition of water and flow through the enzymatic reactor.

The enzymatic reactor consisted of a 26.3 cm long 316 stainless steel 9.53 mm (<sup>3</sup>/<sub>8</sub> in) O.D. tubing with 6.22 mm (0.245 in) I.D. and it was positioned in the middle of the oven just above the air fan, which induced a slight vibration in the reactor. The enzymatic reactor was followed by a micro-metering valve (Autoclave Engineers, Erie, PA, USA), which was used to control the flow rate of product mixture. Upon depressurization, samples were collected in 7 mL vials inserted in a side-armed thick-walled custom made glass tube, which was connected to a rotameter (Matheson, Newark, CA, USA) and a gas meter (AL225, Canadian Meter Co. Ltd., Cambridge, ON). CO<sub>2</sub> passed through the flow meter and the gas meter before being vented in order to measure the flow rate at ambient conditions. The temperature of the oven (Fisher F15 Econotemp lab oven, Nepean, ON) and the temperature of the MICA band heater (BR530 Tru-Temp Electric Heat, Edmonton, AB) on the micro-metering valve was controlled within ±2 °C of the desired temperature using a PID controller (CN6161, Omega Engineering Inc., Stamford, CT, USA) via thermocouples (J-type, Tru-Temp Electric Heat, Edmonton, AB).

The experimental set-up used to conduct continuous enzymatic reactions (Fig 6.1) was designed to combine the advantages of systems previously used by Sovova and Zarevúcka [2] and Rezaei and Temelli [1]. For instance, the idea of pre-heating the reactants prior to injecting them into the enzyme bed was adopted from Sovova and Zarevúcka [2] while the idea of pumping reactants continuously, as opposed to putting the reactants in an on-line reservoir [2] or into the bottom of the enzymatic reactor [4], was taken from Rezaei and Temelli [1]. Nevertheless, the experimental setup used had some unique features. For instance, a longer and narrower reactor (26.3 cm x 6.22 mm I.D) packed with glass wool and enzyme was used to prevent, among other things, the occurrence of channelling. Interestingly, Laudani et al. [5], who recently published an excellent study on enzymatic esterification in SC-CO<sub>2</sub>, which was not available when the system was designed and built, also used a long and narrow (75 cm x 4 mm I.D.) enzymatic reactor. Aside from being longer, the enzymatic reactor was suspended over the oven fan in such a way as to induce a slight vibration in it. Such a vibration was believed to prevent glycerol build-up on enzyme's active sites, an issue previously encountered by Hampson and Foglia [4] and attributed to the low solubility of glycerol in SC-CO<sub>2</sub>. Besides, the system was designed to mix oil and SC-CO<sub>2</sub> prior to the addition of water so as to ensure that the SC-CO<sub>2</sub> was saturated with oil in order to improve the oil and water mixing. This approach differed slightly from that of Rezaei and Temelli [1] who used the mixer to blend oil, water and SC-CO<sub>2</sub>.

### 6.2.3. *Reaction protocols*

Fifteen reactions were conducted at  $11.0 \pm 0.2$  MPa while keeping canola oil and deionized distilled water (DDW) mass flow rates constant at  $1.91 \pm 0.02$  g/s and  $0.31 \pm 0.02$  g/s, respectively. Such flow rates correspond to a oil-to-water molar ratio of 1:7.86. The effect of enzyme load for these reactions was investigated by conducting experiments with 0.5, 1.0 and  $1.5 \pm 0.03$  g of enzyme firmly packed with a stainless steel rod between two equal layers of borosilicate 8  $\mu\text{m}$  glass wool fibers (Pyrex fiber glass, Corning Inc., Corning, NY, USA) in the enzymatic reactor. For each of these runs, a fresh batch of enzyme was used. The effects of temperature and  $\text{CO}_2$  flow rate were also considered for these runs by performing reactions at 40, 45 and  $50 \pm 2$  °C and at 0.5, 1.0 and  $1.5 \pm 0.03$  L/min of  $\text{CO}_2$  measured at ambient conditions. Samples were taken every hour for the first two hours and then every half hour for the remainder of each 6 h reaction.

### 6.2.4. *Compositional analysis*

Compositional analysis of samples collected at 6 h was conducted for all runs. For runs 6-10, compositional analysis was also conducted for samples collected at 3, 4, 5, and 5.5 h. Samples separated into two phases upon standing at ambient conditions and only the oil layer was analyzed using a Lee Scientific Series 600 SFC/GC supercritical fluid chromatograph (SFC) (Dionex, Mississauga, ON) equipped with a fused silica column (10 m  $\times$  50  $\mu\text{m}$  I.D.) with a 0.25  $\mu\text{m}$  thick

stationary phase consisting of 50% n-octyl and 50% methylpolysiloxane (Selerity Technologies, Salt Lake City, UT, USA), a 500 nL timed injector loop and a flame-ionization detector (FID) set at 350 °C. Approximately 110-140 mg of oil product and 22.5 mg of n-docosane (C<sub>22</sub>H<sub>46</sub>) were dissolved in 5 mL petroleum ether/ethyl ether mixture (1:1 v/v). The injector loop was rinsed with a mixture of petroleum ether/ethyl ether mixture (1:1 v/v) using five microliter syringe injections. The loop was then rinsed with the sample mixture using five more microliter syringe injections before opening the injector for 1.8 s and starting the column temperature/pressure program previously used by Temelli et al. [6]. In this program, the column temperature was held at 100°C for 5 min and then increased to 190 °C at a rate of 8°C/min while the pressure was held at 12.2 MPa (120 atm) for 5 min and then increased to 30.4 MPa (300 atm) at a rate of 0.8 MPa/min (8 atm/min) and held there for 3 min. The Dionex AI-450 Chromatography Automated Software Release 3.32 was used to collect and analyze the data.

Response factors, which were 1.45, 1.98, 1.53, 1.26 for FFA, MAG, DAG and TAG, respectively, were obtained by conducting triplicate injections of standard solutions containing 1.0, 2.0, 4.0, 8.0 and 16.0 mg/mL of OA, MO, DO, TO and 4.5 mg/mL of n-docosane. The R<sup>2</sup> for the corresponding calibration curves were 0.9871, 0.9575, 0.9796 and 0.9897 for OA, MO, DO, TO, respectively. The concentrations of FFA, MAG, DAG, and TAG in each sample were calculated by multiplying the response factor for the compound of interest by the amount of n-

docosane added to the sample as internal standard and by the ratio of peak area counts for the component of interest and n-docosane. Concentrations were then converted to moles using the following molar weights: 282.5, 356.6, 621.0 and 879 a.m.u. for FFA, MAG, DAG and TAG, respectively. The choice for these molecular weights was discussed previously in Section 3.2.3.

The percentage of fatty acids in free form or percentage conversion (% *Conv*) was calculated using Eq. (6.1).

$$\% \text{ Conv} = \frac{N_{FFA}}{N_{FFA} + N_{MAG} + 2 \cdot N_{DAG} + 3 \cdot N_{TAG}} \times 100 \quad (6.1)$$

where  $N_{FFA}$ ,  $N_{MAG}$ ,  $N_{DAG}$ ,  $N_{TAG}$  are the average number of moles for FFA, MAG, DAG and TAG in samples analyzed by SFC, respectively.

The amount of glycerol produced was not measured and therefore had to be calculated. In order to calculate glycerol, the molar concentration of each species in the amount of product that was collected as a function of time also had to be calculated. Given that only the number of moles of each species in the samples analyzed by SFC was known, first mole fraction equations such as Eq. (6.2) were written

$$X_{TAG} = \frac{N_{TAG}}{N_{TAG} + N_{MAG} + N_{DAG} + N_{FFA}} = \frac{n_{TAG}^{out}}{n_{TAG}^{out} + n_{MAG}^{out} + n_{DAG}^{out} + n_{FFA}^{out}} \quad (6.2)$$

where  $n_{TAG}^{out}$ ,  $n_{DAG}^{out}$ ,  $n_{MAG}^{out}$  and  $n_{FFA}^{out}$  represent the unknown number of moles of TAG, DAG, MAG and FFA, which were produced by the system every hour and where  $X_{TAG}$  represent the mole fraction of TAG obtained from the SFC analyses of the samples collected between 5 and 6 h. A reorganization of Eq. (6.2) leads to Eq. (6.3). Application of the same procedure for DAG and FFA led to Eqs. (6.4) and (6.5),

$$0 = [n_{TAG}^{out} \cdot (X_{TAG} - 1)] + (n_{DAG}^{out} \cdot X_{TAG}) + (n_{MAG}^{out} \cdot X_{TAG}) + (n_{FFA}^{out} \cdot X_{TAG}) \quad (6.3)$$

$$0 = (n_{TAG}^{out} \cdot X_{DAG}) + [n_{DAG}^{out} \cdot (X_{DAG} - 1)] + (n_{MAG}^{out} \cdot X_{DAG}) + (n_{FFA}^{out} \cdot X_{DAG}) \quad (6.4)$$

$$0 = (n_{TAG}^{out} \cdot X_{FFA}) + (n_{DAG}^{out} \cdot X_{FFA}) + (n_{MAG}^{out} \cdot X_{FFA}) + [n_{FFA}^{out} \cdot (X_{FFA} - 1)] \quad (6.5)$$

where  $X_{DAG}$  and  $X_{FFA}$  represent the mole fractions of DAG and FFA, respectively. Besides Eqs. (6.2-6.5), two additional equations were obtained based on material balance and reaction stoichiometry for glycerol (Eq. (6.6)) and fatty acids (Eq.(6.7))

$$n_{TAG}^{in} = n_{TAG}^{out} + n_{DAG}^{out} + n_{MAG}^{out} + n_{Glycerol}^{out} \quad (6.6)$$

$$0 = n_{DAG}^{out} + 2 \cdot n_{MAG}^{out} + 3 \cdot n_{Glycerol}^{out} - n_{FFA}^{out} \quad (6.7)$$

where  $n_{TAG}^{in}$  represent the number of moles of TAG (canola oil), which was fed into the system per hour and  $n_{Glycerol}^{out}$  represent the unknown number of moles of glycerol produced by the system every hour. Eqs. (6.3-6.7) were solved for each run by introducing the mole fractions for each species from the right side of each



equation into a  $5 \times 5$  matrix and then multiplying the inverse of this matrix by a vector containing the left side of each equation.

#### 6.2.5. *Experimental design and statistical analysis*

A three-variable Box-Behnken design (Table 6.1) was used in this study to efficiently investigate the effects of temperature (40, 45, 50°C), CO<sub>2</sub> flow rate (0.5,

**Table 6.1.** Box-Behnken experimental design with natural and coded variables

Run no.	Natural Variables			Coded Variables		
	Temperature (°C)	Enzyme load (g)	Flow rate (L/min)	Temperature ( $x_1$ )	Enzyme load ( $x_2$ )	Flow rate ( $x_3$ )
1	45	0.5	0.5	0	-1	-1
2	45	1.0	1.0	0	0	0
3	40	0.5	1.0	-1	-1	0
4	50	1.0	1.5	1	0	1
5	45	1.5	1.5	0	1	1
6	45	1.5	0.5	0	1	-1
7	40	1.0	1.5	-1	0	1
8	45	0.5	1.5	0	-1	1
9	50	1.0	0.5	1	0	-1
10	50	1.5	1.0	1	1	0
11	45	1.0	1.0	0	0	0
12	45	1.0	1.0	0	0	0
13	40	1.0	0.5	-1	0	-1
14	50	0.5	1.0	1	-1	0
15	40	1.5	1.0	-1	1	0

1.0, 1.5 L/min) and enzyme load (0.5, 1.0 and 1.5 g) while keeping the required number of experiments low. All fifteen experiments used in this design were randomized. Triplicate SFC analyses were conducted on the 6 h sample of each run. The average % *Conv* obtained was fitted into Eq. (6.8).

$$y = \beta_0 + \beta_1 x_1 + \beta_2 x_2 + \beta_3 x_3 + \beta_{12}(x_1)(x_2) + \beta_{13}(x_1)(x_3) + \beta_{23}(x_2)(x_3) + \beta_{11}(x_1)^2 + \beta_{22}(x_2)^2 + \beta_{33}(x_3)^2 \quad (6.8)$$

where  $y$  is % *Conv*,  $\beta_i$  are coefficients and  $x_1$ ,  $x_2$  and  $x_3$  are the coded variables (Table 6.1) for reaction temperature, enzyme load and flow rate, respectively. Coefficients  $\beta$  and the maximum hydrolysis conversion were determined using the Box-Behnken Design in the software Design Expert 7.1.3 [7]. Design Expert was also used to conduct the analysis of variance (ANOVA) and to validate the model.

### 6.3. Results and discussion

#### 6.3.1. Establishment of experimental test parameters

The levels of reactant concentrations, SC-CO<sub>2</sub> flow rate and enzyme load tested were based on a number of considerations, including the inherent limitations of the system. The oil-to-water molar ratio was set to 1:8 based on the hydrolysis study discussed in Chapter 5 and on another study by Guthalugu et al. [8] concerning the optimization of enzymatic hydrolysis of soy deodorizer distillate using *Candida rugosa*. However, to establish the actual oil and water flow rates, the

limitation was the minimum water flow rate of 0.005 g/min that could be consistently achieved by the high-performance liquid chromatography (HPLC) pump used to deliver water. Consequently, the oil flow rate was set at 0.032 g/min to achieve the targeted molar ratio of 1:8 for oil-to-water. Given the difficulty in varying the flow rate of water without changing either the oil flow rate or the oil-to-water molar ratio, the water and oil flow rates were kept constant.

Tested SC-CO<sub>2</sub> flow rate levels were also established in a similar fashion. The initial range was determined based on higher glycerol production reported using 1.0 L/min rather than 3.7 L/min [1] and another report [2] claiming, without providing any data, practically complete conversion while conducting hydrolysis using <0.5 L/min SC-CO<sub>2</sub>. Given that the available rotameter could only measure flows between 0.5-1.5 L/min, it dictated the possible range that could be investigated. As previously stated, one of the unique features of the experimental set up was its longer and narrower reactor. Although it would be desirable to have it even longer and slightly narrower, its current dimensions were limited by the oven's cross-sectional length and ease of packing. This, in turn, determined its maximum enzyme holding capacity of 1.5 g.

As stated in Section 6.1, the pressure was set to 10 MPa to decrease production of MAG and DAG while maximizing FFA production and increasing water solubility to prevent its accumulation on enzyme active sites. Indeed, based on values reported by Fattori et al. [9], canola oil solubility at 10 MPa and 40-50 °C

was < 0.5 mg oil/g CO<sub>2</sub> whereas that of water was 1.70 and 2.96 mg water/g CO<sub>2</sub> at 40 and 50 °C, respectively [10]. Given that preliminary blank reactions conducted with no enzyme at higher temperature (100°C) in a batch reactor resulted in negligible conversion, that Fujita and Himi [11] as well as Rezaei and Temelli [1] independently reported negligible conversion when conducting blank hydrolysis reactions at 100 °C and 55 °C, respectively, no reactions were carried out without the addition of enzymes into the reactor.

### 6.3.2. *Composition of the product mixture*

Analysis of the lipid layer of the product mixture was conducted by SFC. Such analytical method allows the separation and quantification of fats into classes without modifying the oil chemically. The typical SFC chromatogram shown in Figure 6.2 illustrates how the internal standard (n-docosane) gave two peaks while FFA, DAG and TAG classes were represented by several peaks thereby reflecting the different types of fatty acids and/or positional isomers present in the hydrolyzed canola oil sample. This chromatogram also makes it apparent that the first product of hydrolysis, DAG, is more predominant than MAG. Table 6.2 shows a portion of the data obtained. From these, it is evident that the molar concentration of MAG at 45 °C was lower and much more dependent on enzyme load and flow rate than that of DAG. From this table it is also apparent that the glycerol content was relatively low.

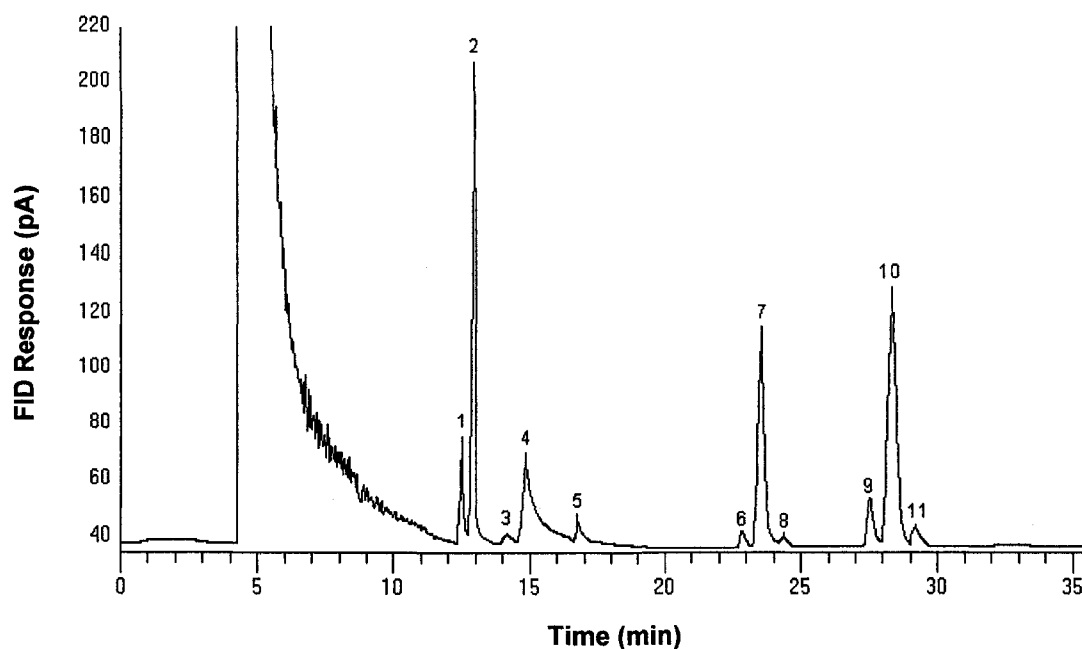


**Figure 6.2.** Typical supercritical fluid chromatogram of a sample collected from the enzymatic hydrolysis of canola oil in supercritical carbon dioxide (SC-CO<sub>2</sub>) after 6 h of continuous reaction; (1,2) internal standard, (3,4) FFA, (5) MAG, (6-8) DAG, (9-11) TAG.

**Table 6.2.** Composition\* of samples obtained between 5 and 6 h of continuous enzymatic hydrolysis of canola oil in supercritical carbon dioxide at 45 °C as a function of enzyme load and flow rate.

Enzyme load (g)	0.5		1.0	1.5	
	0.5	1.5	1.0	0.5	1.5
FFA (mmole)	0.408	0.459	0.493	0.462	0.572
MAG (mmole)	0.138	0.068	0.053	0.024	0.086
DAG (mmole)	0.209	0.216	0.184	0.175	0.114
TAG (mmole)	0.246	0.221	0.202	0.259	0.133
Glycerol (mmole)	0.095	0.080	0.081	0.071	0.086

\* Average of triplicate SFC analysis.

### 6.3.3. Response surface model

The complete Box-Behnken experimental design is presented in Table 6.3 with the process variables tested and the experimental ( $Y_{\text{exp}}$ ) % *Conv* obtained.

**Table 6.3.** Box-Behnken experimental design with percentage conversion obtained experimentally and those predicted by the response surface model

Run no.	Process variables			$Y_{\text{Exp}}^*$ (% <i>Conv</i> )	$Y_{\text{Pred}}$ (% <i>Conv</i> )	Residual
	Temperature (°C)	Enzyme load (g)	Flow rate (L/min)			
1	45	0.50	0.50	24.21	26.16	-2.0
2	45	0.99	1.01	32.76	32.39	0.4
3	40	0.51	0.97	28.14	24.82	3.3
4	50	1.01	1.47	38.68	38.58	0.1
5	45	1.53	1.52	44.61	42.77	1.8
6	45	1.50	0.50	28.68	28.37	0.3
7	40	1.03	1.48	35.54	37.33	-1.8
8	45	0.50	1.51	28.32	28.52	-0.2
9	50	1.01	0.53	33.48	30.94	2.5
10	50	1.51	0.99	32.98	34.41	-1.4
11	45	1.02	0.97	31.99	32.28	-0.3
12	45	1.02	1.01	32.49	32.59	-0.1
13	40	1.02	0.48	28.41	29.18	-0.8
14	50	0.50	0.99	25.31	26.51	-1.2
15	40	1.51	1.00	32.12	32.86	-0.7

\* Results are based on average of triplicate SFC analysis.

When fitting these experimental data to the second order polynomial model (Eq. (6.8)) using Design Expert 7.1.3 [7], the ANOVA results shown in Table 6.4 indicated that the model was significant but that some terms, such as  $A^2$ ,  $AB$  and  $AC$ , were largely insignificant. Therefore, these terms ( $A^2$ ,  $AB$  and  $AC$ ) were removed from the model and the ANOVA shown in Table 6.5 was obtained for the reduced model. From these results, it is evident that the reduced model offers a better fit. Indeed, there is only 0.07% chance that a model with an F-value of 14.00 could be due to random errors. It is also evident that terms  $A$  and  $C^2$  are not

**Table 6.4.** Analysis of variance results for the complete response surface quadratic model

Source	Sum of Squares	Degrees of Freedom	Mean Square	F Value	<i>p</i> -value Prob > F
Model	349.08	9	38.79	6.81	0.0240
A-Temperature	5.19	1	5.19	0.91	0.3836
B-Enzyme Load	131.44	1	131.44	23.08	0.0049
C-Flowrate	128.88	1	128.88	22.63	0.0051
AB	3.99	1	3.99	0.70	0.4406
AC	0.42	1	0.42	0.07	0.7962
BC	35.92	1	35.92	6.31	0.0537
$A^2$	0.00	1	0.00	0.00	0.9858
$B^2$	29.05	1	29.05	5.10	0.0735
$C^2$	10.45	1	10.45	1.84	0.2335
Residual	28.48	5	5.70		
Cor Total	377.56	14			

significant ( $\alpha \leq 0.05$ ); however, removing anyone of them considerably lowered the correlation coefficient ( $R^2$ ), which indicated that 91.3% of the variation is explained by this reduced model. Consequently, this reduced model, which is described by Eq. (6.9), was considered to best describe the current results and was therefore used to generate the predicted conversion levels ( $Y_{\text{pred}}$ ) presented in Table 6.3 and the three dimensional plots shown in Figures 6.3 – 6.5.

$$y = 32.393 + 0.837 x_1 + 4.030 x_2 + 4.060 x_3 + 2.934 x_2 x_3 - 2.753 (x_2)^2 + 1.687 (x_3)^2 \quad (6.9)$$

**Table 6.5.** Analysis of variance results for the reduced response surface quadratic model

Source	Sum of Squares	Degrees of Freedom	Mean Square	F Value	<i>p</i> -value Prob > F
Model	344.73	6	57.45	14.00	0.0007
A-Temperature	5.59	1	5.59	1.36	0.2767
B-Enzyme Load	131.83	1	131.83	32.12	0.0005
C-Flowrate	128.86	1	128.86	31.40	0.0005
BC	36.18	1	36.18	8.82	0.0179
B <sup>2</sup>	29.11	1	29.11	7.09	0.0287
C <sup>2</sup>	10.30	1	10.30	2.51	0.1518
Residual	32.83	8	4.10		
Cor Total	377.56	14			



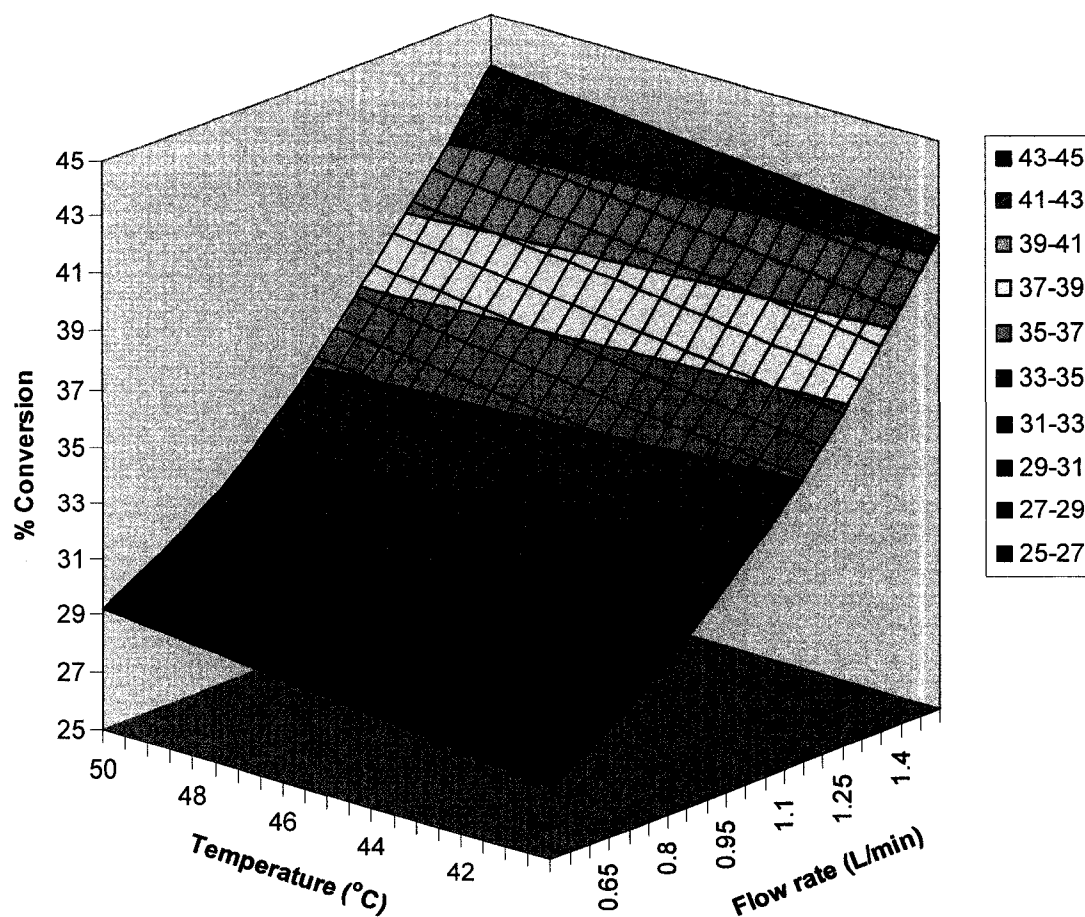


**Figure 6.3.** Effect of temperature and supercritical carbon dioxide flow rate on conversion during the continuous enzymatic hydrolysis of canola oil using 1.5 g of enzyme.

From Eq. (6.9), it is possible to predict that the maximum % *Conv* of 43.2% would be achieved if the system was operated using a Lipozyme IM load of 1.5 g, a SC-CO<sub>2</sub> flowrate of 1.5 L/min and a temperature of 50 °C. Although such maximum conversion level might appear to be low, it is similar to the maximum conversion

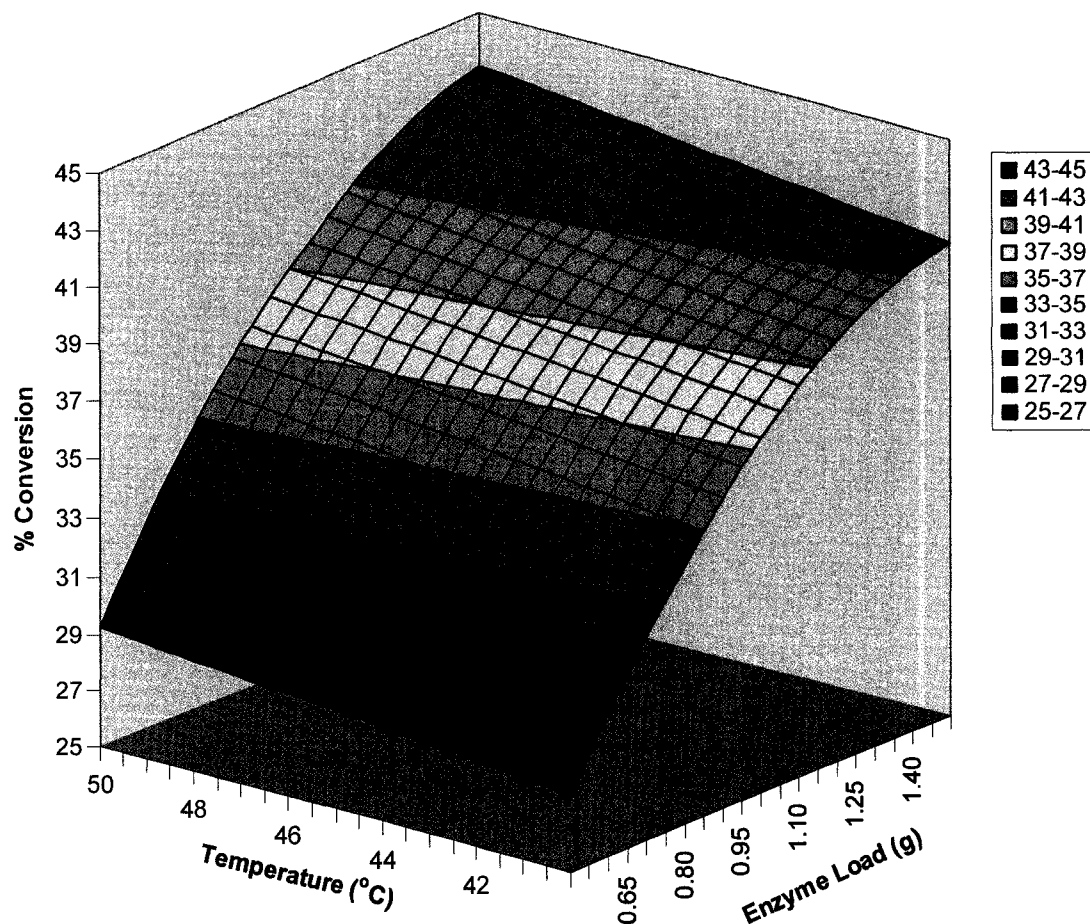


**Figure 6.4.** Effect of temperature and enzyme load on conversion during continuous enzymatic hydrolysis of canola oil using supercritical carbon dioxide flow rate of 1.5 L/min.

rate previously reported [1]. Indeed, Rezaei and Temelli [1] obtained a maximum of 63 to 67% TAG disappearance when conducting reactions at 24-38 MPa, 35-55 °C and a SC-CO<sub>2</sub> flow rate of 3.7 L/min. When the results obtained in this study are converted into percentages of TAG disappearance, and modelled using Design Expert 7.1.3, the maximum conversion obtained was 67%.

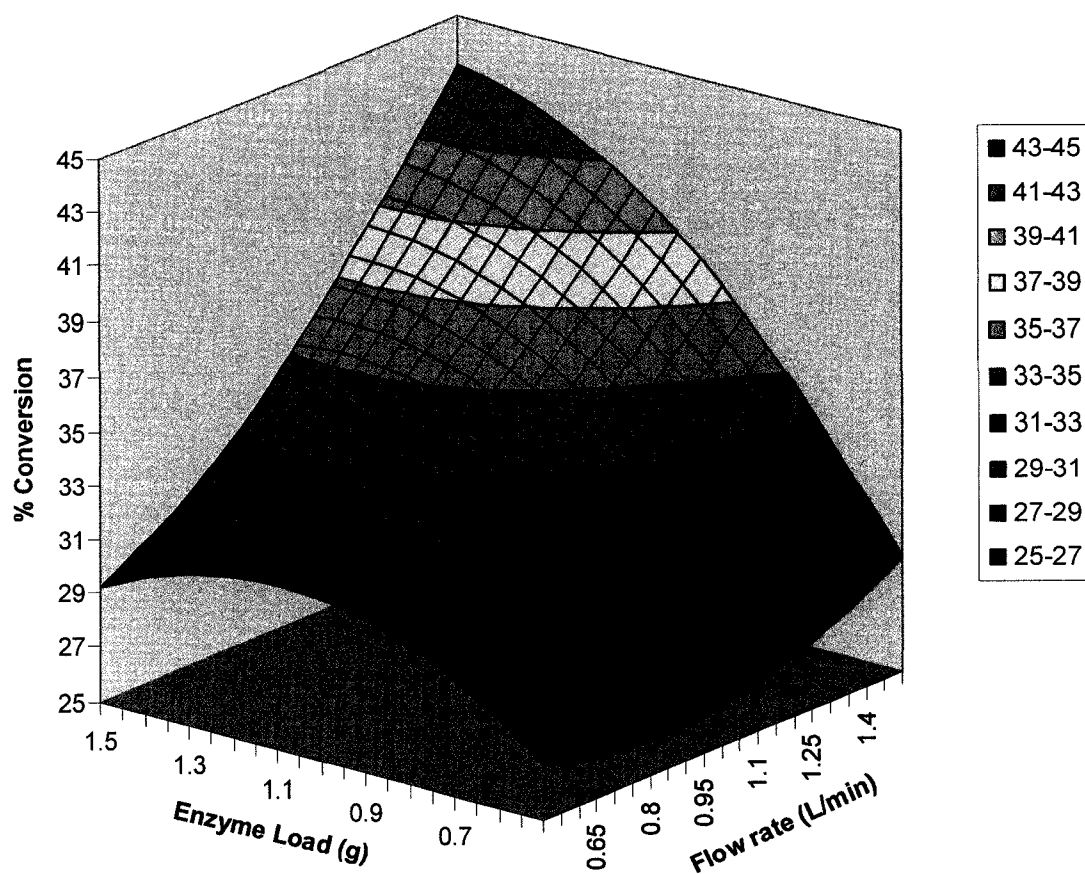


**Figure 6.5.** Effect of enzyme load and supercritical carbon dioxide flow rate on conversion during continuous enzymatic hydrolysis of canola oil at 50°C.

#### 6.3.4. Temperature Effect

From Figure 6.4, it is evident that slightly higher conversions were obtained at 50 °C than at 40 °C. However, the results of the ANOVA (Table 6.5) clearly indicated that temperature did not have a significant ( $p = 0.2767$ ) effect on percent conversion. This demonstrates that Lipozyme IM is not temperature sensitive between 40 and 50 °C, which offer industrial advantages. It also implies that

variation in SC-CO<sub>2</sub> properties due to such a temperature change does not have a significant effect on percent conversion.

#### 6.3.5. *Effect of enzyme load*

Contrary to temperature, the enzyme load had a significant effect ( $p = 0.0005$ ) on hydrolysis conversion: the higher the enzyme load, the higher was the percentage conversion in Figure 6.4. As well, there was a more noticeable increase in hydrolysis conversion when the enzyme load was increased from 0.5 to 1.0 g rather than from 1.0 to 1.5 g. Indeed, the difference in % *Conv* between an enzyme load of 0.5 and 1.0 g was 9.7 whereas that between 1.0 and 1.5 g was only 4.2 at 40, 45 and 50 °C. Besides, Figure 6.5 shows that, at low flow rates, the percentage conversion drops slightly when higher enzyme loads are used. A possible explanation for such results is that the lower SC-CO<sub>2</sub> flow rate (0.5 L/min) was unable to effectively carry water through the enzyme bed length as the enzyme load was increased from 1.0 to 1.5 g enzyme. This might have caused an accumulation of water in the reactor and decreased the rate of product removal and fresh reactant delivery to the active sites of enzymes thereby decreasing conversion. The fact that higher percentage conversion was obtained when reactions were conducted using higher enzyme loads implies that the flow rate of water was adequate for an enzyme load of 1.5 g. However, it also means that water flow rate was too high for reactions conducted at lower enzyme load. In fact, as previously mentioned in Chapter 1, lipase enzymes need to have a mono-layer of water around them in order

for their active sites to function properly, which is partly why they behave better in a non-polar solvent like SC-CO<sub>2</sub>. In addition, a given amount of water is needed for hydrolysis to take place otherwise the lipase will catalyze an esterification reaction. Nonetheless, too much water can also decrease conversion by limiting the access of lipid substrates to the enzyme's active sites.

Although higher hydrolysis conversions were obtained using an enzyme load of 1.5 g, this study was not able to establish if this was the optimal enzyme load for the considered system. Indeed, it is possible that higher conversion rates can be established if reactions are conducted using higher enzyme loads or lower water flow rates. Therefore, reactions should be conducted using either higher enzyme loads or lower flow rates in order to establish the optimal levels.

#### 6.3.6. *Effect of SC-CO<sub>2</sub> flow rate*

The SC-CO<sub>2</sub> flow rate had a significant effect ( $p = 0.0005$ ) on hydrolysis conversion (Fig. 6.3). Higher conversions were obtained using a SC-CO<sub>2</sub> flow rate of 1.5 L/min rather than 1.0 L/min or 0.5 L/min. However, a previous study [1] reported, using a wider reactor (I.D. of 13 mm as opposed to 6.22 mm in this study), lower glycerol production by conducting canola oil hydrolysis using a SC-CO<sub>2</sub> flow rate of 3.7 L/min compared with 1.0 L/min. Assuming that differences in reactor dimensions played a negligible mass transfer effect, the optimal flow rate might lie between 1.5 and 3.0 L/min and further studies should be conducted to establish it.

Nevertheless, this study showed that there is less difference in percentage conversion between reactions conducted using 0.5 and 1.0 L/min SC-CO<sub>2</sub> flow rate rather than 1.0 and 1.5 L/min for the difference was 5.3 and 8.7, respectively (Fig. 6.3). Therefore, percentage conversion dramatically increased with SC-CO<sub>2</sub> flow rate even though residence time of reactants was probably reduced without necessarily diluting the reactants since oil and water flow rates were kept constant. Consequently, to obtain higher conversions at higher SC-CO<sub>2</sub> flow rates, the reaction rates must have increased substantially to compensate for the lower residence time. This was probably compensated for by the changes in the diffusional mass transfer control of the process. Indeed, increasing the flow rate of SC-CO<sub>2</sub> probably increased the availability of substrate, by decreasing the laminar layer around each enzyme, while reducing the amount of products in the vicinity of each enzyme.

Given that Lipozyme IM is very sensitive to moisture content and that the flow rate of SC-CO<sub>2</sub> affects water content in the vicinity of the enzyme, solubility of water in SC-CO<sub>2</sub> must be considered. According to Sabirzyanov et al. [10] the mole fraction of water that is soluble at 10 MPa in SC-CO<sub>2</sub> at 50 and 40 °C is 0.00717 and 0.00414, respectively. The calculated mole fraction of water feed as a function of CO<sub>2</sub> flow rate was 0.013, 0.007 and 0.004 at 0.5, 1.0 and 1.5 L/min CO<sub>2</sub>, respectively. Consequently, when reactions were conducted at 40 °C using 0.5 and 1.0 L/min and at 50 °C using a flow rate of 0.5 L/min, not enough SC-CO<sub>2</sub> was

provided to completely solubilize all the water that was fed to the system and this could have led to some accumulation of water on the lipase active sites thereby lowering conversion levels, especially at flow rates of 0.5 L/min. However, when reactions were conducted at 50°C using higher CO<sub>2</sub> flow rates (1.0 and 1.5 L/min) enough SC-CO<sub>2</sub> was present to completely solubilize the water fed to the system thereby preventing water build-up. The solubility effect might therefore explain the slight, but not significant, differences between temperatures as a function of flow rate observed in Fig. 6.3. Nevertheless, these results highlight the fact that optimum moisture content is a crucial parameter for continuous lipase hydrolysis of TAG using Lipozyme IM and should therefore be further investigated in order to increase percentage conversion.

#### **6.4. Conclusions**

The effects of temperature, enzyme load and SC-CO<sub>2</sub> flow rate on Lipozyme IM hydrolysis of canola oil into FFA were investigated using a Box-Behnken design. The percentage conversions obtained for each run were modeled using a polynomial equation, which was used to generate response surface plots describing the effect of each tested parameter on percentage conversion. Statistical analysis revealed that temperature did not have a significant ( $p = 0.2767$ ) effect on percent conversion, which implies that Lipozyme IM's catalytic activity and SC-CO<sub>2</sub> properties did not affect conversion between 40 and 50 °C. Nevertheless, significantly ( $p = 0.0005$ ) higher hydrolysis conversions were obtained at higher

enzyme loads (1.5 g), which meant that the flow rate of water was adequate for an enzyme load of 1.5 g but might be too high for lower enzyme loads. Higher SC-CO<sub>2</sub> flow rate (1.5 L/min) also significantly ( $p = 0.0005$ ) increased hydrolysis conversion probably because increasing the flow rate of SC-CO<sub>2</sub> increased the availability of substrate while reducing the amount of products in the vicinity of each enzyme. The maximum percentage conversion predicted by the model was 43.2% (67% TAG disappearance) when reactions were conducted at 50 °C using a SC-CO<sub>2</sub> flow rate of 1.5 L/min and an enzyme load of 1.5 g. Although these results are encouraging, more investigations are required to establish the optimal enzyme load and SC-CO<sub>2</sub> flow rate.

## 6.5. References

- [1] K. Rezaei, F. Temelli, Lipase-catalyzed hydrolysis of canola oil in supercritical carbon dioxide. *J. Am. Oil Chem. Soc.* 77 (2000) 903.
- [2] H. Sovova, M. Zarevucka, Lipase-catalysed hydrolysis of blackcurrant oil in supercritical carbon dioxide. *Chem. Eng. Sci.* 58 (2003) 2339-2350.
- [3] K. Rezaei, F. Temelli, On-line extraction-reaction of canola oil using immobilized lipase in supercritical CO<sub>2</sub>. *J. Supercrit. Fluids* 19 (2001) 263.
- [4] J.W. Hampson, T.A. Foglia, Effect of moisture content on immobilized lipase-catalyzed triacylglycerol hydrolysis under supercritical carbon dioxide flow in a tubular fixed-bed reactor. *J. Am. Oil Chem. Soc.* 76 (1999) 777.
- [5] C.G. Laudani, M. Habulin, Z. Knez, G.D. Porta, E. Reverchon, Immobilized lipase-mediated long-chain fatty acid esterification in dense carbon dioxide: Bench-scale packed-bed reactor study. *J. Supercrit. Fluids* 41 (2007) 74-81.
- [6] F. Temelli, J.W. King, G.R. List, Conversion of oils to monoglycerides by glycerolysis in supercritical carbon dioxide media. *J. Am. Oil Chem. Soc.* 73 (1996) 699.



- [7] Stat-Ease Inc., Design Expert version 7.1.3, Minneapolis, MN, 2007.
- [8] N.K. Guthalugu, M. Balaraman, U.S. Kadimi, Optimization of enzymatic hydrolysis of triglycerides in soy deodorized distillate with supercritical carbon dioxide. *Biochem. Eng. J.* 29 (2006) 220-226.
- [9] M. Fattori, N.R. Bulley, A. Meisen, Carbon dioxide extraction of canola seed: Oil solubility and effect of seed treatment. *J. Am. Oil Chem. Soc.* 65 (1988) 968.
- [10] A.N. Sabirzyanov, A.P. Il'in, A.R. Akhunov, F.M. Gumerov, Solubility of water in supercritical carbon dioxide. *High Temp.* 40 (2002) 203-206.
- [11] K. Fujita, M. Himi, Hydrolysis of glycerol trioleate and extraction of its fatty acid under CO<sub>2</sub> supercritical conditions. *Nippon Kagaku Kaishi* 1 (1995) 79-82.

## **7. Summary, conclusions and recommendations**

This thesis research investigated a number of lipid reactions in supercritical carbon dioxide (SC-CO<sub>2</sub>) with the aim of not only understanding the role of key processing parameters on product yield, but also to generate the kinetic data needed for process design targeting the production of monoacylglycerol (MAG), diacylglycerol (DAG) and free fatty acids (FFA). The glycerolysis, esterification and hydrolysis reactions investigated in this body of work were evaluated from the standpoint of understanding the effects of supercritical media, pressure, and reactant concentrations. It thus seems fitting to briefly summarize the findings, assess these issues for each reaction and recommend alternative ways of conducting these reactions to improve yields.

### **7.1. Comparison of reactions and dynamic equilibrium product compositions obtained**

Table 7.1 summarizes the dynamic equilibrium product concentrations obtained during glycerolysis, esterification as well as non-catalyzed and enzymatic hydrolysis. The table provides ranges of concentrations for each chemical species so as to reflect the different concentrations obtained at various processing conditions. For instance, when non-catalytic hydrolysis was conducted using 1:70 oil/water ratio, the concentration of FFA, MAG, DAG, triacylglycerol (TAG)

was 96, 2, 1.4 and 0.6, respectively. However, when hydrolysis was conducted using 1:3 oil/water, the concentration of FFA, MAG, DAG, TAG was 59, 16, 18 and 7, respectively. From these results, it is clear that near complete hydrolysis is attainable using the non-catalytic method but that more optimization work is required to achieve similar conversions using the enzymatic method.

**Table 7.1.** Range of FFA, MAG, DAG and TAG concentrations obtained while conducting glycerolysis, esterification and hydrolysis at various initial reactant concentrations and pressures in SC-CO<sub>2</sub>.

	Concentration (mol %)			
	FFA	MAG	DAG	TAG
Glycerolysis <sup>1</sup>	13-17	66-71	13-15	0-1
Esterification <sup>2</sup>	4-50	25-82	13-22	1-6
Non-catalytic Hydrolysis <sup>3</sup>	59-96	2-16	1.4-18	0.6-7
Enzymatic Hydrolysis <sup>4</sup>	41-57	2-14	11-24	13-26

<sup>1</sup> 10-30 MPa, 4-8% (w/w) water, 250 °C

<sup>2</sup> 10-30 MPa, 1:0.1, 1:1 and 1:2 glycerol/oleic acid, 250 °C

<sup>3</sup> 10-30 MPa, 1:3, 1:17 and 1:70 oil/water, 250 °C

<sup>4</sup> 10 MPa, 0.5-1.5 g enzyme, 0.5-1.5 L/min SC-CO<sub>2</sub>, 40-50 °C

Figure 7.1 presents a comparison of the products formed as a function of time during glycerolysis (Chapter 3), esterification (Chapter 4) and hydrolysis (Chapter 5). Hydrolysis of TAG takes approximately 2.5 h to reach dynamic equilibrium. Thus, if the MO formation curve for esterification is shifted by 2.5 h,

then the dynamic equilibrium concentration for esterification is reached at approximately the same time as for glycerolysis (Fig. 7.1). In other words, conducting glycerolysis-hydrolysis using the conditions outlined in Chapter 3 takes

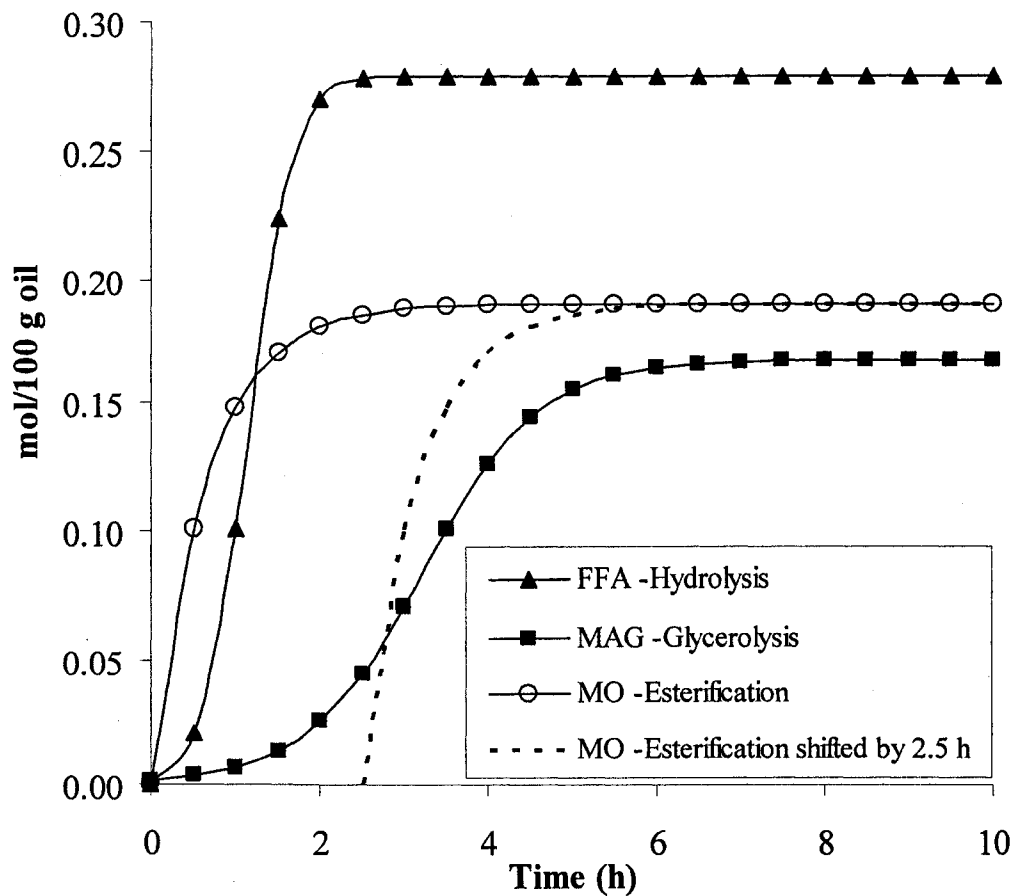


**Figure 7.1.** Products formed as a function of time during hydrolysis, glycerolysis and esterification conducted at 10 MPa and 250 °C: (▲) amount of FFA formed by hydrolysis using 1:17 initial oil/water molar ratio, (■) amount of MAG formed by glycerolysis using 8% (w/w of glycerol) initial water, and (○) and (----) amount of monoolein formed by esterification using 1:0.1 initial glycerol/oleic acid molar ratio when time zero is set at 0 and 2.5 h, respectively.

approximately the same amount of time as if hydrolysis was conducted first and then esterification was conducted next without any time delay between the two reactions. However, to increase the glycerolysis reaction rate, FFA could be added to the initial reactants. By so doing, there would be no need for the glycerolysis reaction to wait for the hydrolysis products to induce the reaction since the esterification of FFA could readily occur thereby triggering glycerolysis by producing emulsifiers (DAG and MAG), which would in turn promote a more rapid glycerolysis. Apart from increasing the reaction rate, the addition of FFA would effectively catalyze the reaction without having to add non-food grade material or catalyst to the system. FFA would also be an inexpensive catalyst since FFA could be extracted directly from the product mixture using SC-CO<sub>2</sub> and used in the next batch.

Extensive kinetic modeling was conducted for the glycerolysis, esterification and non-enzymatic hydrolysis reactions where all possible reaction steps were taken into account. The rate constants for all these reaction steps were determined and used to establish the mechanism of each of these reactions at various processing conditions within the limitations and assumptions of the kinetic models used. Such an approach, along with the corresponding findings, has not been reported previously and is essential for optimal process design. Nonetheless, this thesis research provides only the reaction kinetics perspective and a complete fundamental understanding of the complex reaction systems can only be achieved once

thermodynamics (phase behaviour and solubility aspects) and mass transfer perspectives are taken into account and a simultaneous assessment of all three perspectives is accomplished. However, results make it clear that partial conversion can be achieved for any of these reactions. Indeed, reactions may be interrupted when the desired partial mixture is achieved. For instance, in the case of glycerolysis and esterification, it is possible to use the information generated to produce designer oil mixtures with targeted amounts of MAG and DAG in the product.

## **7.2. Effect of supercritical carbon dioxide**

Similar results for glycerolysis, esterification and hydrolysis were achieved in SC-CO<sub>2</sub> and SC-N<sub>2</sub>, which means that SC-CO<sub>2</sub> does not actively participate in the catalysis of any of these reactions. It also means that nitrogen, which is currently used in conventional glycerolysis, esterification and hydrolysis to prevent oxidation, can be replaced with carbon dioxide without significantly affecting the rate of the reaction. Substituting carbon dioxide for nitrogen would allow the incorporation of such a reaction step as a unit operation in a larger SC-CO<sub>2</sub> extraction-reaction or extraction-reaction-fractionation-reaction process. Such a process could, for instance, have canola seeds as the feed material and emulsifiers as an end product for use in various product applications such as ice cream or coffee whiteners. Indeed, by first extracting the oil from canola seed using SC-CO<sub>2</sub> and then feeding

the oil-laden SC-CO<sub>2</sub> mixture into a reactor containing glycerol, MAG could be formed in a system requiring a single pressurization step. Similarly, mono- and diolein could be formed by first extracting the oil from canola seeds using SC-CO<sub>2</sub>, feeding the oil-laden SC-CO<sub>2</sub> mixture into a reactor full of water, conduct complete hydrolysis, separate oleic acid from the other FFA along a temperature gradient SC-CO<sub>2</sub> separation column, and finally use the SC-CO<sub>2</sub> to accumulate the oleic acid into a reactor containing excess glycerol where production of mono- and diolein would occur via esterification. Such novel approaches can also be applied to other fats and oils for the synthesis of various designer lipids.

Given that SC-CO<sub>2</sub> does not affect the rate of glycerolysis, SC-CO<sub>2</sub> could also be used to conduct continuous glycerolysis. This could indeed be achieved by flowing reactants through a series of frits inside of a 250 °C column. The frits would enhance the mixing of reactants in SC-CO<sub>2</sub> media. Although a continuous glycerolysis system in nitrogen [1, 2] and continuous enzymatic glycerolysis in SC-CO<sub>2</sub> [3-5] were previously reported, the literature lacks information on continuous glycerolysis in SC-CO<sub>2</sub>.

The enzymatic hydrolysis study (Chapter 6) clearly demonstrated that higher SC-CO<sub>2</sub> flow rate significantly ( $p = 0.0005$ ) increased hydrolysis conversion. Such a result suggests that increasing the SC-CO<sub>2</sub> flow rate increased the availability of substrate while reducing the amount of products in the vicinity of each enzyme. However, the optimum flow rate for the current system was not achieved.

Nevertheless, since the percentage conversion increased greatly between reactions conducted at 1.0 and 1.5 L/min compared to those conducted at 0.5 and 1.0 L/min, it is believed that 1.5 L/min is very close to the optimum flow rate. Therefore, investigations using the method of steepest ascent [6], which is a procedure to sequentially and rapidly move in the direction of the maximum hydrolysis conversion, should be used to establish the optimum flow rate. In addition, to take into account the effect of mass transfer on the system, various flow rates (hence various Reynolds Numbers) could be investigated to determine the transition out of the suspected diffusion-controlled region.

### **7.3. Effect of pressure and temperature**

Conducting glycerolysis-hydrolysis reactions at various pressures demonstrated that the maximum rate of MAG formation ( $MAG_{max}$ ) at 20 MPa was significantly higher ( $p \leq 0.05$ ) than that at 30 MPa, but similar ( $p > 0.05$ ) to that at 10 MPa. In an attempt to identify which reactions were more susceptible to pressure, esterification and hydrolysis reactions were conducted at 10 and 30 MPa. The result obtained was most unexpected. Indeed, similar rates ( $p > 0.05$ ) of MAG formation were obtained for esterification reactions conducted at 10 and 30 MPa and the maximum rate of FFA formation ( $FFA_{max}$ ) during hydrolysis was also not affected ( $p > 0.05$ ) by pressure. However, similar to glycerolysis, the  $FFA_{max}$  was delayed at 30 MPa during hydrolysis. It is therefore possible that the higher amount



of SC-CO<sub>2</sub> present at 30 MPa dilutes the reactants thereby decreasing the interactions between oil and water and slowing down the process for both hydrolysis and glycerolysis reactions. The fact that MAG<sub>max</sub> during glycerolysis was affected by pressure and that FFA<sub>max</sub> during hydrolysis was not, might be due to either differences in phase behaviour or SC-CO<sub>2</sub> dilution effect that increases the amount of water bound to glycerol.

Besides pressure, the role of temperature in the esterification and hydrolysis reactions was also investigated and results clearly showed higher yields with increasing temperature to 250 °C. Such results were expected since temperature affects the reactants miscibility as well as providing the required activation energy. Nevertheless, temperature and pressure might also have considerable impact on phase behaviour and future work should therefore involve determination of phase behaviour as a function of pressure and temperature.

The fact that higher or equal yields are obtained at 10 MPa has considerable economical impact because equipment designed to work at 10 MPa is common and more economical. In addition, a pressure of 10 MPa can be reached without the use of a high pressure pump because, as previously mentioned in Chapter 3, when the pressure inside of a sealed autoclave at ~20 °C is equivalent to the pressure inside of a CO<sub>2</sub> cylinder (5.5-6 MPa), the pressure will increase to 10 MPa upon heating the autoclave to 250 °C. Therefore, when reactions are conducted at 10 MPa, no additional compressor or CO<sub>2</sub> pump is required.

In the enzymatic hydrolysis study, pressure was set to 10 MPa in order to decrease the solubility of MAG and DAG in SC-CO<sub>2</sub> and thereby promote their conversion to FFA and glycerol. For this reason the effect of pressure was not directly investigated but the effect of temperature, which also impacts SC-CO<sub>2</sub> density, was investigated. However, variation in SC-CO<sub>2</sub> properties due to investigated temperature changes (40 to 50 °C) did not have a significant effect ( $p = 0.2767$ ) on percent conversion. Therefore, one can conclude that variation in SC-CO<sub>2</sub> properties due to the tested temperatures does not have a significant effect on percent conversion and that Lipozyme IM's activity does not significantly change within the tested temperature range.

#### **7.4. Effect of reactant concentrations**

Based on the glycerolysis and hydrolysis reactions conducted, increased conversions were obtained as the water content was increased. As previously suggested, the increased conversion with additional amount of water might not only be due to the Law of Mass Action but it might also be linked to the inherent properties of hot pressurized water (subcritical water) in promoting acid/base reactions.

The calculated level of water formed during esterification was similar to that which was initially present in hydrolysis reactions conducted using stoichiometric amount of water (1:3) (Fig. 5.6). However, during hydrolysis FFA were produced

(Fig. 5.4) and during esterification FFA were converted to MAG, DAG and TAG (Fig. 4.4). The question is then, if the same amount of water was present in these two reactions, why did hydrolysis occur in one and esterification in the other? The difference between the two reactions lies in the amount of glycerol present in each reaction. Indeed, during hydrolysis the maximum concentration of glycerol formed was  $< 0.1$  mol/100 g oil while the glycerol concentration in the esterification reaction conducted using 1:0.1 glycerol/oleic acid ratio was never less than 3 mol/100 g oil (Fig. 4.6). It therefore appears that, the water produced during esterification reactions conducted using 1:0.1 glycerol/oleic acid ratio was not used for hydrolysis of the product most probably because at least a portion of the water was bound by the glycerol. However, when esterification reactions were conducted with lower levels of glycerol, such as 1:2 glycerol/oleic acid ratio, less glycerol was available at dynamic equilibrium ( $< 0.04$  mol/100 g oil) and a lower proportion of water was bound, which resulted in lower dynamic equilibrium MAG production (Fig. 4.6). Such a “drying effect” caused by glycerol also explains why more than the stoichiometric amount of water was necessary in order to obtain complete hydrolysis of TAG.

The glycerol “drying effect” also affected glycerolysis. Indeed, as demonstrated by the kinetic data, the only reaction responsible for the initial TAG breakdown required to initiate glycerolysis is the one involving water and TAG to form DAG and FFA; once DAG and FFA are present, then MAG can be formed.

However, the level of glycerol used in the glycerolysis reactions was similar to that used while conducting esterification using a 1:0.1 glycerol/oil ratio (glycerol concentration  $>3$  mol/100 g oil); therefore, similar to esterification, some water was most probably bound to the glycerol. Consequently, the initiation of glycerolysis reaction required greater than stoichiometric amount of water. This fact is clearly shown in Figure 5.7 where similar amounts of water were present in the hydrolysis reactions conducted at 1:17 oil/water and for the glycerolysis conducted at 8% water in glycerol. This figure also depicts the negligible slope in glycerolysis water concentration compared with the one observed for hydrolysis. This indicates that although hydrolysis initially occurs, the water used is later partly replenished by the esterification reaction.

Although the effect of initial reactant concentration was not directly investigated during the enzymatic hydrolysis study (Chapter 6), it was possible to indirectly determine that the flow rate of water was probably too high. Indeed, if it had been too low, increasing the enzyme load would not have increased conversion since there would not have been enough water to sufficiently hydrate all the enzymes in order to keep them active. However, significantly ( $p = 0.0005$ ) higher conversions were obtained with the highest load of enzyme, which means that higher conversion could possibly be obtained if either the flow rate of water is decreased or the enzyme load is increased. Given that the HPLC pump used to deliver water was already set to its minimum flow rate, it might be simpler to

increase the enzyme load by modifying the enzymatic reactor or adding another reactor in series.

## 7.5. References

- [1] S.S. Chang, L.H. Wiedermann, Continuous manufacture of monoglycerides, United States Patent 3,079,412, 1963.
- [2] R.R. Allen, R.L. Campbell, Process for the manufacture of fatty acid esters, United States Patent 3,313,834, 1967.
- [3] M.A. Jackson, Monoglyceride production via enzymatic glycerolysis of oils in supercritical CO<sub>2</sub>, United States Patent 5,747,305, 1998.
- [4] M.A. Jackson, J.W. King, Lipase-catalyzed glycerolysis of soybean oil in supercritical carbon dioxide. *J. Am. Oil Chem. Soc.* 74 (1997) 103.
- [5] H. Nouredini, D.W. Harkey, M.R. Gutsman, A continuous process for the glycerolysis of soybean oil. *J. Am. Oil Chem. Soc.* 81 (2004) 203-207.
- [6] D.C. Montgomery, Response surface methods and designs, in: *Design and Analysis of Experiments*, John Wiley & Sons, Hoboken, NJ, 2005.

## **Appendix A. Detailed equipment description and operation**

### **A.1. Supercritical high temperature batch reactor**

#### *A.1.1. Detailed description of the supercritical high temperature batch reactor*

The supercritical high temperature batch reactor (SC-HTBR) system was custom made to conduct batch glycerolysis, hydrolysis, and esterification reactions in supercritical carbon dioxide media and to collect samples as a function of time. As previously shown in Figure 3.1, the system was made up of a number of components namely the compressor, reactor, magnetic stirrer and electric heaters with their controller. The compressor (Cat-No 554.2141, Nova-Werke AG, Effretikon, Switzerland) was used to pressurize carbon dioxide (CO<sub>2</sub>) or nitrogen (N<sub>2</sub>) into the system. This apparatus was air driven (0.4-0.8 MPa air pressure) and capable of pressurizing gas up to 70 MPa [1]. The reactor used (Fig. A.1.1) was a stainless steel 200 mL test autoclave (Cat-No 546.0103, Nova-Werke AG, Effretikon, Switzerland) with a maximum working pressure of 70 MPa at 350 °C [2]. The cap of the autoclave had three ports (Fig A.1.1), one for the J-type thermocouple, one for the inlet and one for the exit streams as shown in Figure A.1.2. Inside the autoclave, a 6.35 mm (¼ in) outside diameter (O.D.) sampling tube extended from the inside of the cap on the exit port to 2 mm from the bottom of the autoclave. This line was bent so as to avoid contact with the glass encased magnetic stirrer obtained from Fisher Scientific Ltd. (Nepean, ON). All the tubing

connections (see Fig. A.1.2), including the sampling port, were made with 6.35 mm (1/4 in) O.D. high pressure tubing from either Nova Swiss (Nova-Werke AG, Effretikon, Switzerland) or Autoclave Engineers (Snap-tite Inc., Erie, PA, USA).

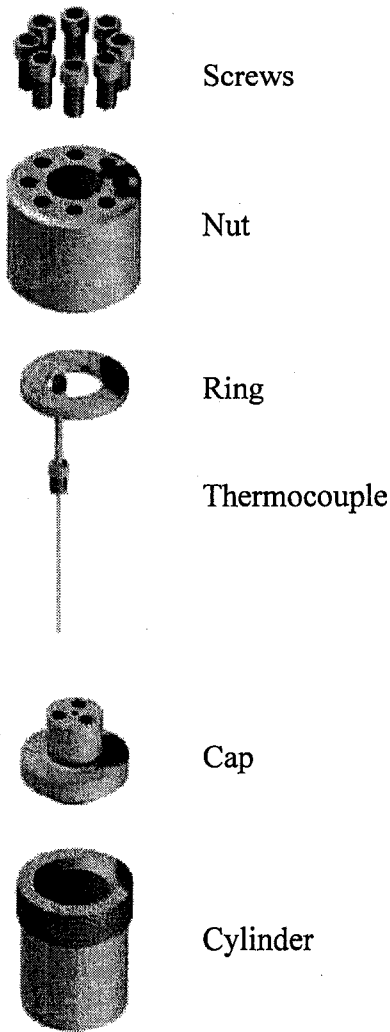


**Figure A.1.1.** Nova Swiss test autoclave with the given name of each part.

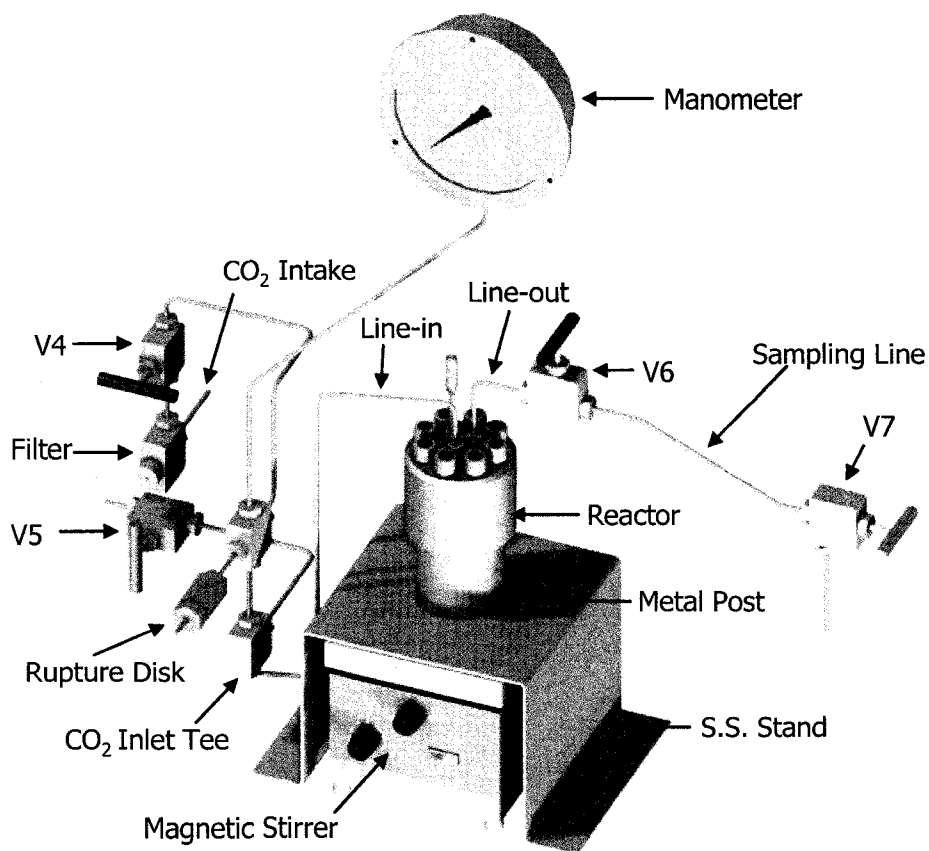


**Figure A.1.2.** Three dimensional scale drawing of some parts of the SC-HTBR system.

The tees, filter, rupture disk and valves were from Nova Swiss (Nova-Werke AG, Effretikon, Switzerland) while the manometer (McDaniel Controls Inc., Boutte, LA, USA) was bought from Wika Instruments Ltd. (Edmonton, AB) and calibrated locally. The magnetic stirrer used was placed under a custom made stainless steel stand with two metal poles welded on top of it, which were used to fix the reactor to the stand while ensuring that it was centered and in line with the magnetic stirrer.



The autoclave was heated with two MICA heating bands custom made by Tru-Temp Electric Heat Ltd. (Edmonton, AB) and was controlled by a custom built PID temperature controller (Fig. A.1.3). Heating bands were isolated by a heat shield, which was custom made using fibre glass cloth, fibre glass insulation and aluminum reinforcement sheets.

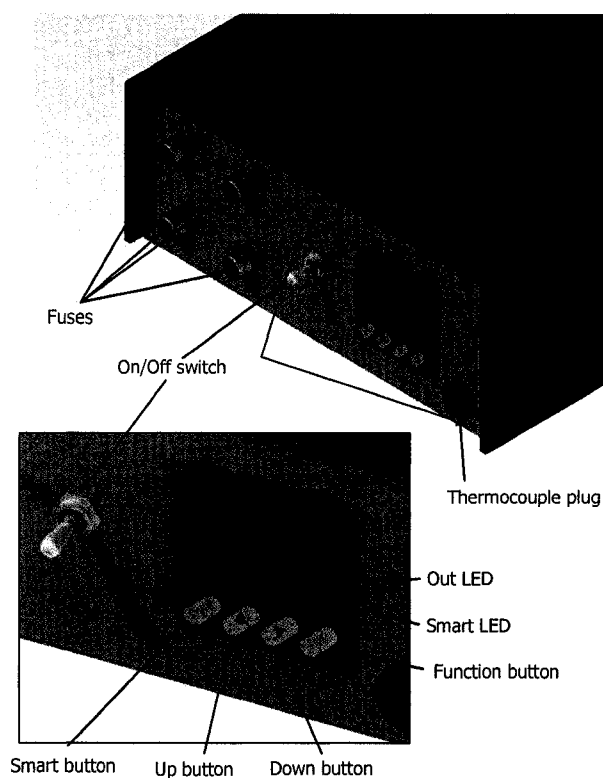


**Figure A.1.3.** Scale drawing of the temperature controller.

#### *A.1.2. Detailed operating procedure*

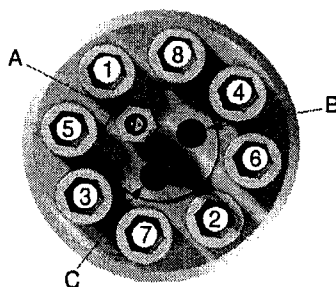
Following is the detailed operating procedure used to conduct the batch glycerolysis, esterification and hydrolysis reactions in SC-CO<sub>2</sub> and SC-N<sub>2</sub>.

- Start-up procedure:
  - Connect the high temperature system to the 70 MPa port on the Nova Swiss compressor.
  - Connect the vacuum trap line to the end of the sampling port via a rubber tubing line.
  - Clean equipment parts.
    - Wash cylinder, cap, glass-encased magnetic stirrer, thermocouple and tubing (see Fig. A.1.1 and A.1.2) with water and soap. For resistant stains, use ethanol or acetone. Avoid use of abrasives especially on the sealing surface of the cap and cylinder.
    - Wash valves with soapy water in sonication bath.
    - Rinse well with water, then ethanol and then with distilled water.
    - Air-dry with pressurized air or leave to dry over night.
  - Lubricate all threads (to prevent galling) with graphite.
  - Add the glass encased magnetic stirrer to the cylinder of the reactor.
  - Pipette the required amounts of reactants into the cylinder while ensuring that the bevelled sealing surfaces of the cylinder is kept clean.
  - Cap the cylinder
    - Place the cylinder into the custom made reactor clamp.
    - Align the cap so that the “3” on the side of the cap is in-line with the green mark on the reactor clamp.

[Note: When anhydrous reactants are required, cover the cylinder with aluminum foil and then make two small holes in the foil and add reagents. In the first hole, inject tank pressure nitrogen and in the other hole add reagents. Block the sampling (exit line) port on the cap with a rubber stopper and then quickly remove the foil on the cylinder and slide on the cap. Purge the cylinder by introducing tank pressure nitrogen through one port and vent through the other. After purging, block all ports with rubber stoppers.]

- Seal the reactor
  - Place the ring on the cap with the bevelled side downwards.
  - Screw the nut while holding the cap so that it remains aligned.
  - Screw nut-screws crosswise following the order given in Fig. A.1.4 with a torque-wrench in three separate steps: 0–30–52 Nm.

- Screw temperature probe in port “A” as illustrated in Fig. A.1.4.
- Install the autoclave between the posts on the stainless steel stand.
- Fix the heating clamp around the autoclave by tightening the two hex bolts on both heating clamps.
- Connect all the tubing lines to the autoclave.
- Install the “heat shield” around the heating clamps and plug-in the thermocouple.



○ **Figure A.1.4** Diagram of bolts and fittings position on the nut.

- Purge the reactor with tank pressure CO<sub>2</sub>.
  - Close valves V4, V5 and V6.
  - Open the CO<sub>2</sub> tank valve and valve 1 and 3 on the compressor (see Fig. A.1.5)

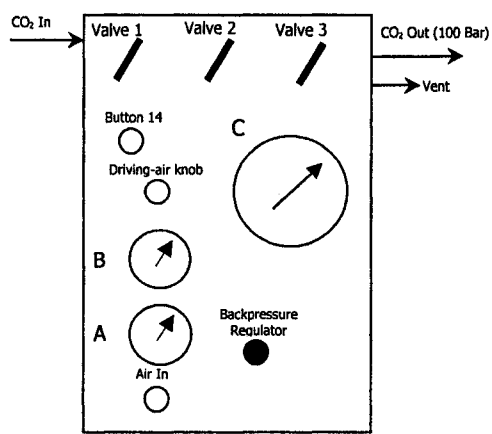


**Figure A.1.5.** Schematic of the front control panel of the Nova Swiss compressor.

- Fill the reactor with CO<sub>2</sub> by slowly opening valve V4. Once the pressure reaches >4 MPa, close V4.
  - Empty the reactor by slowly opening valve V5 just long enough to decrease the pressure to <1 MPa.
  - Repeat (fill/empty cycle) five times.
  - Fill the reactor with CO<sub>2</sub> and then close valve V4.
- Start moderate stirring by turning the knob on the magnetic stirrer to 12 o'clock position as shown in Fig. A.1.6.

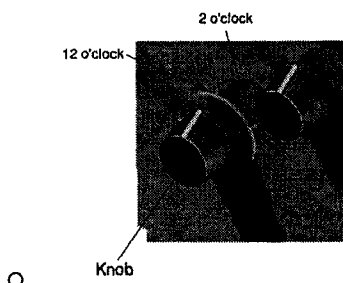


**Figure A.1.6.** Knob positions on the magnetic stirrer.

- Pressurize the system to the desired pressure: press Button 14 (Fig. A.1.5) to start the compressor. When the desired pressure is reached on manometer C, slowly open V3 and then V4. Adjust the pressure using the backpressure regulator (Fig. A.1.5).
  - Heat-up the reactor to the desired temperature.
    - Increase the stirring by turning the knob on the stirrer to 2 o'clock position (see Fig. A.1.6).
    - Press “FUNC” once or until “SP” appeared, set the desired temperature using “▲▼” then press “FUNC” to confirm your choice.
- Sampling procedure:
    - Ensure that V6 is firmly closed and open V7.
    - Start the vacuum pump.
    - Apply vacuum to sampling tube at the outlet of V7.
    - Close V7 while still under vacuum and then remove the vacuum line.
    - Fill sampling tube by opening V6.
    - Place waste container in the sampling holder. Screw a clean tube stub on the outlet of V7 and collect content of sampling tube in waste container by slowly opening V7.

- Repeat previous steps and then place a labelled, ashed pre-weighed 7 mL glass vial into the sampling holder and collect content of sampling tube in it.
- Shut-down procedure:
  - Turn off the temperature controller.
  - Turn off the magnetic stirrer.
  - Turn off the vacuum pump.
  - Collect the contents of the reactor by connecting a vacuum flask to the outlet of V7, open V6 and then slowly open V7.
  - Depressurize the compressor by closing the CO<sub>2</sub> tank and then slowly opening valve 2.
  - When all the manometers read 0 MPa, open all valves.
  - Remove the heat-shield and leave the system to cool over-night.

### *A.1.3. References*

- [1] Operating Manual NovaSwiss Diaphragm-Type-Compressors, Air driven for 15'000 and 45'000 PSI.
- [2] High-pressure extraction plant documentation K-SCE 01 for Norac Technologies Inc., Alberta, Canada. Prepared by KASYCO GmbH, 1986.

## **A.2. Supercritical continuous enzymatic reactor**

### *A.2.1. Description of the continuous enzymatic reactor*

The supercritical continuous enzymatic reactor (SC-CER) was designed and custom built to conduct continuous enzymatic reactions in supercritical carbon dioxide (SC-CO<sub>2</sub>). A schematic of the system is shown in Figure A.2.1 and Section 6.2.2 provides a complete description of the system.

### *A.2.2. Detailed operating procedure*

The following is the detailed operating procedure for conducting continuous enzymatic reactions in SC-CO<sub>2</sub> using the SC-CER.

- Start-up procedure:
  - Load enzymes between two equal layers of borosilicate 8 µm glass wool fiber (Pyrex fiber glass, Corning Inc., Corning, NY, USA).
  - Install the reactor inside the oven. Install the sample holder with a collection vial in it and hook it up as seen in Figure A.2.1.
  - Close V1e, V2e, V3e, V4e, and V5e (Fig. A.2.1.1).
  - Open the CO<sub>2</sub> tank and then open V1e and V2e to introduce tank pressure CO<sub>2</sub> in the system. Check for leaks.
  - Close V1e and start the compressor to pressurize CO<sub>2</sub>. Adjust the pressure using the backpressure regulator.
  - Turn on the oven and set the desired temperature on the PID controller.
  - Once the compressor reaches the desired pressure, open V1e to pressurize the system.
  - Open V5e and adjust the flow rate of SC-CO<sub>2</sub> indicated on the flow meter using V6e.
  - Open V3e and V4e and immediately start the Gilson and Varian HPLC pumps.
  - Record the time and the reading on the gas meter.
  - Frequently monitor the pressure, temperature and flow rate of the system.

- Sampling procedure:
  - Disconnect the cap of the sample holder and the flow meter connection tube from the sample holder.
  - Replace the sample holder with another one containing a clean collection vial.
  
- Shut-down procedure:
  - Stop the Varian and Gilson pumps and close V3e and V4e.
  - Record the time and the gas flow reading.
  - Stop the compressor and close the CO<sub>2</sub> tank.
  - Leave the system to depressurize on its own.
  - Turn off the temperature controller and the oven.

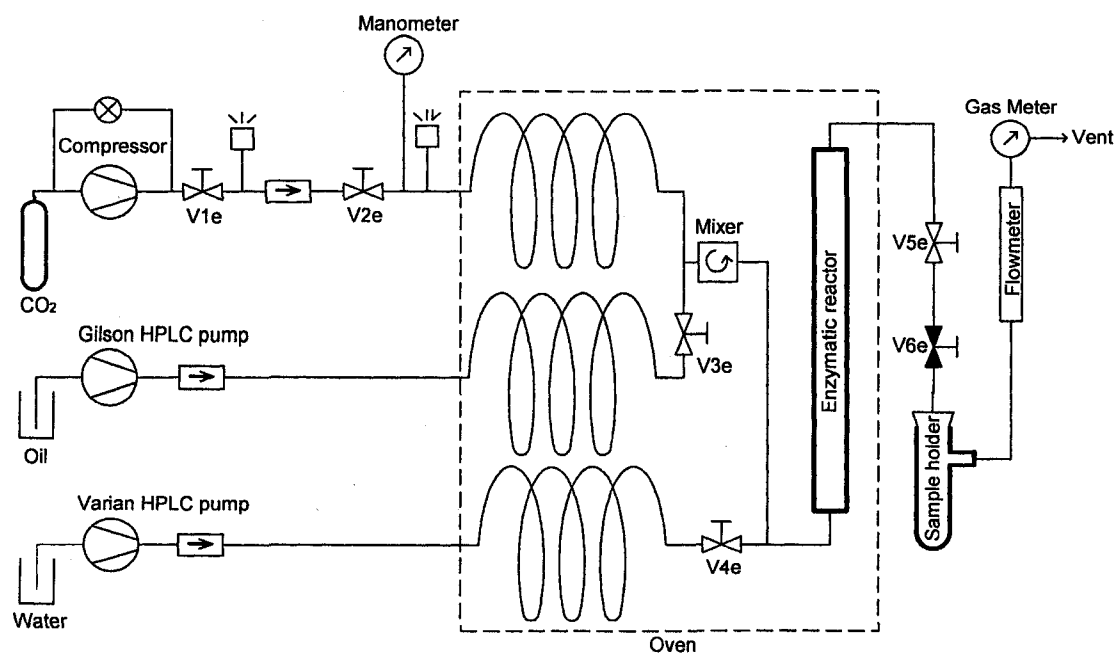


**Figure A.2.1.** Schematic of the experimental system used to conduct continuous enzymatic reactions in supercritical carbon dioxide.